The role of Protein Tyrosine Phosphatase PTPN22 in T cell signalling and autoimmunity

Shatakshi Sood

Degree of Doctor of Philosophy – The University of Edinburgh – 2015

Declaration

I, the undersigned, hereby declare that this thesis is my own composition, the work presented in the thesis has been conducted by myself, unless acknowledged otherwise, and it has not been submitted for any other degree or professional qualification except as specified.

Shatakshi Sood Date

Acknowledgements

Completion of this doctoral thesis would not have been possible without the patience, guidance and training from my supervisor Professor Rose Zamoyska. I am grateful for the opportunity to work on this project, and her encouragement particularly at difficult times when nothing made sense! Thank you for believing in me (not to mention the Jekyll and Hyde experiments) and making me push myself harder.

I would also like to thank my second supervisor Professor David Gray for his encouraging support, constructive feedback and valuable career advice. I am grateful to his lab's generous supply of home made antibodies.

I would like to express my sincere gratitude to "The Darwin Trust of Edinburgh" for offering me the PhD studentship and giving me a chance to achieve a doctoral degree. I am really grateful to Wellcome Trust for the financial support in my 4th year of study.

A big thank you to Dr. Rebecca Brownlie for all the initial training in setting up the project, her help with the arthritis experiments and more importantly for her continued motivation in tough times. I am very grateful to Dr. Robert Salmond for his patience in reading the painful first drafts and providing critical feedback and constructive comments for writing this thesis.

I am very thankful to Dr. Martin Waterfall not only for his technical assistance with flow cytometry experiments but also for looking out for me. Thank you for the many insightful discussions, lengthy conversations, survival tips and most of all your encouragement and invaluable support. I would like to thank Kay Samuel for meticulously proof reading the final manuscript. To Dr. Katrina Gordon a massive thank you for being an incredible source of motivation and strong determination.

I would like to acknowledge the support from the animal staff, Bette the lab fairy and everyone in IIIR who have helped with reagents, advice, corridor banter and made the department a pleasant to work.

Thank you to all the past and present members of the Zamoyska lab for sharing the team spirit and making it a humble learning experience. Dr. Stefano Caserta (for valuable discussion and feedback during the lab meetings and otherwise), Dr. Jessica Borger (for sharing plasmids and my woes with transduction experiments), Dr. Graeme Cowan (for his keen eye for technical details and help with statistical analysis), Dr. Thomas Tan (for protocols and brainstorming sessions), Celine (for her assistance with optimizing ELISA experiments and her magical western blots), David (for tissue culture, irradiating spleens and good natured humorous motivation), Xioyan (for lending helping hands on long experiment days) and Kaija my accomplice in this great adventure. From sharing a protocol to a house, we've have been there for one another through good times and bad - thank you for making it such a memorable journey!

My heartfelt thanks go to all my friends and office buddies, in particular my best friend-Abeer, Anjali, Anna, Binny, Des, Divya, Diwa, Gaurav, Juan (my evil twin), Kate, Lek, Matthew, Mehandru, Nouf, Pooja, Regina, Sourabh, Tua and Valentina. All of you have provided the vital "support system", put up with bouts of mood swings and endless complains but more importantly accepted me with all my flaws and quirkiness. I fall short of words to express the magnitude of your friendship and support. I would not have reached this far sane and survived the PhD writing hell alone. Cheers guys, we made it through!

Mum and Dad, I would not be here, had it not been for your innumerable sacrifices. I know this PhD means as much to you as it does to me. This thesis is a proof of your unfaltering support, love and valuable life lessons. You have being my anchor, my confidant, my mentor and I dedicate this thesis to you both. I'd like to thank my brothers, Roshim and Rishi and my sister-in-law Ruchika, who have encouraged me, stood by me and humoured me during the most darkest and toughest moments. It is through their eyes that I saw the light at end of the proverbial PhD tunnel. Of course, the fabulous next generation Sood family kids, Roshtu, Vanya and Parnika have effortlessly brought joy, laughter and love into my life by just being themselves.

Abstract

Signals via the T cell receptor (TCR) are critical for the development of T cells in the thymus, maintenance of a self-tolerant peripheral T cell repertoire and the activation of T cells in secondary lymphoid organs. A dynamic balance between tyrosine phosphorylation and dephosphorylation is essential for the maintenance of homeostasis and proper regulation of the immune system. The cytoplasmic phosphatase, PTPN22 (protein tyrosine phosphatase non-receptor type 22) is involved in negative modulation of signal transduction through the TCR and plays a central role in regulating lymphocyte homeostasis.

Genome wide association studies reveal that point mutations in PTPN22 confer an increased risk of developing multiple autoimmune diseases in humans. The precise function of PTPN22 and how mutations contribute to autoimmunity is controversial. Loss-of-function mutations in PTPN22 are associated with elevated T effector cell expansion and autoreactive B cells in both humans and mice.

A thorough dissection of the molecular involvement of PTPN22 and its allelic variant R619W is important to delineate its role in autoimmunity, to this end we utilised the *Ptpn22*$^{-/-}$ mice generated in our laboratory. In order to address whether R619W allelic variant is a gain- or loss-of-function mutation, we expressed both PTPN22^{WT} and PTPN22^{R619W} constructs in primary activated *Ptpn22*$^{-/-}$ T lymphocytes using lentiviral transduction. Surprisingly expression of either wild type or variant phosphatase showed no affect on cytokine production. Preliminary results from bone marrow chimeras generated by retroviral expression of PTPN22^{WT} and PTPN22^{R619W} in *Ptpn22* deficient mice showed reduced T cell activation compared to *Ptpn22*$^{-/-}$ T cells. PTPN22^{WT} appeared to be more suppressive of T cell responses than variant PTPN22^{R619W}. Consistent with studies conducted in comparable knock-in mouse models, our data point to the variant PTPN22^{R619W} as being a partial loss of function allele.

To elucidate the mechanism of PTPN22 action in context of an autoimmune disease, we investigated the effect of *Ptpn22* deficiency on the phenotype of SKG mice. The

SKG mouse harbours a point mutation (W163C) within the carboxyl terminal SH2-domain of ZAP-70, which results in decreased TCR signalling and impaired thymocyte development with defective positive and negative selection. These mice are prone to developing $CD4^+$ T cell mediated autoimmune arthritis that closely resembles rheumatoid arthritis in humans.

We found that thymus differentiation was partially restored in SKG *Ptpn22*$^{-/-}$ thymocytes and *Ptpn22* deficiency enhanced TCR mediated signalling in SKG *Ptpn22*$^{-/-}$ thymocytes relative to SKG thymocytes. Consistent with increased signalling observed in the thymocytes, there was improved *in vitro* proliferation and IL-2 production of $CD4^+$ T lymphocytes from SKG *Ptpn22*$^{-/-}$ mice compared to SKG mice. By contrast to SKG mice, SKG *Ptpn22*$^{-/-}$ mice developed less severe mannan-induced arthritis and showed decreased proportions of Th17 and higher numbers of regulatory T cells. These results show that removal of PTPN22 can compensate, at least partially, for the deficient ZAP-70 activity in the SKG mouse, thus linking PTPN22 and ZAP-70 to the same signalling pathway.

This study advances our understanding of how manipulating TCR signals impacts on downstream T cell functions, suggesting PTPN22 may be a valuable target for the treatment of autoimmune diseases. Further studies to determine physiological role of the phosphatase and its disease-associated variants could provide insight into mechanism of immune activation, tolerance and autoimmunity.

Lay Summary

T cells fight against infections but occasionally can turn on themselves. Failure to regulate immune responses increases the risk of autoimmunity and tumour development. One such protein tyrosine phosphatase acting as a molecular switch to negatively regulate T cell function is PTPN22. Interestingly, genetic studies show that aberrations in this phosphatase are associated with autoimmune diseases. A thorough dissection of the molecular involvement of PTPN22 is important to delineate its role in autoimmunity. To this end, we utilised a mouse model where we have deleted the PTPN22 protein in the mouse cells. Consistent with the role of PTPN22 as an inhibitor of T cell signalling, PTPN22KO mouse show increased T cell activity, however these mice fail to develop any autoimmunity.

To understand the mechanism of PTPN22 action in context of an autoimmune disease, we investigated the effect of loss of *Ptpn22* deficiency on the phenotype of SKG mice. The SKG mice is a naturally occuring mouse strain which spontaneously develops arthritis that resembles rheumatoid arthritis in humans due to mutation in a molecule, ZAP-70 that positively regulates T cell function. Arthritis can also be elicited in these SKG mice by injection of fungal products (such as mannan). We crossed the *Ptpn22* deficient mouse with the SKG mouse to generate SKG *Ptpn22*$^{-/-}$ mice. Our results show that loss of PTPN22 resulted in less incidence and severity of mannan induced arthritis on the SKG background. This study shows that lack of a negative regulator (PTPN22) can partially compensate for the dysfunction in a positive regulator (ZAP-70) therefore linking these two molecules to similar signalling pathway.

This study advances our understanding of how manipulating T cell signals impacts on downstream T cell functions, suggesting PTPN22 may be a valuable target for the treatment of autoimmune diseases. Further studies to determine physiological role of the phosphatase and its disease-associated variants could provide insight into mechanism of immune activation, tolerance and autoimmunity.

Table of Contents

Table of Figures

List of Tables

Abbreviations

ADAP - Adhesion and Degranulation-Promoting Adaptor Molecule

Ag - Antigen

AICD - Activation Induced Cell Death

AP1- Activator Protein 1

APC - Antigen Presenting Cell

Bcl 2 - B Cell Lymphoma Protein 2

Bcl 6 - B Cell Lymphoma Protein 6

BCR - B Cell Receptor

BM - Bone marrow

$Ca2^{+}$ - Calcium

CamK - $Ca2^{+}$ - Calmodulin Dependent Kinase

CARD - Caspase Recruitment Domain

CARMA1 - CARD and MAGUK Containing Scaffold Protein 1

CCL - Chemokine CC Ligand

CCR - C-C Chemokine Receptor

CD - Cluster of Differentiation

CDR - Complementarity Determining Region

CFDA - Carboxyfluorescein Diacetate N-Succinimidyl Ester

CID - Combined Immunodeficiency

CLP - Common Lymphoid Progenitor

CMP - Common Myeloid Progenitors

CMV - Cytomegalovirus

Csk - C-terminal Src Kinase

cTEC - Cortical Thymic Epithelial Cell

CTL - Cytotoxic T Lymphocyte

CTLA4 - Cytotoxic T Lymphocyte Antigen 4

CXCL - Chemokine (C-X-C) Ligand

DAG - Diacylglycerol

DC - Dendritic Cell

DISC - Death Inducing Signaling Complex

DLL4 - Notch Delta - Like Ligand 4

DN - Double Negative $CD4^-$ $CD8^-$ Thymocyte

DP - Double Positive $CD4^+CD8^+$ Thymocyte

ELISA - Enzyme Linked Immunosorbent Assay

EOMES - Eomesodermin

ER - Endoplasmic Reticulum

ERK - Extracellular Signal Regulated Kinase

ETP - Early-T Cell Progenitor

FACS - Fluorescence Activated Cell Sorting

FADD - Fas Associated Death Domain

FCS - Fetal Calf Serum

Foxp3 - Forkhead Box P3

FRET - Foerster Resonance Energy Transfer

FSC - Forward Scatter

FTOC - Fetal Thymic Organ Culture

Gads - Grb2-Related Adapter Downstream of Shc

Grb2 - Growth Factor Receptor Bound Protein

h - hour

HEK - Human embryonic kidney

HPK1 - Hematopoietic Progenitor Kinase

i.p. injection - Intraperitoneal Injection

i.v. injection - Intravenous Injection

ICAM - Intracellular Adhesion Molecule

Id - Inhibitor of DNA-Binding

IFN - Interferon

IFNGR - IFN Gamma - Receptor

Ig - Immunglobulin

IL - Interleukin

IL-2R - IL-2 Receptor

IL-7R - IL-7 Receptor

IMDM - Iscove's Modified Dulbecco's Medium

IP3 - Inositol 1,4,5 - Trisphosphate

IS - Immunological Synapse

iSP - Immature Single Positive Thymocytes

ITAM - Immunoreceptor Tyrosine-Based Activation Motif

Itk - IL-2 Induced Tyrosine Kinase

JNK - c-Jun N-Terminal Kinase

Kd - Knockdown

kDa - Kilodalton

KLRG-1 - Killer Cell Lectin-Like Receptor G1

KO - Knockout

LAT - Linker of Activated T Cells

LFA-1 - Leukocyte Function-Associated Antigen 1

LIME - Lck-Interacting Membrane Protein

LN - Lymph Nodes

mAb - Monoclonal Antibody

MAPK - Mitogen-Activated Protein Kinase

MFI - Mean Fluorescence Intensity

MHC - Major Histocompatibility Complex

Min - Minute

MPECs - Memory Precursor Effector Cells

mRNA - Messenger RNA

mTEC - Medullary Thymic Epithelial Cells

NFAT - Nuclear Translocation of Nuclear Factor of Activated T Cells

NFκB - Nuclear Factor Kappa B

NK - Natural Killer Cell

NKT - Natural Killer T Cell

p:MHC - Peptide MHC Complex

PAG - Phosphoprotein Associated with Glycosphingolipid-Enriched Microdomains

PBMC - Peripheral Blood Mononuclear Cell

PBS - Phosphate Buffered Saline

PCR - Polymerase Chain Reaction

PDBu - Phorbol 12, 13 dibutyrate

PD1- Programmed Cell Death 1 Receptor

PEST - Proline - Glutamic acid - Serine - Threonine

PFA - Paraformaldehyde

pHSC - Pluripotent Hematopoietic Stem Cell

PI3K - Phosphoionositide 3-Kinase

PIP2 - Phosphatidylinositol-4,5-Bisphosphate

PKA - Protein Kinase A

PLCγ - Phospholipase C γ

PSGL - 1-P-Selectin Glycoprotein Ligand - 1

PTK - Protein Tyrosine Kinase

PTP - Protein Tyrosine Phosphatase

PTPN - Protein Tyrosine Phosphatase, Non Receptor Type

RA - Rheumatoid arthritis

RAG - Recombinase Activating Gene

RANKL - Receptor Activator of Nuclear Factor Kappa-B Ligand

Rap1- Ras-proximity -1

RasGRP - Ras Guanyl Nucleotide-Releasing Protein

RIAM - Rap-1 GTP interacting adapter molecule

RNA - Ribonucleic Acid

S - second

S1P1 - Sphingosine-1-Phosphate Receptor 1

SD - Standard Deviation

SFK - Src Family Kinase

SH - Src Homology Domain

siRNA - Short Interfering RNA

SKAP - Src Kinase associated protein of 55 kDa

SLEC - Short-Lived Effector Cell

SLP-76 - SH2 Domain-Containing Leukocyte Phosphoprotein of 76 kDa

SOS - Son of Sevenless

SP - Single Positive

SSC - Side Scatter

STAT5 - Signal Transducer and Activator of Transcription 5

TCM - Central Memory T Cell

TCR - T Cell Receptor

Tdt - Terminal-Deoxynucelotide Transferase

TEM - Effector Memory T Cell

TGFβ - Transforming Growth Factor Beta

TMB - 3, 3, 5, 5-Tetramethylbenzidine

TNFα - Tumor Necrosis Factor Alpha

Treg - Regulatory T Cell

Tyr - Tyrosine

VCAM - Vascular cellular adhesion molecule

VSV-G - Vesicular Stomatitis Virus Glycoprotein

WB - Western Blot

WT - Wild-Type

ZAP-70 - Zeta Associated Protein of 70 kDa

Chapter 1: Introduction

1.1 An Overview of the Immune system

The mammalian immune system functions to protect the hosts against a wide range of pathogenic organisms. All the major circulating immune cells arise from the pluripotent hematopoietic stem cells (pHSCs), which further differentiate into the myeloid stem cell or the common lymphoid progenitors. Protection by the immune system is established by execution of four related activities: recognition of foreign pathogens, elimination of the pathogen by effector responses, tightly controlled self regulation of the immune response and formation of immunological memory. Two components of the immune system: innate and adaptive immunity collaborate together to protect the host system.

1.2 Innate immunity

Innate immunity is defined as the "hard wired responses" encoded in their mature form by germline genes of the host and is inherited from parent to child. The innate immune system recognizes conserved molecular patterns on microorganisms known as pathogen-associated molecular patterns (PAMPs) through a limited and invariant repertoire of receptors called pattern recognition receptors (PRRs) (Murphy et al., 2012). It constitutes the first-line of host defence and comprises of physical and chemical barriers, which together with the molecular and cellular components provide a rapid-response mechanism to prevent microbial invasions.

The first hurdle for the pathogen involves breaching the barriers protecting the host. These include anatomical barriers such as the skin, the internal epithelia and the mucosal membranes lining the respiratory, gastrointestinal and genitourinary tracts. A variety of soluble factors contribute to innate immunity, either present constitutively in biological fluids (such as lysozyme, complement proteins) or that are released from cells that are activated following recognition of invading pathogens (e.g. cytokines and chemokines). Integral cellular mediators of the innate immune system originate from the myeloid lineage and include macrophages, neutrophils,

eosinophils, basophils, mast cell, dendritic cells (DCs), and some cells of the lymphoid lineage such as natural killer (NK) and natural killer (NKT) T cells.

1.3 Adaptive immunity

Although the innate immune system has evolved sufficiently to provide generalised rapid sensing and elimination of pathogens, it is limited in its ability to recognise the rapidly evolving microorganisms. The adaptive immune system overcomes the constraints of limited diversity and provides a more specific targeted immune response. The adaptive immune system arises from the lymphoid lineage of pHSCs and comprises B and T lymphocytes that are characterised by their unique cell surface antigen (Ag) receptors (BCR and TCR, respectively). These antigenic receptors are custom tailored through a process of somatic gene recombination to generate diverse repertoires of receptors to recognise various pathogens. The adaptive immune response confers the host with Ag specific immunological memory, thereby permitting a more effective host response against the specific pathogens when encountered again.

1.3.1 The Generation of BCR and TCR Diversity

Both B and T lymphocytes originate from the common lymphoid precursor (CLP). While the B cells develop within the bone marrow and differentiate into mature B cells (plasma cells), which secrete antibodies with specificity similar to that of the BCR. While T cell precursors are generated in the bone marrow, they develop in the thymus as naïve T cells which upon activation differentiate into effector T cells.

The BCR comprises membrane-bound immunoglobin that is composed of four polypeptides – two identical 50 kD heavy chains (H) and a pair of identical 25 kD kappa (κ) or lamda (λ) light chains (L) held together by disulphide bonds. The N-terminal amino acid sequence of both the heavy and light chains forms the Ag-binding region and varies extensively between antibody molecules, known as the variable (V) region. The variable regions of heavy and light chain form the hypervariable loops, creating a surface complementary to antigen, commonly called as complementarity-determining regions 1, 2 and 3 (CDR1, CDR2, CDR3). The

variable region of the H chain is assembled from individual gene segments, classified as variable (V), diversity (D) and joining (J). The carboxyl terminal of the heavy chains comprises the constant region, (C) region, which determines the functional activity of the antibody molecule. The five main antibody classes IgM, IgD, IgG, IgA and IgE are determined by their corresponding heavy chains and denoted by Greek letters (μ, δ, γ, α and ε respectively). IgG is the most abundant in humans (Murphy et al., 2012).

The majority of TCR consists of a heterodimer of two different polypeptide α and β chains that are structurally similar to the antigen-binding fragment (Fab) of an immunoglobin molecule. The TCR α chain is made up of three gene segments, the variable amino terminal (V), joining (J) and the constant regions and the TCR β chain is composed of V, D (diversity) and J segments. A minor subset of T cells bears an alternative TCR made of a different pair of polypeptides (γ) and (δ), called γδ T cells. The γδ T cells mainly reside in the skin epithelium and mucosa rich tissue such as the gut and have a less diverse TCR repertoire (Girardi, 2006).

The generation of diversity of lymphocyte receptors is similar in T and B cells. The V, D and J gene segments are randomly assembled by DNA recombination, mediated by the recombinase-activating genes 1 and 2 (RAG1/RAG2) to generate variable regions, that when fused to the constant (C) region form Ag receptors with unlimited diversities. The clonal diversity is generated by multiple mechanisms first by the combinatorial variation in the V-D-J gene segment joining, second by junctional diversity occurring as a result of inaccurate splicing creating frame shift mutations and third, by insertion of nucleotides at the V-D and V-J junction by the enzyme deoxyribonucleotidyl transferase (TdT) (Cabaniols et al., 2001; Parkin and Cohen, 2001). Mice lacking either of the *Rag* gene, present with a complete block in the lymphocyte development (Mombaerts et al., 1992).

1.3.2 B cells

In humans B cells constitute approximately 15% of peripheral blood leukocytes and undergo a developmental program in the bone marrow by staged maturation from pro-B cell, to pre-B cell and finally into immature B cells with membrane-bound

immunoglobin, BCR. In the Pro-B cell stage the recombinase enzyme catalyses rearrangement of the immunoglobin heavy-chain locus with D_H to J_H joining, followed by secondary rearrangement of V_H regions joining the D_H-J_H segments. Successful rearrangement of the heavy chain VDJ locus leads to expression of intact μ heavy chain, further rearrangements ceases and the pro-B cells become pre-B cells. In the pre-B-cell stage, the V and J regions of λ or κ light chains are rearranged. The successful assembly of VJ rearranged light chains combined with the μ chains forms immature B cell expressing IgM molecules (Pieper et al., 2013). On reaching the immature stage, B cells exit the bone marrow and migrate to the spleen where they undergo further differentiation into naïve, follicular, or marginal zone B cells. The successfully rearranged heavy and light chains are subject to allelic exclusion, ensuring that only one of the two alleles of a gene is expressed. As well as allelic exclusion, light chains also display isotypic exclusion; that is expression of only one type of light chain, either κ or λ by an individual B cell (Pieper et al., 2013). Upon stimulation by antigen, B cells can undergo class switching to express a different Ig heavy chain. Somatic hyper mutation in mature B cells generates further diversity of the BCR to generate clones with enhanced Ag binding. Affinity maturation ensures that the clones with highest affinity survive and mature into antibody- producing cells (Pieper et al., 2013).

In contrast to conventional B cells described above (also referred as B2 cells), B1 cells are derived from the foetal-liver hematopoietic stem cells that are long lived and are particularly found in the peritoneal cavity and in gut-associated lymphoid tissues. These self-renewing B1 cells produce a significant portion of IgM natural autoantibodies in serum that are crucial for defence against encapsulated bacteria. B-1 cells are further subdivided into B1-a ($CD5^+$) and B1-b ($CD5^-$) subsets (Hardy, 2006). Unlike the conventional B2 cells, the B1 cells can respond to antigens independent of T cells. B1-a cells and their natural antibody products provide innate protection against bacterial infections in naive hosts, whereas B1-b cells function independently as the primary source for long-term adaptive antibody responses to polysaccharides during infection (Engel et al., 2011). The hallmarks of B1 B cells are their polyreactivity and their low affinity for various ligands, a possible consequence

of positive selection by self-Ags. However, their low threshold of activation makes them highly reactive to high loads and/or altered self-Ags, which could potentially exacerbate autoimmune disease (Engel et al., 2011). B1-a cells can contribute to autoimmunity by the autoreactivity of natural antibodies, the production of IL-10 cytokine and enhanced antigen presentation capabilities (Duan and Morel, 2006).

1.3.3 T cells

T cells develop through various stages in the thymus (discussed later in **1.4**) and can be broadly divided into two major classes depending on the selective surface expression of the glycoprotein CD4 or CD8 producing $CD4^+$ or $CD8^+$ T cells respectively. After T cells leave the primary lymphoid tissues (BM and thymus) they home to secondary lymphoid tissues (lymph nodes (LN) and spleen) and continuously circulate between blood and lymphatic circulatory systems. Naïve T cells are multipotent and survive in the periphery by contact of the TCR with ligands of self-peptide major histocompatibility complex (MHC) and exposure to interleukin 7 (IL-7) (Sprent and Surh, 2011). Once naïve T cells encounter specific Ag they undergo activation and clonal expansion of the Ag specific T cells. $CD4^+$ and $CD8^+$ T cells differentiate into functionally different subsets following exposure to antigen, contingent on the integration of multiple signals from the local microenvironment **(Fig 1.1)**.

$CD4^+$ T cells

Resting naïve $CD4^+$ T (designated as Th) cells release very low levels of cytokines. Upon stimulation by antigen presented in context of MHC II and signalling via the IL-2 receptor Th cells progress to Th0 cells that mainly secrete IL-2. Depending on the milieu of cytokines present, the Th cells can differentiate into a variety of lineages, for example, Th1, Th2 or Th17 subsets (Sallusto and Lanzavecchia, 2009). In the past, a classical model assigned $CD4^+$ effector T cells either into Th1 and Th2 subsets, each with its own distinct cytokines, transcription factors and functions (Mosmann et al., 1986). The lineage specification of the different $CD4^+$ T cells subsets depend on the concerted actions of cytokine-induced signal transducer and

activator of transcription (STAT) factors and "master regulators", transcription factors, which provide cell extrinsic feedback loops by production of cytokines, as well as cell-intrinsic transcriptional networks guiding each developmental program (Murphy and Reiner, 2002). The development of the Th1 subset, results from the sequential actions of STAT1 induced by IFNγ and STAT4 induced by IL-12 that ultimately promote expression of T-bet, a central transcription factor important for Th1 programming. The Th2 subset is induced by IL-4 induced STAT6 signalling which upregulates the transcription factor GATA3 (Murphy and Reiner, 2002). Th1 cells are associated with protection against intracellular pathogens and virally infected targets while the Th2 phenotype regulates humoral immunity and is involved in protection against extracellular pathogens (Zhu et al., 2010).

Recently in addition to the well characterized Th1 and Th2 subsets, a number of other functional Th subsets have been described for $CD4^+$ T cells, including Th17, T regulatory (Treg), Th3 and T follicular helper (Tfh), which secrete different cytokines to facilitate specific immune responses. Transforming growth factor β (TGF-β) and IL-6 are crucial factors involved in the *de novo* differentiation of Th17 (Bettelli et al., 2006; Veldhoen et al., 2006) and IL-23 is required for their survival and expansion (Aggarwal et al., 2003). Alternatively, Th17 cells can also be induced by IL-6, IL-1β and IL-23, independent of TGF-β and these "alternatively - derived" Th17 cells are more pathogenic than those derived from TGF-β and IL-6 alone (Bedoya et al., 2013). Differentiated Th17 cells produce a variety of cytokines including IL-17A, IL-17F, IL-21, IL-22, GM-CSF, TNFα, IL-9, IL-10 and IFNγ depending upon the cytokine milieu present at the time of differentiation (Bedoya et al., 2013). IL-17A is considered to be the primary effector cytokine secreted by Th17 and can elicit the production of other inflammatory cytokines by fibroblasts and epithelial cells, such as IL-6, IL-8, GM-CSF and MCP-1 (Cooke, 2006). The central modulator of the Th17 is the retinoic acid-related orphan nuclear receptor γ (RORγT), which drives the transcription of IL-17A and IL-17F (Ivanov et al., 2006). Other transcription factors involved in directing naïve $CD4^+$ T cell towards Th17 differentiation include STAT3, interferon regulatory factor 4 (IRF4), the aryl hydrocarbon receptor (AHR), NOTCH and basic leucine zipper transcription factor

(BATF) (Bedoya et al., 2013). IL-6 and IL-23 activates STAT3 and regulate expression of RORγT. STAT3 deficiency impairs RORγT expression leading to elevation of T-bet and the nuclear transcription factor Forkhead box P3 (Foxp3) (Bedoya et al., 2013). STAT3 is thought to further enhance cell commitment to the Th17 lineage by directly binding the *IL17* gene promoter (Bedoya et al., 2013). Elevated levels of IL-17 are implicated in multiple autoimmune conditions such as multiple sclerosis, psoriasis, rheumatoid arthritis, systemic lupus erythematous and experimental autoimmune encephalomyelitis (EAE) (Cooke, 2006).

$CD4^+CD25^+$ regulatory T cells (Tregs) are vital for maintaining immune tolerance by counter-balancing adaptive immune responses (Liston and Gray, 2014). Adoptive transfer of purified $CD4^+CD25^-$ T cells from normal mice into nude mice that lack T cells of their own resulted in development of number of autoimmune diseases such as thyroiditis and gastritis (Sakaguchi et al., 1995). Depending on the site of development Tregs are broadly classified, into natural Tregs (nTregs) that develop in the thymus or induced Tregs (iTregs), which develop in the periphery upon T cell activation (Josefowicz and Rudensky, 2009). The expression of Foxp3, an X-chromosome encoded member of the winged-helix protein family of transcription factors, is crucial for the function and maintenance of both subsets (Fontenot et al., 2003). IL-2 has been shown to play an important role in the maintenance of nTregs and stimulation of nTregs in response to IL-2 provides regulation of IL-2 producing effector T cells (Fontenot et al., 2005). The differentiation of naïve $CD4^+$ T cells into iTregs was found to be dependent on cytokines such as TGF-β, IL-4 and IL-10 (Apostolou and von Boehmer, 2004). Additionally, TGF-β induced signals are critical for the expression of Foxp3, the size of the peripheral Treg compartment and the suppressive function of Tregs (Marie et al., 2005). The *Foxp3* gene is highly conserved with similar functions in mouse and man and mutations in Foxp3 protein results in severe and fatal autoimmune pathologies affecting multiple organs in both species (Rudensky, 2011). Differentiation of both Th17 and Treg subsets of $CD4^+$ T cells are overlapping and are determined by the concentration of TGF-β; at low doses, TGF-β synergises with proinflammatory cytokines, IL-6 and IL-21 to promote expression of the IL-23 receptor favouring Th17 differentiation whereas at high

doses it favours the Foxp3 mediated repression of RORγT favouring iTreg differentiation (Zhou et al., 2008).

Th3 is a unique subset of Tregs, which differentiates from naïve $CD4^+$ T cells following ingestion of an oral antigen. This subset is known to secrete TGF-β, assist in IgA secretion and suppress functions of both Th1 and Th2 cells. It resembles Treg in the expression of CD4 and CD25, however there are controversial reports about expression of Foxp3 in these cells. (Gol-Ara et al., 2012).

The Tfh subsets are characterised by the surface expression of PD-1, ICOS, Bcl-6, IL-21 and chemokine receptor CXCR5, which mediates their recruitment into B cell follicles to regulate development of Ag-specific B cell immunity (Crotty, 2011).

$CD8^+$ T cells

On encountering Ag presented by MHC I molecules, naïve $CD8^+$ T cells undergo rapid proliferation, generating large populations of clonally expanded Ag-specific T cells which can differentiate into either effector T cells known as cytotoxic T lymphocytes (CTLs) or long-lived memory cells (Williams and Bevan, 2007).

$CD8^+$ T cells require antigen stimulation, CD28-dependent co-stimulation, and IL-12 or Type I interferons (IFNs) for activation and commitment to clonal expansion and effector cell differentiation (Williams and Bevan, 2007). CTLs recognise their target cells expressing cognate peptide-MHC I complexes and facilitate their clearance by either direct lysis or by production of antiviral cytokines TNF and IFNγ cytokines (Barry and Bleackley, 2002). Two major pathways of cytotoxicity have been described in CTL: Ca^{2+} dependent perforin/granzyme and Ca^{2+} independent Fas ligand (FasL) mediated apoptosis, these are mediated by TCR signalling. The first mechanism requires rearrangement of effector-cell cytoplasm, resulting in release of lytic granules containing perforin and granzyme B at the immunological synapse. Perforin is a potent pore forming protein, which creates pores in the membrane of target cells, enabling delivery of granzyme B that cleaves various intracellular substrates, including pro-apoptotic factors such as Bid (Barry and Bleackley, 2002). CTLs express Fas ligand (CD95, also known as death receptor) and initiate apoptosis

of target molecules by binding Fas-molecules on target cells via caspase dependent, death-inducing signalling complex (DISC) (Barry and Bleackley, 2002).

A majority (90-95%) of clonally expanded CTLs die by apoptosis after antigen clearance and the surviving effector cells are able to differentiate into long lived memory $CD8^+$ T cells which produce low levels of perforin, granzyme B and IL-2 (Murali-Krishna et al., 1998). Memory T cells can be divided into effector (T_EM; $CCR7^-CD62L^-$) or central (T_cM; $CCR7^+ CD62L^+$) subsets based on the expression of chemokine receptor CCR7 and L-selectin, CD62L (Sallusto et al., 2014).

1.3.4 Antigen Presentation

In contrast to B cells that are capable of recognising antigens on their own, Ag recognition by αβ T cells requires Ag to be processed into peptides that are presented in context of MHC molecules. MHC molecules are highly polygenic and polymorphic as they are encoded by several different sets of genes arranged into large clusters in the genomes and can have allelic variants differing by up to 20 amino acids. MHC polymorphisms occur mainly in the peptide-binding groove to increase the diversity of peptides that can be bound by MHC molecules. MHC molecules are divided into two classes – MHC class I which is expressed on the surface of all nucleated cells and presents peptide antigens to $CD8^+$ T cells and MHC class II that are predominantly expressed on professional antigen presenting cells (APC) such as dendritic cells (DCs), macrophages and B cells and present peptides to $CD4^+$ T cells (Kindt et al., 2007).

Both class I and class II MHC molecules are structurally similar, comprising a heterodimeric α and β peptide binding domain and two Ig-like domain (Rudolph et al., 2006). In class I MHC, the peptide binding cleft ($\alpha_1\alpha_2$) binds peptides of 8-10 amino acids in length whereas the binding pocket in class II MHC molecules is less restricted and can bind peptides up to 13-17 amino acids in length. MHC class II molecules are more flexible as they are formed through non-covalent association of two polypeptides chains (α and β) (Rudolph et al., 2006).

MHC class I molecules mainly bind antigenic peptides derived from intracellular proteins that are endogenously processed by immunoproteases within the cytosol of APC and are transported to the endoplasmic reticulum (ER) via a family transporters associated with Ag processing-1 and-2 (TAP-1 and TAP-2). Within the ER, TAP and chaperon proteins act as a scaffold for the assembly of MHC class I molecules (α and β_2M) with the peptides. These chaperons include tapasin, that stabilises the TAP1/2 heterodimer, calnexin that helps to retain partially assembled MHC molecules until they are fully formed, and calreticulin, which stabilises the MHC class I to receive the peptide (Sadasivan et al., 1996). The newly assembled pMHC complex is then translocated to the plasma membrane through the Golgi complex.

By contrast MHC class II molecules, bind peptides derived from pathogens that are ingested in intracellular vesicles or from the extracellular proteins that are internalized by endocytosis. During assembly of the MHC class II molecule (αβ) in the ER, the binding cleft is blocked by the preassembled trimeric protein called invariant chain (Ii) while the cytoplasmic tail of Ii expresses a motif, which targets the complex to the endosomal/lysosomal compartment via trafficking through the Golgi complex. Subsequently the Ii chain is gradually degraded by proteolysis. However, a short fragment of Ii called class II associated invariant chain peptide (CLIP) remains bound within the peptide binding groove, to prevent premature binding of antigenic peptide (Kindt et al., 2007). The human leukocyte Ag HLA-DM, structurally related to MHC class II molecules is primarily located within the endosomal compartment and facilitates the exchange of CLIP for the antigenic peptide, enabling the stable pMHC to be directed to the cell surface (Denzin and Cresswell, 1995).

1.4 Immunological Tolerance & Autoimmunity

The immune system has evolved to achieve effective immunity against foreign pathogens without mounting detrimental responses to self thus preserving the integrity of the host's own tissues. Immunological tolerance is a state of unresponsiveness towards self and maintenance of immune competence and reactivity to all the other foreign antigens (Murphy et al., 2012). The inability to

remain tolerant to self is the fundamental cause of autoimmunity. A number of immune tolerance induction mechanisms work in synchrony to maintain the fine balance between effective immunity and autoimmunity. The mechanisms of immune tolerance are classically divided into two categories: central tolerance and peripheral tolerance. To review the mechanisms controlling the induction of tolerance in T cells it is important to first discuss the development of T cells within the thymus.

1.4.1 T Cell Development

T cells are derived from the common lymphoid progenitors (CLP) that originate from the pHSCs found in the fetal liver and bone marrow. These CLPs migrate to and colonise the thymus where they can differentiate into T, B or NK cells (Ardavin et al., 1993). Following lineage commitment, developing thymocytes undergo a series of TCR rearrangements with eventual assembly of TCR complexes maturing into γδ T cell and αβ T cell lineages. The different developmental stages are marked by expression of cell surface receptors **(Fig 1.2)**. The αβ T cells diverge further into $CD4^+$ T cells, $CD8^+$ T cells, NKT cells and Tregs (Rothenberg et al., 2008).

The interaction of thymocytes with thymic stromal cells drives the development of the T cell lineage. The thymus is made up of an outer cortex and an inner medulla region that comprise distinct epithelial stromal cells known as cortical thymic epithelial cells (cTECs) and medullary thymic epithelial cells (mTECs) respectively (Anderson and Takahama, 2012). *Nude* mice, lack a thymus and thus mature cTECs due to loss of function of the transcription factor, FoxN1 and consequently the thymus, is completely devoid of all T cells (Manley and Blackburn, 2003). T cell development is initiated by the recruitment of the CLPs to the thymus by P-selectin an adhesion molecule, that is expressed on thymic endothelial cells (TECs) (Rossi et al., 2005) and by chemokines such as chemokine ligand (CCL) 21, CCL25 and CXCL12 expressed by TECs (Liu et al., 2006). The unique thymic microenvironment not only provides supportive cytokines such as c-kit ligand and IL-7 that maintain and expand early thymic precursors (ETP), but also crucially provides an environment that is rich in Notch ligand Delta-like ligand 4 (DLL4) (Rothenberg et al., 2008; Schmitt and Zuniga-Pflucker, 2002). There is accumulating

evidence that Notch signalling is critical for determination of T cell fate during maturation from pHSCs. It has been shown to favour T cell development over B cell formation, as *Notch*$^{-/-}$ mice demonstrate an early block in T cell development (Pui et al., 1999; Radtke et al., 1999) and overexpression of constitutively active Notch-1, by retroviral transduction, resulted in development of immature $CD4^{+}CD8^{+}$ double positive (DP) cells in the BM (Pui et al., 1999).

The early thymic progenitors (ETP) enter the outer cortex and lack expression of the co-receptors CD4 and CD8 and are referred to as double negative (DN) cells. The DN population can be subdivided into four sequential stages (DN1, DN2, DN3 and DN4) characterised by the surface expression of CD44, an adhesion molecule and CD25, the alpha chain of IL-2 receptor. In addition, proliferation and survival of ETPs in the DN population is dependent on signals from IL-7 and IL-7R and from tyrosine kinase receptor c-kit and its ligand and stromal cell factor (SCF). The DN1 population is phenotypically defined as c-$kit^{+}CD44^{+}CD25^{-}$, is very heterogenous and can give rise to all subsets of T cells including NKT and γδ T cells. As the DN1 cells proliferate they commence up-regulation of CD25, and enter the DN2 stage becoming $CD44^{+}CD25^{+}$. The DN2 stage is further subdivided into DN2a (c-kit^{hi}) and DN2b (c-kit^{med}). During the DN2 stage of development, cells commence the rearrangement of the TCRβ, γ and δ genes. Finally at the DN3 ($CD44^{-}CD25^{+}$) expression of both c-kit and CD44 is turned off and the cells can be further subdivided as DN3a ($CD27^{lo}$) pre-β or $CD27^{hi}$ DN3b γδ cells (Rothenberg et al., 2008). In the DN3 stage, the first checkpoint for committed αβ thymocytes verifies proper TCR gene rearrangement and is known as β–selection. It requires the thymocytes to signal through a pre-TCR consisting of a properly rearranged TCRβ chain, pre-TCRα chain, CD3 complex and ζ chain (Carpenter and Bosselut, 2010).

The assembly of the pre-TCR complex signals allelic exclusion of the *TCRβ* locus, proliferation and down-regulation of CD25 expression so that cells enter the DN4 stage ($CD44^{-}CD25^{-}$) and differentiation into $CD4^{+}$ $CD8^{+}$ double positive (DP) thymocytes. Inability of pre-TCR complex to associate with CD3ζ chain halts the development at DN3 stage, so thymocytes with out-of-frame TCRβ rearrangements

do not receive survival signals and undergo apoptosis (Malissen and Malissen, 1996). In addition, any defects in the *Rag1, Rag2* genes causing failure in rearrangement of β chain, or defects in pre-*TCRα, TCRβ, CD3ζ* and *CD3ε* genes, causes the results in absence of DP thymocytes which are blocked in the DN3 stage (Fehling et al., 1995; Malissen et al., 1995; Mombaerts et al., 1992; Shinkai et al., 1992).

In the DP stage thymocytes stop proliferating and down-regulate the expression of IL7R (CD127). The *Tcrb* locus, encoding TCRβ proteins becomes inaccessible and the accumulation of RAG1 and RAG2 proteins initiates rearrangement of the *Tcra* locus, encoding the TCRα chain, resulting in the surface expression of the TCRαβ complex (Germain, 2002). DP thymocytes undergo positive selection and CD4/CD8 lineage determination within the cortex. Nearly ~90% of double positive thymocytes express TCRs that interact so weakly with available self-peptide MHC that signals required to sustain viability are not generated resulting in cell death (Huesmann et al., 1991). Thymocytes with TCRs with intermediate affinity for self-peptide MHC receive survival signals and are positively selected (Starr et al., 2003). By contrast, thymocytes expressing TCRs with high affinity for self-peptide MHC complex are induced to undergo either clonal deletion or inactivation in the medulla.

DP thymocytes that survive positive selection within the cortex undergo CD4/CD8 lineage commitment to differentiate into either $CD4^+$ or $CD8^+$ single positive (SP) cells in the medulla. Interaction of the DP thymocytes with cTECs, upregulates the expression of C-C chemokine receptor, (CCR7) and receptor activator of nuclear factor kappa- B ligand (RANKL). These DP thymocytes follow the signals emanating from mTECs (ligands for CCR7 - CCL19 and CCL21 and the receptor for RANKL, RANK) and migrate into the medulla (Anderson and Takahama, 2012; Petrie and Zuniga-Pflucker, 2007). It is in medulla, that negative selection takes place, removing SP thymocytes with autoreactive TCRs from the repertoire and establishing central tolerance.

1.4.2 Central Tolerance

The downside of generation of diverse repertoire of T and B cells by random recombination events during development in the thymus and bone marrow is the production of a large number of self-reactive TCRs and BCRs, respectively. Central tolerance is the process that works to eliminate the autoreactive T and the B cells. Indeed, many self-reactive clones are eliminated efficiently in the thymus and clonal deletion plays a central role in immunological tolerance (Hogquist et al., 2005). Other mechanisms of tolerance induction such as anergy (Schwartz, 2003) and receptor editing (McGargill et al., 2000) have been described, however they contribute less significantly than clonal deletion.

Central tolerance is achieved by the deletion of autoreactive thymocytes through negative selection and is critically dependent on the interaction of thymocytes with other cells in the thymic microenvironment. The medulla is enriched with two types of antigen presenting cells – mTECs and DCs both of which are crucial for negative selection (Anderson and Takahama, 2012). The medullary TECs are known sites of promiscuous gene expression and are therefore capable of expressing a large diversity of "tissue specific antigen" (TSA) that represent antigens expressed outside the thymus (Palmer, 2003). The expression of these TSAs are driven by a transcription factor known as autoimmune regulator (AIRE) that is selectively expressed by the mTECs thus enabling the negative selection of tissue-specific autoreactive T cells in the medulla (Anderson et al., 2002). The critical role of AIRE in tolerance induction is illustrated by the multi-organ autoimmunity developing in patients and mice deficient for AIRE (Anderson et al., 2002; Peterson et al., 1998). The autoimmune disease observed in various mouse strains that have impaired medullary characteristics further elucidates the importance of the medullary architecture for establishing central tolerance: REL-B deficient mice, Nik^{aly}/Nik^{aly}, which carry the alymphoplasia mutation in Nik (nuclear factor-κB (NF-κB)-inducing kinase); lymphotoxin-β receptor (LT-βR)- deficient mice and tumor necrosis factor (TNF)-receptor-associated factor-6 (TRAF-6)-deficient mice. All of these mutant mouse strains show reduced levels of AIRE, which promotes the expression of peripheral tissue-specific antigens by mTECs (Hogquist et al., 2005).

In addition to mTECs, the majority of thymic DCs are resident in the medulla and have an important role in central tolerance as they can cross-present antigens that are synthesized by mTECs and inducing the apoptosis of self-reactive thymocytes (Gallegos and Bevan, 2004). mTECs might also contribute to central tolerance through their regulated expression of co-stimulatory molecules such as CD40, CD80 (B7-1) and CD86 (B7-2) (Hogquist et al., 2005).

The thymic architecture spatially separates positive (cortex) and negative selection (medulla) events during thymocyte development, however a key question for understanding clonal deletion is how a DP thymocyte can discriminate between various peptide-MHC ligands and initiate distinct positive and negative selection signals. The strength of interaction between the TCR and pMHC complexes expressed by the TECs is a crucial parameter of selection; with thymocytes that recognise self-peptide MHC with low affinity undergo positive selection, whereas those with high affinity undergo negative selection (Starr et al., 2003). There are currently two proposed mechanisms of how a developing thymocyte might make the distinction between low and high affinity signals. First is a "zipper" model, which suggests that low and high affinity interactions trigger qualitatively different responses, (Palmer and Naeher, 2009). It is based on the observation that a single pMHC complex can engage and activate multiple TCRs over time and by increasing the number of TCR interactions, serial triggering leads to multiplication of pMHC induced TCR signals (Rachmilewitz and Lanzavecchia, 2002; Valitutti et al., 1995). The model posits that a high-affinity TCR-pMHC complex induces a stable "zippering" between the membrane proximal domains of CD8 α and β TCR chains, which causes stronger signal transduction leading to negative selection. Conversely a low-affinity interaction leads to incomplete zippering and partial phosphorylation of CD3 immunoreceptor tyrosine-based activation motif (ITAM), consequently triggering positive selection (Palmer and Naeher, 2009).

The second model is the kinetic proof reading model of T cell activation, which takes into account the dwell time of pMHC complex binding with the TCR (McKeithan, 1995). This model proposes that a high-affinity pMHC would occupy the TCR for a longer time (slower off-rate) and have a longer half-life providing sufficient time for

the formation of fully activated TCR-CD3 complexes while a low-affinity pMHC would have a faster off-rate and a shorter half-life resulting in partial activation of TCR-CD3 complexes (Kalergis et al., 2001; Kersh et al., 1998; Savage and Davis, 2001). Support for this model comes from surface plasmon resonance studies that show that high-affinity pMHC ligands occupy the TCR for a longer period of time with slower-off rates (Alam et al., 1996). In terms of signal transduction, low-affinity ligands would induce a set of early TCR signals, whereas the high-affinity ligands would induce both early and late TCR signals (Palmer, 2003).

Differential activation of signalling pathways has been shown to direct the fate of developing thymocytes. One signalling pathway proposed to be involved in positive versus negative selection is the extracellular signal regulated kinase (ERK) belonging to mitogen activated protein kinase (MAPK) pathway. Low affinity-pMHC (positive selecting) ligands induce ERK activation more slowly and over long sustained periods of time resulting in positive selection. Whereas the high-affinity negative selecting ligands induce a rapid and robust ERK activation, which is associated with death (Mariathasan et al., 2001; McNeil et al., 2005). Additionally the cellular localisation of ERK is influenced by signal strength and determines the positive and negative selection in thymocytes, with strong signals recruiting ERK to the plasma membrane while weak positively selecting signals recruiting ERK to the Golgi complex (Daniels et al., 2006). Another key T cell specific protein, called thymocyte expressed molecule involved in selection (THEMIS), seems to be involved in determining the strength and kinetics of Ca^{2+} influx and phosphorylation of ERK (Fu et al., 2009). This facilitates TCR recognition of very fine differences in affinities (analogue input) and converts it into clear-cut selection outcome (digital output).

Finally, changes in gene expression induced by high-affinity interaction are also known to be important in cells undergoing clonal deletion. Two genes that are consistently upregulated are Nur77 and Bim, which are important in inducing self-reactive thymocytes to apoptose (Baldwin and Hogquist, 2007).

1.4.3 Peripheral Tolerance

Negative selection in the thymus does not eliminate all self-reactive lymphocytes, in part because not all self-antigens are expressed in the thymus. This holds true for epitopes recognized by T cells causing EAE, MS or T1D, where the limited availability of these epitopes in thymus results in incomplete negative selection, such that the escaping T cell clones can be activated in the periphery where these antigens are more abundant (von Boehmer and Melchers, 2010). In addition, autoreactive T cells escape negative selection in the thymus when their TCR avidity for self-pMHC is sufficiently low (Liu et al., 1995; Zehn and Bevan, 2006). Therefore, peripheral tolerance mechanisms act to control the activation of potentially self-reactive mature T cells to prevent them from causing autoimmunity.

One of the principle regulatory mechanisms in maintenance of peripheral immune tolerance is mediated by regulatory T cells, which express Foxp3 and suppress immune responses through numerous mechanisms, including production of anti-inflammatory cytokines, direct cell-cell contact and by modulating the activation state and function of APCs (Sakaguchi et al., 2008; Vignali et al., 2008). The development and function of Tregs is dependent on the activity of Foxp3. Induced knockout or spontaneous mutation of mouse Foxp3 gene (Scurfy mice) led to a systemic autoimmune disease associated with absence of Tregs (Fontenot et al., 2003; Hori et al., 2003; Khattri et al., 2003). Similarly, mutations in the human Foxp3 gene cause immunodysregulation, polyendocrinopathy, enteropathy X-linked syndrome (IPEX) a fatal disorder known to share several features with common scurfy mice. In addition, to high constitutive expression of IL-2 receptor alpha chain (CD25) Tregs are positive for CTLA4 and GITR and express low levels of the IL-7 receptor alpha chain (CD127) (Shevach, 2009). Tregs are generated in the thymus by intermediate affinity interaction with agonist ligands therefore recognition of self-reactive TCR ligands is a key event initiating Treg development (Itoh et al., 1999; Jordan et al., 2001). Besides TCR signal strength, costimulation signals mediated by CD28 and IL-2 are required for survival of Tregs (Hsieh et al., 2012). Both *in vitro* and *in vivo* studies have shown the importance and ability of cytokine TGFβ in

converting mature T cells to the Treg lineage in the peripheral lymphoid organs (Apostolou and von Boehmer, 2004).

Ignorance is one of the simplest mechanisms of peripheral tolerance mechanism, wherein low-affinity self-reactive T cells ignore self-antigen in the periphery either because the self-antigens are sequestered in sites that are not easily accessible 'immune privileged sites' e.g. the physical blood-brain or because they are not present in sufficient quantities to overcome a threshold and trigger a T cell response (de Souza et al., 2010). Alternatively, encounters of T cells with self-antigens in the absence of co-stimulatory signals, might lead to a state of long-term hyporesponsiveness or functional inactivation called anergy that is characterised by an active repression of TCR signalling and IL-2 expression (Schwartz, 2003).

Co-stimulatory pathways provide the secondary signal crucial for T cell activation and is achieved mainly by the interaction of the CD28 molecules on T cells and the B7 molecule family (CD80 and CD86) present on the surface of APCs (de Souza et al., 2010). Besides promoting T cell activation, co-stimulatory pathways can also provide negative signals that inhibit T cell responses. Two key molecules that are upregulated in anergic cells are programmed death 1 receptor (PD-1), its ligand PD-L1 and cytotoxic T-lymphocyte-associated protein 4 **(**CTLA4). Evidence that PD-1 plays a critical role in control of self-reactivity is demonstrated by development of lupus-like autoimmune disease in mice lacking PD-1 (*Pdcd-1*$^{-/-}$), which develop lupus-like autoimmune disease (Nishimura et al., 1999). CTLA4 is a CD28 homologue with inhibitory function (Krummel and Allison, 1995; Walunas et al., 1996). *Ctla4*$^{-/-}$ mice show lethal lymphoproliferative disorder (Tivol et al., 1995), in addition CTLA4-deficient CD4^{+} T cells are resistant to anergy induction *in vivo* (Perez et al., 1997).

Another effective mechanism of peripheral tolerance is deletion of autoreactive T cells by activation induced cell death (AICD). Two apoptotic pathways exist in mammals – a cell intrinsic and a cell extrinsic pathway, which converge when the caspase cascade is activated (Leavy, 2008). The cell extrinsic pathway is induced by engagement of the Fas receptor (CD95) by FasL (CD178) and induction of Bim-

dependent triggering of a Bcl-2 and Bcl-xL regulated mitochondrial death pathway (Marrack and Kappler, 2004). Mice that carry mutations in Fas (Fas-deficient *lpr* or *lpr*^{cg} mice or FasL-deficient *gld* mice) are not able to engage the AICD pathway develop progressive lymphadenopathy and splenomegaly (Cohen and Eisenberg, 1991). Defects in the Fas pathway in humans are also associated with autoimmune lymphoproliferative syndrome (de Souza et al., 2010). Initiation of the cell-intrinsic pathway involves the activation of pro-apoptotic B-cell lymphoma 2 (Bcl-2)-family members such as Bcl-2-interacting mediator of cell death (Bim). Mice deficient for Bim are also resistant to apoptosis, and with age these mice spontaneously develop immune complex-mediated glomerulonephritis (Bouillet et al., 1999). In contrast to AICD, the killing of the antigen-activated T cells during down-regulation of an immune response to an acute infection requires Bim and not Fas (Bouillet et al., 2002).

1.4.4 Autoimmunity

When mechanisms of self-tolerance fail autoimmunity ensues and the subsequent malfunction of the immune system resulting in inflammation and tissue destruction causes autoimmune disease. Autoimmunity is thought to result from a combination of genetic variants and acquired environmental triggers such as infections (Rioux and Abbas, 2005). Classic examples include type 1 diabetes, a chronic polygenic disease in which the pancreatic β-cells (which produce insulin) are selectively destroyed by autoreactive $CD8^+$ T cells and innate immune cells (Lehuen et al., 2010) and rheumatoid arthritis resulting from the uncontrolled inflammation of synovial joints driven by a dysregulation of Th1 immune response (Burmester et al., 2014).

The environmental triggers for autoimmune diseases act in the presence of genetic predisposition to the disease. Many studies implicate infection as a trigger for developing autoimmune diseases mainly, as it can readily disrupt peripheral tolerance by exposure of self to the immune system through breakdown of immune system barriers (Javierre et al., 2011). In addition, there is the alternative, or perhaps complementary, process of molecular (antigenic) mimicry, whereby an antigen of a microorganism or a constituent of food that sufficiently resembles a self-molecule

can induce a cross-reactive autoimmune response (Kindt et al., 2007). This is highlighted by the detection of serum autoantibodies that also recognise pathogenic epitopes, for example the anti-SM autoantibodies obtained from SLE patients are also reactive with the EBNA-1 epitope of Epstein Barr virus (Javierre et al., 2011).

Genetic susceptibility has a major role in autoimmunity. Genome wide association studies have identified polymorphisms in over 200 bona fide loci, which contribute to autoimmune diseases and many of which are common to different autoimmune diseases (Cho and Gregersen, 2011). These include genes encoding molecules of MHC complex, TCR and BCR, and those important in maintenance of peripheral tolerance and apoptosis such as Bim.

1.5 T Cell Receptor Signal Transduction

T cells are central players in the adaptive immune system and effective adaptive immunity relies critically on the antigen specific activation of naive resting lymphocytes. T cells are activated by ligation of a clonotypic T cell receptor with antigenic peptide bound to MHC molecules presented on the surface of antigen presenting cells. This interaction originates with engagement of the TCR at the immunological synapse, which further triggers, several signal transduction pathways that involve protein kinases, protein phosphatases, adapter proteins, second messengers and key intermediates (Mustelin and Tasken, 2003).

The first signalling molecules that are activated following TCR ligation feed into radiating and intricately branched network of signalling cascades that culminates with the induction of gene transcription, which then initiates a diverse array of developmental and functional events such as differentiation, proliferation and cytokine production that are optimally tailored to provide an appropriate immune response. In addition, the selection, survival and proper development of T cells also depend on signals emanating from the TCR.

The complex signalling cascade resulting in T cell activation can be conveniently divided into signal initiation, propagation and diversification, each of which involves

a separate yet interconnected module of signalling molecules that are regulated to fine-tune the TCR response.

1.5.1 TCR Signal Initiation

The TCR complex consists of the TCRαβ (or TCRγδ) heterodimer plus three pairs of the invariant signalling protein CD3 subunits (CD3ε-CD3γ, CD3ε-CD3δ and CD3ζ-CD3ζ) (Wucherpfennig et al., 2010). T cell signalling is initiated by engagement of the TCR-CD3 complex with the processed antigenic peptide bound to MHC molecules on the surface of antigen presenting cells. The TCR-CD3 complex lacks intrinsic enzymatic activity and relies on the recruitment and activation of the Src family of protein kinases (SFKs): Lck (p56-Lck) and (p59-Fyn) (Palacios and Weiss, 2004; Salmond et al., 2009) which bind the cytoplasmic domains of the TCR co-receptors CD4 and CD8 (Veillette et al., 1988). SFKs are important for providing tonic survival TCR signals in naïve T cells (Seddon and Zamoyska, 2002). Approximately 40% of Lck is constitutively active in naïve cells that maintain a basal state of phosphorylation of TCR associated CD3ζ chains (Nika et al., 2010; Stefanova et al., 2002). The activity of Lck is tightly regulated by the phosphorylation states of two tyrosine (Tyr) residues – the inhibitory residue Tyr^{505} in the C-terminal domain and the activating Tyr^{394} residue in the catalytic domain. Phosphorylation of Tyr^{505} residue by C-terminal tyrosine Src kinase (Csk) stabilises an inactive closed conformation of Lck. The complete kinase activity of Lck is achieved by relieving the closed inactive form; by dephosphorylation of the Tyr^{505} residue by the phosphatase, CD45 and the auto-phosphorylation of Tyr^{394} residue, which stabilises the active open confirmation **(Fig 1.3 insert)**. The activating tyrosine residue is dephosphorylated by several phosphatases including CD45 and the cytosolic phosphatases PTPN6 and PTPN22.

Once activated, Lck phosphorylates the immunoreceptor tyrosine based activation motifs (ITAMs) present on the cytoplasmic domain of the CD3 subunits. These phosphorylated ITAMs provide docking sites for the recruitment of zeta-associated protein kinase of 70 kDa (ZAP-70) via its tandem Src homology-2 (SH2) domains (Chan et al., 1992). The binding of ZAP-70 molecules to the ITAMs unlocks ZAP-70

from its inactive configuration (Deindl et al., 2007), allowing it to be auto-phosphorylated and activated by phosphorylation at the Tyr^{493} residue by Lck. This promotes its kinase activity and results in further downstream phosphorylation of its target substrates, that including the key adaptor molecule, linker for activation of T cells (LAT) (Smith-Garvin et al., 2009).

1.5.2 TCR Signal Propagation

The presence of 10 ITAMs in the TCR complex, allows up to 10 ZAP-70 molecules to cluster to the TCR-CD3 complex. Two adapter molecules, LAT and SH2 domain containing leukocyte phosphoprotein of 76-kDa (SLP-76), comprise the important first targets of ZAP-70 in this multi molecular complex and form the focal point for integration and activation of multiple signalling pathways (Acuto et al., 2008). Both LAT and SLP-76 are crucial for TCR signalling as loss of either LAT or SLP-76 results in complete loss of TCR signal transduction (Smith-Garvin et al., 2009). The cytosolic tail of LAT contains nine conserved tyrosine residues (Sommers et al., 2004), which upon phosphorylation following TCR engagement binds SH2 domain containing proteins, including phospholipase C gamma (PLC-γ), phosphoionositide 3-kinase (PI3K), the adapters Grb2 and Grb2-related adapter downstream of Shc (Gads) (Smith-Garvin et al., 2009). SLP-76 is recruited to the LAT through its constitutive interaction with Gads. The complex of LAT-Gads-SLP76 complex forms LAT signalosome (Malissen et al., 2005) **(Fig 1.3)** and is responsible for the recruitment of several other signalling molecules such as PLC-γ, the adaptors Gads2, Nck and ADAP (adhesion and degranulation promoting adaptor protein), the Rho family GTPase exchange factor Vav, IL-2 induced tyrosine kinase (Itk) and hematopoietic progenitor kinase 1 (HPK1) (Koretzky et al., 2006; Smith-Garvin et al., 2009).

The cooperative binding of LAT and SLP-76 serve to precisely nucleate a large effector complex, which result in the activation of PLC-γ by Itk-mediated phosphorylation. Activated PLC-γ hydrolyses and cleaves the membrane lipid, phosphatidylinositol 4,5-bisphosphate (PIP_2) producing the second messenger inositol 1, 4, 5 – triphosphate (IP_3) and diacylglycerol (DAG) **(Fig 1.3)**.

PLC-γ mediated IP_3 production stimulates the Ca^{2+} permeable ion channel receptors IP_3R on the ER membrane to release Ca^{2+} from intracellular storage reserves into the cytoplasm. On depletion of the ER Ca^{2+} reserves, there is a sustained influx of extracellular Ca^{2+} by the 'store operated' mechanism of Ca^{2+} entry through the CRAC channels in the plasma membrane (Oh-hora and Rao, 2008). Increase in the intracellular levels of Ca^{2+} due to sequential release from the internal and external reserves acts as an important trigger for activation of transcriptional factors and signalling proteins such as calcineurin and Ca^{2+} calmodulin dependant kinase (CaMK) (Smith-Garvin et al., 2009). Ca^{2+} activates calcineurin that dephosphorylates the nuclear factor of activated T cells (NFAT), this results in its translocation to the nucleus where it complexes with activator protein (AP-1) that results in the production of IL-2 (Rao et al., 1997; Smith-Garvin et al., 2009).

TCR induced production of DAG results in the activation of two major signalling pathways involving Ras and Protein Kinase C (PKCθ). Ras, a small G protein activated by GTP, is required for the activation of the serine threonine kinase Raf-1 that initiates a cascade of protein kinases known as the mitogen activated protein kinase (MAP Kinase) pathway. Phosphorylation of the end product of this pathway MAP kinase (ERK-1 and ERK-2) allows it to activate Elk, a transcription factor necessary for the activation of Fos. Phosphorylated Fos associates with Jun and together they are known as AP1, which is an essential transcription factor for T cell activation (Genot and Cantrell, 2000).

The other signalling pathway regulated by DAG is PKCθ, a PKC family member with specific lipid binding domain for DAG. PKCθ is implicated in the regulation and activation of crucial transcription factor nuclear factor kappa B (NF-kB). TCR stimulation leads to the assembly of a trimolecular membrane bound complex of proteins that include CARMA1, BCL-10 and MALT1. This complex, once assembled drives the activation of IKK (inhibitor of κB kinase). a multiprotein enzyme which phosphorylates the inhibitor of κB, (IκB). In resting cells, IκB bound NF-κB is retained it in the cytosol. IKK mediated phosphorylation of IκB, releases NF-κB which migrates to the nucleus, where it activates genes involved in the function, survival and homeostasis of T cells (Hayden and Ghosh, 2011).

1.5.3 TCR Signal Diversification

Antigen stimulation of T cells induces their strong adhesion to the APCs. This adhesion is mediated mainly by activation of surface integrin molecules on T cells. The major integrins expressed by T cell surface are leukocyte function associated antigen-1 (LFA-1) and very late antigen (VLA-4), which bind their respective ligands: intracellular adhesion molecules (ICAM-1) and vascular cellular adhesion molecule (VCAM), and fibronectin on other immune cells, endothelial cells, fibroblasts and extracellular matrix proteins. TCR mediated signalling results in conformational change of the integrins which increases their affinity for their ligands triggering 'inside-out' signals from TCR to integrins (Menasche et al., 2007).

The signals that regulate integrin activation following TCR stimulation are still unclear, however the small GTPase Ras-proximity-1 (Rap1) is thought to be an important player, by increasing TCR induced adhesion to ICAM-1 (Katagiri et al., 2003; Sebzda et al., 2002). In addition, some elements of the LAT signalosome are also known to be critical for the inside out signalling and include the cytosolic adaptor ADAP that constitutively associates with another adapter protein, Src kinase-associated phosphoprotein of 55 kDa (SKAP-55). Both of which interact with SLP-76 in the signalosome. The ADAP/SKAP-55 complex recruits RAP-1 via a third adapter, Rap1-GTP interacting adapter molecule (RIAM). This is constitutively bound to SKAP-55 and associates with activated RAP-1 upon TCR ligation, resulting in the localisation of RAP-1 to the membrane (Smith-Garvin et al., 2009). Activated RAP-1 is also known to associate with the regulator of cell adhesion and polarisation enriched in lymphoid tissues (RAPL), which is localised in the membrane and binds to LFA-1(Katagiri et al., 2003).

This model of ADAP/SKAP-55 mediated activation of RAP1 initiated LFA-1 signalling is a major pathway of integrin activation in many T cell subsets, however an alterative route of LFA-1 activation by Tregs has been reported. Using a knock-in mouse containing a point mutation in the kinase domain of ZAP-70 (ZAP-70AS), Au-Yueng *et al.* showed that the kinase activity of ZAP-70 could be selectively inhibited in *in vitro* cultured ZAP-70AS T cells by a specific small molecule

inhibitor (Au-Yeung et al., 2010). 70AS). They further showed that inhibition of ZAP-70 kinase activity in peripheral T cells abrogated the activation and effector function of T cell subsets, but interestingly had no effect on GTP-bound RAP-1 activity of the Treg subset (Au-Yeung et al., 2010). Recruitment of kinase dependent SLP-76- VAV1/ADAP to LAT does not occur in the absence of phosphorylation of tyrosine residues on LAT, however ZAP-70 itself can act as an adaptor molecule for 'inside-out' signalling. Therefore, signals initiated from the TCR can diversify either through the generation of LAT signalosome or through the associated adaptor function of ZAP-70 kinase.

1.5.4 Regulation of TCR signalling

As outlined above, signals through the TCR are driven by an array of biochemical events that ultimate lead to activation of multiple effector pathways. Activation of T cells is actively regulated both positively and negatively to allow the signals to be controlled and halted and to ensure an appropriate response. The negative regulation of TCR signalling is mediated both through by regulating the pathways and the different molecules involved in the signalling cascade and include inhibitory membrane-bound receptors such as CTLA4, PD1 and CD5 which recruit tyrosine phosphatases (Acuto et al., 2008). The importance of these receptors in TCR signalling is underscored by the observation that deficiency of PD1 and CTLA4 results in lupus like disease and lymphoproliferative disease in humans and mice respectively (Nishimura et al., 1999; Tivol et al., 1995). Even though CD5 deficiency does not cause any immune disorders, the mice display altered T cell development (Tarakhovsky et al., 1995). In addition, no overt phenotype is seen in mice lacking inhibitory membrane scaffold proteins such as phosphoprotein associated glycosphingolipid-enriched microdomains (PAG) and Lck-interacting membrane protein (LIME) despite their pivotal role in recruiting kinases and phosphatases to the immunological synapse, suggesting there are multiple mechanisms that compensate for the loss of these molecules (Acuto et al., 2008).

One of the most critical and actively regulated module of TCR signalling event is the SFK component, Lck. Opposing actions of Csk and CD45, either phosphorylates or

dephosphorylates the inhibitory Tyr^{505} residue resulting in inactive or active forms of Lck (Veillette et al., 2002). In addition, the activity of Lck is also regulated by dephosphorylation of the activating Tyr^{394} residue by cytoplasmic phosphatase PTPN22, which is recruited to the plasma membrane via its association with Csk (Cloutier and Veillette, 1996, 1999). Furthermore, fine-tuning of the TCR signals to distinguish between strong and weak ligands occur by dephosphorylation of the active site of Lck by another phosphatase, SHP-1 in the presence of weak antagonist signals (Stefanova et al., 2003). Conversely, in the presence of strong agonist TCR signals, ERK is rapidly activated and phosphorylates Ser59, which prevents the SHP-1 binding, thus keeping Lck active to sustain TCR signals and further amplify ERK activity (Stefanova et al., 2003).

The activity of SFK within the lipid rafts may be regulated by the transmembrane adapter molecule PAG. In resting T cells, Csk is localised to the lipid rafts by interaction of its SH2 domain with constitutively phosphorylated PAG tyrosine residues Tyr^{314}/ Tyr^{317} (in mice and humans respectively) (Brdicka et al., 2000). The association of PAG with Csk enables Csk to modify both Lck and Fyn in resting cells by phosphorylating the negative regulatory tyrosine residues, promoting a closed conformation. Upon TCR ligation Fyn phosphorylates PAG at the Tyr^{314} residue (Filby et al., 2007; Yasuda et al., 2002), which releases Csk and results in its loss from the lipid rafts (Davidson et al., 2007). Of note, PAG association with Csk is probably not the the only mechanism by which Csk gets to the membrane, as $PAG^{-/-}$ mice do not show any T cell phenotype and Csk was independently recruited to the plasma membrane (Dobenecker et al., 2005; Xu et al., 2005).

Adaptor proteins, Dok-1 and Dok-2 have been reported to be involved in attenuating the TCR signalling (Yasuda et al., 2007). Dok can associate with several negative regulators including SHP-1, Csk and RasGAP (Dong et al., 2006). Recently Schoenborn et al. described a potential interaction between Dok1 and Csk that may contribute to negative regulation of Lck activity in response to TCR ligation (Schoenborn et al., 2011). Consistent with their role in negatively regulating TCR, $Dok1^{-/-}$ $Dok2^{-/-}$ mice have increased TCR induced IL-2 production and proliferation with prolonged phosphorylation of ZAP-70, LAT, SLP-76 and Akt. Furthermore,

these mice develop a lupus-like renal disease with high anti-double stranded DNA antibody titers (Dong et al., 2006; Yasuda et al., 2007).

In addition to regulating the early/proximal signalling mechanism, downstream adaptor SLP-76 can also be a target of negative regulation. The serine/threonine kinase HPK1 upon Lck-mediated activation inducibly binds the SH2 domain of SLP-76 and phosphorylates a serine residue; Ser^{376}. This mediates recruitment of the 14-3-3 family of ubiquitously expressed regulatory proteins (Di Bartolo et al., 2007). Recruitment and HPK1 mediated phosphorylation of SLP-76 occurs 10-15 minutes post TCR stimulation and lasts up to an hour (Di Bartolo et al., 2007) suggesting a late time point in regulation of the TCR signalling cascade. In support of its role as a negative regulator, HPK-1 deficiency results in enhanced TCR-dependent tyrosine phosphorylation of SLP-76, PLCγ, LAT, Vav1 and ZAP-70, leading to development of a severe form of EAE in mice (Shui et al., 2007).

Besides phosphorylation, early T cell receptor responses are also modulated by ubiquitin ligases of Casitas B-lineage lymphoma family (CBL) through degradation of components of the TCR signalling machinery, including CD3ζ, ZAP-70, PLCγ, phosphoinositide 3-kinase (PI3K) and PKCθ (Loeser and Penninger, 2007). The Cbl family of proteins comprising of c-Cbl and Cbl-b, are ubiquitously expressed in hematopoietic cells and contain a ring finger domain through which they interact with E2 ubiquitin ligases (Thien and Langdon, 2001). c-Cbl is highly phosphorylated upon TCR stimulation. It is recruited to the TCR-CD3 complex through its interaction with src-like adaptor protein SLAP in T cells. In addition c-Cbl can associate via its SH2 domain with tyrosine phosphorylated Lck, Fyn, ZAP-70 and LAT leading to their ubiquitylation (Janssen and Zhang, 2003). c-$Cbl^{-/-}$ mice have increased thymocyte numbers, with DP cells being hyper-responsive to stimuli, demonstrating increased phosphorylation of CD3, TCRβ, Lck and Fyn (Murphy et al., 1998). Furthermore, in mice deficient in c-Cbl there is increased expression of TCR, CD3, CD4, CD5 and CD69 (Murphy et al., 1998; Naramura et al., 2002). In agreement with its role in negative regulation of TCR signals, overexpression of c-Cbl in Jurkat T cells leads to the inhibition of the transcription factors AP1 and NFAT (Rellahan et al., 2003).

1.6 Phosphatases

Protein phosphorylation is a widely used in post-translational modification and is a fundamental part of cellular information processing regulating numerous physiological functions, including immune defences. The human genome encodes at least 518 protein kinases (PTKs) of which 90 are specific for phosphorylation of tyrosine residues (Mustelin et al., 2004). Protein tyrosine phosphatases (PTPases) are enzymes that remove the phosphates from the Tyr substrates. A dynamic balance between tyrosine phosphorylation and dephosphorylation is crucial for the maintenance of homeostasis and proper regulation of the immune system. Aberrations in phosphorylation can have profound consequences, such as dysregulation in apoptosis or cell cycling, and the onset of malignancies. Protein tyrosine phosphatases play a crucial role in keeping T cells in a resting state in the absence of antigens as well as reversion of activated T cells back to the resting phenotype upon removal of the activating stimulus (Mustelin et al., 2004).

Based on their structure and specificities of target substrates human PTPases can be divided into four major subfamilies; class I, class II, class III which all use cysteine as a nucleophile for catalysis and class IV PTPs which use aspartic acid as a nucleophile (Alonso et al., 2004). Class I PTPases represent the largest sub-family containing 99 members, further subdivided into 38 well known “classical” tyrosine specific which have mouse homologues and 61 “dual specific” PTPases (DSPs) which have diverse substrate specificities (Andersen et al., 2004). The classical PTPs can be further divided into non-receptor (NRPTPs), intracellular PTPs that contain a single catalytic domain and various amino- or carboxy- terminal domains. Examples include SHP1, SHP2 and the PEST family of phosphatases including PTPN22 and the transmembrane receptor like PTPs (RPTPs). The latter generally have an extracellular, putative ligand binding domain, a single transmembrane region and one or two cytoplasmic PTP domains and include CD45 and CD148 phosphatases (Andersen et al., 2004).

The DSPs which also belong to class I phosphatase contain VH1-like phosphatases (as the first DSP cloned was the VH1 protein from *Vaccinia* virus) that have very

diverse specificities such as: phospho-tyrosine and phospho-threonine for MAP kinase phosphatases (MKPs): phospho-inositides in the case of PTEN (Alonso et al., 2004). Class II phosphatases contain only one member, the low molecular weight PTP (LMPTP) that consists of a single-phosphatase domain. Class III phosphatases have 3 members, CDC25A, CDC25B and CDC25C. These cysteine based PTPs dephosphorylate inhibitory tyrosines on CDKs to initiate progression of cells through the cell cycle (Honda et al., 1993). The last group, class IV PTPs use aspartate – based mechanisms for catalysis and has 4 members known as EyA but their biological function remains unknown (Tootle et al., 2003).

1.7 Phosphatases in autoimmunity

Protein tyrosine phosphatases (PTPs) act in a coordinated manner with protein tyrosine kinases to control cell signalling thereby regulating various physiological processes (Tonks, 2006). Both receptor-type and non-receptor type PTPs have been implicated in TCR mediated signal transduction. Some positively regulate lymphocyte activation and development (CD45 and CD148), whereas others inhibit these processes (SHP1, PTPN2, PTPN22, PTP-PEST). Alteration of the expression or activity of PTPs involved in TCR signal regulation has been shown to cause immunopathology in mice and recent genome wide association studies have identified a large number of single nucleotide polymorphisms in PTPs that are linked to several human autoimmune diseases (Consortium, 2007; Todd et al., 2007). These studies highlighted the link between dysfunctional regulation of phosphorylation and disease, underscoring the need to elucidate the underlying regulatory mechanisms controlled by phosphatases.

CD45 *(PTPRC)*

Protein Tyrosine Phosphatase receptor Type C (PTPRC), also known, as CD45 is a large 180 - 220 kDa receptor type PTP encoded by the *PTPRC* gene, which is abundantly expressed in all hematopoietic cells except red cells and exists in different functional isoforms {reviewed in (Hermiston et al., 2003; Vang et al., 2008)}. Structurally, CD45 comprises of an N terminal extracellular domain of

variable length, followed by fibronectin-type repeats, a transmembrane segment and a cytoplasmic tail containing 2 consecutive PTP domains, of which only membrane proximal domain is functionally active and is capable of auto-inhibition by homodimerasation (Xu and Weiss, 2002). CD45 positively regulates T cell activation by dephosphorylating the inhibitory tyrosine residues of SFKs Lck and Fyn (Tyr^{505} in Lck and Tyr^{528} in Fyn) (Ostergaard et al., 1989). CD45 is an important regulator of signal transduction via the TCR complex at multiple stages of T cell development, evident from the studies demonstrating that CD45 deficient mice have few peripheral T cells owing to impaired thymic development (Byth et al., 1996; Kishihara et al., 1993). Similar to its role in T cells, CD45 dephosphorylates the C terminal tyrosine of Lyn in B cells however their activation is only partially compromised in CD45-deficient mice (Katagiri et al., 1999).

Some studies also implicate a negative role for CD45. Where it is responsible for dephosphorylating the positive regulatory site on Lck (Tyr^{394}) thus leading to Lck inactivation (Mustelin et al., 1989). Given the ability of CD45 to dephosphorylate the activatory and inhibitory tyrosine of SFKs, these two functions need to be differentially regulated in cells. It is possible that phosphorylation state of Lck dictates the action of CD45 resulting in the dephosphorylation of the activating or inhibitory tyrosine residue. It is thought that CD45 is temporally sequestered from the vicinity of Lck once it is activated, so that it cannot be inactivated. In keeping with this idea, several studies show that CD45 is transiently present in the lipid rafts, sufficient to activate Lck, but is excluded from the immune synapse upon activation (Edmonds and Ostergaard, 2002; Freiberg et al., 2002; Penninger et al., 2001). In addition to directly modulating Lck and Fyn, CD45 also dephosphorylates PAG at Y314, inhibiting Csk recruitment from the cytosol, which in turn phosphorylates the inhibitory Tyr^{505} residue on Lck downregulating its function in activated T cells (Davidson et al., 1997).

In accordance with the function of CD45 in promoting cell activation, the nucleotide polymorphism C77G in the gene encoding CD45 gene that results in impaired dimerization of CD45 has been found at greater frequency in a cohort of patients with multiple sclerosis and autoimmune hepatitis than in healthy controls (Jacobsen

et al., 2000). Though a subsequent study was unable to replicate these results (Barcellos et al., 2001). Therefore evidence from studies in both mouse and human studies highlight the importance of CD45 in regulation of the immune system and its perturbation maybe linked to autoimmunity.

CD148 *(PTPRJ)*

Similar to CD45, CD148 is a receptor-type PTP encoded by *PTPRJ*, however it is distinguished from CD45 in possessing an extracellular domain containing five fibronectin-type repeats and only a single PTP domain. Although in humans CD148 is expressed in both B and T cells, in mouse high expression is only seen in B cells and not in T cells (Hermiston et al., 2009). Mice lacking CD148 show partially blocked B cell development and decreased B cell activation due to increased phosphorylation of the inhibitory C terminus residue (Tyr^{507}) of major B cell SFK, Lyn (Zhu et al., 2008). The functions of both CD45 and CD148 are analogous and perhaps redundant, in support of this notion, mice lacking both CD45 and CD148 show a greater block in B cell development and BCR signalling than mice with either CD45 or CD148 deficiency (Zhu et al., 2008). In addition augmented expression of CD148 in CD45-deficienct Jurkat T cells 'rescues' the defect in TCR signalling further supporting the complementary roles of CD45 and CD148 in T cell signalling.

SHP1 *(PTPN6)*

SHP-1 (encoded by *PTPN6)* and SHP-2 (encoded by *PTPN11)* are two related mammalian intracellular PTPs containing tandem amino-terminal SH2, domains, a central phosphatase domain and a carboxyl terminal domain with potential tyrosine phosphorylation sites {reviewed in (Lorenz, 2009; Vang et al., 2008)}. While the expression of SHP-1 is restricted to hematopoietic cells and epithelial cells, SHP-2 is ubiquitously expressed. The predominant mechanism of activation of SHP-1 is mediated by engagement of its SH2 domains, through which it interacts with receptors carrying an immunoreceptor tyrosine based inhibitory motif (ITIM) in their cytoplasmic tails.

The immunological importance of SHP-1 comes from the study of motheaten mice that have mutant SHP-1, which is characterized by spotty hair loss and abnormal immune system functioning and leukocyte types (Shultz et al., 1997; Shultz et al., 1993; Tsui et al., 1993). T lymphocytes from these mice are hyper-responsive to TCR stimulation (Pani et al., 1996). Defects in T cell development have been observed, and the thymus involutes at an early stage (Shultz et al., 1997). Together these studies suggest that T cell activation is negatively regulated by SHP-1, in part this is mediated through direct dephosphorylation of ZAP-70, resulting in decreased downstream signalling (Brockdorff *et al*., 1999).

In contrast to SHP-1, the closely related SHP-2 does not appear to be a negative regulator (Neel et al., 2003; Vang et al., 2008). SHP-2 has been shown to influence TCR signalling by dephosphorylation of PAG in transfection studies involving catalytically inactive SHP-2. Additionally SHP-2 is known to positively regulate the MAP kinase pathway (Zhang et al., 2004). Unlike SHP-1, deletion of the SHP-2 gene is embryonically lethal in mice (Saxton et al., 1997). Like CD45, lower levels of SHP-1 protein have been detected in patients with systemic lupus erythematosus (SLE) (Huck et al., 2001) whereas, gain of function mutations in SHP-2 result in Noonan's syndrome (Tartaglia et al., 2001).

TC-PTP *(PTPN2)*

T cell-protein tyrosine phosphatase is an ubiquitously expressed intracellular PTP, encoded by *PTPN2* that is characterised by an N-terminal PTP domain and a proline-rich C-terminal region {reviewed in (Doody et al., 2009)}. It exists as two isoforms and it is particularly important in signalling in the Jak-STAT pathway. Mice deficient in PTPN2 have impaired B and T cell functions (Dupuis et al., 2003). Mice with conditional PTPN2 deficiency in T cells demonstrate a cell-intrinsic role for PTPN2 in T cells, having augmented positive selection of thymocytes, accumulation of T cells with effector/memory phenotype in the peripheral lymphoid organs. PTPN2 knockout mice develop autoantibodies as they age (Wiede et al., 2011). At the cellular level, PTPN2-deficient T cells show increased phosphorylation of tyrosine residues. In keeping with the role of PTPN2 in cytokine-receptor signalling,

conditional PTPN2-deficient T cells show increased proliferation and show greater IL-2 induced STAT5 activation than WT cells (Wiede et al., 2011). Therefore, PTPN2 negatively regulates T cell activation by inhibiting both TCR and IL-2 receptor signalling. Furthermore, several reports have identified PTPN2 as a susceptibility locus for autoimmune diseases such as type 1 diabetes, rheumatoid arthritis and Crohn's disease (Burton, 2007; Consortium, 2007; Smyth et al., 2008; Todd et al., 2007). Recently, the type-1 diabetes-linked PTPN2 variant rs1893217(C) was associated with decreased IL-2R signalling and reduced PTPN2 expression in $CD4^+$ T cells (Long et al., 2011).

PTP-PEST *(PTPN12)*

PTP-PEST is an intracellular PTP, which belongs to the family of proline-, glutamic acid-, serine- and threonine-rich (PEST) family of phosphatases encoded by *PTPN12* that is ubiquitously expressed {reviewed (Veillette et al., 2009)}. PTP-PEST is an important regulator of cell migration and adhesion as shown by overexpression studies in fibroblasts or transformed cell lines and PTP-PEST deficient mouse fibroblasts (Veillette et al., 2009). PTP-PEST is important for normal cellular physiology as mice lacking PTP-PEST exhibit embryonic lethality with severe abnormalities in embryonic vascularisation, mesenchyme formation, liver development and neurogenesis (Sirois et al., 2006). Overexpression of PTP-PEST in B cell or T cell lines resulted in suppression of antigen receptor signalling (Arimura et al., 2008; Davidson and Veillette, 2001). T cell specific deletion of PTP-PEST showed that PTP-PEST was not necessary for T cell development and primary T cell responses. However, it was required for secondary T cell activation and inhibition of anergy (Davidson et al., 2010). These activities correlated with the selective capacity of PTP-PEST to dephosphorylate Pyk2, a substrate of Fyn, involved in adhesion and migration. In keeping, with it important role in adhesion, lack of PTP-PEST resulted in enhanced formation of homoaggregates between T cells in *Ptpn12*$^{-/-}$ T cells compared to wild-type T cells. Further the PTP-PEST deficiency reduced susceptibility to EAE and the affect was attributed to the decrease in the secondary T cells responses (Davidson et al., 2010).

1.8 Protein Tyrosine Phosphatase Non receptor Type 22 (*PTPN22)*

Another member of the PEST family of phosphatases is PTPN22, which belongs to the non-receptor like subfamily of class I phosphatases (Cohen et al., 1999; Matthews et al., 1992). The human gene *PTPN22* maps to chromosome 1p13.3-13.1 and encodes an 807 amino acid residue, intracellular tyrosine phosphatase protein referred as lymphoid specific phosphatase LYP (referred as human PTPN22 from this point onwards) in humans and proline enriched phosphatase (PEP, referred as mouse PTPN22 from this point onwards) in mice (Cohen et al., 1999; Matthews et al., 1992). Both human and mouse PTPN22 are closely related and share overall 70% homology with 89% identity in their catalytic phosphatase domain and 61% homology in the C-terminal domain (Cohen et al., 1999; Matthews et al., 1992) and are expressed exclusively in hematopoietic cells (Matthews et al., 1992) and are approximately 105kDa and 110kDa in size respectively (Cohen et al., 1999).

The intracellular distribution of PTPN22 has been controversial. For mouse PTPN22, it was initially reported to reside primarily in the nucleus when overexpressed in HeLa cells (Flores et al., 1994), and mapping of the potential nuclear localization signal identified a requirement for residues 788 - 802 in the P4 domain (Flores et al., 1994). By contrast, another study that overexpressed HA-tagged PTPN22 in Jurkat cells found it to be abundant in cytoplasm with low nuclear compartmentalization (Gjorloff-Wingren et al., 2000).

This study also showed that the C-terminus was important for the observed cytoplasmic enrichment, while deletion of both the C-terminal domain or N-terminal catalytic domain abolished low level nuclear localisation (Gjorloff-Wingren et al., 2000). Another study using epitope overexpression or GFP-labelling showed that human PTPN22 was found exclusively in the cytoplasm, with low nuclear localisation (Chien et al., 2003; Cohen et al., 1999). Seemingly, most PTPN22 is distributed in the cytoplasm, whilst a fraction translocates to nucleus under certain conditions.

1.8.1 Structure of PTPN22

The PEST family of proteins is a group of three intracellular phosphatases that contain PTPN22, PTP-PEST (also referred as PTPN12) and PTP-hematopoietic stem cell fraction (PTP-HSCF, also termed as brain derived phosphatase, BD1 or PTP20). They share a common structural organisation with an amino terminal phosphatase domain, a highly divergent central region containing proline rich motifs and a carboxyl-terminal homology (CTH) (Veillette et al., 2009).

The N-terminal of PTPN22 contains a conserved serine phosphorylation site at position 35 and catalytic phosphatase domain between residues 23 to 288 (Matthews et al., 1992). Although the catalytic domain for mouse PTPN22 has not been crystallized, it may to be very similar to human PTPN22 as they share about 90% homology. The crystal structure of the catalytic domain of human PTPN22 reveals, a phosphotyrosine recognition loop (amino acid 54 - 60), a WPD loop (amino acid 193 - 204) and a phosphatase signature motif responsible for catalysis (amino acid 226 - 233) (Tsai et al., 2009; Yu et al., 2007). Furthermore, the ability to enzymatically dephosphorylate tyrosine is critically dependent on residues C227 and D195 within the PTPN22 catalytic domain, which work by acting as nucleophilic acceptors of a phosphate moiety and facilitate the hydrolysis of the phosphate-enzyme intermediates (Wu et al., 2006).

The interdomain region connecting the amino-terminal and the C-terminal end spans 300 amino acids. Mutational analysis has revealed that the human PTPN22 interdomain region between amino acid residues 300-320 forms an intramolecular interaction with the catalytic domain and inhibits enzymatic activity, thus important in self-regulation of phosphatase (Liu et al., 2009). Furthermore, there is evidence that Lck regulates human PTPN22 by tyrosine phosphorylation at the Tyr^{536}, present in the interdomain region (Fiorillo et al., 2010). Bottini et al. proposed a model where binding of human PTPN22 to Csk recruits it to the membrane, in close proximity to Lck, which then phosphorylates PTPN22 on Tyr^{536} to turn off its activity thus potentiating T cell signalling. In support of the model, overexpression of mutant human PTPN22 Y536F results in reduced NFAT/AP1 luciferase reporter

activation, inhibited CD69 expression and increased phosphatase activity of immunoprecipitated PTPN22 Y536F compared to wild-type PTPN22 (Fiorillo et al., 2010).

The C-terminal domains of both human and mouse PTPN22 contain highly conserved proline rich regions called P1, P2, P3 and P4 (Cohen et al., 1999).It is known to interact with the SH3 domain of Csk via the P1 motif (Cloutier and Veillette, 1996; Cohen et al., 1999). The structural basis of the association between Csk and mouse PTPN22 became clear following the co-crystallization studies of the Csk SH3 domain and PTPN22 derived P1 peptide (Ghose et al., 2001). The residues PPPLPERTPES-F**IV**, which form the first polyproline motif P1, were shown to abrogate Csk binding when individually substituted by alanine residues (underlined residues) (Gregorieff et al., 1998). In addition, two hydrophobic residues (residues indicated in bold) located towards the carboxyl terminal of the P1 core motif were shown to be important for the high affinity Csk-PTPN22 association (Gregorieff et al., 1998) **(Fig 1.4)**. Although the P2-P4 motifs are conserved between mouse and human, no specific function or association for these domains have been established. In addition, PTPN22 contains five PEST domains between amino acid residues 607-802. These are frequently found in proteins with high turnover (Rogers et al., 1986). Pulse chase analyses have shown that the resting cell half-life of PTPN22 in resting cells is greater than 5h (Flores et al., 1994), suggesting that it is not rapidly degraded.

Human PTPN22 has three splice variants, designated at LYP 1–3 (Cohen et al., 1999; Wang et al., 2010). The full-length protein of LYP1 (807 amino acid), is the most abundant of the 3 isoforms. LYP2 is the shortest splice form and contains only the first P1 motif within the C-terminal due to an alternative stop codon resulting in truncation of the protein (Cohen et al., 1999). The LYP3 variant results from an alternative splicing and has a different C-terminus containing a 28 amino acid deletion between P1 and P2 motifs (Wang et al., 2010). LYP 1 is the most studied variant and not much is known about the other two variants. No equivalent isoforms have been described for mouse PTPN22.

Human PTPN22 protein is not highly expressed in resting naïve cells. Cohen et al. showed that expression of PTPN22 is upregulated at 24 hours post stimulation with anti-CD3 Ab or PHA with a further increase noted at 48 hours (Cohen et al., 1999). LYP1 expression was seen in Jurkat cell lines, Ramos and Daudi B cell lines but not in myeloid cell lines like K562 or U937 (Cohen et al., 1999). Mouse PTPN22 expression is high in all cells of the immune system including T cells, B cells, immature dendritic cells, macrophages, mast cells, natural killer cells (NK), natural killer T cells (NKT) and neutrophils with particular high expression in NK and NKT cells (Arimura and Yagi, 2010).

1.8.2 Function of PTPN22 in T cells

The role of PTPN22 in T cell activation was hypothesised from initial studies showing that it forms a complex with the cytoplasmic protein tyrosine kinase, Csk (Cloutier and Veillette, 1996). Csk potently suppresses T cell activation by phosphorylating the inhibitory tyrosine residue of the SFKs Lck and Fyn, thereby antagonising the action of CD45 (Veillette et al., 2002). Cloutier and colleagues show that nearly 25-50% of the total cellular mouse PTPN22 is in complex with 5-6% of Csk in resting mouse T cells (Cloutier and Veillette, 1996). Later, similar results were confirmed with human PTPN22 in primary human T cells (Vang et al., 2012). Overexpression of wild-type mouse PTPN22 in a mouse T cell hybridoma (BI-141) showed pronounced inhibition of TCR-induced protein tyrosine phosphorylation and cytokine production (Cloutier and Veillette, 1999). Similarly overexpression of mouse PTPN22 in anti CD3/CD28 stimulated Jurkat T cells showed reduced cell activation, as determined by an NFAT/AP-1 luciferase reporter system (Gjorloff-Wingren et al., 1999). The inhibitory action of PTPN22 was shown to be dependent on its enzymatic activity, as mutants lacking the C-terminal domain were unable to exert similar effects (Gjorloff-Wingren et al., 1999). In addition, overexpression studies comparing wild-type mouse PTPN22 with a mutant lacking the Csk-binding P1 domain, and co-expression of wild-type mouse PTPN22 with Csk in Jurkat T cells, suggested that physical interaction between PTPN22 and Csk enables synergistic inhibition of TCR signalling through their combined ability to phosphorylate the inhibitory tyrosine residue Tyr^{505} (via Csk) and dephosphorylate

the activatory tyrosine Tyr^{394} (via PTPN22) on Lck (Cloutier and Veillette, 1999; Gjorloff-Wingren et al., 1999).

Using human Jurkat T cell lines, substrate-trapping analysis was conducted by mutating the C227S/D195A sites of PTPN22 within the phosphatase domain. These studies indicated that CD3ε, CD3ζ, ZAP-70, valosin containing protein (VCP), Vav, Grb-2 and E3 ubiquitin ligase, c-Cbl were all substrates of PTPN22 (Cohen et al., 1999; Hill et al., 2002; Wu et al., 2006). Furthermore, PTPN22 was shown to dephosphorylate both Lck and ZAP-70 at their activating tyrosine residues, Tyr^{394} and Tyr^{493}, respectively *in vitro* (Wu et al., 2006). More evidence that Lck is a physiological substrate for PTPN22 came from studies showing increased Lck phosphorylation in TCR-stimulated *Ptpn22*-deficient T cells (Brownlie et al., 2012; Hasegawa et al., 2004) and in human Jurkat T cells treated with chemical PTPN22 inhibitors (Vang et al., 2012). Another bona fide substrate for PTPN22 is CD3ζ that is dephosphorylated *in vitro* by recombinant PTPN22 (Wu et al., 2006) and also shows increased phosphorylation in primary human T cells treated with PTPN22 inhibitors (Vang et al., 2012).

Human PTPN22 was shown to be a negative regulator of TCR signalling in various *in vitro* studies. A pivotal study by Begovich *et al.* used RNAi to knockdown PTPN22 reported an increase in NF-κB transcription (Begovich et al., 2004). Another putative substrate of PTPN22, identified using a substrate profiling approach, is Src-kinase associated protein of 55 kDa homolog, SKAP-HOM, an adapter protein that is important in lymphocyte adhesion regulation (Yu et al., 2011). Although *in vitro* studies suggest SKAP-HOM to be a putative PTPN22 substrate, direct evidence that PTPN22 controls phosphorylation of Tyr^{75} in SKAP HOM under physiologic condition is lacking. In summary, these studies stress the importance of PTPN22 as a potent negative regulator with a very receptor proximal point of action.

The inhibitory role of PTPN22 in normal T cells has further been demonstrated by characterization of *Ptpn22*-deficient mice. The mice revealed an age dependent increase of effector and memory cells in both the $CD4^+$ and $CD8^+$ T cell peripheral populations (Hasegawa et al., 2004). Phenotypically the mice exhibited increased

size of lymph nodes and spleen with spontaneous generation of germinal centres along with elevated serum antibody levels (Hasegawa et al., 2004). *In vitro* generated effector $CD4^+$ T cells displayed increased phosphorylation of Tyr^{394} on Lck and concomitant ZAP-70 and MAPK activation, elevated calcium levels and increased proliferation in response to TCR stimulation (Hasegawa et al., 2004). Despite presenting with skewed lymphocyte populations and activated phenotype, the *Ptpn22*$^{-/-}$ mice failed to develop any autoimmune or lymphoproliferative disease on C57BL/6 background. Nonetheless, combining PTPN22 deficiency with a specific point mutation in CD45 (E613R), which alone drives a lupus-like disease on a mixed 129/B6 but not a wild-type C57BL/6 background (Majeti et al., 2000), resulted in lupus-like disease and accelerated memory T cell formation on a C57BL/6 background (Zikherman et al., 2009).

Our group independently generated a *Ptpn22*-deficient mouse model and showed that there was a concomitant increase in the Treg cell numbers, that counter balanced the increased effector cell numbers observed in *Ptpn22*-deficient mice (Brownlie et al., 2012). In addition, we showed that there was an increase in the intrinsic suppressive capacity of Treg from *Ptpn22*$^{-/-}$ mice, as demonstrated by the ability to suppress effector T cell proliferation and colitis in *Rag*$^{-/-}$ mice (Brownlie et al., 2012). Furthermore, this study provided evidence that *Ptpn22* deficiency resulted in increased RAP1 phosphorylation in effector T cells and increased LFA-1 mediated adhesion in Tregs, suggesting that PTPN22 modulates integrin-dependent T cell migration and adhesion (Brownlie et al., 2012).

Initial studies from *Ptpn22*-deficient mouse models showed no differences in activation markers, proliferation and phosphorylation of PTPN22 substrates in wild-type and *Ptpn22*$^{-/-}$ naïve T cells, suggesting that PTPN22 function was mainly important in effector cells (Brownlie et al., 2012; Hasegawa et al., 2004). However, a recent study from our group showed that naïve T cell responses were influenced by loss of PTPN22 (Salmond et al., 2014). Using OT-I TCR transgenic *Ptpn22*-deficient mice (that have transgenic expression of MHC class I- restricted ovalbumin (Ova) specific TCR), we showed that naïve *Ptpn22*$^{-/-}$ OT-I T cells had increased ERK phosphorylation and proliferation in response to low-affinity peptides compared with

wild-type OT-I T cells. In contrast, responses to high affinity peptide were comparable between the two genotypes, suggesting that in naïve T cells PTPN22 may function to limit signalling by weak agonists and self-antigens but does not impede responses to strong agonists antigens (Salmond et al., 2014). Also PTPN22 was shown to be important for regulating homeostatic proliferation, as in absence of PTPN22, increased lymphopenia-induced proliferation, driven by low affinity self-peptide MHC was noted in naïve *Ptpn22*$^{-/-}$ T cells compared to wild-type T cells both on polyclonal and OT-I transgenic backgrounds (Salmond et al., 2014).

In summary, experiments using genetic or pharmacologic manipulation of PTPN22 provide strong evidence that the phosphatase serves as a negative regulator of signalling through the TCR.

1.8.3 The role of PTPN22 in other cell populations

PTPN22 is expressed in primary B cells (Arimura and Yagi, 2010; Zikherman et al., 2009) and can be dynamically regulated. *In vitro* CpG stimulation resulted in an increase in mRNA and protein expression of PTPN22 in B cells (Dai et al., 2013), whereas lipopolysaccharide (LPS) stimulation suppressed expression (Arimura and Yagi, 2010). The *Ptpn22*-deficient mice, showed no difference in total peripheral B cell numbers or alteration in signalling through the BCR, as evidenced by normal calcium mobilisation following BCR engagement (Hasegawa et al., 2004). Modest increase in selected IgG subtypes and B cell rich germinal centres were seen in *Ptpn22*$^{-/-}$ mice (Hasegawa et al., 2004), however, disinhibited T cell function could account for the observed alteration in the germinal centres rather than perturbed B cell signalling defects (Maine et al., 2014; Zikherman et al., 2009).

A previous report provided some evidence for role of PTPN22 in B cell signalling. Reduction of PTPN22 protein by expression of antisense PTPN22 cDNA in the immature mouse-B cell line WEHI-231, resulted in a decrease in BCR-induced apoptosis, which is a crucial event in the elimination of potentially autoreactive immature B cells (Hasegawa et al., 1999). Thus indicating a possible role for PTPN22 in promoting negative selection of immature B cells. PTPN22 may also play a role in malignant B cell signalling. A recent report showed that high levels of

PTPN22 was found in chronic lymphocytic leukaemia (CLL) blasts and knock-down of PTPN22 or inhibition of its enzymatic function promoted BCR-triggered apoptosis in CLL blasts, suggesting that PTPN22 may act to protect malignant cells from antigen receptor-induced cell death (Negro et al., 2012).

PTPN22 is highly expressed in myeloid cells such as dendritic cells and macrophages (Arimura and Yagi, 2010; Heng and Painter, 2008). Myeloid cells function by secreting proinflammatory cytokines, initiating host defences, presenting antigen and providing secondary costimulation signals. They carry out these functions by recognising environment signals via the myeloid cell pattern-recognition receptors (PRR) (Broz and Monack, 2013). A recent study showed that PTPN22 selectively promotes type I interferon production via PRR in human and mouse macrophages and DCs (Wang et al., 2013). Efficient type I interferon induction after TLR engagement requires activation of the signalling cascade that involves phosphorylation of interferon response factors (IRFs), IRF3 and IRF7 and is critically dependent upon the Lys63 linked auto-ubiquitination of the E3 ligase TNF receptor associated factor 3 (TRAF3) (Hacker et al., 2011).

PTPN22 selectively associates with TRAF3 in myeloid cells and promotes Lys63 linked auto-ubiquitination of TRAF3 following stimulation through PRR, resulting in production of type I interferon, which was reduced in *Ptpn22*$^{-/-}$ or *Ptpn22* knock-down myeloid cells (Wang et al., 2013). In addition, the effect of PTPN22 in the TLR pathway was not mediated by PTPN22 catalytic activity, but instead was reliant upon scaffolding properties within the C-terminal domain of the protein, as treatment of mouse bone marrow derived macrophages or a macrophage cell lines with pharmacologic inhibitors of PTPN22 demonstrated no effect on TLR-stimulated type I interferon production (Wang et al., 2013). Furthermore, another study showed that PTPN22 is differentially expressed in the M1 (classically activated) and M2 (alternatively activated) macrophages and PTPN22 suppresses M1 polarization of macrophages and reciprocally promotes the expression of M2-associated genes (Chang et al., 2013). PTPN22 was shown to play a protective role in inflammatory bowel disease, as loss of PTPN22, rendered mice more susceptible to dextran sulphate sodium (DSS) induced colitis (Chang et al., 2013).

Therefore PTPN22 has a dual role in regulation of immune cell signalling, wherein it restricts and dampens signalling downstream of the TCR in the adaptive immune system and selectively promotes functions of myeloid cells in the innate immune system.

1.8.4 Association of C1858T polymorphism in PTPN22 with autoimmune diseases

The recognition that the *PTPN22* gene is a major risk factor for autoimmunity was initiated by identification of a single nucleotide polymorphism (SNP) in *PTPN22* exon 14, which substituted cytosine at position 1858 with a thymine (1858C>T) and was associated with an increased predisposition to type 1 diabetes (Bottini et al., 2004), rheumatoid arthritis (Begovich et al., 2004) and systemic lupus erythematosus (SLE) (Kyogoku et al., 2004). The *PTPN22-C1858T* confers a change of amino acid at position 620 (619 in mouse) from arginine (R) to tryptophan (W) within the P1 motif (Bottini et al., 2004) **(Fig 1.4)**. The SNP was further shown to disrupt the interaction of Csk with PTPN22, resulting in diminished binding of Csk with PTPN22 (Bottini et al., 2004). Since its initial finding, hundreds of reports supporting the link between C1858T and increased predisposition to autoimmune diseases have been published {reviewed in (Bottini and Peterson, 2014)}. Furthermore, genome-wide association studies conducted in humans show that the 1858C>T SNP in *PTPN22* ranks as the second highest risk factor for development of rheumatoid arthritis (after MHC) and the third highest risk factor for type 1 diabetes (Todd et al., 2007).

The frequency of *PTPN22 1858T* allele varies significantly among different populations. In Europe, a northeast to southwest gradient exists, with the highest frequency of 15-17% observed in the North European countries. Moving southwest the frequency of allele decreases to 7-8% and decreases even further to 2-3% in the southern Italian and Sardinian populations (Bottini and Peterson, 2014; Burn et al., 2011). *PTPN22 C1858T* allele is rare (< 1%) in African, Middle Eastern, Native American and Asian populations (Bottini and Peterson, 2014; Burn et al., 2011).

While the associated risk with many autoimmune diseases have been well established with the *PTPN22 1858T* allele, many autoimmune diseases do not share this susceptibility locus including ulcerative colitis and Crohn's disease (Diaz-Gallo et al., 2011; van Oene et al., 2005), multiple sclerosis (Begovich et al., 2005) and psoriasis (Criswell et al., 2005). These findings indicate that the *PTPN22* C1858T polymorphism is a common risk factor for some, but not all autoimmune diseases.

In addition to autoimmune diseases, *PTPN22 1858 C>T* also affects susceptibility to infectious diseases. Carriers of the 1858T allele are at increased risk of bacterial infections, including invasive pneumococcal infections, bacterial pulmonary infections in patients with chronic mucocutaneous candidiasis and to leprosy (Bottini and Peterson, 2014). Remarkably, the R620W variant has been associated with reduced risk of developing tuberculosis (Bottini and Peterson, 2014; Burn et al., 2011). Presumably, while the R620W is a common risk allele for some autoimmune disease, the modest protective effect that it provides against the infections may be a reason for its maintenance in the human population.

Besides the 1858C>T SNPs of *PTPN22*, other SNPs have also been identified, one of which is located within the catalytic domain, *PTPN22* 788 G>A and confers a R263Q amino acid change (Carlton et al., 2005). The R263Q mutation was shown to be associated with a lower risk of development of RA in a larger cohort (Rodriguez-Rodriguez et al., 2011). While the R263Q mutation is demonstrated to decrease the phosphatase activity of the PTPN22, compared to the wild-type protein, as shown by reduced ability to down regulate ERK phosphorylation, NFAT activation and *in vitro* phosphatase activity of the Q263 variant (Orru et al., 2009). Interestingly, the authors found an association between the R263Q variant and reduced risk of SLE, indicating that this loss-of function variant actually provides a protective effect against autoimmunity (Orru et al., 2009).

The point mutation of PTPN22 associated with autoimmunity has been the focus of both human ($PTPN22^{R620W}$) and mouse ($PTPN22^{R619W}$) *in vitro* studies over the last 10 years with conflicting results. Overexpression of $PTPN22^{R620W}$ in Jurkat cells showed significant inhibition of TCR signalling and was hence assumed to be a

'gain-of function' mutation (Vang et al., 2005). An initial study utilising primary T cells transfected either with $PTPN22^{WT}$ or $PTPN22^{R619W}$ showed a decrease in IL-2 production upon anti-CD3 antibody stimulation in $PTPN22^{R619W}$ compared to cells expressing $PTPN22^{WT}$ (Vang et al., 2005). In addition, expression of $PTPN22^{R619W}$ showed decreased phosphorylation of proximal signalling molecules like CD3ζ and LAT, which correlated to reduced levels of ERK activity (Vang et al., 2005). In support, a study with primary human T cells isolated from carriers of $PTPN22^{R620W}$ polymorphism demonstrated impaired calcium flux and upregulation of activation markers upon TCR activation (Rieck et al., 2007). By contrast, the point mutation has been described as a hypomorph mutation wherein transfection of $PTPN22^{R620W}$ in Jurkat cells alone or in the context of Csk, resulted in higher pERK than $PTPN22^{WT}$ following TCR stimulation (Zikherman et al., 2009). Further support for the loss-of-function model comes from two independently generated R619W knock-in mice, analogous to the human R620W variant, both of which describe a phenotype similar to the PTPN22- deficient mouse (Dai et al., 2013; Zhang et al., 2011). The most recent of the papers show that R619W knock-in mice fails to develop signs of autoimmunity on the B6 background but on a mixed 129/B6 genetic background, the mice manifested systemic autoimmunity characterized by high-titers of autoantibodies and vasculitis, lymphoid infiltrates in multiple organs (Dai et al., 2013).

Interestingly, neither the PTPN22 KO nor R619W mutation is sufficient to develop spontaneous autoimmunity on B6 background therefore the use of established autoimmune models or multiple gene knock-outs/ mutations have been used to study this gene in a disease specific context (Maine et al., 2012; Maine et al., 2014; Yeh et al., 2013; Zheng and Kissler, 2013; Zikherman et al., 2009). The SKG mouse strain, on the BALB/c background contains a spontaneous point mutation W163C in the SH2 domain of ZAP-70 and are prone to develop $CD4^+$ T cell mediated chronic autoimmune arthritis in the mice that resembles human rheumatoid arthritis when maintained in conventional facilities (Sakaguchi et al., 2003). The arthritis is characterized with progressive symmetric progression of inflammation from interphalangeal joints of the forepaws and hind paws to larger joints (wrists and

ankles) (Sakaguchi et al., 2003). Arthritis can also be elicited under specific pathogen free (SPF) conditions either through antigen non-specific activation of innate immunity, (e.g. by administration of crude or purified fungal extracts) or by provoking homeostatic proliferation of self-reactive T cells upon transfer to the T cell-deficient environment of nude mice (Yoshitomi et al., 2005). To investigate the effect of PTPN22 on T cell signalling in context of an autoimmune disease, we crossed the SKG mice with mice containing global deletion of *Ptpn22*.

1.9 Thesis Aims

The overall aims of this thesis are to understand how intracellular signals and the interplay of various signalling molecules influence downstream T cell function. Signals through the T cell receptor are transmitted initially by the SFK, Lck whose activity is modified by the phosphatase PTPN22. PTPN22 is a known negative regulator of T cell signalling, however the precise dissection of molecular involvement of PTPN22 at various stages of signal transduction cascade is yet to be elucidated. Several studies show that there is a robust association between the R620W polymorphism in PTPN22 with development of autoimmune diseases. However whether the substitution renders PTPN22 a more or less potent regulator of T cell signalling is still controversial. We therefore used the *Ptpn22*$^{-/-}$ mice to address the following aims in this thesis.

- To characterise the functional effects of the R619W polymorphism in primary murine T cells using lentiviral transduction technology.
- To identify the signalling pathways in which PTPN22 is involved to gain further insight into its function.
- To understand the molecular mechanism of PTPN22 action in the context of an autoimmune disease.

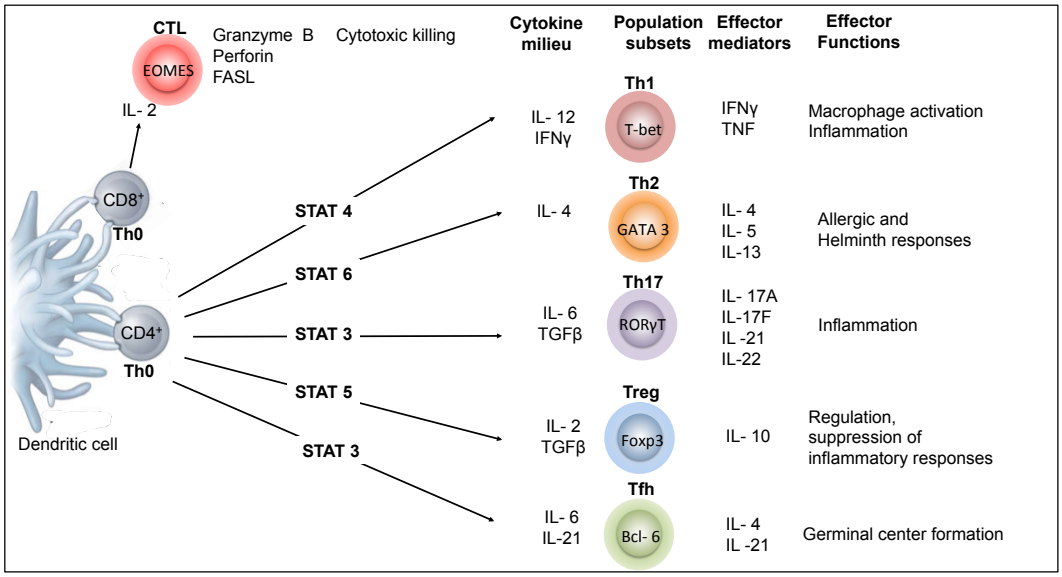

Figure 1.1 Differentiation of Effector T cells (adapted from Swain *et al* 2012 and O'Shea *et al* 2010)

Following recognition of a specific antigen presented by antigen presenting cells, naïve T cells undergo several rounds of division and differentiate into different effector subsets depending on the presence of the cytokine milieu and characterised by their cytokine profile and transcription factors.

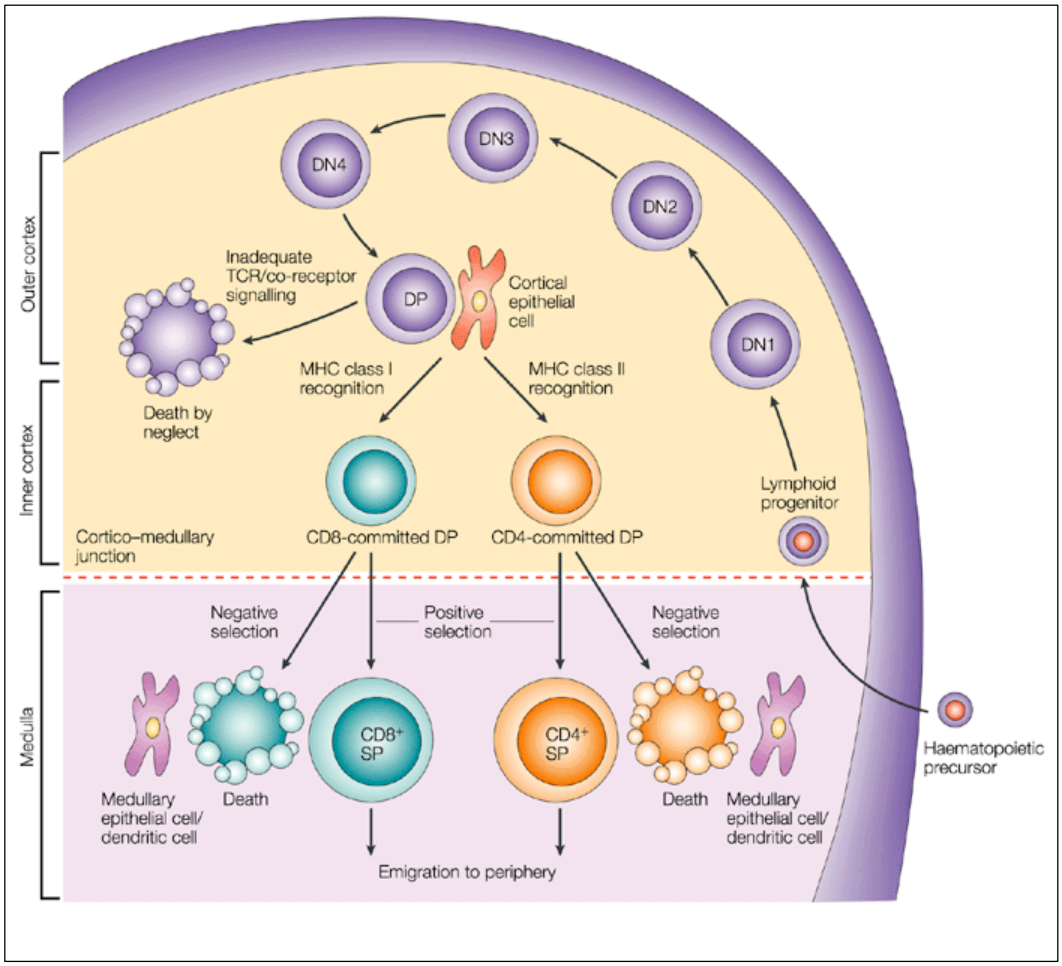

Figure 1.2 T cell development in thymus (From Germain, 2002)
Committed progenitor lymphoid cells migrate from the bone marrow into the thymus. The early thymic precursors (ETP) that enter the cortex lack expression of TCR, CD4 and CD8 markers, and are termed as double negative (DN). As the cells progress through the subsequent DN2 to DN4 stages they express the pre TCR composed of pre TCRα chain and rearranged TCRβ chain. At the DN4 stage the cells express both CD4 and CD8 and are termed as double positive (DP). The DP cells then undergo positive selection, which critically depends on interaction of TCR with self-peptides; most of the cells die as they have very low affinity towards self-peptide (death by neglect), those which react with increased affinity are deleted by negative selection (in medulla) on those cells which have intermediate affinity are positively selected and mature into $CD4^+$ or $CD8^+$ SP cells and migrate from medulla into peripheral lymphoid organs.

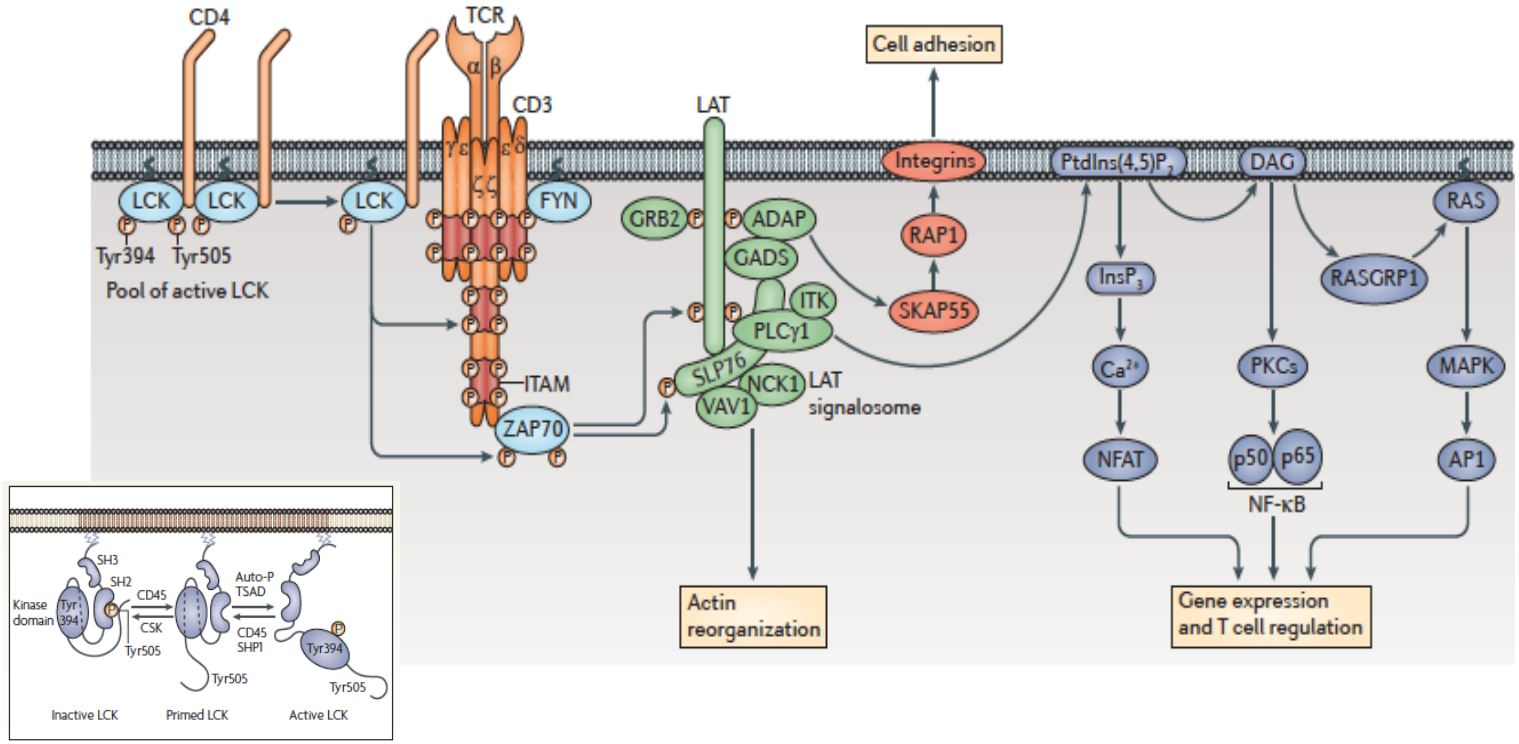

Figure 1.3 Overview of T cell receptor signalling (Adapted from Brownlie *et al.* 2013 and Acuto *et al.* 2008)
Following TCR/CD3 engagement by pMHC, Lck is activated and recruited to the TCR/CD3 complex Lck then phosphorylates the ITAM motifs within the CD3 subunits. The activity of Lck is tightly regulated by Csk, which phosphorylates the inhibitory (Tyr505) maintaining Lck in inactive state. Activation of Lck is mediated by CD45 by dephosphorylating Tyr505 residue, thereby counteracting activity of Csk. The T-cell specific adaptor protein (TSAD) then binds to and positively regulates Lck. Together, Csk, CD45 and TSAD are involved in maintaining an equilibrium between inactive, primed and active states of Lck (insert). The phosphorylated ITAMs provide docking sites for recruitment of ZAP-70, which is activated by phosphorylation by Lck. ZAP-70 further recruits and phosphorylates SLP-76 and LAT, which form the LAT signalosome and recruit more signalling molecules. The LAT signalosome propagates the signals to three major signalling pathways; Ca^{2+}, MAPK and NFκB pathway leading to mobilization of transcription factor critical for gene expression. Signals via the TCR are also important for actin reorganization and activation of integrin mediated inside out signalling.

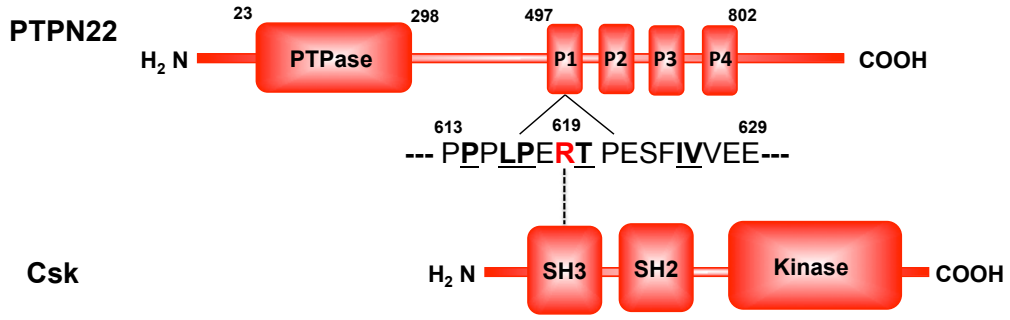

Figure 1.4 Structural requirement for Csk and PTPN22 interaction.
A schematic representing the primary structure of Csk and PTPN22 and the residues required for the interaction. Csk is a kinase and comprises of N-terminal SH3, SH2 and a C-terminal catalytic domain. Structurally PTPN22 comprises of an N-terminal phosphatase domain connected via the interdomain to a non-catalytic proline rich carboxyl terminal. The location of P1-P4 proline motifs are shown. The proline motif located within the P1 region of PTPN22 important for interacting with Csk is highlighted, with the essential amino acids critical for binding underlined. The position of the autoimmunity linked single nucleotide polymorphism that is mutated to tryptophan (R619W) is highlighted in red.

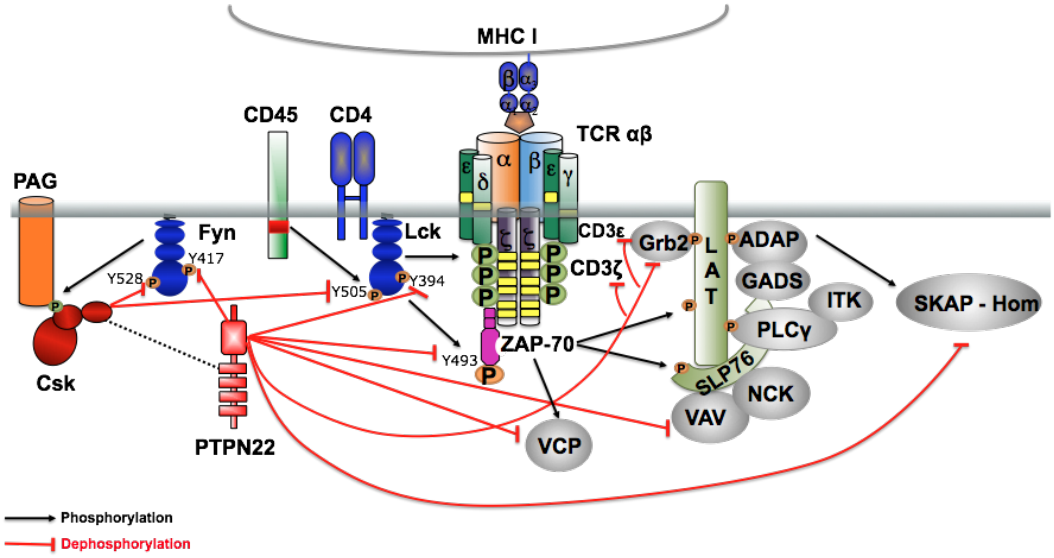

Figure 1.5 PTPN22 negatively regulates T cell signalling by dephosphorylating multiple proximal signalling molecules (Adapted from Burn *et al* 2011 and Bottini *et al,* 2014).
Substrate trap experiments show that PTPN22 interacts with multiple proximal signalling molecules and attenuates TCR signalling by dephosphorylating them on activating tyrosine residues, which include Tyr394, Tyr 417 and Tyr 493 on Lck, Fyn and ZAP-70. Other putative substrates that undergo PTPN22 mediated dephosphorylation include TCR - CD3ζ, CD3ε chains, adaptors Grb2, Vav and valosin containing protein (VCP). Recently *in vitro* studies have identified Tyr72 on SKAP to be a potential substrate of PTPN22.

Chapter 2: Materials and Methods

2.1 Buffers and Solutions

2.1.1 Buffers for plasmid DNA miniprep

Buffer P1

50mM Tris Acetate, pH 8.0 (Calbiochem-Novabiochem UK)

10mM Ethylene diamine tetra acetic acid (EDTA) (Sigma-Aldrich UK)

100μg mL^{-1} RNAse A (Invitrogen, UK)

Buffer P2

0.2N Sodium Hydroxide (Sigma-Aldrich UK)

1% SDS (Fisher-Scientific, UK)

Buffer P3

3M Potassium Acetate (Sigma-Aldrich UK)

2.1.2 Luria Bertini Broth

10gL^{-1} Tryptone (Sigma-Aldrich UK)

10gL^{-1} Sodium Chloride (Sigma-Aldrich UK)

5gL^{-1} Yeast Extract (Sigma-Aldrich UK)

2.1.3 Luria Bertini Agar

10gL^{-1} Tryptone (Sigma-Aldrich UK)

10gL^{-1} Sodium Chloride (Sigma-Aldrich UK)

5gL^{-1} Yeast Extract (Sigma-Aldrich UK)

14gL^{-1} Agar (Sigma-Aldrich UK)

2.1.4 TAE Buffer (10X)

48.5 gL^{-1} Tris Base (Fisher-Scientific, UK)

11.4 ml Glacial acetic acid (Fisher-Scientific, UK)

20mL of 0.5M EDTA (pH 8.0)

2.1.5 TE Buffer

10mM Tris pH 8.0 (Fisher-Scientific, UK)

1mM EDTA (Sigma-Aldrich, UK)

2.1.6 HBS Buffer 2X (pH 7.12)

281mM Sodium Chloride (Sigma-Aldrich, UK)

100mM HEPES (Sigma-Aldrich, UK)

1.5mM Disodium hydrogen phosphate (Na_2HPO_4)

2.1.7 Western Blot Lysis Buffer

20mM Tris pH 7.5 (Fisher Scientific, UK)

150mM Sodium Chloride (Sigma-Aldrich UK)

1% Triton X 100 (Fluka–Sigma-Aldrich UK)

1% Maltoside (Merck Millipore)

2mM EDTA (Sigma-Aldrich UK)

1mM Sodium Orthovanadate (Sigma-Aldrich UK)

1/100 Protease inhibitor cocktail (Sigma-Aldrich UK)

1mM Sodium Fluoride (Sigma-Aldrich UK)

2.1.8 Western Blot 4X Reducing Sample Buffer

160mM Tris-HCl pH 6.8 (Fisher Scientific, UK)

40% v/v Glycerol (Sigma-Aldrich, UK)

10% v/v SDS (Fisher Scientific, UK)

0.05% w/v Bromophenol blue (Sigma-Aldrich, UK)

9%v/v β-2-mercapthoethanol (Sigma- Aldrich, UK)

2.1.9 Western Blot Running Buffer

NuPAGE® MOPS SDS Running Buffer 20X for Bis-Tris gels (Invitrogen, UK)

2.1.10 Western Blot Transfer Buffer

20mM Tris-Cl pH 7.5 (Fisher Scientific, UK)

150mM Glycine (Fisher Scientific, UK)

20% Methanol (Fisher Scientific, UK)

2.1.11 Western Blot Wash Buffer

1X PBS (Gibco BRL, UK)

0.1% Tween-20 (Scientific Laboratories Supplies, UK)

2.1.12 Red Cell ACK Lysis Buffer (pH 7.4)

150mM Ammonium Chloride (Sigma-Aldrich UK)

10mM Potassium bicarbonate (Sigma-Aldrich UK)

0.1mM EDTA (Sigma-Aldrich UK)

2.1.13 Flow Cytometry (FACS) Buffer

1X Phosphate Buffered Saline pH7.2 (PBS; Gibco BRL, UK)

$5gL^{-1}$ Bovine Serum Albumin (Fisher Scientific, UK)

0.05% Sodium Azide (Sigma-Aldrich UK)

2.1.14 Magnetic Activated Cell Separation (MACS) Buffer

1X PBS (Gibco BRL, UK)

2mM EDTA (Sigma-Aldrich UK)

0.5% BSA (Sigma-Aldrich UK)

2.1.15 ELISA Wash Buffer

1X Phosphate Buffered Saline pH7.2 (Gibco BRL, UK)

0.05% Tween-20 (Scientific Laboratories Supplies, UK)

2.2 Cell Lines

2.2.1 293T

293T cell line (Takara; Clontech, UK), also called HEK was established from human embryonic kidney cells. These cells constitutively express the simian virus 40 (SV40) large T antigen. This is an easily transfected cell line and was used for generating high titers of lentivirus (Section 2.6).

2.2.2 NIH-3T3

The cell line was established from the primary mouse embryonic fibroblasts cells that were cultured by a designated protocol (primary mouse cells were transferred every 3 days at $3x10^5$ cells, thus the name 3T3). NIH- 3T3 cells were established from the Swiss NIH mouse using the same protocol. The NIH -3T3 cell line was a kind gift from the laboratory of Dr. Amy Buck (University of Edinburgh) and was used for estimating the titer of lentivirus particles generated in the 293T cells.

2.3 Mouse Models

All mouse strains used were maintained and bred under pathogen-free conditions, at the University of Edinburgh animal facilities, in accordance with the U.K. Home Office and local ethically approved guidelines. Wild type BALB/c and C57BL/6 mice were bred in house.

2.3.1 *Ptpn22*$^{-/-}$ mice

Mice with global deletion of *Ptpn22* were generated by the introduction of *lox*P recombination sites flanking exon 1 and crossing them with transgenic mice expressing Cre recombinase driven by the gene encoding protamine (*Prm*-Cre) and then backcrossed either to C57BL/6 mice for four generations (*Ptpn22*$^{-/-}$) or with H-2K^{b} restricted OT-I strain with a congenital deficiency in mature B cells and T cells (*Rag1*$^{-/-}$) background.

2.3.2 SKG *Ptpn22*$^{-/-}$ mice

The SKG mice on BALB/c background contains a spontaneous homozygous W163C mutation in the C-terminal SH3 domain of ZAP-70 (Sakaguchi et al., 2003) and were a kind gift from Prof. Shimon Sakaguchi (Osaka University, Japan). The SKG mice were backcrossed for greater than 8 generation onto the *Ptpn22* deficient mouse line to generate SKG *Ptpn22*$^{-/-}$ mice.

2.4 Peptide

The OT-I transgenic TCR is designed to recognize ovalbumin residues 257 – 264. The SII**N**FEKL (Ser, Ile, Ile, Asn, Phe, Glu, Lys, Leu) octapeptide is the naturally occurring epitope presented to T cells by the MHC class I molecule, H-2K^{b}. Several different variants of Ova peptide, which differ by one amino acid at the 4th position (shown in bold) are used to alter the TCR affinity. N4 (Asparagine) being the strongest peptide, T4 (Threonine) being intermediate and G4 (Glycine) with lowest affinity.

2.5 Cell isolation, purification and culture

2.5.1 Cell Culture Medium

Iscove's Modified Dulbecco's Medium (IMDM) (Sigma Aldrich UK)

Supplemented with:

5% Heat inactivated Fetal Calf Serum (FCS) (Serotec, UK)

100U mL^{-1} Streptomycin (Sigma-Aldrich UK)

100μg mL^{-1} Penicillin (Sigma-Aldrich UK)

$2x10^{-3}$ M L-Glutamine (Sigma-Aldrich UK)

$5x10^{-5}$ M β-2- Mercaptoethanol (Sigma-Aldrich UK)

2.5.2 Isolation of thymocytes and peripheral T cells for *in vitro analysis*

Mouse brachial, axillary, cervical, inguinal and mesenteric lymph nodes were harvested from age matched controls. For some experiments thymus (mice used for thymic analysis unless otherwise stated were always 6-7 week old) and spleen were also removed. Single cell suspension was prepared by teasing the organs through a 70μm sterile cell strainer (BD Falcon, USA) with the end of 2mL syringe plunger. The cells were then washed by centrifugation at 300*g* for 5 min (Heraeus-Multifuge 3S-R) and supernatant discarded before resuspension in fresh culture medium. Splenocytes were subjected to ACK lysis (5 mL for 3 min on ice), after which they were washed, re-filtered with a fresh 70μm sterile cell filter and resuspended in culture medium. An aliquot of cells was either counted on the CASY-1 automated cell counter according to manufacturer's instruction (Scharfe System, Germany) or with a haemocytometer with 0.1% Trypan blue (Fluka-Sigma-Aldrich, Germany) to allow exclusion of dead cells.

2.5.3 Purification by negative selection using Dynabeads® (Invitrogen, UK)

For *in vitro* $CD4^+$ T cell proliferation assays, the T cells were enriched for $CD4^+$ cells by negative selection using Dynabeads. Briefly, the single cell suspension of pooled lymph nodes taken from four individual mice were labelled with rat anti-mouse antibodies produced in-house (kindly provided by the Prof. David Gray, University of Edinburgh) (see **table 2.1**) at saturating concentrations in IMDM medium supplemented with 2% FCS, at a cell density of $2x10^8$ cells mL^{-1}, by incubating for 30 min, in the dark, at 4°C (fridge). During the incubation, the cells were gently mixed after 15 min. While the cells were incubating with primary antibodies, sheep anti-rat IgG Dynabeads (Life-Technologies, UK) were prepared by washing twice with 5mL of medium supplemented with 2% FCS. After the 30 min incubation, the samples were washed twice with the 2% FCS medium and resuspended at $1x10^7$ cells $mL^{-1.}$ The washed Dynabeads were added to the samples at 1:2 beads/cell ratio and incubated for an additional 20 min at 4°C with constant rotation. After the incubation, the unwanted cells, which were bound to the dynal beads were removed using a magnetic particle concentrator (Dynal) and the supernatant, containing the enriched $CD4^+$ T cells, transferred to a fresh 15 mL Falcon tube (Corning, UK). The bound beads were removed from the magnet and resuspended in 5 mL of fresh medium and the bead isolation repeated before transferring the supernatant to the 15 mL Falcon tube. Transferred cells were finally washed, counted and resuspended at the required cell concentration in culture medium containing 5% FCS.

Table 2.1 Antibodies used for isolation of $CD4^+$ T cells using anti-rat IgG dynabeads

Specificity	Clone	Host	Stock Conc.	Dilution
MHC class II	M5114	Rat	8mg mL^{-1}	1:400
CD8a	53 – 6.72	Rat	1.2mg mL^{-1}	1:100

2.5.4 Cell sorting using Flow Cytometry

A BD FACSAria I (BD Biosciences, UK) was used to sort $CD4^+$ naïve ($CD45^{hi}CD25^-$) T cells, following the enrichment with Dynabeads. Antibody-labelled cells were suspended in 0.22µm filtered FACS buffer and passed through a 70µm cell filter (BD Falcon, USA) to remove any cell clumps. The cells were resuspended at $1x10^7$ cells mL^{-1} in sterile FACS buffer and then purity sorted with FACSAria cell sorter (BD biosciences, UK) collecting the naïve cells in 1 mL of FCS containing 1% Penicillin/Streptomycin. After sorting, the cells were washed once in complete medium, counted and resuspended at the final desired concentration.

2.6 Lentivirus production and Titration

293 T cell culture and passage

Iscove's Modified Dulbecco's Medium pH7.4 (IMDM) (Sigma Aldrich UK)

Supplemented with:

10% Heat inactivated Fetal Calf Serum (FCS) (Serotec, UK)

100U mL^{-1} Streptomycin (Sigma-Aldrich UK)

100µg mL^{-1} Penicillin (Sigma-Aldrich UK)

$2x10^{-3}$ M L-Glutamine (Sigma-Aldrich UK)

The 293T cell line was maintained in 10 mL of culture medium in 75mL tissue culture flasks (Nunc, Denmark) at a cell density of $0.5x10^6$ cells per flask, incubated at 37°C/5%CO_2, in a humidified incubator. After the cells were confluent the culture medium was aspirated and the cells were gently washed once with 10 mL of 1X PBS and then trypsinized with 3 mL of 1% trypsin (Lonza, UK) by incubating for 3 min at room temperature. The sides of the tissue culture flask was gently tapped to dislodge the cells, following which 7 mL of culture medium was added and cells were washed by centrifuging at 300*g* (Heraeus-Multifuge 3S-R) for 5 min. The cells were then

seeded at $0.5x10^6$ cells per 75mL tissue culture flask (Nunc, Denmark) in 10 ml of fresh culture medium.

Lentivirus production in 293 T cells

To generate lentivirus 4.5×10^6 293T cells were plated in culture medium containing 10% FCS without any antibiotics in 10 cm tissue culture plates (Nunc, Denmark). The following day a DNA mixture containing 4.5µg of envelope protein, pMDG2-VSV-G, 11.5µg of psPAX2, packaging plasmid and 16µg of viral vector resuspended in 562.5µL of TE buffer and 62.5µL of $CaCl_2$ (2.5M stock) solution was prepared. The DNA/ $CaCl_2$ solution was quickly mixed with 625µL of 2X HBS (section 2.1.7) by vortexing. The DNA/ $CaCl_2$/ HBS solution was immediately added onto the cells. After overnight incubation the medium was changed to fresh medium containing 10mM sodium butyrate (Sigma, stock solution prepared at 10µM). This medium was collected 30 h later and spun at 4000*g* (Heraeus-Multifuge 3S-R) for 5min to remove cell debris. The virus supernatant was either used fresh or was concentrated by centrifugation, using a 45Ti rotor (Beckman Coulter) for 2h at 50,000*g*. The viral pellet was resuspended in 50µL medium at 4°C and aliquots (50µL) were snap frozen in liquid nitrogen and stored at -80°C.

Lentivirus Titration

To titrate lentivirus batches, $1x10^5$ 3T3 cells were plated in 24-well tissue culture plate (Nunc, Denmark) one day prior to infection. 10µL of concentrated lentivirus was added to 1mL of medium and then serially diluted 10 fold. 24 h post infection the supernatant was aspirated and the cells were washed with PBS once and then transferred into 12*75mm FACS tubes (BD biosciences, UK). The percentage of GFP^+ cells was evaluated by a MACSQuant (Miltenyi, Germany) flow cytometer and lentiviral titer was calculated using the following formula:

$$Viral\ titer = \frac{no.of\ 3T3\ cells\ plated\ \ \%\ GFP\ positive\ cells}{(Dilution\ of\ Virus\ used)} \times 1000$$

2.7 Lentivirus transduction of activated T cells

To transduce in vitro generated polyclonal or OT-I cytotoxic T-lymphocytes (CTLs), the activated T cells were washed, by centrifugation at 300g (Heraeus-Multifuge 3S-R) for 5 min and the cell pellet was resuspended, at 106 cells per 1 mL of viral supernatant with 20ng mL-1 recombinant human IL2 (rhIL2; Peprotech, UK) and 4μg polybrene (Sigma-Aldrich, UK). Control cells were resuspended at the same density in culture medium containing the concentration of rhIL2 and polybrene. 1mL of the cell suspension was added to each well of a 24-well plate and the cells spin-infected by centrifuging at 500g for 45 min at 32°C. Following the centrifugation the medium was gently removed, without disturbing the cell pellet and replaced with 1mL of complete culture medium containing 20ng mL-1 rhIL2 followed by incubation at 37°C/5%CO2 in a humidified incubator. The efficiency of transduction efficiency was assessed by expression of GFP by flow cytometry.

2.8 Amaxa nucleofactor transfection of T cells

Designed based on kind advice from Dr. Jessica Borger

Prior to transfection, 1mL of Mouse T cell Nucleofactor medium (supplemented with 20ng mL^{-1} rhIL2, 5% FCS, 2mM glutamine, 1mL of component A and 10μL of component B) supplied with the Mouse T cell Nucleofector kit (Lonza, Switzerland) was aliquoted into a 12-well plate (Nunc, Denmark) and incubated at 37°C for a minimum of 30 min. The *in vitro* generated CTLs, were density separated on lympholyte (Cedarlane, UK), to remove dead cells, counted and washed once with 1X PBS to remove the medium containing serum proteins. The cells were then resuspended at a concentration of $1x10^7$ cells in 100μL of Mouse T cell nucleofector solution (supplied with Nucleofector kit) containing 10μg plasmid, then transferred to a cuvette and electroporated using the $CD8^+$ T cell parameter, X-001 of the Amaxa Nucleofector Device (Lonza, Switzerland). The cells were transferred immediately to the pre-warmed aliquoted medium (described above) and incubated for 4 h at 37°C/5% CO_2, in a humidified incubator. Following 4 h of incubation, the cells were resuspended in 12 mL of complete IMDM culture medium (supplemented with 20ng

mL^{-1} of rhIL2) before aliquoting 4 mL of the cell suspension to each of 3 wells of a 12-well plate and incubated for further 4 h.

2.9 Molecular Biology Techniques

2.9.1 Plasmid DNA Constructs

The cDNA encoding mouse PTPN22 was cloned from the full-length image clone: 30077916. $PTPN22^{R619W}$ variant was generated by site directed mutagenesis at base 1858, where a C>T mutation conferred the change of Arg (R) at aa 619 to a Trp (W). Dr Jessica Borger kindly provided the full-length cDNA $PTPN22^{WT}$, $PTPN22^{R619W}$, $PTPN22^{WT}$-YFP and $PTPN22^{R619W}$-YFP fusion protein constructs cloned in CMV promoter vectors (pCMV- Sport6 and pMAX for YFP, respectively). The bicistronic lentiviral vector pLVX-EF1α was purchased from Takara Clonetech, UK.

2.9.2 Agarose Gel Electrophoresis

Electrophoresis of DNA was performed on standard horizontal electrophoresis apparatus (Biorad, UK). Depending on the size of the DNA to be visualised, 0.75% to 1% w/v DNA grade agarose gels were prepared in 1X TAE (section 2.1) and stained by incorporation of 0.5μg mL^{-1} of ethidium bromide. Prior to loading, DNA was mixed in with 1μL of DNA loading buffer (Thermo Scientific; 10mM Tris-HCl pH 7.6, 0.03% bromophenol blue, 0.03% xylene cyanol FF, 60% glycerol and 60mM EDTA pH 8.0) and electrophoresed at 100V until optimal band separation was achieved. DNA was visualized with ultra-violet light and photographed using a Gel-documentation system (Syngene). Molecular weights of DNA bands were estimated by the relative electrophoretic mobility of DNA ladders Hyperladder 1 (Bioline,UK) and 1kB ladder (New England Biolabs, UK).

2.9.3 Restriction Endonuclease Digestion

A total of 5μg of DNA diluted in sterile distilled water and 5μL 1X NEBuffer (supplied with variable $MgCl_2$ concentrations, New England Biolabs, UK), with 100μg mL^{-1} of BSA and 1U of appropriate restriction endonuclease was digested in a final volume of 50μL restriction digestion mixture reaction in 0.5 mL eppendorf

tubes (Fisher-Scientific, UK). The samples were incubated at 37°C for 1 h, unless specified otherwise and where advised the enzyme was heat inactivated by incubating at 65°C for 5 min.

2.9.4 Gel Extraction of DNA

The restriction digested DNA fragments were separated by gel electrophoresis (described in **2.9.2**) and DNA fragments of required molecular weight were excised from the gel using a scalpel. Using the GeneClean III kit (qBiogene) according to manufacturer's protocol, the gel slice was weighed and 3 volumes of NaI solution (supplied with kit) was added and incubated at 55°C to melt the gel slice. Depending on the final volume of the mixture, GLASSMILK (silica beads) were added to the NaI/DNA solution, mixed well and incubated at room temperature for 5 min following which the DNA bound to the beads were pelleted by centrifuging at 16060*g* (Biofuge Fresco, Heraeus) for 1 min. The pellet was washed twice with 0.5mL of wash buffer and air-dried. The DNA pellet was then resuspended in equal volume of TE buffer as that of added silica beads.

2.9.5 Ligation

Ligation of insert and vector DNA was generally performed at 3:1 equimolar ratio, thus approximately 600ng insert DNA to 200ng of vector DNA, was ligated in a total volume of 10µL containing 1µL of 10X ligase buffer (New England Biolabs, UK; 50mM Tris-HCl, 10mM $MgCl_2$, 1mM ATP, 10mM DTT, pH 7.5 @ 25°C) and 1U T4 ligase (New England Biolabs, UK). Cohesive-end ligation were incubated at 16°C for 1 h and blunt-end ligation reaction at 4°C overnight.

2.9.6 Transformation

Competent DH5α cells (Life-Technologies UK) were thawed on ice for 10 min prior to incubation with 50ng plasmid DNA or 400ng of ligation mixture at 4°C for 20 min. Following which the cells were heat shocked at 42°C for 30s and immediately incubated on ice for 2 min. Pre-warmed SOC medium (Invitrogen, UK) was added to each transformation reaction and incubated for 1 h at 37°C with constant shaking.

50µL and 100µL of cells were spread onto LB agar plates containing appropriate antibiotic selection and incubated at 37°C overnight.

2.9.7 Cloning of PTPN22-StrepTAG into lentiviral vector

Sequences of oligonucleotides designed for generation of C terminal double Streptag separated by glycine-serine linker (WSHPQFEK-GGGSGGGSGGGS-WSHPQFEK) are listed in **Table 2.2**. PCR overlap extension was performed on $PTPN22^{WT}$ or $PTPN22^{R619W}$ template cDNA using Phusion High- Fidelity DNA polymerase (Finnzymes, New England Biolabs, UK) and oligonucleotides StrepTAG 1F, OnestrepTAG -1F (listed in **Table 2.2)**. The following thermal cycling conditions; an initial denaturation step at 98°C for 1 min followed by 3 cycles of 98°C denaturation for 30 s, 47°C annealing for 30 sec, 72°C for 30 s for nucleotide extension and then 27 cycles of 98°C denaturation for 30 s, 65°C annealing for 30 s and 72°C for 1 min nucleotide extension, and a final incubation at 72°C for 10 min was used. The second round PCR reaction to amplify 470 bp fragment used 1µL of first reaction PCR product as DNA template with oligonucleotides StrepTAG 1F and 3' overlapping primer OneStrepTAG-1R (listed in **Table 2.2)** using the same thermal cycling conditions. The PCR product was cloned back using unique restriction site *XcaI* and *NotI* restriction enzyme site encoded within the OneStrepTAG-1R oligonucleotide (**Table 2.2** underlined) into PTPN22 cDNA cloned in Sport 6 vector. The clones were confirmed by DNA sequencing. The full-length cDNA $PTPN22^{WT}$Streptag or $PTPN22^{R619W}$Streptag fusion protein tagged constructs were subsequently subcloned into bicistronic GFP reporter lentiviral vector using unique restriction enzyme sites *EcoRI* and *NotI*.

Table 2.2 Sequences of Oligonucleotides used for generation of PTPN22 StrepTAG fusion lentiviral constructs

Primer[1]	Oligonucleotide Sequence[2]
StrepTAG 1F **(F1)**	3'-TCTCCCAGAAAGAACTCTAG-5'
Onestrep TAG-1F **(R1)**	5'CTTTCTCGAACTGCGGGTGGCTCCAAGCGCTCATATT CCAAGCTGATGGC-3'
OneStrepTAG-1R **(R2)**	5'-TACTCTAGAGCGGCCGCC**TTA**TTTCTCGAACTGCGGGTGGCTCCACGATCCACCTCCCGATCCACCTCCGGATCCACCTCCTTTCTCGAACTGCGGGTGGCTCCAAGCGCT-3'

[1] The sense of the oligonucleotide is indicated in parentheses.

[2] *NotI* restriction enzyme site is underlined, stop codon is shown in bold (black) and the overlapping between primers is highlighted.

2.9.8 Sequencing

The generated recombinant PTPN22-Streptag clones were confirmed by commercial sequencing carried out by GenePool (University of Edinburgh, Edinburgh, UK). **Table 2.3** shows the details of primer sequences used for sequencing. The raw sequencing files was analysed using the free online sequence analysis program (BioEdit Sequence Alignment Editor) (Hall, 1999). The pair-wise sequence alignment was performed in BioEdit software between the obtained sequencing results and construct clones. This program was also used to view chromatograms generated by GenePool sequencing results.

Table 2.3 Oligonucleotides used for the sequencing of generated PCR products

Primer	Sequence[1]
M-13 F	5'-GTAAAACGACGGCCAGT-3'
PTPN22 cDNA R2	3'-TCTTCGAATCAGCACTATTCGG-5'
StrepTAG 1F	3'-TCTCCCAGAAAGAACTCTAG-5'

[1] The sense of the oligonucleotide is indicated in parentheses.

2.9.9 Miniprep for Plasmid DNA Isolation

E.coli containing the plasmid DNA were cultured overnight in 2mL of LB medium with antibiotic selection. The bacteria was pelleted at 10000 rpm for 10 min and resuspended in 200µL of buffer P1. An equal volume of buffer P2 was added, gently mixed and incubated on ice for 5 min. 200µL of chilled buffer P3 was added and the tube was inverted several times followed by 10 min incubation on ice. The tubes were then centrifuged at 16060*g* (Biofuge Fresco, Heraeus) for 10 min at 4°C and the supernatant was transferred to another tube and 600µL of isopropanol was added and incubated on ice for 1 h. The plasmid DNA was pelleted by centrifuging at 16060*g* (Biofuge Fresco, Heraeus) for 10 min at 4°C, washed once with 70% ethanol, air dried for 5 min and resuspended in 30µL of TE buffer.

2.9.10 Large Scale Plasmid Isolation

Plasmid DNA was purified from *E. coli* cultures using the NucleoBond® Xtra Midi Plus purification kit protocol (MACHEREY- NAGEL, Germany). Briefly, *E.coli* harbouring the gene of interest were cultured overnight in 200mL of LB medium with selection antibiotic. The bacteria were pelleted at 42205*g* (RC56 Sorvall, rotor SLA3000) for 10 min at 4°C and resuspended in 8mL of RES buffer. An equal volume of LYS buffer was added, gently mixed followed by addition of 8mL of NEU buffer, mixed by inverting 5-10 times. After incubation the cells were centrifuged at 4347*g* (Heraeus-Multifuge 3S-R) for 5 min. The supernatant was passed over an equilibrated NucleoBond® Xtra Column Filter and washed once with the buffer EQU following which the filter was discarded and column was washed with WASH buffer. The plasmid DNA was eluted from the column with 5mL of ELU buffer and 3.5ml of isopropanol was added, vortexed and incubated at room temperature for 5 min. The mixture was then passed through the NucleoBond Finalizer filter. The filter was washed once with 2mL of ethanol and air dried by expelling air through the filter (n ≥5). The DNA was eluted from the filter with 400 - 800µL of TE buffer (Section 2.1).

2.9.11 Concentration of DNA by Ethanol Precipitation

To concentrate plasmid DNA, one- tenth volume of 3M Sodium acetate (pH 5.2) was added to the DNA solution, followed by two volumes of 95% ethanol and allowed to incubate for 10 min at room temperature. The DNA was pelleted by centrifuging at 16060*g* (Biofuge Fresco, Heraeus) for 10 min. The pellet was then washed once with 70% ethanol air-dried and resuspended in TE buffer.

2.10 Western Blot (WB)

2.10.1 Sample Preparation

The cells were pelleted by centrifugation 300*g* (Heraeus-Multifuge 3S-R) for 5 min and supernatant discarded. The pellet was resuspended at $1x10^8$ cells per 1 mL of lysis buffer **(**described in **2.1.8)** with freshly added protease inhibitors and incubated for 30 min on ice. The lysates were subsequently microfuged at 16060*g* (Biofuge Fresco, Heraeus) for 10 min at 4°C to separate the nuclear fraction. The post-nuclear supernatants were transferred to clean 1.5mL eppendorf tubes (Fisher-Scientific, UK) and if not used immediately were labeled and stored at -20°C. For whole cell lysates, the samples were defrosted and an 10µL aliquot of $2x10^6$ cells was mixed with 2µL of distilled water and 4µL of 4X sample buffer **(**section 2.1**)** and boiled for 5 min at 95°C on a heat block. The samples were briefly centrifuged prior to loading it on a gel.

2.10.2 Immunoprecipitation with Streptactin magnetic beads

Streptactin magnetic beads were prepared by taking an aliquot of 50µL of beads and were washed twice by addition of 500µL of lysis buffer (containing protease inhibitors) and retaining the beads by magnetic separation in each wash by placing against the magnet. The beads were finally resuspended in 100µL of lysis buffer and stored at 4°C until use. 15µL of the washed beads were added to 100µL of cell lysate and incubated overnight at 4°C with constant rotation. The beads were microfuged very briefly at low speed (95*g* for 30 sec) and were separated from the supernatant by placing the eppendorf tubes against the magnet. The supernatant was discarded and the beads were washed thrice with lysis buffer containing protease inhibitors by

placing against the magnet, removing the supernatant each time and retaining the beads. After the final wash step, the beads were resuspended in 20µL of 4X reducing sample buffer (section 2.1) and processed as explained in the section above.

2.10.3 Gel running

NuPage Novex Bis-Tris 4-12% (Life Technologies, USA) was placed in an electrophoresis system (BioRad, UK) with running buffer (Novex, Life Technologies,USA). The protein ladder (Precision Plus Protein Standards All Blue, Bio-Rad, US) and samples were loaded and the gel was run at 100V for 1 h in cold cabinet with constant stirring.

2.10.4 Transfer protocol

The resolved proteins were transferred onto PVDF membranes (Millipore, USA) using wet transfer apparatus from (BioRad, UK). Firstly the PVDF membrane was activated by soaking in 100% ice-cold methanol for 30 s and then equilibrated in ice-cold transfer buffer (section 2.1). Two pieces of filter paper (Whatman Ltd, UK) and two sponges were immersed in the transfer buffer. The gel was removed from the running cassette and equilibrated in the transfer buffer by shaking for 10 min on the shaker (Stovall, lifesciences) at room temperature. The transfer sandwich was set-up, comprising the outer sponge, filter paper, gel and the PVDF membrane layered sequentially from the negative cathode of the transfer cassette, care was taken to remove any air bubbles while placing the gel and the PVDF membrane. The transfer was performed at 100V for 105 min at 4°C. The blotted membrane was blocked for 1h at room temperature in Odyssey blocking buffer (Li-Cor, UK). The blot was incubated with the primary antibodies (listed in table 2.4) in Odyssey blocking buffer containing 0.1% Tween 20 overnight at 4°C. Subsequently the membrane was washed in wash buffer thrice for 15 min and then incubated with appropriate secondary antibody (listed in table 2.4) in 20 mL wash buffer containing 0.1% SDS for 45 min at room temperature. The membrane was washed again three times for 15 min with wash buffer and acquired in PBS using the Odyssey Scanner (Li-Cor, UK). All incubation and washing steps were carried out under continuous shaking.

2.10.5 WB analysis and Quantification

All the western blots were quantified using the Odyssey infrared fluorescence imaging systems. The advantages of using the Odyssey are that the fluorescent signal is directly proportional to the amount of target protein over a wide range of concentrations and two different targets can be identified simultaneously on a single blot with spectrally distinct secondary fluorescent antibodies **(Table 2.4)**. Following the acquisition the relative band intensities were compared by densitometry using Image Studio Lite (Li-Cor Odyssey software). The software calculates the background by taking the median values of the background above and below the drawn rectangle, which is then subtracted from the final reading. The resulting integrated intensity (counts per mm^2) was recorded.

Table 2.4 Antibodies for Western Blot

Specificity	Conjugated	Clone	Host	Usage conc.	Manufacturer
Primary Antibody					
Human PTPN22			Goat	1:667 (Stock 100µg)	RND systems (AF3428)
Mouse PTPN22		P1 (588-654)	Rabbit	1:1000 (stock 5mg mL^{-1})	Genentech
ZAP-70		29/Zap70 Kinase	Mouse	1:2000 (stock 250µg mL^{-1})	BD transduction laboratories
Actin		13E5	Rabbit	1:5000	Cell signaling
Secondary Antibody					
Anti-goat	Alexa Fluor 680		Donkey	1:5000 (stock 2mg mL^{-1})	Cat. A21084, Life Technologies, USA

Specificity	Conjugated	Clone	Host	Usage conc.	Manufacturer
Anti-rabbit	IRDye 800		Donkey	1:10,000 (stock 1mg mL^{-1})	Cat. 611-731-127 Rockland, USA
Anti-mouse	Alexa Fluor 680		Goat	1:5000 (stock 2mg mL^{-1})	Cat. A21058, Life Technologies, USA
Anti-rabbit	Alexa Fluor 680		Goat	1:5000 (stock 2mg mL^{-1})	Cat. A21109, Life Technologies, USA

2.11 Enzyme Linked Immuno-Sorbant Assay

Cytokine ELISAs were performed on supernatants that were previously harvested from culture plates and stored at -20ºC. IL-2 production was measured with mouse IL-2 Ready-Set-Go Kit (Cat 88-7024). The kit was used according to the manufacturer's protocol. Briefly, capture antibody (provided by the kit) was coated onto 96 well plate (NUNC, maxisorp, Denmark) in 50µL/well of the supplied coating buffer by incubating at 4°C overnight. The following day the plates were blocked for 1 h at room temperature with 100µL of blocking buffer (supplied with the kit). Optimum dilutions of supernatant along with doubling dilution of recombinant protein standards were added in a total volume of 50µL/well of blocking buffer. The standards were always assayed in duplicates and the supernatants were assayed in triplicates. The plates were then incubated on an oscillatory shaker (Stovall, lifesciences) for 2 h at room temperature. 50µL of the secondary-biotinylated antibody (supplied with the kit) diluted in the blocking buffer were added to each well and plates were incubated for 1 h at room temperature. Streptavidin-peroxidase (supplied with the kit) was added in 50µL/well in blocking buffer and incubated for 45 min at room temperature. 50µL of 3, 3, 5, 5-Tetramethylbenzidine (TMB), the colorimetric substrate of peroxidase was added (supplied with kit). When the blue

color change was noted (or maximum 10 min), the reaction was stopped by addition of 0.18M H_2SO_4 (Carl Roth, UK) and the plates were read at 450nm on microplate reader (Fluoroscan II, Labsystems) within 30 min. The plates were washed vigorously 3-5 times after every subsequent step with ELISA wash buffer (Section 2).

2.12 T cell based functional assays

2.12.1 *In vitro* T cell activation

For antigen-specific stimulation, single cell suspension of lymph node cells and/or splenocytes were incubated at density of $5x10^6$ cell mL^{-1} in 5 mL of complete medium, in 6-well tissue culture plate (Nunc, Denmark) containing either 2.5µg mL^{-1} of concanavalin A (for polyclonal T cells) (Sigma-Aldrich, stock 10mg mL^{-1}) or 10nM of SIINFEKL (N4) peptide (for OT-I transgenic T cells) (Cambridge peptides stock $1x\ 10^{-3}$M) at 37°C/5%CO_2 in a humidified incubator.

2.12.2 *In vitro* generation of CTLs

Ptpn22$^{+/+}$ and *Ptpn22*$^{-/-}$ OT-I CTLs were generated by incubating $3x10^7$ total splenocytes in 25mL filtered capped tissue culture flasks (Nunc, Denmark) with 10nM SIINFEKL (N4) peptide at 37°C/5%CO_2 in a humidified incubator for 2 days. Following 2 days of incubation the cells were washed twice with 1X sterile PBS and then incubated for another 2 days with complete culture medium containing 20ng mL^{-1} rhIL2 (PeproTech, UK) in 75mL tissue culture flasks (Nunc, Denmark) at cell density of $2.5x10^6$ cells mL^{-1}. A similar procedure was followed for *in vitro* generation of polyclonal CTLs, except that the cells were activated with 2.5µg mL^{-1} of concanavalin A, as described above.

2.12.3 *Ex vivo* cytokine production

$5x10^5$ cells of *ex-vivo* lymphocytes were plated in each well of a 96-well round bottom plate and were stimulated in a final volume of 200µL of culture medium containing a final concentrations of 0.05µg mL^{-1} phorbol 12,13-dibutyrate **(**PDBu) (Sigma-Aldrich, stock 1mg mL^{-1}) and 0.5µg mL^{-1} of ionomycin (Sigma) in the

presence of 5μg mL^{-1} Brefeldin A (Sigma) by incubation for 4 h at 37°C 5%/ CO_2, in a humidified incubator. Unstimulated controls were incubated in 200μL of culture medium containing only 5μg mL^{-1} Brefeldin A. Following 4 h of incubation the cells were washed and stained with Live/Dead Aqua (Molecular Probes, Life Technologies, UK) dye in PBS for 10 min at room temperature and the cells were then fixed and permeabilised for intracellular detection of cytokines (see **2.14.2**).

2.12.4 Cell Proliferation

Labelling with Cell trace Violet

For the measurement of *in vitro* proliferation, single cell suspension of FACS sorted $CD4^{+}$T cells were labelled with Cell Trace Violet (Molecular Probes, Life Technologies, UK) according to the manufacturer's protocol. Briefly, the cells were resuspended at $3x10^6$ cells mL^{-1}, in pre-warmed PBS and Cell Trace was added at a concentration of 2.5μM with continuous gentle mixing followed by incubation in the dark for 20 min at 37°C 5%/ CO_2 in a humidified incubator. Excess dye was quenched by adding an equal volume of pre-warmed culture medium and incubating for 5 min at room temperature. The cells were then centrifuged 300*g*, and resuspended in culture medium at a final concentration of $1x10^6$ cells mL^{-1}. 100μL of labelled cells were pipetted into each well of a round-bottomed 96-well plate and prepared for stimulation. An aliquot of labelled cells was checked by flow cytometry to ensure uniform labelling.

Activation of T cells using irradiated splenocytes

Irradiated splenocytes from BALB/c *Rag2*$^{-/-}$ mice (kindly provided by Prof. Judith Allen, University of Edinburgh) were used as a source of antigen presenting cells. Briefly, a single cell suspension of splenocytes was prepared and the red blood cells were lysed with ACK red cell lysis buffer and the cell suspension was irradiated at 30Gy (Cs^{137}, Gamma Service Medical, GmBH). Irradiated splenocytes were washed thrice with culture medium and then counted and resuspended at a final concentration of $2x10^6$ cells mL^{-1}. The cells were mixed with 0, 0.04, 0.2 and 1μg mL^{-1} of anti-mouse CD3ε antibodies (eBiosciences, UK) and were added in 2:1 ratio

to the Cell Trace labelled $CD4^+$ cells (described above) and the plate was incubated at 37°C 5%/ CO_2, in a humidified incubator. The cell proliferation was assessed by doubling reduction of Cell Trace Violet dye fluorescence at day 3 by flow cytometry

2.12.5 Ca^{2+} Flux Assay

N.B: This assay is very temperature sensitive and during the entire assay including harvest of organs, buffers were maintained at room temperature at all times unless otherwise specified.

We wanted to compare the ability to detect Ca^{2+} flux in thymocytes or lymphocytes from three different strains of mice. Therefore, in order to avoid the bias in measurement of Ca^{2+} Flux, the cells from the different strains of mice were stimulated simultaneously in a single 5mL round bottom FACS tube (BD biosciences, USA). The different cell populations were identified by staining them with a varying concentration of Carboxyfluorescein diacetate N-succinimidyl ester (Vybrant CFDA-SE, Invitrogen, UK), a commonly used intracellular dye as a marker for cell proliferation.

Single thymocyte cell suspension resuspended at $3x10^7$ cells mL^{-1}, in pre-warmed 1X PBS was labelled with CFDA-SE dye at final concentration of either 0.02μM or 0.012μM, by incubating for 10 min in the dark at 37°C 5%/ CO_2. Cells from third strain left unlabelled but incubated as above. The excess dye was quenched by addition of an equal volume of pre-warmed culture medium containing 10% FCS and washed by centrifugation at 300*g*. The cells were counted using an automated cell counter, CASY-1 and mixed in 1:1:1 ratio at final cell concentration of $3x10^7$ cells mL^{-1}. An aliquot of cells were checked for proportions by acquisition on a MacsQuant (Milltenyi, Germany) flow cytometer. The cells were then resuspended at $1x10^7$ cells mL^{-1} and loaded with 2μM of the ratiometric Indo-1 dye (Life Technologies, USA) in pre-warmed PBS. The samples was incubated at 37°C/5% CO_2 for 40 min after which the excess dye was quenched by addition of culture medium containing 1% FCS and washing. At this point, the sample was split into three groups for labelling with biotinylated (bio) antibodies (10μg mL^{-1}) (e.g. Group 1: TCR-bio, Group 2: TCR-bio with CD4-bio and Group 3:CD3-bio with CD4-bio)

(eBiosciences, UK) in 100µL of 1% cell culture medium and incubated for 20 min at room temperature in dark. Thereafter, the samples were washed and resuspended in 600µL of culture medium containing 1% FCS, and supplemented with 2.5mM $CaCl_2$ and 2.8mM $MgCl_2$ for acquisition on LSR II flow cytometer (BD Biosciences, USA). The filter configurations for the assay on LSRII are 530/30 PMT A (Indo-1-blue) and 405/20 PMT B (Indo-1) on the UV trigon. After 45 s of running the samples, 1µg mL^{-1} of Streptavidin-PE was added to induce surface protein crosslinking via the bound biotinylated antibodies. The sample was then acquiring for 8 min, before stimulating the cells were with 1µg mL^{-1} of ionomycin (Sigma-Aldrich, UK) that served as a positive control.

The detection of cellular levels of Ca^{2+} is calculated based on the ratio of the Indo-1 bound to calcium (emitted at 420nm, violet) and free calcium (emitted at 510nm, blue) which is displayed as a parameter over time. Hence before activation the presence of excess dye within the cell population gives a predominant violet signal and hence low ratio value, whereas upon activation the dye changes from violet to blue and hence the Indo-1 ratio increases over time.

2.12.6 Analysis of pERK phosphorylation

Different populations of *ex vivo* thymocytes were labelled with varying concentration of Cell Trace Violet (0, 0.1 and 0.012 µM) and mixed in 1:1:1 ratio. The cells resuspended at $1x10^7$ cells mL^{-1} in serum-free culture medium were stained with 10µg mL^{-1} of biotinylated anti-mouse CD3 and CD4 antibodies by incubating for 20 min on ice in the dark. The samples were washed by addition of 200µL FACS buffer and centrifuging at 300*g* from 3 min once, the cells were then resuspended at $1x10^7$cells mL^{-1} in FACS buffer and split by aliquoting 100µL of cells in round bottomed FACS tubes (BD Biosciences, USA), in triplicates were possible. Tubes were then placed in a 37°C water bath and stimulated by crosslinking with 1µg mL^{-1} of streptavidin conjugated fluorophore (PE or FITC) antibody for different lengths of time (0, 2, 5 and 10 min). The controls included were unstimulated cells, PDBu and UO126 inhibitor. The unstimulated control received an equivalent amount of serum-free culture medium. The reaction was stopped at the desired time point by addition

of 2% v/v paraformaldehyde (PFA) (Acros, USA) and incubated for minimum of 15 min at RT. Amongst the various fix/permeabilisation methods PFA/methanol (described in **2.14.2**) showed best results for the pERK intracellular staining.

ERK phosphorylation was monitored in OT-I CTLs by stimulating with $1x10^{-7}$ M G4 peptide. A similar procedure was followed except that the cells were not pooled and different time points (0, 2.5, 7.5 and 22.5 min) were considered for the assay.

2.13 Induction and scoring of arthritis

Six to eight week-old mice were injected intraperitoneally with 50mg mannan in reconstituted in sterile PBS once. Mice were weighed and observed for clinical signs weekly for 4 weeks. Signs of arthritis was assessed by visual scoring where 0 = no joint swelling, 1 = mild to moderate swelling, 2 = substantial swelling of wrist or ankle and 3 = severe swelling of wrist or ankle. Scores for all the wrists and ankles were combined for each mouse.

2.14 Cell treatments

Depending on the kind of functional assay carried out, the cells were treated with various reagents to either inhibit or serve as a positive control for the assay.

PP2 treatment for inhibition of SFK

Cells at a concentration of $1x10^7$/mL were incubated in complete medium supplemented with 10μM PP2 (Gibco BRL, UK) for 15 min at 37°C/5%CO_2 and were then fixed with 2% PFA by incubating at room temperature for 20 min

Sodium Orthovanadate (Na_3VO_4) treatment to inhibit cellular phosphatases

Cells at a concentration of $1x10^7$/mL were incubated in complete medium supplemented with 100mM Na_3VO_4 (Sigma-Aldrich, UK) for 15 min at 37°C/5%CO_2 and then fixed with 2% PFA by incubating at room temperature for 20 min.

Phorbol 12,13 – dibutyrate (PDBu) treatment

Cells at a concentration of $1x10^6$/mL were incubated in complete medium supplemented with 0.1μM PDBu (Sigma-Aldrich, UK) for 10 min at 37°C/5%CO_2 and then fixed with 2% PFA by incubating at room temperature for 20 min.

U0126 treatment for MEK Inhibition

Cells at a concentration of $1x10^6$/mL were incubated in complete medium supplemented with 20μM U0126 (Calbiochem-Novabiochem, UK) for 10 min at 37°C/5%CO_2 and then fixed with 2% PFA by incubating at room temperature for 20 min.

2.15 Flow cytometry and Antibodies

2.15.1 Surface Staining

The expression of cell surface markers both *ex vivo* and in *in vitro* activated T or treated cells was assessed using flow cytometry. A minimum of 0.5-$1x10^6$ cells were pipetted into a conical bottomed 96-well plate (Greiner Bio-One, Germany), centrifuged (300*g*, 5 min) and resuspended in 30μL of PBS containing a 1:750 dilution of Live/Dead Aqua Stain (Molecular Probes, Life Technologies, UK). The cells were stained in the dark by incubating at room temperature for 10 min. The excess stain was washed off by addition of 100μL FACS buffer and centrifuging (300*g*, 5 min). The samples were then subsequently stained with fluorescence or biotin-conjugated antibodies (listed in **Table 2.5**) by incubating for 30 min on ice in 30μl of FACS buffer antibody mix followed by a wash step. For biotinylated primary antibodies, a secondary incubation for 15 min on ice with either streptavidin-conjugates (BD-Biosciences, UK) (listed in **Table 2.5**) or Alexa Fluor (Molecular probes, Life Technologies, UK) (listed in **Table 2.4**) was performed. Finally the samples were washed in FACS buffer and resuspended in 50-300μL of FACS buffer and acquired on either LSR II (BD, Biosciences, USA), Canto II (BD Biosciences, USA) or MacsQuant (Miltenyi, Germany) flow cytometers.

2.15.2 Intracellular Staining

Cell surface staining protocol was performed as normal. Importantly, the live/dead viable staining was always done prior to fixing. Following the final wash of the surface stains, intracellular staining with antibodies (listed in **Table 2.6**) was performed with one of the following protocols depending on the application.

Foxp3 Intracellular staining Kit (Cat. 00-5523-00, eBioscience, USA)

This kit was used specifically for intracellular staining of Foxp3 transcription factor, according to the manufacturer's recommendations. Briefly, cells were resuspended in 100µL of diluted fixation/permeabilisation buffer (supplied with the kit) and the samples were incubated for 20 min at room temperature (or left overnight at 4°C if required). Thereafter the samples were centrifuged (600*g*, 3 min), buffer was removed and the pellet fully resuspended, washed twice with 1X permeabilisation buffer (600*g*, 3 min), after which the samples were stained by incubating in 30µL of permeabilisation buffer containing the antibody for minimum 30 min at 4°C in dark. The samples were finally washed with permeabilisation buffer and resuspended in 100µL of FACS buffer for acquisition on either LSR II (BD, Biosciences, USA) or MacsQuant (Miltenyi, Germany) flow cytometers.

BD Cytofix/ CytoFix Fixation Permeablisation Kit (Cat. 555023, BD Bioscience, UK)

This kit was used when assessing *ex vivo* cytokine production and for intracellular staining of Streptag, as the FoxP3 buffer completely quenched the GFP reporter expression. Intracellular staining was performed with one of the following protocols depending on the application Briefly, cells were resuspended in 100µL of diluted fixation/ permeabilisation buffer and the samples incubated for 20 min at 4°C (or left overnight at 4°C if required). Thereafter the samples were centrifuged (600*g*, 3 min), buffer was removed and the samples were incubated with 1X BD permeabilisation buffer for 30 min at 4°C and washed (600*g* 3 min), after which the resuspended

samples were stained by incubating in 30µL of permeabilisation buffer containing the antibody for a minimum 30 min (and maximum overnight at 4°C) at 4°C in dark. The samples were finally washed with permeabilisation buffer and resuspended in 100µL of FACS buffer for acquisition on MacsQuant (Miltenyi, Germany) flow cytometer.

Paraformaldehyde (PFA) and Methanol procedure for Phospho-stainings.

This intracellular staining protocol was followed for phospho-staining assays (pERK) and provided the best results compared to other intracellular protocols. The samples were fixed in 2% final concentration of PFA for 20 min at room temperature, washed once with 1X PBS by centrifuging at 600 *g* for 3 min and permeabilized in 90% ice-cold methanol for 30 min on ice. The samples were then washed in FACS buffer by centrifuging at 600 *g* for 3 min and then stained for 30 min by incubation on ice in the dark with the respective intracellular antibodies. Samples stained with biotinylated antibodies were subsequently stained with a secondary streptavidin-conjugated fluorophore (BD-Biosciences, UK) or Alexa Fluor (AF) (Molecular probes, Life Technologies, UK) (listed in **Table 2.4** & **2.5)** for 30 min on ice in dark. After staining the samples were washed and resuspended in 100µL FACS buffer on either LSR II (BD, Biosciences, USA) or MacsQuant (Miltenyi, Germany) flow cytometers.

2.15.3 Flow Cytometry Data Analysis

Flow cytometry data was analysed with FlowJo software v.9.6 (TreeStar Inc.). All samples were first gated on intact lymphocytes, thymocytes or splenocytes using the side scatter (SSC) versus the forward scatter (FSC). The dead cells were excluded from analysis, by gating the live/ dead stained cells against forward scatter, following which doublet or aggregated cells were removed from analysis by gating for single cells through FSC-area (FSC:A) versus FSC-height (FSC:H) or FSC width (FSC:W) depending on optimal profile discrimination. Subsequent gating was dependant on

population distribution profiles and appropriate antigen-fluorophore marker fluorescence intensity used in the particular experiment.

Table 2.5 Flow Cytometry Antibodies

Surface Staining					
Primary Antibodies					
Figure	**Specificity**	**Clone**	**Host**	**Conjugate**	**Supplier**
4.5; 4.6	Anti-Mouse CD3	145-2C11	Armenian hamster	Biotin	eBioscience, USA
4.5, 4.6	Anti-Mouse CD4	RM4-5	Rat	Biotin	BD Pharmingen, USA
4.2; 4.8; 4.9; 4.11; 5.11	Anti-Mouse CD4	RM4-5	Rat	Pacific blue	Biolegend, USA
5.2; 5.3	Anti-Mouse CD4	RM4-5	Rat	FITC	BD Pharmingen, USA
4.14; 5.9; 5.13	Anti-Mouse CD4	RM4-5	Rat	PerCP-Cy 5.5	Biolegend, USA
4.5; 4.6	Anti-Mouse CD4	RM4-4	Rat	APC	Biolegend, USA
4.4; 4.7; 4.8	Anti-Mouse CD5	53-7.3	Rat	APC	BD Biosciences, USA
3.4; 3.5	Anti-Mouse CD8a	53-6.7	Rat	BV421	Biolegend, USA
4.11; 5.9	Anti-Mouse CD8a	eBioH 35-17.2	Rat	FITC	eBioscience, USA
4.2	Anti-Mouse CD8a	53-6.7	Rat	PE	eBioscience, USA
4.5; 4.6	Anti-Mouse CD8a	53-6.7	Rat	PerCP	Biolegend, USA

4.8; 4.9	Anti-Mouse CD8a	MCD0817	Rat	PeTxRed	Life Technologies, USA
4.2; 4.15; 5.13	Anti-Mouse CD25	PC61.5	Rat	APC	eBioscience, USA
3.8; 4.2; 4.12; 5.10	Anti-Mouse/ human CD44	IM7	Rat	APC-eFluor780	eBioscience, USA
3.7	Anti-Mouse CD45.1	A20	Rat	APC	Biolegend, USA
3.7	Anti-Mouse CD45.2	104	Rat	PE	Biolegend, USA
4.13, 5.2	Anti-Mouse CD45RB	C363.16A	Rat	PE	eBioscience, USA
3.8; 4.12	Anti-Mouse CD62L	MEL-14	Rat	PE	eBioscience, USA
5.10	Anti-Mouse CD62L	MEL-14	Rat	APC	eBioscience, USA
4.3	Anti-Mouse CD69	H1.2F3	Hamster	Biotin	Biolegend, USA
4.5; 4.6	Anti-Mouse TCRβ	H57-597	Armenian Hamster	Biotin	BD Pharmingen, USA
4.4	Anti-Mouse TCRβ	H57-597	Armenian Hamster	FITC	eBioscience, USA
5.13	Anti-Mouse CTLA-4	UC10-4B9	Rat	PE	Biolegend, USA
4.8; 4.9	Anti-Mouse TCR Vβ3	KJ25	Mouse	FITC	eBioscience, USA
4.8; 4.9	Anti-Mouse TCR Vβ5	MR9.4	Mouse	PerCP	eBioscience, USA
4.8; 4.9	Anti-Mouse TCR Vβ8.1/8.2	KJ16	Mouse	PE	eBioscience, USA

4.8; 4.9	Anti-Mouse TCR Vβ11	CTVB11	Mouse	FITC	eBioscience, USA
Secondary Reagents and Antibodies					
4.3	Streptavidin			PerCP	Biolegend, USA
4.5, 4.6	Streptavidin			PE	Biolegend USA

Table 2.6 Flow Cytometry Antibodies-Intracellular staining

Intracellular Primary Antibodies					
Figure	**Specificity**	**Clone**	**Host**	**Conjugate**	**Supplier**
3.3	Streptactin			Streptactin chromeo 642	IBA, Germany
3.13; 4.7	Anti-Phospho p44/42 MAPK (pERK)		Rabbit mAb		Cell Signalling, USA
5.11	Anti-Mouse IFNγ	XMG1.2	Rat	Alexa Fluor 488	Biolegend, USA
3.5	Anti-Mouse IFNγ	XMG1.2	Rat	PE	BD Pharmingen, USA
5.11	Anti-Mouse TNF	eBio4B10	Mouse	PerCP - Cy5.5	eBioscience, USA
3.5	Anti-Mouse TNF	MP6-XT22	Rat	APC	Biolegend, USA
4.14; 4.15; 5.13	Anti-Mouse/Rat FoxP3	FJK-16s	Rat	Pacific Blue	eBioscience, USA
5.12	Anti-Mouse IL-10	JES5-16E3	Rat	PeCy7	Biolegend, USA
5.11;5.12	Anti- Mouse IL-17	Ebio17B7	Rat	APC	eBioscience, USA

2.16 Statistical analysis

Statistical analyses were done using Prism 6 software (GraphPad Software Inc, USA). When comparing two samples significance was calculated using the parametric student's t-test, unpaired, and two-tailed. Significance was denoted with the following cutoffs: *P<0.05, **P<0.01, ***P<0.001. Multiple samples were compared using one-way ANOVA with post-ANOVA Holm-Sidak or Tukey's methods for multiple t-tests with the following cutoffs: * $p \leq 0.05$.

Chapter 3: Role of PTPN22 and its variant R619W in T cell signalling

3.1 Introduction

Autoimmune diseases are characterized by dysfunction of the immune system resulting in the failure to remain tolerant to 'self' antigens thus causing aberrant attack against self-tissues and organs. Autoimmunity is a consequence of both genetic predisposition and environmental factors. Alleles of *PTPN22* have emerged as the strongest common genetic risk factor for human autoimmunity outside of the major histocompatibility complex (Bottini et al., 2006). Studies implicating a *PTPN22* allelic variant, R620W, in susceptibility to numerous autoimmune diseases attests the biological importance of its immune regulatory role (Begovich et al., 2004; Bottini et al., 2004; Kyogoku et al., 2004).

PTPN22 shares a similar structure, bearing 89% sequence homology in the catalytic domain, and 61% homology in the C-terminal domain between man and mouse (Cohen et al., 1999). Given the high degree of homology (70%) between the phosphatases, the role of human PTPN22 is likely to be analogous to that of murine PTPN22 protein. It is therefore perplexing that studies involving the PTPN22^{R620W} (PTPN22^{R619W} in mouse) polymorphisms, which disrupts the association of PTPN22 with Csk, present conflicting results with regards to the functional consequences of the polymorphism in humans and comparable knock-in (KI) mouse model which phenotypically resembles the PTPN22 KO mouse and is a loss-of-function mutation (Dai et al., 2013; Zhang et al., 2011).

An early study conducted using peripheral T cells isolated from type-1 diabetes patients with heterozygous expression of the PTPN22 R620W polymorphism showed reduced IL-2 production after stimulation with CD3/CD28 (Vang et al., 2005), suggesting that the variant was a gain-of-function allele. Additionally over expression of PTPN22^{R620W} in primary human T cells resulted in significant inhibition of TCR induced tyrosine phosphorylation of Lck at Tyr394, TCR-CD3ζ

chain, LAT and demonstrated a more efficient reduction in calcium mobilisation and phosphorylation of ERK as compared to expression of the more common variant *PTPN22* allele (Vang et al., 2005). Likewise, Aarnisalo *et al* observed a significant decrease in IL-2 secretion by PTPN22^{R620W} CD4^{+} T cells relative to PTPN22 expressing CD4^{+} T cells from T1D patients (Aarnisalo et al., 2008). In addition, CD4^{+} T cells from the PTPN22^{R620W} carriers showed a profound decrease in calcium flux in response PHA stimulation (Aarnisalo et al., 2008). Collectively, these data supported the idea that PTPN22^{R620W} is a gain-of-function mutation that inhibited T cell signalling more potently than PTPN22. In support, another study reported a reduced TCR-induced calcium mobilisation in memory T cells, among homozygous PTPN22^{R620W} carriers (Rieck et al., 2007). TCR-stimulated IL-10 was significantly reduced in PTPN22^{R620W} T cells, production of IL-2, IFN-γ and TNF-α and proliferation of CD4^{+}CD25^{-} T cells were similar to that of PTPN22 controls suggesting that the variant is associated with alteration in cytokine balance (Rieck et al., 2007). More support for a PTPN22^{R620W} gain-of-function model in T cell activation came from a study of SLE, wherein patients expressing the PTPN22^{R620W} variant demonstrated a skewing of cytokines profiles towards higher IFN-α serum levels (Kariuki et al., 2008).

The effects of PTPN22^{R620W} polymorphism is not only limited to T cells, healthy cohorts expressing PTPN22^{R620W} showed a significant decrease in number of memory B cells with impaired calcium flux compared to PTPN22 controls in response to stimulation via the BCR (Rieck et al., 2007). Recent studies by Arechiga *et al.* further identified the role of PTPN22^{R620W} in BCR signalling pathway wherein it reduced Syk, PLCγ and Akt phosphorylation compared to cells expressing the common variant PTPN22 allele (Arechiga et al., 2009).

In contrast to the numerous studies indicating that PTPN22^{R620W} is more efficient at suppressing T cell signalling compared to PTPN22, a recent study conducted in a group of patients with myasthenia gravis found elevated IL-2 production by stimulated PBMCs in PTPN22^{R620W} carriers (Lefvert et al., 2008) thus supporting a loss-of-function effect for the PTPN22^{R620W} variant in opposition to the previous studies. Further support for the loss-of-function model came from two groups that

independently reported the generation of knock-in mice expressing the analogous mutation R619W in the murine ortholog of PTPN22. Both groups found that the variant exhibited increased TCR signalling with enhanced T cell proliferation and expansion of the effector/memory T cell pool (Dai et al., 2013; Zhang et al., 2011). Furthermore, peripheral $CD4^+$ T cells carrying the homozygous $PTPN22^{R620W}$ substitution from both healthy donors and rheumatoid arthritis patients exhibited augmented ERK phosphorylation and proliferation in response to anti-CD3/CD28 stimulation (Zhang et al., 2011).

Clearly, whether the disease predisposing variant $PTPN22^{R620W}$ is a gain or loss-of-function still needs to be resolved. We therefore chose to investigate the functional consequence of the mouse ortholog of $PTPN22^{R620W}$, $PTPN22^{R619W}$ in T cell signalling by expressing it *in vitro* into primary PTPN22-deficient murine T cells.

3.2 Results

3.2.1 Generation of C-terminal Streptag $PTPN22^{WT}$ and $PTPN22^{R619W}$ lentiviral constructs

The strategy used to generate the $PTPN22^{WT}$ and $PTPN22^{R619W}$ Streptag fusion proteins is outlined in **Figure 3.1**. The Streptag construct was incorporated in the carboxyl terminal of $PTPN22^{WT}$ or $PTPN22^{R619W}$ cDNA using 3' oligonucleotide overhang extension PCR. The overhang extension PCR was generated during two rounds of PCR as shown in **Figure 3.1A**. In the first round, amplification of a 370 bp fragment with primer pair F1 and R1 was carried out (listed in **Table 2.2**) The PCR fragment spanned a region between an amino-terminal *XcaI* restriction site and an elongated 3' end with one copy of Streptag. The 3' primer was designed such that it removed the stop codon and original *NotI* restriction site from the resulting PCR product, thus producing a PTPN22-Streptag fusion protein. Utilising the first PCR product as template DNA, a second round of PCR reaction was carried out with primer pair F1 and R2 producing a 450 bp PCR product. Primer R2 contained a 3' overlapping sequence with primer R1 and the sequence for a second copy of Streptag separated by a glycine serine linker sequence, it also incorporated a stop codon and

NotI restriction site. The two PCR products were identified by agarose gel electrophoresis as shown in lanes 2,3 and 4, 5 (**Fig 3.1B**). The final PCR product was digested with *XcaI* and *NotI* restriction enzymes to produce a 382 bp product, which was inserted back into the full-length cDNA clone contained in pCMV-Sport6 vector utilising the same restriction sites. To generate $PTPN22^{WT}$ and $PTPN22^{R619W}$ lentiviral expression constructs, cDNA encoding the $PTPN22^{WT}$ or $PTPN22^{R619W}$ Streptag fusion protein was excised by digestion with *EcoRI* and *NotI* restriction enzymes and subcloned in an EF1α promoter driven GFP reporter based bicistronic lentiviral vector between the *EcoRI* and *NotI* restriction sites as depicted in **Figure 3.1C**

3.2.2 Generation of recombinant virus in 293T producer cell line and characterization of PTPN22 lentiviral constructs by transient transfection.

Use of the recombinant lentiviral system is a preferred method of gene transfer as it results in stable integration into mammalian cells and directs high level gene expression. **Figure 3.2** illustrates the generation of replication incompetent recombinant lentiviral particles by co-transfection, into the producer cell line 293T, of plasmids coding for viral envelope proteins from vesicular stomatitis virus glycoprotein (VSV-G), viral structural proteins (gag, pol) and the high quality lentiviral plasmid DNA containing either $PTPN22^{WT}$Streptag or $PTPN22^{R619W}$Streptag. The recombinant viral vector is then replicated and assembled into complete pseudotype virus particles that are secreted into the culture medium by the 293T producer cells.

The lentiviral vector is bicistronic and the reporter GFP is encoded downstream of an IRES sequence. Thus PTPN22 and GFP were transcribed from a single transcript but were translated independent of each other; the expression of $PTPN22^{WT}$ and $PTPN22^{R619W}$ was confirmed in transfected 293T by intracellular staining for the fusion tag, Streptag by flow cytometry. Vector only transfected 293T cells served as negative control **(Fig. 3.3A)**. Given that ~99% of the cells were positive for GFP expression with either of the constructs, it was surprising that we only detected about

32% and 48% of the 293 T cells expressing Streptag **(Fig. 3.3A)**. As Streptag is designed for affinity purification of proteins it is possible that detection by flow cytometry could be inefficient, suggesting a problem with signal detection rather than expression of the construct. The expression of PTPN22 in transfected 293T cells was further assessed and confirmed by western blotting, where cell lysates were first immunoprecipitated with streptactin magnetic beads and then subjected to immunoblotting with Goat Anti-Human PTPN22 antibody **(Fig. 3.3B)**. In these experiments, the lentiviral-containing supernatant from 293T cells was tested by transducing the murine 3T3 embryonic fibroblast cell line. **Figure 3.3C** shows that, in comparison to the untransfected controls, nearly 99% and 98% of cells were transduced with vector only control and $PTPN22^{WT}$ generated supernatant respectively, whereas 89% of 3T3 cells were transduced with $PTPN22^{R619W}$ as assessed by the expression of GFP. Taken together, these results show that the 293T cell supernatant contained sufficient lentiviral particles to efficiently infect the target 3T3 fibroblast cells and, subsequently, that Streptag-$PTPN22^{WT}$ and Streptag-$PTPN22^{R619W}$ fusion proteins are similarly expressed.

3.2.3 Efficient lentiviral-induced expression of $PTPN22^{WT}$ and $PTPN22^{R619W}$ in primary PTPN22-deficient T lymphocytes.

Following the initial characterisation of the PTPN22-Streptag fusion lentiviral constructs in 3T3 cell line **(Fig. 3.2A)**, we next wanted to test if we could express $PTPN22^{WT}$ and $PTPN22^{R619W}$ in primary *Ptpn22*$^{-/-}$ T lymphocytes. We used the *Ptpn22*$^{-/-}$ OT-I mouse model, which was generated by back-crossing H-$2K^{b}$-restricted OT-I mice with global deletion of *Ptpn22* (described in section **2.3**).

Primary murine lymphocytes are not only difficult to transduce but the efficiency of transduction is very low in comparison to the human lymphocytes (Zhang et al., 2003). Several studies have established the capacity of lentiviruses to transduce various kinds of non-proliferating cells both *in vitro* and *in vivo*, however some cell types such as early progenitor hematopoietic stem cells and resting T lymphocytes are refractory to transduction unless dividing (Frecha et al., 2010). Furthermore, the

efficiency of lentivirus-mediated gene transfer into T cells depends on a combination of various factors such as cycling status of the cells, high viral titers and optimal timing of transduction (Zhang et al., 2003).

Fig 3.4A outlines the summary of optimised protocol utilised for the transduction of *in vitro* generated *Ptpn22*$^{-/-}$ OT-I CTLs with PTPN22^{WT} and PTPN22^{R619W} lentiviral constructs. For the transduction of *in vitro* generated *Ptpn22*$^{-/-}$ OT-I CTLs two strategies were employed: (1) co-culturing activated *Ptpn22*$^{-/-}$ OT-I T cells with transfected 293T packaging cells **(Fig. 3.4 B)** or (2) by "spin infection" with the produced lentiviral supernatant from transfected 293T **(Fig. 3.4 C)**. Both the strategies showed similar transduction efficiency, of up to 70% at 24 hours post transduction, as assessed by GFP expression by flow analysis. Therefore all subsequent experiments were done using spin-infection technique. Cell viability of the transduced cells was determined by staining with TO-PRO-3, an impermeant dye that intercalates into DNA in necrotic and apoptotic cells. The flow cytometry plots (**Fig. 3.4)** show that cell death in transduced *Ptpn22*$^{-/-}$ T cells expressing either phosphatase was similar, as determined by the percentage of TO-PRO-3 positive cells. Furthermore, in the TO-PRO-3 negative population, the expression profile for GFP expression was similar for both PTPN22^{WT} and PTPN22^{R619W} transduced cells (~70%). These results demonstrate that both PTPN22^{WT} and PTPN22^{R619W} can be expressed with high efficiency in primary mouse *Ptpn22*$^{-/-}$ OT-I CTLs cells. Successful expression of both PTPN22 proteins in *Ptpn22*$^{-/-}$ OT-I CTLs cells was a promising result which allowed us to further address the functional effect of expression of PTPN22^{WT} and PTPN22^{R619W} in *Ptpn22*$^{-/-}$ OT-I CTLs.

3.2.4 Effects of re-expression of PTPN22^{WT} and PTPN22^{R619W} on cytokine production by *Ptpn22*-deficient cells.

To investigate the effects of PTPN22^{R619W} on the functional consequences of T cell activation, we examined the *in vitro* production of cytokines by *Ptpn22*$^{-/-}$ OT-I CTLs expressing either PTPN22^{WT} or PTPN22^{R619W}. A recent study from our group showed that CD8^{+} effectors from *Ptpn22*$^{-/-}$ OT-I TCR transgenic mice had higher levels of cytokine expression in response to stimulation with lower affinity peptides

compared to *Ptpn22*$^{+/+}$ CD8^{+} cells both *in vitro* and *in vivo* (Salmond et al., 2014). Therefore, we sought to determine if re-expression of either PTPN22^{WT} or PTPN22^{R619W} in *in vitro* generated *Ptpn22*$^{-/-}$ OT-I CTLs had any affect on cytokine production in response to re-stimulation through the TCR.

Briefly, *in vitro* generated *Ptpn22*$^{+/+}$ and *Ptpn22*$^{-/-}$ OT-I CTLs (described in detail in section **2.12** and outlined in **Fig 3.4A**) were transduced with vector only, PTPN22^{WT}Streptag or PTPN22^{R619W}Streptag constructs. After 24 h of transduction, the cells were re-stimulated with the weak agonist SIITFEKL (T4), and very weak agonist SIIGFEKL (G4) peptides at varying concentration (10^{-8}, 10^{-7},10^{-6} M) for 4 hours in presence of Brefeldin A, and the GFP positive cells were assessed for their expression of IFNγ and TNFα by flow cytometry.

Firstly to ensure that the results obtained were not affected by the transduction procedure, cytokine production from GFP^{+} (transduced) and GFP^{-} (untransduced) *Ptpn22*$^{+/+}$ and *Ptpn22*$^{-/-}$ OT-I CTLs was compared, after transduction with empty lentiviral vector construct. In response to re-stimulation with the T4, and G4 peptides, more untransduced control CD8^{+} effectors from *Ptpn22*$^{-/-}$ mice expressed IFNγ and TNF than their wild-type counterparts (left panel, **Fig 3.5A**). Similarly, a higher proportion of GFP^{+} *Ptpn22*$^{-/-}$ cells produced IFNγ and TNF than vector only transduced GFP^{+} wild-type cells upon stimulation with either 10^{-6} M of G4 or T4 (right panel, **Fig 3.5A**). Of note, the fewer cells displayed in the GFP gated plots is because the fixing and permeabilisation protocol resulted in loss of GFP expression so some of the GFP positive cells were lost from the analysis (right panel, **Fig 3.5A**). Nonetheless, these results are in agreement with our recently published data showing that *Ptpn22*$^{-/-}$ OT-I CTLs produced more cytokines than wild-type OT-I CTLs cells in response to re-stimulation with low affinity peptide (Salmond et al., 2014).

Having established that the process of transduction did not impact upon the differences observed in cytokine production between the wild-type *Ptpn22*$^{+/+}$and *Ptpn22*$^{-/-}$ mice, we next examined the cytokine production in transduced *Ptpn22*$^{-/-}$ OT-I CTLs expressing either vector only, PTPN22^{WT} or PTPN22^{R619W}. The efficiency of transduction determined 24 h post transduction by analysis of GFP

expression was 70% for both PTPN22^{WT} and PTPN22^{R619W} transduced cells (**Fig. 3.4 C**). The GFP positive cells from both PTPN22^{WT} and PTPN22^{R619W} transduced OT-I CTLs cells were assessed for their expression of IFNγ and TNF by flow cytometry. PTPN22 has been previously demonstrated to act as a negative regulator of TCR signalling and shown to reduce cytokine production in primary human T cells following stimulation via TCR (Aarnisalo et al., 2008; Arechiga et al., 2009; Vang et al., 2005). Therefore, it was surprising that expression of either PTPN22^{WT} or PTPN22^{R619W} in CD8^{+} effectors did not result in a decrease in cytokine expression, with the percentages of IFNγ^{+} and TNFα^{+} cells comparable to the vector transduced control *Ptpn22*$^{-/-}$ cells (**Fig. 3.5B**). These results suggest that the lentiviral induced expression of either PTPN22^{WT} or PTPN22^{R619W} in differentiated *Ptpn22*$^{-/-}$ CTLs was not sufficient to significantly temper TCR-induced cytokine production, with similar amounts of cytokines been produced as the control *Ptpn22*$^{-/-}$ T cells.

3.2.5 Comparison of effects of PTPN22^{R619W} and PTPN22^{WT} expression in PTPN22-deficient cells on lymphopenia-induced T cell expansion

PTPN22-deficient mice on a C57BL/6 background have increased numbers of effector and memory cells (Brownlie et al., 2012; Hasegawa et al., 2004). The increase in the effector and memory cell population in PTPN22-deficient mice has been attributed to a disruption of T cell homeostasis as demonstrated by the increased ability of naïve *Ptpn22*$^{-/-}$ T cells to proliferate when co-transferred into a lymphopenic host compared to their *Ptpn22*$^{+/+}$ counterparts (Brownlie et al., 2012). In support, recent work from our group has shown that the increased homeostatic proliferation in both naïve polyclonal and OT-I *Ptpn22*$^{-/-}$ T cells was driven by low affinity interactions with MHC molecules loaded with self-peptide (Salmond et al., 2014). As two independent studies have confirmed that the phenotype of T cells from PTPN22^{R619W} the knock-in mouse is similar to that of *Ptpn22*$^{-/-}$ mice (Dai et al., 2013; Zhang et al., 2011), we hypothesised that we might see differences in the homeostatic proliferation between PTPN22^{R619W} and PTPN22^{WT} transduced T cells. In order to compare the effects of PTPN22^{R619W} and PTPN22^{WT} on lymphopenia-

induced proliferation, we performed adoptive T cell transfer experiments. *In vitro* generated $CD8^+$ CTLs from *Ptpn22*$^{-/-}$ OT-I mice ($CD45.2^+$) were transduced with vector only, $PTPN22^{WT}$streptag or $PTPN22^{R619W}$streptag plasmids. Wild-type $CD8^+$ CTLs ($CD45.1^+$) transduced with vector only served as control. Following 24 hours of transduction the control wild-type *Ptpn22*$^{+/+}$ CD8+ CTLs were mixed 1:1 with *Ptpn22*$^{-/-}$ $CD8^+$ CTLs transduced with vector, or with $PTPN22^{WT}$Streptag or with $PTPN22^{R619W}$Streptag and a total of $2x10^6$ cells were injected intravenously into RAG KO mice (n=3) as illustrated by the schematics in **Figure 3.6**. The transduction efficiency of each population was comparable before injection **(Figure 3.7)**. After 30 days, the mice were sacrificed and the LNs and spleens were harvested and analysed for the presence of $CD45.1^+GFP^+$ (*Ptpn22*$^{+/+}$) and $CD45.2^+GFP^+$ (*Ptpn22*$^{-/-}$) cells. Very few cells were recovered in any of the three groups (**Figure 3.8A).** Although not statistically significant, decreased numbers of *Ptpn22*$^{-/-}$ $CD8^+$ T cells were recovered from all three groups (i.e. transduced either with vector, $PTPN22^{WT}$ or $PTPN22^{R619W}$) compared to the *Ptpn22*$^{+/+}$ vector transduced control **(Figure 3.8B)** suggesting either that *Ptpn22*$^{-/-}$ did not expand as well as the wild-type *Ptpn22*$^{+/+}$ cells or that they did not survive as well. Additionally analysis of the *Ptpn22*$^{+/+}$ and *Ptpn22*$^{-/-}$ T cells within the different groups for the proportions of effector ($CD62L^{lo}CD44^{hi}$) or central memory ($CD62L^{hi}CD44^{hi}$) as assessed by expression for CD44 and CD62L markers showed no difference **(Figure 3.8 C and D)**.

To our surprise, there was no expression of GFP in either *Ptpn22*$^{+/+}$ or *Ptpn22*$^{-/-}$ $CD8^+$ T cells recovered from any of the groups suggesting that either the transferred transduced cells were outcompeted by untransduced cells or that the transduced cells lost the expression of the GFP reporter **(Figure 3.9)**. As the recovery *Ptpn22*$^{+/+}$ or *Ptpn22*$^{-/-}$ OT-I T cells from either of the groups was very low, failure to survive or low level of expansion due to homeostatic proliferation cannot be ruled out. Indeed a previous report found that naïve TCR transgenic donor T cells expand to a lesser extent than polyclonal C57BL/6 T cells in RAG KO hosts (Kieper et al., 2005). Therefore, based on the findings of this study and our results we decided to adoptively transfer activated polyclonal T cells transduced with the $PTPN22^{WT}$ or $PTPN22^{R619W}$ phosphatase constructs into RAGKO hosts.

As before, i*n vitro* activated polyclonal T cells from *Ptpn22*$^{-/-}$ mice (described in section **2.3)** were transduced with vector only, PTPN22^{WT}streptag or PTPN22^{R619W}streptag plasmids whereas wild-type *Ptpn*22$^{+/+}$ activated T cells were transduced with vector only control. The level of transduction efficiency of wild-type *Ptpn*22$^{+/+}$ and *Ptpn22*$^{-/-}$ T cells transduced with vector only was comparable and expression of either phosphatase in *Ptpn22*$^{-/-}$ T cells assessed by GFP expression was similar (**Figure 3.10)**. The cells were mixed as before and are detailed in schematic figure **3.6** with additional control groups of recipient mice injected with untransduced *in vitro* activated *Ptpn22*$^{+/+}$ and *Ptpn22*$^{-/-}$ T cells and untransduced *ex vivo* wild-type *Ptpn22*$^{+/+}$ and *Ptpn22*$^{-/-}$ T cells **(Figure 3.11A)**. Of note, the previous study examined homeostatic proliferation by adoptive transfer of naïve T cells (Kieper et al., 2005), however due to limitation of lentiviral transduction technique, we transferred activated T cells and therefore the additional *ex vivo* untransduced group served as a positive control for the assay. In case the loss of GFP expression in the previous experiment was due to length of time (30d) the cells were in the recipient, mice were sacrificed 10 days post cell transfer and LNs and spleens were analysed. Even though we recovered increased total cell numbers in both LNs and Spleen within all the groups in this experiment compared with the previous experiment suggesting adoptively transferred cells did expand **(Figure 3.11B)**, once again there was complete loss of GFP expression in the adoptively transferred cells in all the groups even at this earlier time point **(Figure 3.11A)**.

Overall the transduced T cells either from the polyclonal or TCR transgenic wild-type or *Ptpn22*$^{-/-}$ mice harbouring the lentiviral constructs did not maintain the transgene expression *in vivo,* suggesting there was silencing of the introduced transgene or deletion of gene modified cells *in vivo.* Indeed, examination by PCR for the presence of the Streptag in DNA extracted from the lymph nodes of these mice showed no bands for the incorporated tag compared to positive control suggesting loss of the transduced cells. Disappointingly, therefore, it cannot be concluded from these data if there are any differences in the ability of expressed PTPN22^{WT} and PTPN22^{R619W} to affect homeostatic proliferation of *Ptpn22*$^{-/-}$ T cells.

3.2.6 Transient transfection of PTPN22 and PTPN22^{R619W} YFP fusion constructs showed reduced ERK phosphorylation

To address the functional effects of the allelic variant in TCR signalling, Ag-induced phosphorylation of ERK was assessed in *Ptpn22*$^{-/-}$ OT-I T cells transiently transfected with constructs encoding PTPN22^{WT}-YFP or PTPN22^{R619W}-YFP fusion proteins by electroporation. The advantage of using fusion proteins was that, unlike the bicistronic lentiviral vector where expression of GFP reporter protein was independent of PTPN22 protein expression, YFP expression was a direct indication of PTPN22 protein expression.

To optimise and determine the effects of DNA transgene expression in *Ptpn22*$^{-/-}$ T cells, *in vitro* generated CD8^{+} CTLs from *Ptpn22*$^{-/-}$ OT-I mice were transfected with increasing concentration of DNA (2.5 μg, 5μg, 10μg per 5x10^{6} cells) using the Amaxa transfection system (described in section **2.8**). The expression of PTPN22 was assessed by analysis of YFP expression by flow cytometry following incubation for 8 hours post transfection **(Fig. 3.12)**. **Figure 3.12** shows expression of a titration of different concentrations of PTPN22-YFP fusion proteins 8 hours after electroporation. YFP expression was detected in cells transfected with all concentrations of DNA tested with an increase of YFP expression proportional to the increasing amount of DNA. The frequency of YFP^{+} cells and the relative level of YFP expression gauged by MFI, was much lower in PTPN22^{WT} as compared to PTPN22^{R619W} transfected cells at all DNA concentrations **(Fig. 3.12)**. Cell death assessed by staining with TO-PRO3 was similar in cells transfected with either PTPN22^{WT} or PTPN22^{R619W} **(Fig. 3.12)**. It was therefore determined that a 10μg DNA dose resulted in maximal cell transfection efficiency without resulting in excessive cell death.

To investigate the effect of PTPN22^{WT} and PTPN22^{R619W} on TCR signalling, the time-course of ERK phosphorylation (pERK) was assessed in PTPN22^{WT} and PTPN22^{R619W} transfected *Ptpn22*$^{-/-}$ cells following stimulation with 10^{-7}M of G4 (low affinity) peptide for 2.5, 7.5 and 22.5 minutes, stimulation was terminated at

respective time points by addition of PFA followed by staining with pERK specific antibody and pERK was quantified at a single cell level by flow cytometry **(Fig 3.13)**.

Figure 3.13A illustrates the gating strategy employed to permit assessment of pERK based on the different amount of expression of YFP. As the PTPN22^{WT}-YFP construct was never expressed as brightly as the other two constructs, three gates were applied: YFP^{-}, YFP^{lo} and YFP^{hi}, based on GFP control vector expression while the untransfected cells served as negative control. Expression of either phosphatase construct reduced the proportions of pERK^{+} cells following TCR stimulation in comparison to *Ptpn22*$^{-/-}$ transfected with GFP only vector **(Fig 3.13B)**. As noted earlier the expression of PTPN22^{WT} was lower than that of PTPN22^{R619W} so the YFP^{lo} population was compared between all samples **(Fig 3.13 C, middle panel)**. Furthermore the data show that the decrease in pERK was dependent on the levels of PTPN22^{R619W}-YFP expression, with proportionally fewer pERK^{+} cells present in YFP^{hi} compared to the YFP^{lo} population. The difference in pERK in PTPN22^{WT} or PTPN22^{R619W} transfected cells was not significantly different from *Ptpn22*$^{-/-}$ cells at low levels of PTPN22 expression. However high levels of expression of PTPN22^{R619W} (assessed by YFP^{hi}) showed a significant three-fold decrease in levels of ERK phosphorylation compared to *Ptpn22*$^{-/-}$ transfected with GFP only vector **(Fig. 3.13C right panel).** Unfortunately lack of YFP^{hi} population in PTPN22^{WT} transfected cells prevented a comparison of whether the variant reduced pERK activation more or less than PTPN22^{WT}. Taken together, these data show that re-expression of both PTPN22^{WT} and PTPN22^{R619W} inhibits ERK phosphorylation but whether PTPN22^{R619W} is a more or less potent inhibitor of TCR mediated signalling than PTPN22^{WT} remains to be determined.

3.3 Discussion

In this chapter we aimed to address the functional consequences of PTPN22^{R619W} expression and characterise the role of this disease predisposing variant on lymphocyte activation. We first optimized the expression of PTPN22^{WT} and PTPN22^{R619W} in *Ptpn22*$^{-/-}$ T cells using lentiviral transduction technology (**Fig. 3.4)**

and studied the subsequent effect of expression on cytokine production from *Ptpn22*$^{-/-}$ T cells in response to stimulation. The transduction efficiency of either phosphatase, evaluated by GFP expression was similar and very efficient (**Fig. 3.4)**. Restimulation of these cells with varying doses of different affinity peptides led to production of IFNγ and TNF. However the re-expression of either PTPN22^{WT} or PTPN22^{R619W} into *Ptpn22*$^{-/-}$ T did not alter the percentage of IFNγ^{+} and TNF^{+} cells compared to control *Ptpn22*$^{-/-}$ T lymphocytes transduced with vector **(Fig 3.5B)**. This result was surprising, as PTPN22 has been previously demonstrated to act as a negative regulator of TCR signalling and that loss of expression of PTPN22 primarily impacts effector T cell activation (Brownlie et al., 2012; Hasegawa et al., 2004).

There are several possible interpretations of these data. One is that PTPN22 expression in differentiated CTLs is not important as these cells are intrinsically rewired to function without PTPN22. A way to test this possibility would be to treat the wild-type *Ptpn22*$^{+/+}$ CTLs with chemical inhibitors against PTPN22 and assess the cytokine production compared to uninhibited controls. However it is unclear whether any of the available inhibitors are specific enough and it would be difficult to rule out that they may be affecting other phosphatases. If indeed PTPN22 has no effect in differentiated CTLs the level of cytokine expression should remain the same. The expression level of PTPN22 in both mouse and human is upregulated upon T cell activation (Arimura and Yagi, 2010). It is possible that the lentiviral-induced expression of both PTPN22^{WT} and PTPN22^{R619W} into *Ptpn22*$^{-/-}$ T cells is insufficient to impact upon cytokine production. In support of this latter view, is the observation that decrease in phosphorylation of ERK following TCR stimulation was directly proportional to the levels of PTPN22 expression and at low level of expression, both PTPN22^{WT} and PTPN22^{R619W} showed similar levels of inhibition of ERK phosphorylation **(3.13 C)**. In addition, the comparison of endogenous levels of PTPN22 expression with the lentiviral induced expression of PTPN22^{WT} and PTPN22^{R619W} by western blot could not be done at the time due to lack of detection antibody and would be worth pursuing in future studies.

Work from our group has established that PTPN22 is particularly important in controlling responses to weak antigens, whereas responses to strong agonist peptides are often comparable in the presence or absence of PTPN22 (Salmond et al., 2014). Therefore we analysed the ability of *Ptpn22*$^{-/-}$ OT-I CTLs transduced with PTPN22^{WT} and PTPN22^{R619W} construct to expand following adoptive transfer into a lymphopenic hosts. These assays were performed by directly comparing expansion of transduced *Ptpn22*$^{-/-}$ cells with control wild-type *Ptpn22*$^{+/+}$ OT-I CTLs transduced with vector and transferred together into a single host. As transduction efficiency of both wild-type *Ptpn22*$^{+/+}$ and *Ptpn22*$^{-/-}$ OT-I CTLs was consistently 50-80% of cells **(Fig 3.7)**, we transferred the cells directly without sorting. In contrast to the published literature showing increased homeostatic proliferation of *Ptpn22*$^{-/-}$ T cells than their wild-type *Ptpn22*$^{+/+}$counterparts (Brownlie et al., 2012; Salmond et al., 2014) we recovered proportionally fewer *Ptpn22*$^{-/-}$ cells than wild-type *Ptpn22*$^{+/+}$ OT-I CTLs within all groups although total cell recovery was extremely poor **(Fig 3.8B)**. Of note, the published studies addressed the homeostatic proliferation of naïve T cells whereas, due to limitation of the transduction procedure, we adoptively transferred activated cells, which resembled effector cells. Unlike the naïve T cells, the survival and proliferation of antigenic-specific memory cells are largely independent of MHC and driven by cytokines (Surh and Sprent, 2000) and it is likely that *Ptpn22*$^{-/-}$ CTLs, which were generated *in vitro* with IL-2, underwent activation induced cell death due to cytokine withdrawal to a greater extent than the wild-type *Ptpn22*$^{+/+}$ CTLs (Schluns and Lefrancois, 2003).

Another complication with the interpretation of data from the adoptive transfer experiments was the inability to recover GFP^{+} cells within any of the groups for both the *Ptpn22*$^{+/+}$ or *Ptpn22*$^{-/-}$ T cells. The loss of GFP reporter could be possibly due to either transgene silencing or competitive outgrowth of untransduced population over the transduced cells. Lentiviruses are emerging as a promising tool for gene transfer due to their ability to transduce both dividing and non-dividing cells at high efficiencies. Whether lentiviruses are also subjected to transgene silencing, however, is still controversial (He et al., 2005; Ma et al., 2003; Pfeifer et al., 2002). The molecular basis for gene silencing in lentiviruses has been attributed to cytosine

methylation of DNA and chromatin structure modification (He et al., 2005). In contrast a recent report comparing the ability of different lentiviral promoters to maintain *in vivo* gene expression in murine T cells showed that the expression of the reporter was most efficiently maintained in an EF-1alpha promoter lentiviral vector in adoptively transferred cells for 2 weeks (Gilham et al., 2010). If loss of GFP expression was due to transcriptional repression rather than transgene deletion, use of methylase inhibitors could be a way to retrieve the expression. Also it is difficult to ascertain whether the loss of reporter expression correlates with loss of transgene as GFP protein expression was independently driven by IRES. The inability to detect the presence of the Streptag sequence by PCR in DNA recovered from the cells suggested that the transferred transduced GFP^{+} cells either died upon transfer or were outgrown by untransduced cells with time as the cells were not sorted before adoptive transfer.

It is difficult to draw any conclusion from the adoptive transfer experiments given the loss of reporter expression and generation of bone marrow chimeras may be a better approach at understanding the function of PTPN22 in the biological context. I generated some preliminary results from naïve T cells recovered from RAGKO chimeras reconstituted with *Ptpn22*$^{-/-}$ bone marrow transduced with vector only, $PTPN22^{WT}$ and $PTPN22^{R619W}$ retroviral constructs, which showed that either construct reduced T cell activation compared to *Ptpn22*$^{-/-}$ T cells. $PTPN22^{WT}$ appeared to be more suppressive of T cell responses than variant $PTPN22^{R619W}$ consistent with the idea that $PTPN22^{R619W}$ was a partial loss of function allele. However we then switched from retrovirus to lentivirus transduction hoping for more efficient gene transfer and further repeats with the retrovirus system were not obtained to consolidate the preliminary results.

Finally to circumvent the problem of loss of reporter expression in transduced cells, *Ptpn22*$^{-/-}$ OT-I CTLs were transfected with $PTPN22^{WT}$ and $PTPN22^{R619W}$ YFP fusion proteins using an Amaxa nucleofection technique. To assess the functional effect of PTPN22 in signalling, phosphorylation of ERK was tested in the cells transfected with $PTPN22^{WT}$ and $PTPN22^{R619W}$ in response to a time course of stimulation with G4, a low affinity peptide recognized by the OT-I TCR. We found that ERK

phosphorylation was decreased by expression of either PTPN22^{WT} or PTPN22^{R619W} constructs when compared to vector only transduced *Ptpn22*$^{-/-}$ control cells **(Fig 3.13B middle)**. No difference in the percentage of pERK^{+} cells was seen between cells expressing PTPN22^{WT} and PTPN22^{R619W} at low levels, but high levels of PTPN22^{R619W} showed less ERK phosphorylation than *Ptpn22*$^{-/-}$ control cells suggesting a dose dependent response in inhibition **(Fig 3.15C right panel)**.

As up to 25 - 50% of PTPN22 has been shown to be bound to 5% Csk in a resting mouse T cell (Cloutier and Veillette, 1996), it is likely that when PTPN22 is expressed alone in cells, it might alter the PTPN22/Csk complex stoichiometry and potentially lead to mislocalisation, resulting in off target effects in respect to dephosphorylation. To address this possibility Weiss and colleagues co-expressed PTPN22 along with Csk in Jurkat cells and showed that when analysing the different populations of GFP expressing cells (from low, intermediary and high) there was a dose dependent effect on ERK phosphorylation following TCR signalling (Zikherman et al., 2009). Furthermore, the authors show that Jurkat cells transfected with either PTPN22^{R620W} or its mouse ortholog PTPN22^{R619W} showed greater levels of ERK phosphorylation compared to wild-type controls when expressed alone or in combination with Csk, thus concluding that PTPN22 R620W is in fact a loss-of-function allele, arguing that overexpression levels of the protein must be carefully controlled for and also studied in the context of Csk (Zikherman et al., 2009). In addition, since multiple TCR signalling regulators are known to interact with Csk-SH3 domain in T cells (Davidson et al., 1997), some of these phosphatases might exist in equilibrium and overexpression of PTPN22 may effect the relative affinity of various protein-protein interaction therefore the interpretation of result showing expression of PTPN22^{R619W} decreased ERK phosphorylation needs to be considered carefully.

In conclusion it remains contentious whether the R619W substitution increases or decreases functional capacity of PTPN22. Studies from two groups independently reporting generation of PTPN22 R619W KI mice, a model for a disease-associated *PTPN22* single-nucleotide polymorphism (Dai et al., 2013; Zhang et al., 2011) showed that the effect of the KI mutation on T cells was very similar to that reported

for the knock-out (KO) mice therefore suggesting that the SNP acts, in mice at least, as a loss-of-function allele. The observed discrepancy resulting in different functional consequences of the mutation in human and mice could be attributed to the species-specific difference.

3.4 Figures

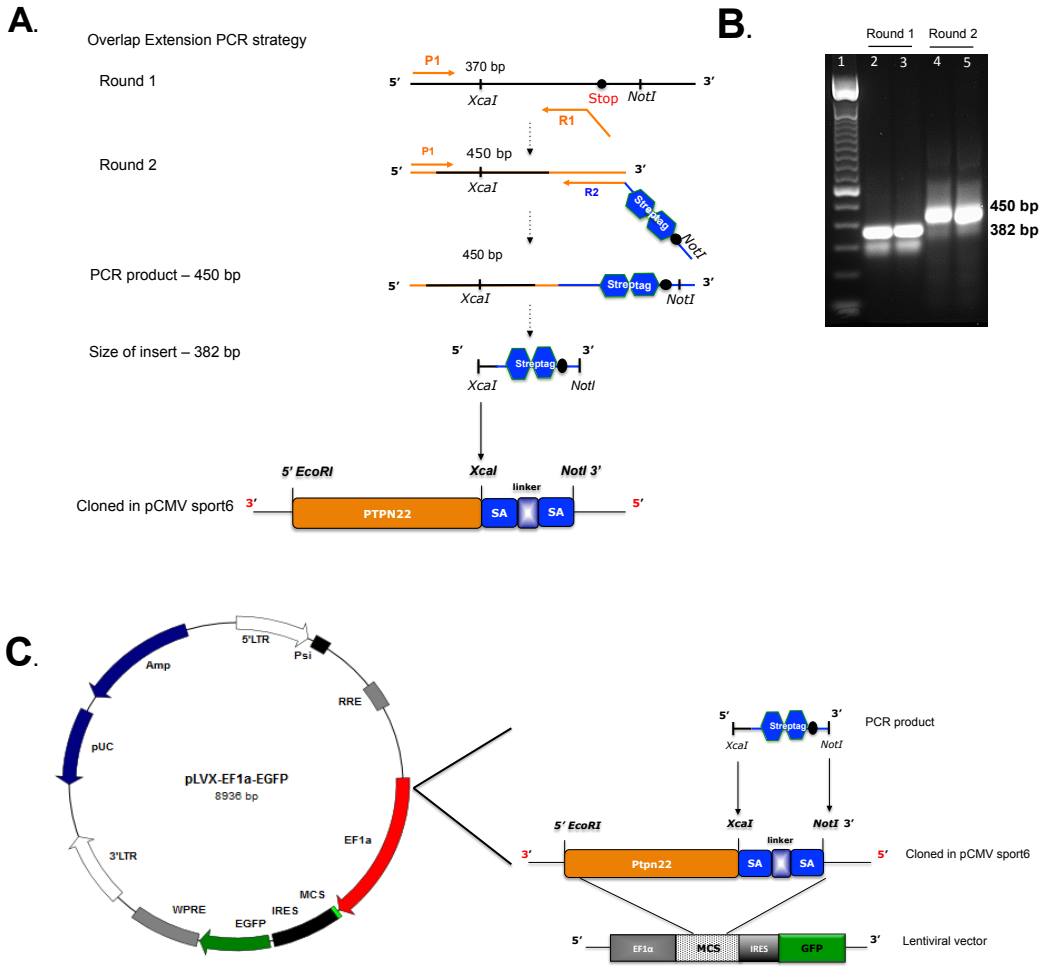

Figure 3.1 Generation of PTPN22^{WT} and PTPN22^{R619W} Streptag fusion lentiviral constructs
Illustration of the PCR-based epitope tagging method employed to generate the Streptag fusion PTPN22 constructs. **(A)** Linear representation of the amplification region of the template plasmid along with the primers and restriction sites. The Streptag was introduced at the 3' terminal by overlap extension PCR, first round amplifying 370 bp region between primer pair P1 and R1 spanning across *XcaI* restriction sites and abrogating the stop codon and *NotI* restriction site and the second round further extending the 3' end of first PCR product with 3' overlapping primer R2 (overlapping primer sequence region on R2 shown in *orange*) to generate a 450 bp PCR product complete with a stop codon and *NotI* restriction site. The PCR product was cloned back into the pCMV Sport6 vector using *XcaI* and *NotI* restriction sites in the 3' to 5' orientation (indicated as *red*). **(B)** The PCR products produced were verified by visualization with agarose gel electrophoresis. Lane 1 shows the 10 kb ladder while lanes 2 and 3 show the first PCR product (370 bp) for PTPN22^{WT} and PTPN22^{R619W} respectively and lanes 4 and 5 show the second PCR product (450 bp) for PTPN22^{WT} and PTPN22^{R619W} with two copies of Streptag. **(C)** The wild-type and the R619W full length C-terminal Streptag PTPN22 cDNA were ligated into the pLVX-EF1α-IRES-ZsGreen1pLVX Vector using the indicated restriction sites. The vector is bicistronic with the GFP reporter downstream of an IRES.

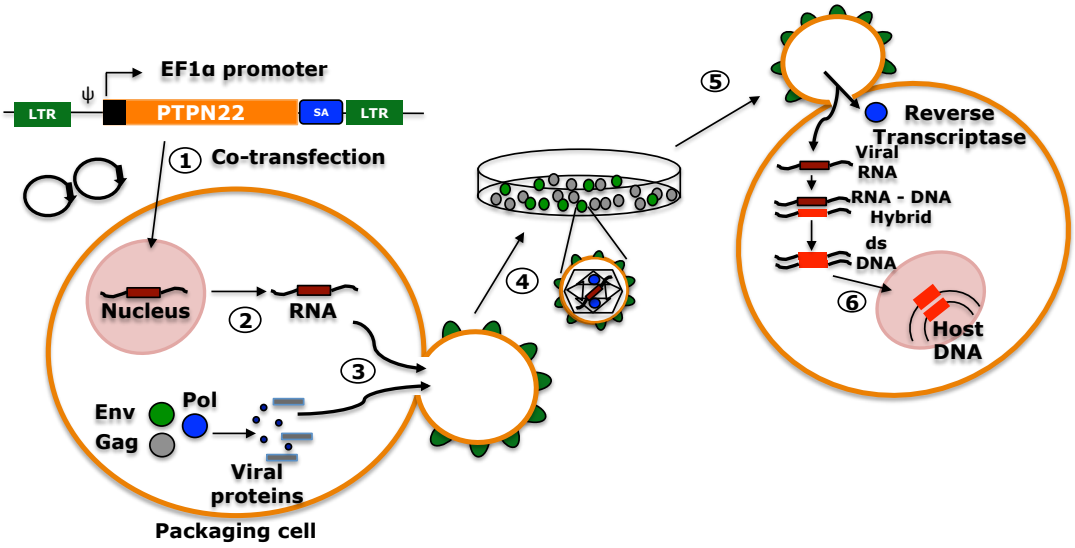

Figure 3.2 Production of recombinant lentiviral particles in 293T cells
Lentiviral construct containing full-length cDNA of PTPN22 was **(1) transfected** into 293T cells along with viral packaging elements using calcium phosphate. The DNA is **(2) transcribed** into RNA and along with the viral structural proteins it is **(3) packaged** into replication incompetent pseudo virus particles that are **(4) released** in the culture medium, which is collected and used to **(5) infect** target cells. On infection the viral RNA is **(6) integrated** into host DNA via reverse transcription.

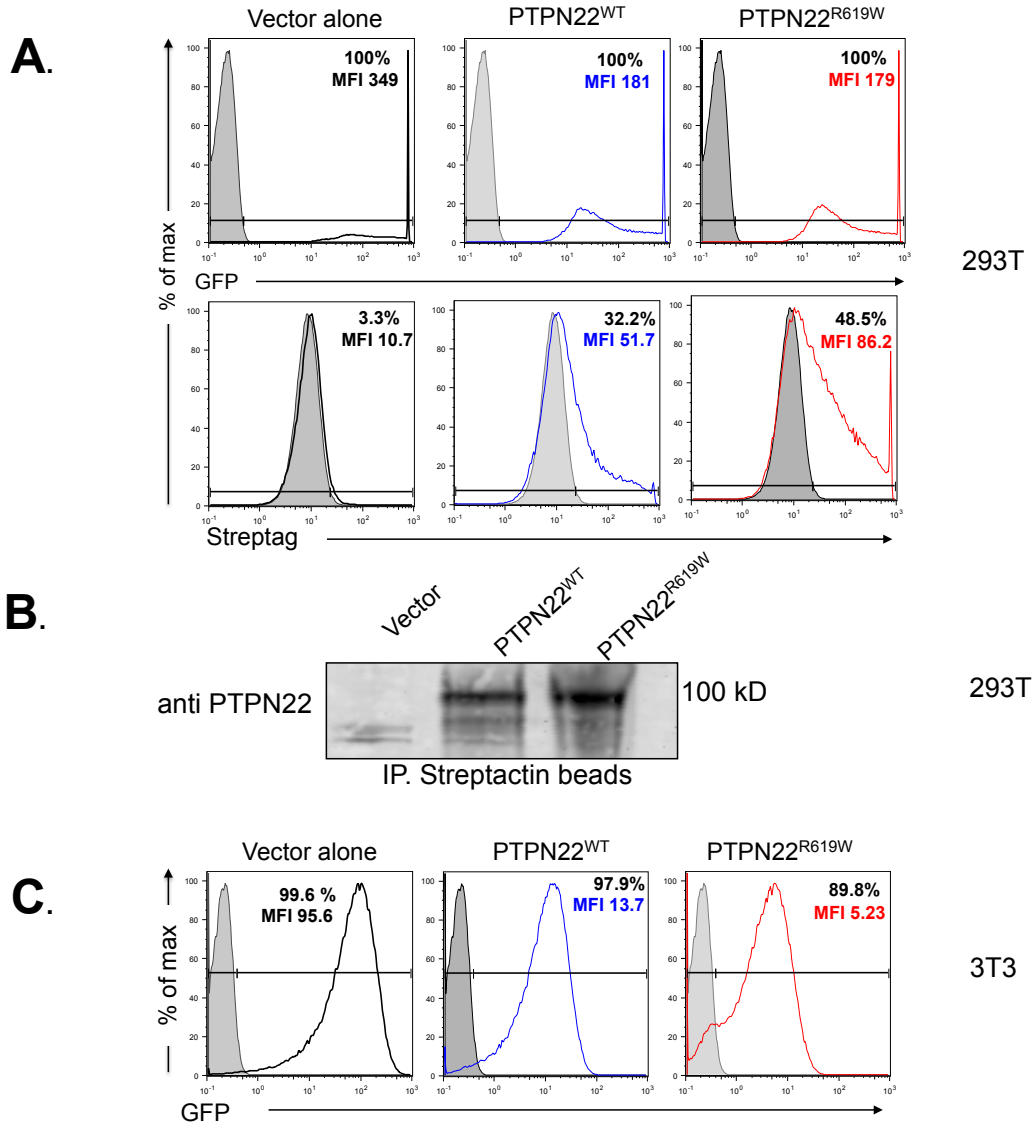

Figure 3.3 Characterisation of PTPN22 Streptag constructs and lentivirus mediated transfection of 3T3 cell line.

(A) 293T cells were transiently transfected with indicated cDNAs, 2 days following transfection, the cells were harvested and intracellular staining for the fusion Streptag was performed following which it was analysed by flow cytometry. The FACS histogram shows expression of GFP (top panel) or Streptag (bottom panel) in 293T cell lines transfected with either vector alone (black line), $PTPN22^{WT}$ (blue line) or $PTPN22^{R619W}$ (red line) compared to untransfected cells (grey shaded). The percentage and MFI of GFP^{+} and $Streptag^{+}$ population is indicated on the graphs. **(B)** Streptag tagged $PTPN22^{WT}$ and $PTPN22^{R619W}$ 293T transfected lysates were recovered by immunoprecipitation with streptactin magnetic beads and determined by immunoblotting with Goat Anti-Human PTPN22 antibody **(C)** The 3T3 cell line was infected with lentiviral supernatant generated from either vector alone (black line), $PTPN22^{WT}$ (blue line) and $PTPN22^{R619W}$ (red line), efficiency of transfection determined by expression of GFP by flow cytometry compared to untransduced cells (grey shaded).

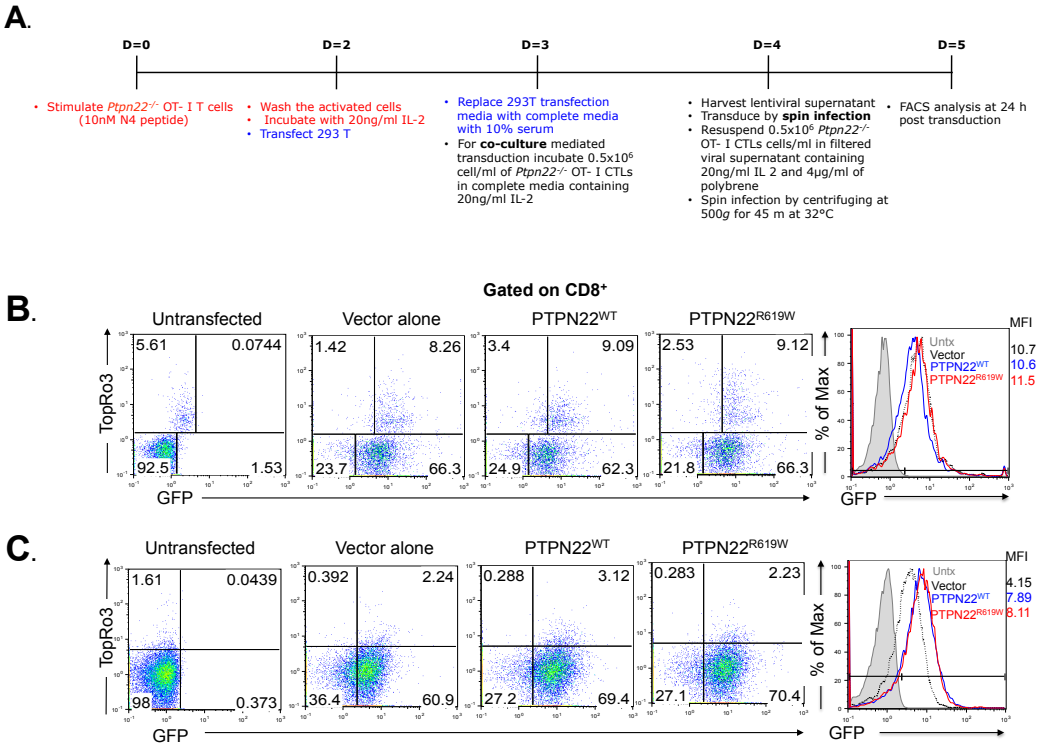

Figure 3.4. Lentiviral transduction of primary murine *Ptpn22*$^{-/-}$ OT-I T cells.
(A) Summarised protocol for lentiviral mediated transduction (steps of lentivirus generation in 293T shown in blue text on scheme) of *in vitro* generated *Ptpn22*$^{-/-}$ OT-I CTLs (described in **2.12** and shown in red text on the scheme) either by **(B)** co-culture with transfected 293T cells or **(C)** by incubation with generated lentiviral supernatant. The histogram shows expression of GFP in transduced CD8^{+} T cells either with vector only (black dotted line), PTPN22^{WT} (blue line) or PTPN22^{R619W} (red line) compared to untransduced cells (grey shaded) assessed at 24 h post transduction.

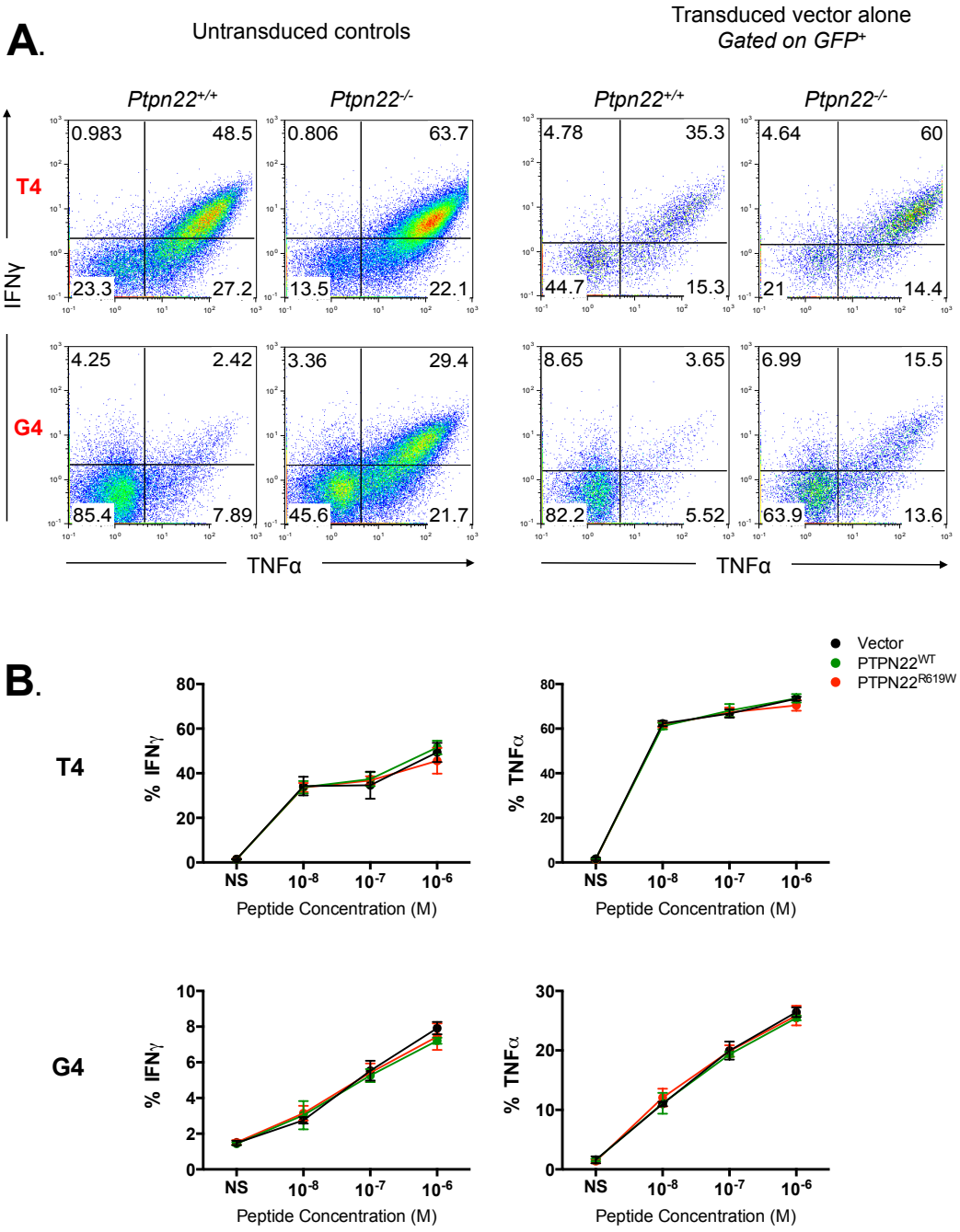

Figure 3.5 Intracellular cytokine production in PTPN22^{WT} and PTPN22^{R619W} transduced *Ptpn22*$^{-/-}$ OT-I CTLs

(A) Cytokine expression was assessed in untransduced (left panel) or vector only transduced GFP^{+} (right panel) *Ptpn22*$^{+/+}$ and *Ptpn22*$^{-/-}$ OT-I CTLs following stimulation with either 10^{-6} M T4 or G4 peptide. **(B)** The bar chart shows average percentages ± SD of IFNγ and TNFα expressing GFP positive *Ptpn22*$^{-/-}$ cells transduced either with vector only (black line), PTPN22^{WT} (green line), or PTPN22^{R619W} (red line) following re-stimulation with varying concentration (10^{-8}, 10^{-7},10^{-6} M) of intermediate (T4) and low affinity (G4) peptide. The results are representative of two individual experiments.

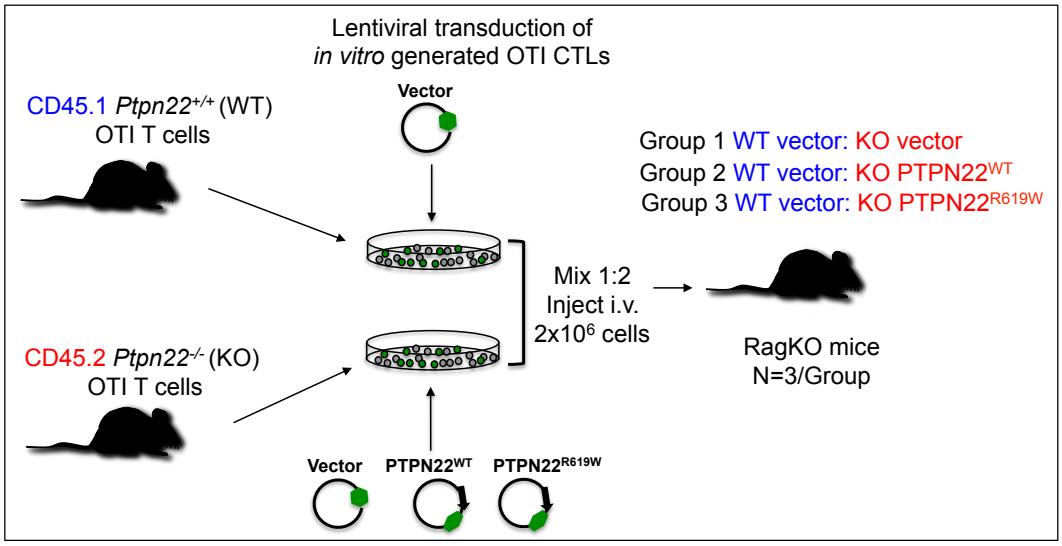

Figure 3.6 Adoptive transfer of lentivirally transduced PTPN22^{WT} and PTPN22^{R619W} *Ptpn22*$^{-/-}$ OT-I CTLs into RAGKO mice

In vitro generated OT-I CTLs (described in **2.12**) from wild-type *Ptpn22*$^{+/+}$ (CD45.1^{+}) mice were transduced with vector only and *Ptpn22*$^{-/-}$ (CD45.2^{+}) cells were transduced with either vector only, PTPN22^{WT} or PTPN22^{R619W}. Transduced CD45.1^{+} wild-type *Ptpn22*$^{+/+}$ and CD45.2^{+} *Ptpn22*$^{-/-}$ cells were mixed and injected intravenously into *Rag1*$^{-/-}$ recipient mice (n = 3) at an ~1:1 ratio (2x10^{6} cells per mouse in total).

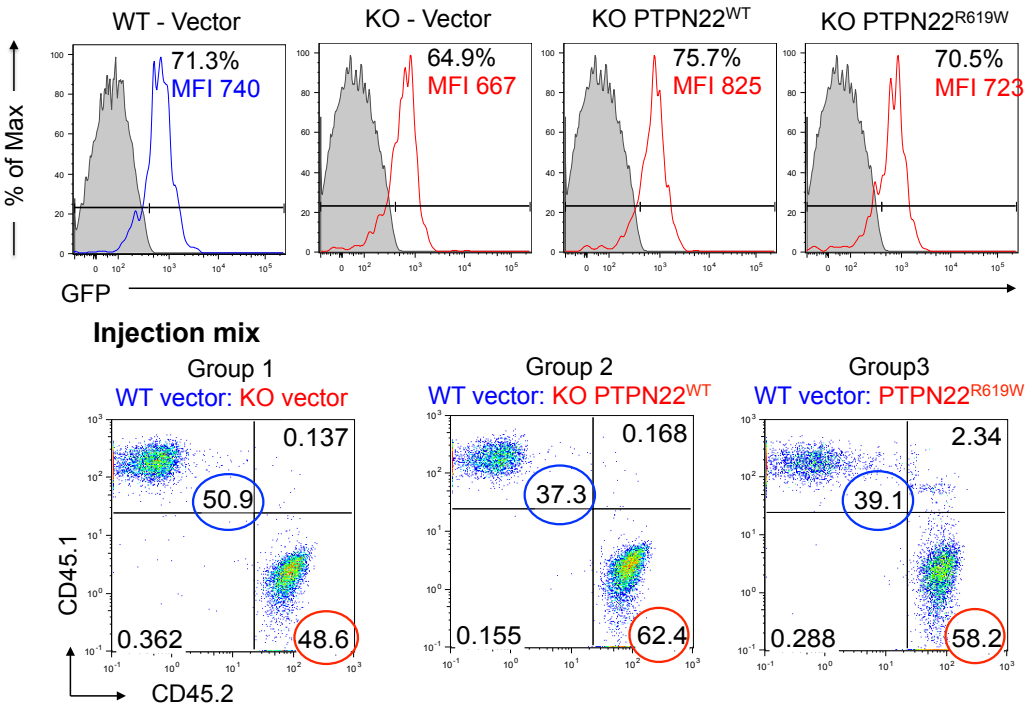

Figure 3.7 *In vitro* transduction efficiency of wild-type *Ptpn22*$^{+/+}$ and *Ptpn22*$^{-/-}$ OT-I CTLs
The histograms (*top* panel) show expression of GFP in wild-type *Ptpn22*$^{+/+}$ OT-I CTLs transduced with vector only (blue line), and *Ptpn22*$^{-/-}$ T cells transduced with either vector only, PTPN22^{WT} or PTPN22^{R619W} (red line) compared to the untransduced control (grey shaded). The percentage of GFP^{+} cells and MFI of GFP population are indicated on the plots. The FACS plots (bottom panel) shows the respective ratios of wild-type (CD45.1^{+}) and *Ptpn22*$^{-/-}$ (CD45.2^{+}) T cells in the three groups before injection; of note groups 2 and 3 did not receive 1:1 ratio of wild-type and *Ptpn22*$^{-/-}$ CD8^{+} T cells but received ~1.5 fold more *Ptpn22*$^{-/-}$ CD8^{+} T cells than wild-type *Ptpn22*$^{+/+}$ CD8^{+} T cells.

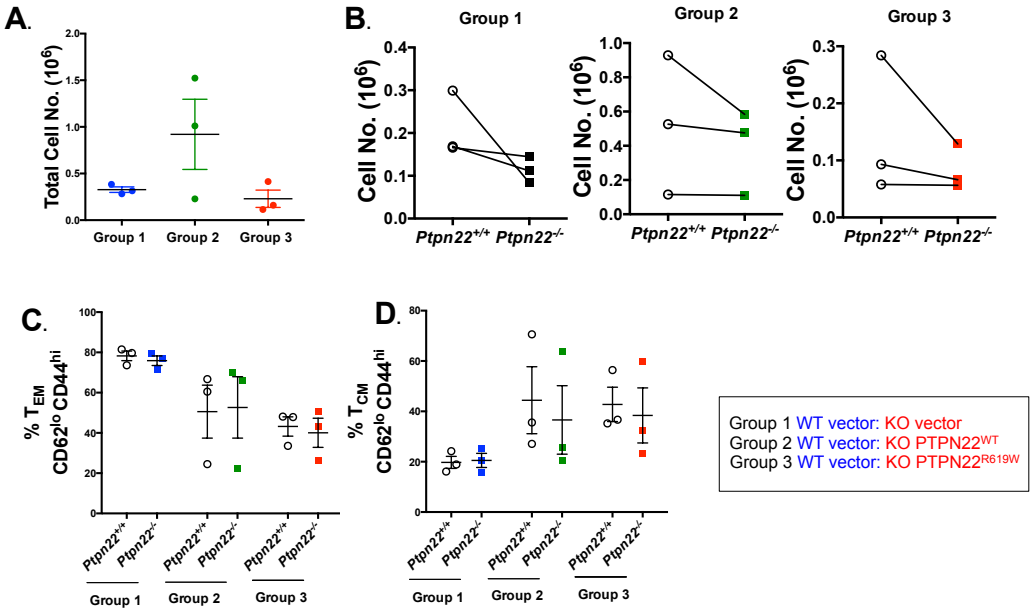

Figure 3.8 Adoptively transferred transduced *Ptpn22*$^{+/+}$ and *Ptpn22*$^{-/-}$ OT-I CTLs did not expand in RAGKO hosts

Lymph nodes and spleen were harvested from the mice 30 days post adoptive transfer (A) The graph shows total cell numbers recovered post transfer in each group (B) Total numbers of CD8^{+} wild-type *Ptpn22*$^{+/+}$ transduced with empty vector (clear circles) and CD8^{+} *Ptpn22*$^{-/-}$ T cells transduced either with vector only (black squares), PTPN22^{WT} (green square) or PTPN22^{R619W} (red square) cells recovered from the mice in the three groups. No difference was observed in the proportions of (C) effector or (D) central memory populations between the wild-type and *Ptpn22*$^{-/-}$ T cells within any of the groups. Each point represents an individual animal (n=3) and the error bars show standard error mean

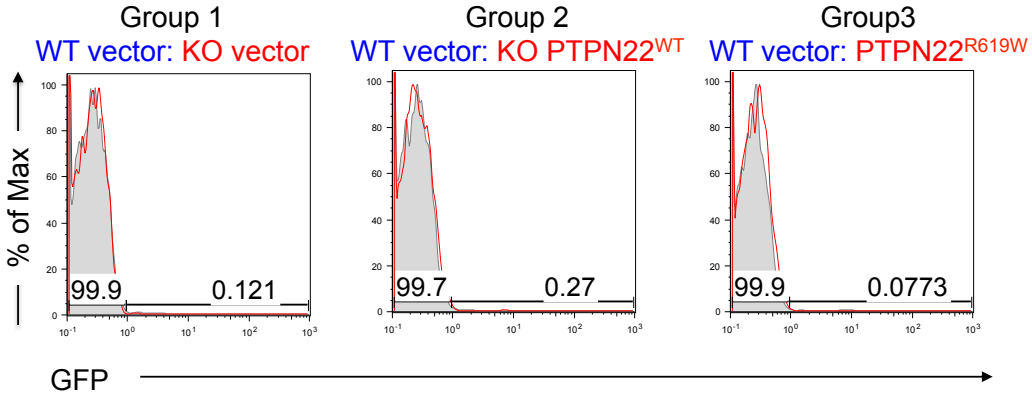

Figure 3.9 Loss of GFP expression following the adoptive transfer

The histograms show the expression of GFP wild-type *Ptpn22*$^{+/+}$ (grey fill) and *Ptpn22*$^{-/-}$ (red line) CD8^{+} T cells recovered from recipient mice 30 days post adoptive transfer in all the three groups. The gates were drawn based on an untransduced control.

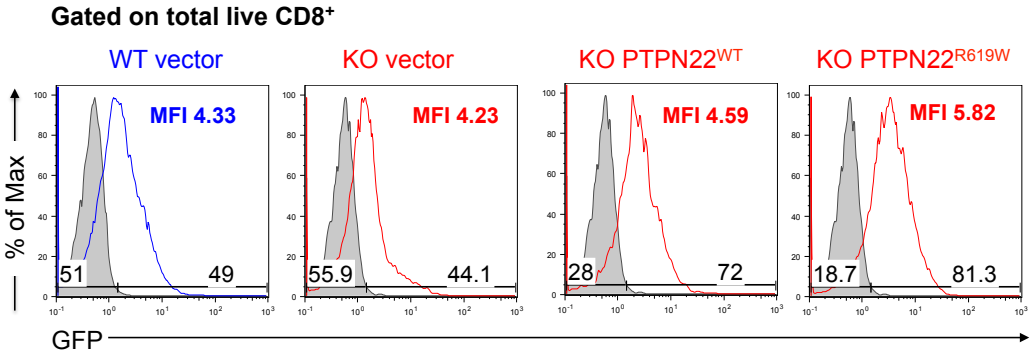

Figure 3.10 *In vitro* transduction efficiency of polyclonal wild-type and *Ptpn22*$^{-/-}$ CTLs
The histograms show expression of GFP in *Ptpn22*$^{+/+}$ T cells transduced with vector only (*blue* line), and *Ptpn22*$^{-/-}$ T cells transduced with either vector only, PTPN22^{WT} or PTPN22^{R619W} (red line) compared to the untransduced control (grey shaded). The percentage of GFP^{+} cells and MFI of GFP population are indicated on the plots.

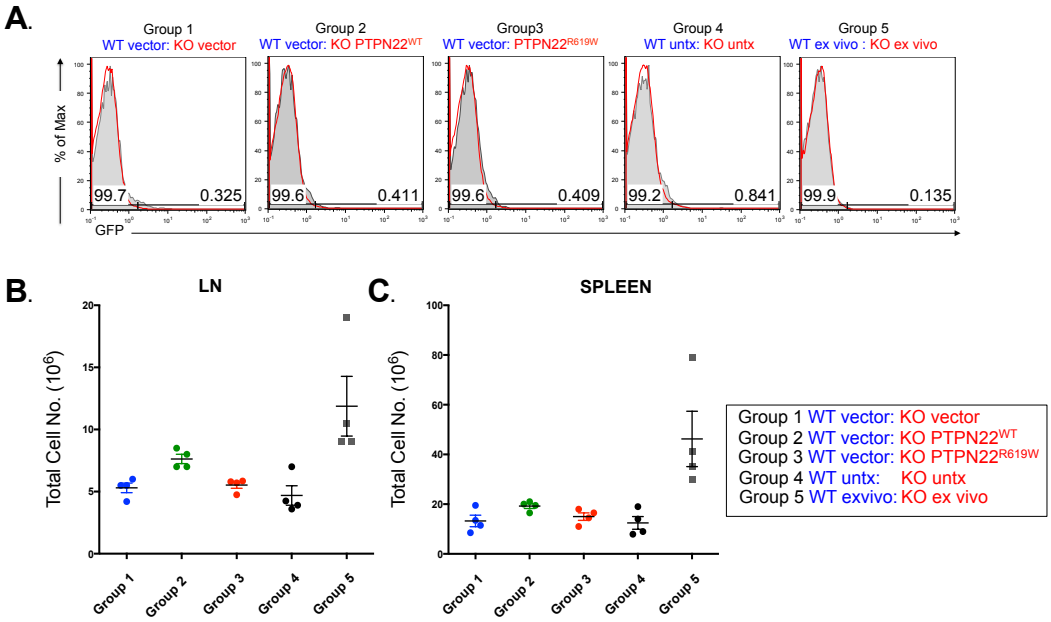

Figure 3.11 Adoptively transferred transduced wild-type *Ptpn22*$^{+/+}$ and *Ptpn22*$^{-/-}$ polyclonal activated T cells expanded in RAGKO hosts but still lost GFP expression.
Lymph nodes and spleen were harvested from the mice 10 days post adoptive transfer. **(A)** The histograms show expression of GFP in wild-type *Ptpn22*$^{+/+}$ T cells transduced with vector (grey shaded) and *Ptpn22*$^{-/-}$ T cells transduced with either vector only, PTPN22^{WT} or PTPN22^{R619W} within the different groups **(B)** The graph shows absolute total cell numbers from LN and spleen recovered post transfer in each group.

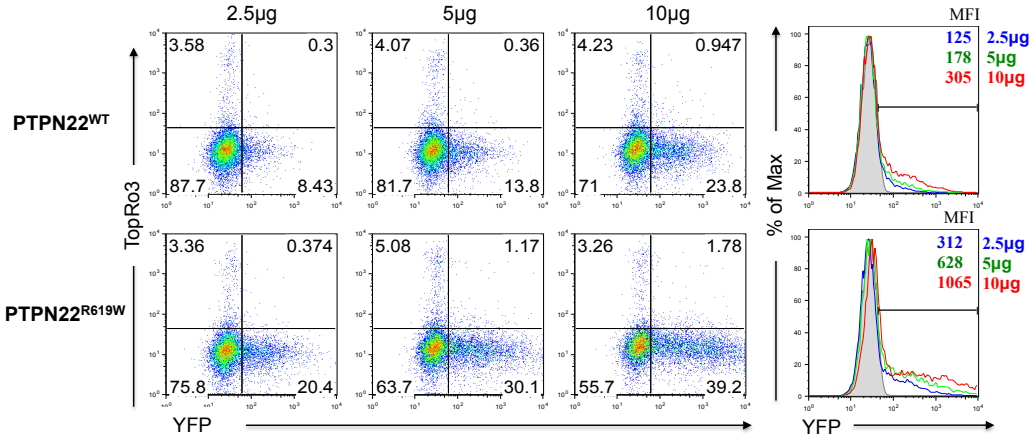

Figure 3.12 Transient transfection of PTPN22^{WT}-YFP and PTPN22^{R619W}-YFP fusion proteins in *Ptpn22*$^{-/-}$ CTLs.
5x10^6 CD8$^+$ CTLs from *Ptpn22* deficient OT-I mice were transfected with Amaxa® nucleofection technology with indicated amounts of (2.5µg, 5µg and 10µg) of PTPN22^{WT} YFP (top panel) or PTPN22^{R619W} YFP (bottom panel) DNA and incubated at 37°C/5% CO_2 for 8 hours. As shown by flow cytometry plots the expression levels of recombinant YFP protein increased proportionally to DNA concentration with either phosphatase construct. The histograms shows the level of YFP expression in transfected cells as compared to no DNA electroporated control (*grey* shaded) with 2.5µg (*blue* line), 5µg (*green* line), 10µg (*red* line) DNA for either PTPN22^{WT} or PTPN22^{R619W} YFP fusion protein. MFIs of YFP$^+$ cells are indicated on the plots and shows that PTPN22^{WT} level in transfected cells remains lower than observed for PTPN22^{R619W}

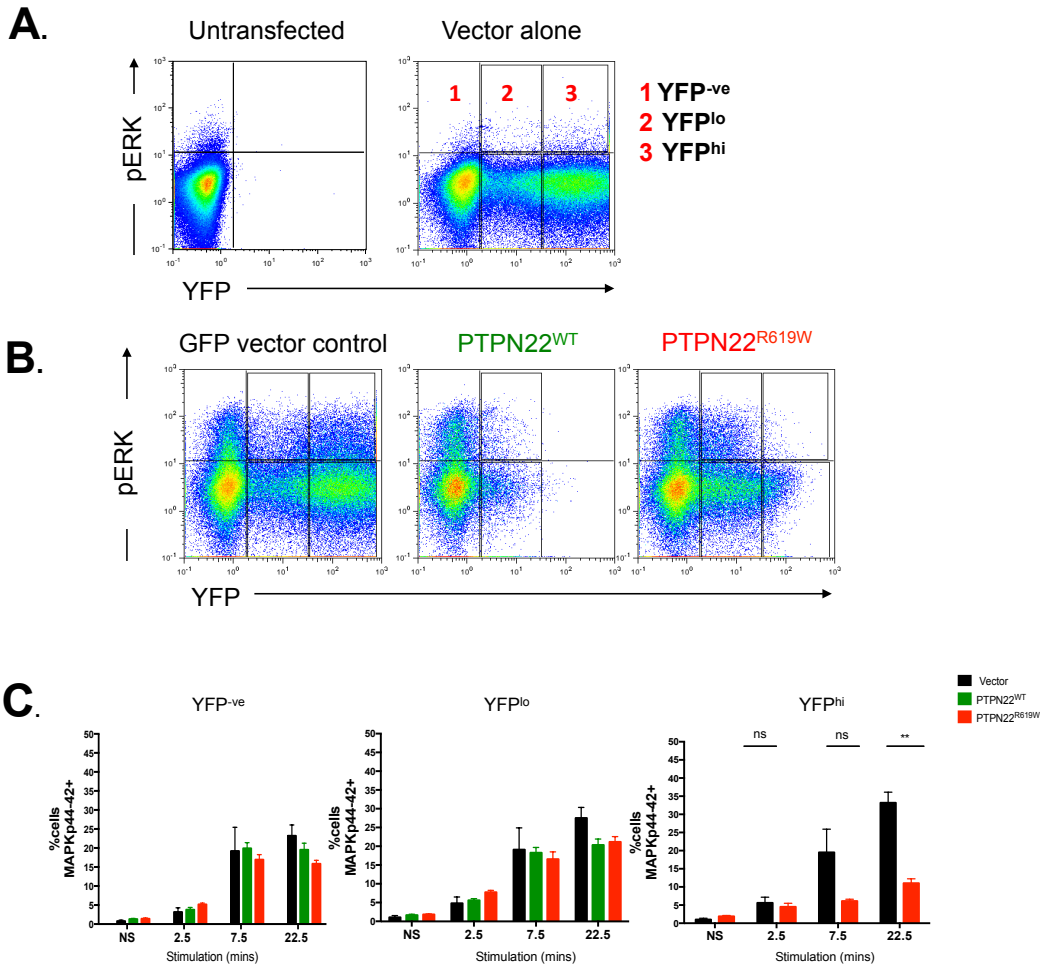

Figure 3.13 High-levels of PTPN22^{R619W}expression inhibit TCR-induced ERK phosphorylation
PTPN22^{WT} and PTPN22^{R619W} transfected *Ptpn22*$^{-/-}$ OT-I CTLs were stimulated for 2.5, 7.5 and 22.5 min with 1x10^{-7} M G4 peptide. Medium only treated cells were analysed as negative controls. **(A)** Illustration of the gating strategy devised to examine the different levels of YFP expression (YFP^{-}, YFP^{lo}, YFP^{hi}) in PTPN22^{WT} and PTPN22^{R619W}YFP fusion protein transfected cells. **(B)** Representative FACS plots showing with proportion of pERK in vector alone, PTPN22^{WT} and PTPN22^{R619W} YFP constructs at 22.5 min post stimulation **(C)** Bar graph shows the relative percentages of pERK^{+}±SD within the different YFP expressing populations in response to peptide stimulation over the time course. Data is representative of two independent experiments. Statistical significance calculated in Prism: Unpaired student's t-test, ns - non significant, **p = 0.002.

Chapter 4: What is the effect of *Ptpn22* deficiency on the SKG phenotype?

4.1 Introduction

The fate of developing thymocytes is dependent on the strength of signals originating from the interaction of T cell receptors with self-peptide/MHC ligands expressed on thymic stromal cells. Cells with overly low self-reactivity die of apoptosis; highly self-reactive clones are eliminated by negative selection while the ones with appropriate self-reactivity are retained through positive selection (Starr et al., 2003). Thus, thymic development ensures the generation of a diverse repertoire of mature $CD4^+$ and $CD8^+$ T cells capable of responding to a wide array of foreign pathogens.

ZAP-70, a Syk family tyrosine kinase that associates with the TCR CD3 and ζ subunits plays a critical role in thymocyte development and mature T cell activation (Chan et al., 1992). Loss of ZAP-70 protein expression in humans leads to severe immunodeficiency characterized by the complete absence of $CD8^+$ T cells and unresponsive mature $CD4^+$ T cells (Chan et al., 1994; Elder et al., 1994). Similarly, ZAP-70-deficient mice present a complete block at double positive (DP) selection stage of thymocyte development resulting in the complete absence of CD4 and CD8 single positive (SP) thymocytes, which could be reconstituted within the thymus following re-expression of ZAP-70 (Negishi et al., 1995). By contrast, single-nucleotide substitutions affecting ZAP-70 and other TCR signalling proximal molecules show partial defects in TCR signalling and are associated with autoimmunity. In SKG mice, a spontaneously-occurring hypomorphic W163C mutation within the carboxyl terminal SH2 domain of ZAP-70 reduces the amount of ZAP-70 protein expression and results in decreased TCR signalling and impaired thymocyte development compared to wild-type BALB/c mice (Sakaguchi et al., 2003). Furthermore, when maintained under conditions where they are exposed to microbes, i.e. not under SPF condition, these mice are prone to spontaneously develop $CD4^+$ T cell-mediated autoimmune arthritis that closely resembles rheumatoid arthritis in humans (Sakaguchi et al., 2003).

Another hypomorphic ZAP-70 mutant mouse strain, ZAP-70 YYAA, which has "knock in" alanine substitutions of tyrosine residues 315 and 319 in the interdomain B of ZAP-70 protein show similar aberration in T cell development to that of SKG mice (Hsu et al., 2009). However, T cells from the YYAA mice are less hyporesponsive to *in vitro* TCR signalling as compared to SKG mice, as shown by slight increases in Ca^{2+} flux and ERK phosphorylation in thymocytes and peripheral T cells (Hsu et al., 2009). Interestingly, unlike SKG mice which develop both spontaneous arthritis and rheumatoid factor autoantibodies, YYAA mice also developed rheumatoid factor antibodies but failed to develop autoimmune arthritis due to differential sensitivity to negative selection in YYAA mice (Hsu et al., 2009).

Graded changes in TCR signalling was first studied by taking advantage of two hypomorphic ZAP-70 mutants, *murdock (mrd), mrtless (mrt)*, each with partial defects in TCR signalling because of amino acid substitutions within the catalytic site of ZAP-70 (Siggs et al., 2007). The *mrd* mutation, which substituted an isoleucine for phenylalanine (I367F) within the kinase catalytic domain, had a modest effect on TCR signalling and thymocyte development, whereas the ZAP-70 *mrt* mutation, arising due to W405R codon change within the catalytic site, completely arrested T cell development at $CD4^+CD8^+$ double positive stage. Neither of the alleles resulted in autoimmunity individually, however autoimmunity arose when these two *Zap-70* gene variants were intercrossed (Siggs et al., 2007) revealing a threshold effect in which partial, but neither mild nor severe, T cell immunodeficiency was sufficient to break tolerance.

The differences in autoimmune syndromes in SKG, YYAA and ZAP-$70^{mrd/mrt}$ mice could be attributed to either the genetic backgrounds or to the differences in TCR signaling resulting from the quantitative and qualitative impairments in ZAP-70. An informative allelic series of ZAP-70 hypomorphic mutants containing increments of *Skg* allele and/or *Zap-70* null allele described recently, provides a model to study how genetic anomaly of T cell signalling contributes to autoimmunity (Tanaka et al., 2010). The study showed a step wise decrease in signalling from +/+, *skg/+, skg/skg* to *skg/-* in response to stimulation via the TCR which correlated with graded alterations in positive and negative selection of T cells in the thymus, thus resulting

in an altered repertoire with accumulation of self-reactive autoimmune T cell clones in a gene-dosage dependent fashion (Tanaka et al., 2010).

Collectively, these studies show that TCR affinity for MHC/peptide ligands play a central role in shaping the peripheral TCR repertoires that is further influenced by TCR signalling thresholds. An association of PTPN22 dysfunction with autoimmunity fits well with the known roles of phosphatases in attenuating signalling pathways integral to immune cellular reactivity (Rhee and Veillette, 2012). However, several key issues need to be addressed which include the substrates of PTPN22, the signalling cascades in which PTPN22 acts and finally the underlying molecular mechanism by which it regulates the adaptive immune responses to maintain or break tolerance.

To further our understanding of the effects of PTPN22 on T cell signalling, we generated double mutant SKG *Ptpn22* deficient mice (SKG *Ptpn22*$^{-/-}$) by back-crossing SKG mice with mice containing global deletion of *Ptpn22*. Substrate trap experiments conducted *in vitro* in Jurkat T cells show that ZAP-70 is one of the substrates of PTPN22, which dephosphorylates the activating Tyr493 residue on ZAP-70 (Wu et al., 2006). The combination of these two mutations provides a unique opportunity to determine the effects of PTPN22 on proximal TCR signalling molecules in the context of an autoimmune disease with a well characterised signalling disruption. We wanted to ask if increasing signalling by loss of a negative regulator would compensate for the decrease in the function of ZAP-70 (positive regulator) in SKG *Ptpn22*$^{-/-}$ mice and whether the two molecules function by affecting similar signalling pathways.

4.2 Results: Thymic development in SKG and SKG *Ptpn22*$^{-/-}$ mice

4.2.1 Impaired T cell development in *SKG Ptpn22*$^{-/-}$ mice

To investigate the effect of *Ptpn22* deficiency on SKG phenotype, we generated ZAP70$^{skg/skg}$ *Ptpn22*$^{-/-}$ double-mutant (hereafter described as SKG *Ptpn22*$^{-/-}$*)* mice. Previous studies have shown that homozygous expression of the hypomorphic

W163C ZAP70 SKG mutation results in decreased signalling through the TCR complex. In developing thymocytes, this decreased signalling results in defective positive and negative thymic selection (Sakaguchi et al., 2003). By contrast, *Ptpn22*-deficiency has no major impact on thymic selection on mice of the C57BL/6 background (Brownlie et al., 2012) and results only in a marginal increase in positive selection in some TCR transgenic strains (Hasegawa et al., 2004). Therefore, we investigated the impact of *Ptpn22* deficiency on thymocyte development in SKG *Ptpn22*$^{-/-}$ mice. As initial experiments, broad phenotypic analysis of the thymus from SKG *Ptpn22*$^{-/-}$ mice was performed.

Previously published data estimated the amount of ZAP-70 protein in thymocytes from SKG mice to be 20 to 25% of wild-type BALB/c levels (Hsu et al., 2009). Assessment of ZAP-70 protein by western blotting from thymi of age matched BALB/c, SKG and SKG *Ptpn22*$^{-/-}$ mice, showed that thymocytes from SKG and SKG *Ptpn22*$^{-/-}$ mice scanned respectively at ~18% and ~24% of BALB/c levels **(Fig 4.1A)**. These data suggest that lack of *Ptpn22* does not affect expression of ZAP-70 protein, with the amount of ZAP-70 protein in SKG *Ptpn22*$^{-/-}$ thymocytes similar to that of SKG thymocytes.

Comparison of thymus lobes taken from SKG *Ptpn22*$^{+/-}$ and SKG *Ptpn22*$^{-/-}$ mice showed no gross phenotypic abnormalities in size or morphology compared to control SKG or BALB/c thymi **(Figure 4.1B)**. The total thymocyte cell numbers from SKG *Ptpn22*$^{+/-}$ and SKG *Ptpn22*$^{-/-}$ were similar to those of SKG mice, however there was a trend for a decrease in thymic cell numbers when compared to BALB/c wild-type mice, which, although not statistically significant, was consistent with an impairment of positive selection **(Fig. 4.1C)**. These results are in agreement with published data, which showed no significant difference in total number of thymocytes and thymic architecture between SKG and BALB/c mice (Sakaguchi et al., 2003). Moreover, there was no significant difference observed in thymocyte number from SKG and SKG *Ptpn22*$^{+/-}$ mice. Therefore, all subsequent analysis compared only SKG with SKG *Ptpn22*$^{-/-}$ mice.

The development process of thymocytes can be further examined by analysis of CD4 versus CD8 expression by flow cytometry (**Fig 4.2A)**. Three distinct stages of thymic T cell development are defined based on the expression of CD4 and CD8: the double-negative (DN) stage ($CD4^-CD8^-$), the DP stage ($CD4^+CD8^+$) and the SP stage ($CD4^+CD8^-$ or $CD4^-CD8^+$). Analysis of DN thymocytes from SKG and SKG *Ptpn22*$^{-/-}$ mice showed no significant difference either in proportion **(Fig 4.2A)** or absolute DN cell numbers **(Table 4.1)** in comparison to the wild-type BALB/c DN thymocytes. Additionally examination of the various subsets of DN; DN1, DN2, DN3 and DN4, facilitated by staining for CD25 and CD44, showed no striking difference in percentages between BALB/c, SKG and SKG *Ptpn22*$^{-/-}$ **(Fig 4.2B)**; the only discernable differences was a marginal decrease in frequency of DN1 subset in SKG *Ptpn22*$^{-/-}$ mice. Overall these results show that there was no block in the progression of thymocytes from DN to DP stage in SKG and SKG *Ptpn22*$^{-/-}$ mice. This is in line with published literature showing that ZAP-70 expression is not crucial in transition of thymocytes from DN to DP (Negishi et al., 1995).

As previously reported for SKG mice (Sakaguchi et al., 2003), the proportions, but not the numbers, of DP cells were significantly increased, whereas both the proportions and the absolute numbers of $CD4^+$ SP and $CD8^+$ SP thymocytes were significantly reduced compared to the wild-type BALB/c control (**Fig 4.2A, Table 4.1)**. Loss of *Ptpn22* did not significantly affect these parameters, with similar increase in percentages of SKG *Ptpn22*$^{-/-}$ DP cells (92.6% ± 0.79) to that of SKG (91.6% ± 0.92) cells. The proportion of SKG *Ptpn22*$^{-/-}$ DP cells was increased compared to BALB/c DP cells (77.63% ± 4.27), which correlated with the slight increment observed in DP thymocyte absolute cell numbers **(Fig 4.2A, Table 4.1)**. As observed in SKG thymocytes, the absolute numbers of $CD4^+$ SP and $CD8^+$ SP cells was profoundly reduced in SKG *Ptpn22*$^{-/-}$ mice **(Table 4.1)**. Further analysis of the CD8 SP thymocytes, revealed that some of the CD8 SP thymocytes in both SKG and SKG *Ptpn22*$^{-/-}$ mice were immature, TCR-negative cells **(Table 4.1)**.

Therefore, thymocyte development in SKG *Ptpn22*$^{-/-}$ mice and SKG mice was similarly affected, in that proportionally fewer DP thymocytes from SKG *Ptpn22*$^{-/-}$ and SKG mice matured into either $CD4^+$ SP or $CD8^+$ SP in comparison to wild-type

BALB/c control (~5 fold less than BALB/c). These data indicate that, in the context of the SKG mutation, *Ptpn22* expression does not have a major influence on overall thymocyte differentiation (**Fig 4.2A, Table 4.1)**.

4.2.2 Positive selection is partially rescued in SKG *Ptpn22*$^{-/-}$ thymocytes

Thymocyte development is an extremely orchestrated process, which is highly dependent on receptor signalling. Signals via TCR are critical for determining positive versus negative selection at the DP stage of development to generate a refined self-restricted and self-tolerant T cell repertoire in the periphery (Gascoigne and Palmer, 2011). The importance of ZAP-70 for T cell development is emphasized by the fact that loss of ZAP-70 completely arrests T cell development at DP stage with the complete absence of $CD4^+$ and $CD8^+$ SPs (Negishi et al., 1995). Partial loss of ZAP-70 as seen in SKG mice, results in defective thymic positive and negative selection which leads to failure in deletion of autoreactive T cells that cause arthritis (Sakaguchi et al., 2003). To determine the effect of *Ptpn22* deficiency on thymocyte differentiation in SKG *Ptpn22*$^{-/-}$ mice a more detailed examination of positive selection in thymocytes was carried out.

Thymocytes undergoing positive selection can be identified by staining for the early activation marker CD69 together with the TCR (Yamashita et al., 1993). **Fig 4.3A** shows the gating strategy for identification of the distinct stages of thymocyte differentiation stages from total live thymocytes. The $CD69^-TCR^-$ cells in gate 1 (purple) represent mostly pre-selection $CD4^+CD8^+$ cells. As the thymocytes initiate positive selection, they express intermediate levels of CD69 and TCR, shown by gate 2 (green) while cells undergoing positive selection expressed high levels of both CD69 and TCR as denoted by gate 3 (orange) and finally as the thymocytes mature into CD4 or CD8 SP cells they stop expressing CD69 and retain high levels of TCR expression as indicated by gate 4 (blue). **Fig 4.3B** shows the proportions of BALB/c, SKG and SKG *Ptpn22*$^{-/-}$ thymocytes in these 4 distinct development stages. The table shows the average proportion of cells in the different positive selecting gates for individual strains with 6-9 mice for each genotype **(Fig 4.3C)**. In comparison to

BALB/c, both SKG and SKG *Ptpn22*$^{-/-}$ thymocytes showed a significant increase ($p<0.0001$) in proportion and numbers of thymocytes, within gate 1 indicating that more thymocytes were retained in the pre-selection stage. Significantly decreased frequencies of SKG and SKG *Ptpn22*$^{-/-}$ thymocytes in comparison to BALB/c thymocytes were noted for all the subsequent stages of progression (gate 2, gate 3) with fewer thymocytes finally maturing into SPs (gate 4). A trend in the increased frequency of cells in gates 2 – 4 is noted in the SKG *Ptpn22*$^{-/-}$ thymocytes compared to SKG but only the increase in frequency within gate 2 was significant ($p<0.01$) **(Fig 4.3 B and C)**

This observation suggested that *Ptpn22* deficiency might potentially affect positive selection in SKG *Ptpn22*$^{-/-}$ thymocytes. To further dissect the impact of loss of *Ptpn22* on thymic differentiation, the expression of TCRβ and CD5 in DP thymocytes was assessed. The level of TCR signalling directly correlates with and quantitatively influences levels of CD5 surface expression in DP thymocytes (Azzam et al., 1998). The TCR levels of SKG and SKG *Ptpn22*$^{-/-}$ DP thymocytes were indistinguishable and were substantially lower than wild-type Balb/c cells **(Fig 4.4A)**. By contrast, the levels of CD5 expression in SKG *Ptpn22*$^{-/-}$ DP thymocytes were markedly increased above that of SKG DP thymocytes **(Fig 4.4A)**, reflecting that the loss of *Ptpn22* enhanced the intensity of TCR signalling.

The levels of both TCR and CD5 are developmentally regulated in thymus and increase from DN to DP to SP stages of development, therefore thymocytes at temporally distinct stages of maturation could be distinguished by gating for CD5 versus TCR (Azzam et al., 1998). The DP population can be subdivided into three subsets on the basis of CD5 versus TCR staining: DP1 ($TCR^{lo}CD5^{lo}$), DP2 ($TCR^{int}CD5^{hi}$) and DP3 ($TCR^{hi}CD5^{int}$) (Saini et al., 2010). Saini *et al*. showed that the timing of CD4-CD8 lineage commitment is determined by ZAP-70 dependent TCR signals and the development of $CD4^+$ and $CD8^+$ T cells were temporally separated and originated from these distinct subsets, with $CD4^+$ SP population arising from the DP2 subset at ~48h and the $CD8^+$ SP population emerging about one day later from the DP3 subset following induction of ZAP-70 expression (Saini et al., 2010). **Fig 4.4B** shows the representative dot plots of CD5 versus TCR in DP

thymocytes from BALB/c, SKG and SKG *Ptpn22*$^{-/-}$. The proportion of cells in each gate from individual mice is tabulated and shown in **Fig 4.4C**. The abundance of both CD5 and TCR depends on the levels and function of ZAP-70 (Otsu et al., 2002) and given that the amount of ZAP-70 protein is reduced due to the W163C point mutation, therefore as expected, the proportion of thymocytes in DP2 and DP3 subsets was significantly reduced in both SKG and SKG *Ptpn22*$^{-/-}$ thymocytes when compared to wild-type BALB/c. Comparison of the proportion of thymocytes within the three subsets indicated comparable proportions in DP1 subset but a significant two fold increase in the proportion of thymocytes over SKG was noted in DP2 ($p = 0.0001$) and DP3 subsets ($p = 0.016$) in SKG *Ptpn22*$^{-/-}$ **(Fig 4.4C)**.

Taken together, *Ptpn22* deficiency increased the frequency of cells within the DP2 subset **(Fig 4.4C)** with a trend towards a modest increase in the absolute numbers of $CD4^{+}$SP thymocytes **(Table 4.1)** in SKG *Ptpn22*$^{-/-}$ mice compared to SKG mice, suggesting a subtle enhancement of positive selection.

4.2.3 *Ptpn22* deficiency enhances signalling through the TCR in SKG thymocytes

Ca^{2+} flux initiated by the activation of PLCγ is an early consequence of TCR signalling and results in NFAT translocation to the nucleus (Masuda et al., 1998). Initial experiments were undertaken to establish whether there was a difference in Ca^{2+} signalling between *Ptpn22*-deficient and wild-type thymocytes on a C57BL/6 background i.e. when normal ZAP-70 was present. Cells from *Ptpn22*$^{-/-}$ thymus was labelled with low concentration of CFSE and mixed with wild-type *Ptpn22*$^{+/+}$ thymocytes in 1:1 ratio and loaded with the Ca^{2+} sensitive fluorescent dye indicator Indo 1. Thymocytes were stimulated by incubating with biotinylated antibodies that were cross-linked by addition of streptavidin. Calcium flux measurement was carried out by assessing the ratio of bound calcium (emitted at 390nm Violet) or unbound calcium (emitted at 500nm Blue) to the Indo-1 dye by flow cytometry. In contrast to a previous study, which showed that CD3 stimulation resulted in greater increase in Ca^{2+} flux in the double positive thymocytes of PTPN22-deficient mice compared with that of wild-type mice (Maine et al., 2012), we found no differences in Ca^{2+} flux

in double positive thymocytes of PTPN22 KO and wild-type mice following stimulation via crosslinking of CD3 with CD4 **(Fig 4.5)**.

As increased expression of CD5 at the DP stage is associated with enhanced TCR signalling (Azzam et al., 2001; Azzam et al., 1998), we sought to determine whether the lack of *Ptpn22* in SKG thymocytes increased the sensitivity to TCR signalling. If so this might explain why DP thymocytes from SKG *Ptpn22*$^{-/-}$ had increased levels of CD5 expression compared to SKG thymocytes **(Fig 4.4A)**. Cells from BALB/c, SKG and SKG *Ptpn22*$^{-/-}$ thymus were labelled with different concentration of CFSE to distinguish each population **(Fig 4.6A)**. As described above, the cells were mixed in 1:1:1 ratio, loaded with the Indo 1 and the thymocytes were stimulated by cross-linking. Cross-linking TCR with CD4 or CD3 with CD4, but not TCR alone, induced a robust peak of intracellular Ca^{2+} flux in wild-type BALB/c DP thymocytes whereas Ca^{2+} flux in SKG thymocytes was impaired, as has been reported previously (Sakaguchi et al., 2003). The absence of *Ptpn22* partially restored the ability of TCR with CD4 or CD3 with CD4 crosslinking to induce Ca^{2+} flux in SKG DP cells, although it was lower than wild-type BALB/c control **(Fig 4.6B)**.

Mitogen activated protein kinase (MAPK) pathways are major pathways induced by TCR stimulation and are critical for T-cell responses (Smith-Garvin et al., 2009). In particular, the ERK cascade is reported to play an important role in the regulation of T cell activation and can be differentially regulated based on TCR signal strength (Daniels et al., 2006). Thymocytes from BALB/c, SKG and SKG *Ptpn22*$^{-/-}$ were labelled with different concentration of Cell trace dye and mixed in ~1:1:1 ratio **(Fig 4.7A)**. The extent of ERK phosphorylation stimulated by antibody-mediated crosslinking of CD3 and CD4 was determined at various time points by FACS analysis using a phospho-Erk antibody **(Fig 4.7B)**. As reported previously, phosphorylation of ERK was markedly reduced in SKG compared to wild-type BALB/c thymocytes (Sakaguchi et al., 2003). SKG *Ptpn22*$^{-/-}$ thymocytes displayed marginally increased ERK phosphorylation compared to SKG thymocytes as shown by increased percentage and MFI of $pERK^{+}$ cells at 2 mins but the response of both SKG and SKG *Ptpn22*$^{-/-}$ thymocytes declined more rapidly than that of BALB/c thymocytes **(Fig 4.7C)**. In response to PdBU stimulation, levels of ERK

phosphorylation were comparable in all 3 mouse strains **(Fig 4.7C)**. This control indicated that there were no intrinsic defects in the ERK MAPK pathway in SKG and SKG *Ptpn22*$^{-/-}$ cells and that the major differences arose from defects in TCR-dependent activation of the pathway.

Collectively, these data showed that *Ptpn22* deficiency improved signalling downstream of the TCR in developing SKG thymocytes, although this seemed stronger for the Ca^{2+} rather than the ERK pathway. These data complement the results obtained in **Fig 4.4A** that showed increased levels of CD5 expression in SKG *Ptpn22*$^{-/-}$ DP thymocytes with comparable TCRβ expression to SKG DP thymocytes, therefore, indicating an increased signalling potential due to lack of *Ptpn22*. These data are also in agreement with published literature showing *Ptpn22* deficiency has direct effects on T cell signal transduction (Brownlie et al., 2012; Hasegawa et al., 2004).

4.2.4 *Ptpn22* deficiency does not alter the TCR repertoire compared to SKG mice

In BALB/c mice, thymocytes expressing TCR Vβ3, Vβ5, Vβ11 and Vβ12 chains are reactive with endogenous viral superantigens encoded by Mtv-8 and Mtv-9, and are subsequently deleted (Matsutani et al., 2006). It has been noted that there is an increased frequency of thymocytes bearing these TCR Vβ subfamilies in SKG mice indicating a failure in negative selection (Hsu et al., 2009). Furthermore, a recent study showed that a graded decrease in TCR signal strength by the expression of aberrant ZAP-70 led to alteration of TCR repertoire due to failure of deletion of self reactive autoimmune clones in the thymus (Tanaka et al., 2010). Therefore we sought to determine if there was any effect of *Ptpn22* deficiency on expression of particular TCR Vβ families.

FACS analysis showed that the frequency of mature $CD4^{+}CD5^{+}$ thymocytes expressing TCR Vβ3, Vβ5 or Vβ11 chains was increased in SKG as compared to wild-type BALB/c thymi (**Fig 4.8**). Additionally a compensational decrease in the proportion of TCR Vβ8.1/8.2^{+} cells which are normally positively selected was noted

in SKG cells. This is in line with published literature (Hsu et al., 2009). Despite increased expression of CD5 and signalling in SKG *Ptpn22*$^{-/-}$ compared to SKG thymocytes, there was no significant difference in the TCR Vβ repertoire representation in either mature CD5^{+} CD4^{+} SP or CD5^{+} CD8^{+} SP SKG *Ptpn22*$^{-/-}$ thymocytes **(Fig 4.9)**. Furthermore, compared to T cells from SKG mice, SKG *Ptpn22*$^{-/-}$ T cells showed no significant differences in the repertoire of peripheral CD4^{+} or CD8^{+} T cells expressing particular Vβs except for Vβ11 **(Fig 4.9)** which could be attributed to very few cells that were acquired.

These data indicate that *Ptpn22* deficiency does not significantly increase negative selection in SKG *Ptpn22*$^{-/-}$ mice compared to SKG mice and the increase in TCR signalling caused by loss of *Ptpn22* is insufficient to cause significant alteration in Vβ repertoire usage. This result is supported by previous studies reporting that *Ptpn22* has minimal role in negative selection (Hasegawa et al., 2004).

4.2.5 *Ptpn22* deficiency does not change the total cell numbers in the periphery in comparison to SKG mice.

Collectively, studying the thymic development in SKG *Ptpn22*$^{-/-}$ mice demonstrated that the loss of *Ptpn22* in SKG *Ptpn22*$^{-/-}$ mice partially rescued positive selection and increased the sensitivity of signalling in thymocytes. We next assessed whether it altered the composition or function in the resulting pool of peripheral T cells.

Previous reports have shown that *Ptpn22*$^{-/-}$ mice of the C57BL/6 background develop splenomegaly and lymphoadenopathy suggesting a dysregulation of the lymphoid compartment (Brownlie et al., 2012; Hasegawa et al., 2004). **Fig 4.10** shows an image of lymph nodes and spleen taken from a 7-week old SKG *Ptpn22*$^{-/-}$ mouse compared to age matched SKG and BALB/c wild-type control mice. The size of the lymphoid organs is similar in all 3 mouse strains, which is further reflected by no significant differences in the total cell numbers in SKG *Ptpn22*$^{-/-}$ compared to SKG and BALB/c wild-type control mice. These data are consistent with published reports of a lack of effect of the SKG mutation on LN and spleen cellularity (Sakaguchi et al., 2003).

4.2.6 Increase in proportion of effectors with age in SKG *Ptpn22*$^{-/-}$ mice.

FACS analysis of peripheral T cells in SKG *Ptpn22*$^{-/-}$ mice showed a similar decrease in proportions of CD4^{+} and CD8^{+} T cells as that of SKG mice **(Fig 4.11)**. Numbers of CD4^{+} and CD8^{+} T cells in lymph nodes **(Table 4.2)** and spleen **(Table 4.3)** from SKG mice were reduced compared with wild-type BALB/c mice as previously reported (Sakaguchi et al., 2003). Consistent with the trend towards an increase in the absolute numbers of CD4^{+} SP thymocytes **(Table 4.1)**, there was an increase in the absolute numbers of CD4^{+} T cells in LN from SKG *Ptpn22*$^{-/-}$ mice as compared to SKG mice, with numbers similar to that of BALB/c mice **(Table 4.2)**. In contrast, there was no increase in the number of CD4^{+} T cells in the spleen **(Table 4.3)**. Additionally SKG *Ptpn22*$^{-/-}$ also showed similar relative increase in B cell numbers as observed in SKG mice and compared to wild-type BALB/c mice **(Table 4.2)**.

Naïve T cells generated under lymphopenic conditions acquire memory-phenotype, showing higher level expression of memory marker CD44 due to extensive homeostatic proliferation (Sprent and Surh, 2011). SKG mice show a lymphopenia induced increase in the effector population in the periphery due to reduced thymic output of CD4^{+} and CD8^{+} T cells (Sakaguchi et al., 2003), whereas the effector/memory population is increased in *Ptpn22*$^{-/-}$ deficient mice due to lack of homeostatic regulation (Brownlie et al., 2012; Salmond et al., 2014). We wanted to assess if the deficiency of *Ptpn22* on the SKG background increased the effector and memory cell population in the periphery of SKG *Ptpn22*$^{-/-}$ mice. Although young (6 week old) SKG *Ptpn22*$^{-/-}$ mice showed no difference in effector/memory T cell pools compared to SKG mice as characterised by CD44 and CD62L expression in CD4^{+} and CD8^{+} T cells by FACS. Further examination of the CD4^{+} and CD8^{+} T cells in the LN of older SKG *Ptpn22*$^{-/-}$ mice (> 5 months) showed increased proportions, but not cell numbers, of effector memory T cell pools compared to SKG mice as determined by CD44^{hi}CD62L^{lo} **(Fig. 4.12)** and CD45RB^{lo} population **(Fig. 4.13)**. Additionally, the increase in effector/memory phenotype was accompanied by a decrease in the frequency of naïve cell (CD44^{lo}CD62L^{hi}) **(Fig 4.12)**. By contrast, the

proportions of $CD44^{hi}CD62L^{hi}$ central memory population were similar in SKG and SKG *Ptpn22*$^{-/-}$ mice. These data show that $CD4^+$ T cells from SKG *Ptpn22*$^{-/-}$ have a significant increase in proportions of $CD44^{hi}CD62L^{lo}$ and $CD45RB^{lo}$ populations, suggestive of T cells responding to endogenous autoantigens or to the lymphopenic environment.

4.2.7 *Ptpn22* deficiency increased the numbers of Tregs in SKG *Ptpn22*$^{-/-}$ mice

Decrease in TCR signal strength due to deficiency of ZAP-70 results in a decrease in the proportion of thymic Tregs in SKG mice, however, in contrast to the thymus, the ratios of Tregs are substantially increased in the lymph nodes and spleen of the SKG mice in comparison to BALB/c mice due to lymphopenia (Tanaka et al., 2010). Our data indicated that the loss of *Ptpn22* in SKG mice altered the signal intensity in the thymocytes of SKG *Ptpn22*$^{-/-}$ mice **(Fig 4.4A)**. TCR signal strength is crucial in development of Tregs, which can develop either in the thymus (natural Tregs; nTregs) or in the periphery upon T cell activation (induced Tregs; iTregs) (Josefowicz and Rudensky, 2009). The increase in number could be explained by the increased number of thymic nTregs, increased induction of iTregs in the periphery, or increased survival/expansion of either or both of these populations. We examined if *Ptpn22* deficiency in SKG mice led to changes in proportions of thymic and peripheral Tregs. The percentages and the absolute cell numbers of $FoxP3^+$ cells were not increased in thymi of young (~7-week-old) SKG *Ptpn22*$^{-/-}$ mice compared to those in SKG mice **(Fig 4.14)** thus suggesting comparable selection of nTregs in both strains. We noted a mild increase in the percentages and the cell numbers of $CD25^+FoxP3^+$ Tregs in both the lymph nodes and spleen in SKG *Ptpn22*$^{-/-}$ mice compared to SKG mice **(Fig 4.15)**.

Taken, together these data suggest that loss of *Ptpn22* enhances T cell signalling in SKG mice leading to the subtle increase in numbers of Tregs. This is line with previously published literature showing *Ptpn22*$^{-/-}$ mice presented with increased proportion and numbers of peripheral Tregs (Brownlie et al., 2012).

4.3 Discussion

The aim of the work presented in this chapter was to determine the impact of *Ptpn22* deficiency on T cell development and signalling in context of SKG background. To this end we compared the SKG *Ptpn22*$^{-/-}$ mice with SKG mice, which contains a spontaneous W163C mutation in the C-terminal domain of ZAP-70 and results in reduced levels of ZAP-70 protein (Sakaguchi et al., 2003) **(Fig 4.1A)**.

PTPN22 is a negative regulator of early TCR signalling that tempers the activity of SFKs, including Lck by dephosphorylation of the activatory tyrosine residue on Lck^{Y394} (Cloutier and Veillette, 1999; Gjorloff-Wingren et al., 1999). Moreover, PTPN22 may also attenuate signals via the TCR by dephosphorylating ZAP-70, CD3ε/ζ and Vav (Wu et al., 2006). ZAP-70 plays a critical role in TCR signalling both during thymocyte maturation and in mature T cell responses (Chan et al., 1992). Thymocyte development and TCR signalling is significantly impaired in SKG mice leading to decreased numbers of CD4$^+$ and CD8$^+$ SP thymocytes and diminished signalling (Sakaguchi et al., 2003; Sakaguchi et al., 2006). Phenotyping of *Ptpn22*$^{-/-}$ mice suggested that *Ptpn22* deficiency may augment positive selection in *Ptpn22*$^{-/-}$ mice, either polyclonal or TCR transgenic, displayed increased fractions and numbers of CD4 SP cells (Hasegawa et al., 2004) and similar results were found in two independently generated PTPN22^{R619W} mice (Dai et al., 2013; Zhang et al., 2011). In another study, Zikherman *et al* described subtle TCR hyperresponsiveness and evidence of increased TCR signal strength among *Ptpn22*$^{-/-}$ immature thymocytes, suggesting that altered antigen receptor thresholds in comparison to wild-type counterparts might contribute to the observed enhancement of positive selection (Zikherman et al., 2009). Thus we focussed initially in the thymus to study the effect of loss of *Ptpn22* on selection and development of SKG mutant mice.

Overall, thymic development was quite similar to SKG mice in the combined SKG *Ptpn22*$^{-/-}$ mice, with reduced numbers of CD4$^+$ SP and CD8$^+$ SP thymocytes and similar distribution of the major thymocytes subpopulations. However, there were subtle changes that indicated that loss of *Ptpn22* partially rescued signalling in developing thymocytes, in particular the increased surface expression of CD5 in

SKG *Ptpn22*$^{-/-}$ as compared to SKG DP thymocytes **(Fig 4.4A)**. Detailed investigation of the distinct maturation stages of DPs by examining the levels of expression of CD5 and TCR revealed significantly greater percentages of DP2 thymocytes in SKG *Ptpn22*$^{-/-}$ relative to SKG **(Fig 4.4B)**. A recent report showed that CD4^{+} SP T cells originate from the DP2 subset (Saini et al., 2010). These results suggest that while *Ptpn22* deficiency did not result in a significant quantitative increment in SP cell numbers but it showed a subtle changes in immature thymocyte populations in SKG *Ptpn22*$^{-/-}$ mice compared to SKG mice. *In vivo* experiments, which tuned proximal TCR signalling by manipulating Src family kinases suggest that "strong" signals promote the development of CD4^{+} T cells (Hernandez-Hoyos et al., 2000; Legname et al., 2000). This could explain the trend towards an increase in CD4^{+} SP numbers observed in SKG *Ptpn22*$^{-/-}$ thymocytes **(Table 4.1)**.

Consistent with increased levels of CD5 expression, DP thymocytes from SKG *Ptpn22*$^{-/-}$ mice showed increased sensitivity compared to SKG thymocytes in signalling through the TCR as seen by improved calcium flux **(Fig 4.6)** and more moderately, ERK phosphorylation **(Fig 4.7)**. However, the SKG *Ptpn22*$^{-/-}$ thymocytes still showed diminished TCR signalling in comparison to the control BALB/c thymocytes, suggesting that *Ptpn22* deficiency could not completely compensate for the reduced signalling capacity of SKG cells. Alteration in the expression and function of ZAP-70, as shown by expression of aberrant ZAP-70, results in graded attenuation in TCR signalling strength (Tanaka et al., 2010) thus supporting our findings that removal of a PTPN22, a negative regulator, is compensating for decreased function of ZAP-70.

CD5 expression has been shown to be associated with TCR affinity (Kassiotis et al., 2003), therefore the increase in CD5 MFI expression in SKG *Ptpn22*$^{-/-}$ DP thymocytes may be indicative of a change in repertoire selection due to loss of *Ptpn22*. Given the subtle changes in positive selection and the improved signals through the TCR, we anticipated differences in the negative selection of the TCR Vβ repertoires. Surprisingly, the data show minimal effect of *Ptpn22* deficiency in negative selection with frequencies of the select autoreactive Vβ members comparable between the two mouse strains both in the thymus **(Fig 4.8)** as well as in

the periphery **(Fig 4.9)**. These findings suggest many possible implications, first that *Ptpn22* is less important in negative selection, which is in line with previous study showing *Ptpn22* deficiency had no effect on negative selection (Hasegawa et al., 2004) and second, that the increase in signalling due to loss of *Ptpn22* was not sufficient to further shift the window of thymic selection seen in the SKG mice (Sakaguchi et al., 2003). Third the strength and kinetics of both Ca^{2+} and ERK signalling are extremely important in positive versus negative selection (Gascoigne and Palmer, 2011). In support of this view is the result showing that the phosphorylation of ERK was less moderately affected in SKG *Ptpn22*$^{-/-}$ mice compared to SKG mice **(Fig 4.7)**. Mariathasan et al. showed that low level but sustained extracellular signal related kinase (ERK) signaling downstream of MAPK, promoted positive selection, but strong and transient ERK activation led to negative selection (Mariathasan et al., 2001). Higher affinity interactions of thymocyte TCR with self-antigen are thought to be required for differentiation of Treg in thymus, suggesting that alteration of TCR signalling might determine the amount of Tregs (Hsieh et al., 2012). However, we did not find any changes in the thymic output of Tregs providing further evidence that *Ptpn22* deficiency did not grossly affect thymic development in SKG *Ptpn22*$^{-/-}$ **(Fig 4.14)**.

We noted an increase in the number of $CD4^+$ T cells, which paralleled the $CD4^+$ T cell numbers in BALB/c mice however such a difference was only noted in the lymph nodes and not in spleen. Of importance is the increased proportion of effector cells characterized as $CD44^{hi}$ $CD62L^{lo}$ or $CD45RB^{lo}$ seen in the periphery of SKG *Ptpn22*$^{-/-}$ mice **(Fig 4.12 and 4.13)** suggesting greater lymphopenia induced expansion early on in development due to decreased thymic output, which was further exacerbated by loss of *Ptpn22*. The increase in effector cells was not surprising as studies conducted in *Ptpn22* deficient mouse model showed increased expansion and function of effector/memory T cell pool, which may stem from loss of the homeostatic regulation of naïve T cells by low affinity self-antigens (Brownlie et al., 2012; Salmond et al., 2014). Furthermore, consistent with our previous study showing that increase in the effector population is counteracted by increased regulatory T cells in periphery of PTPN22-deficient mice (Brownlie et al., 2012) we

also noted a subtle increase in the proportion and the numbers of Tregs in the LNs and spleen **(Fig 4.15)**.

Overall, this chapter highlighted that *Ptpn22* deficiency did not overtly affect thymic development but showed subtle effects on positive selection in SKG *Ptpn22*$^{-/-}$ mice as evident by increased TCR signal strength in immature thymocytes compared to SKG mice. These results show that removal of PTPN22 can compensate, at least partially, for the deficient ZAP-70 activity in the SKG mice, thus linking PTPN22 and ZAP-70 to a common signalling pathway *in vivo*.

4.4 Figures

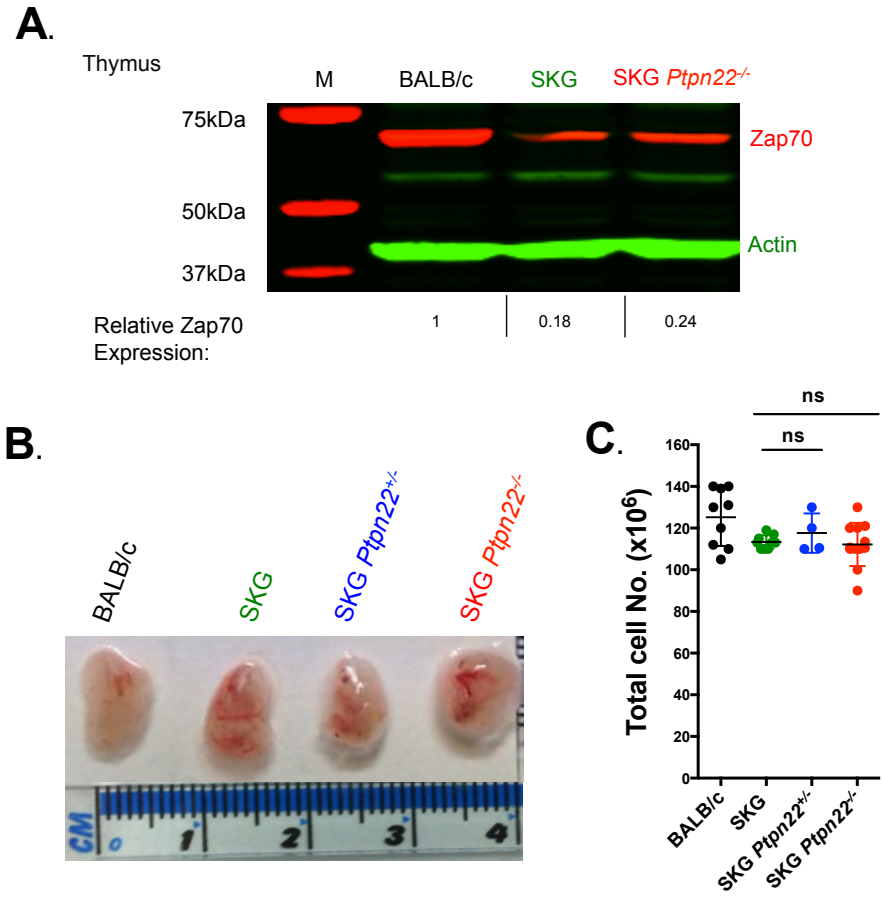

Figure 4.1. *Ptpn22* deficiency does not alter the reduced levels of ZAP-70 on SKG background and total thymic numbers are comparable between SKG and SKG *Ptpn22*$^{-/-}$ mice.
(A) Abundance of ZAP-70 protein in thymocytes from age matched (7week) BALB/c, SKG and SKG *Ptpn22*$^{-/-}$ were analysed by western blotting (pre-cast gel). The blot was sequential blotted for anti-ZAP-70 (BD biosciences) and anti-Actin antibodies overnight at 4°C and for 1 hour at room temperature respectively, and then blotted with anti-mouse (for ZAP-70) and anti- rabbit (for Actin) fluorescent secondary antibodies for 1 hour. The blot was scanned using Li-Cor systems. Relative expression of ZAP-70 was calculated by normalising fluorescence of bands to BALB/c band fluorescence. Experiment is only done once. **(B)** Representative thymi from 7 week old BALB/c, SKG, SKG *Ptpn22*$^{+/-}$ and SKG *Ptpn22*$^{-/-}$ mice. **(C)** Total cell numbers were counted using CASY counter. Data shown are pooled from 3 independent experiments representing BALB/c (black fill circles), SKG *Ptpn22*$^{+/+}$ (green fill circles), SKG *Ptpn22*$^{+/-}$ (blue fill circles) and SKG *Ptpn22*$^{-/-}$ (red fill circles). Dot plots shows group means indicated by the horizontal bars ± SD with each point representing individual mouse. Statistical significance was calculated in Prism using Student's t – test (ns = not significant, where $p \geq 0.01$).

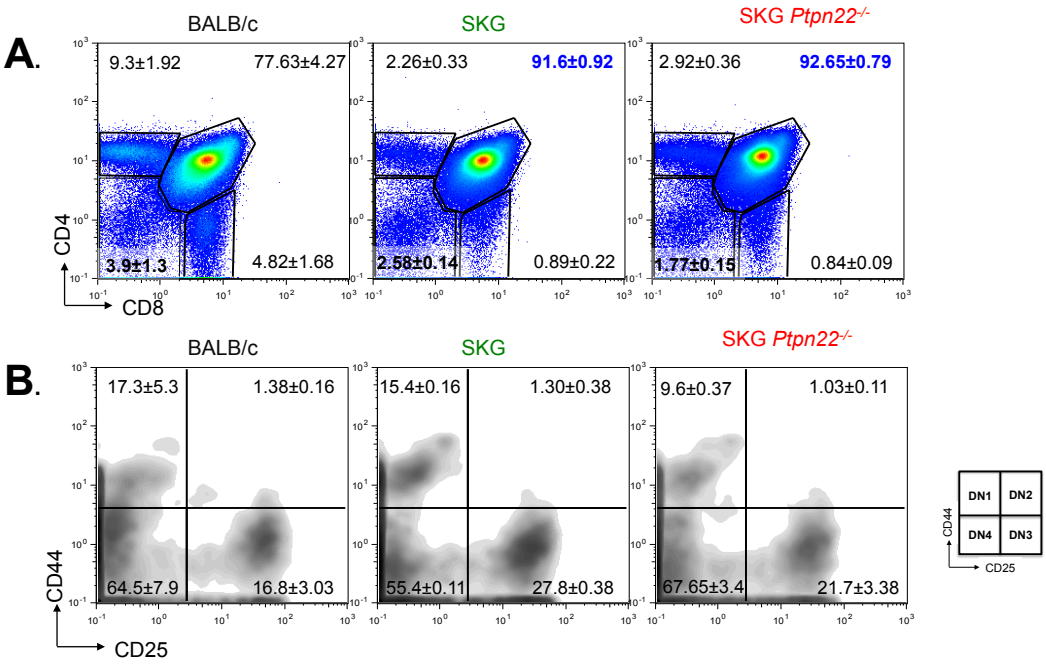

Figure 4.2 Thymic development is impaired in SKG *Ptpn22*$^{-/-}$ mice
(A) Single-cell suspensions from thymi of age matched (7 week) BALB/c, SKG and SKG *Ptpn22*$^{-/-}$ mice were assessed for the proportions of DN ($CD4^-CD8^-$), DP ($CD4^+CD8^+$), CD4SP ($CD4^+CD8^-$) and CD8SP ($CD4^-CD8^+$) by staining for CD4 versus CD8 by flow cytometry. **(B)** Contour plots depicting the sub-stages of the DN population; DN1 ($CD44^+CD25^-$) DN2 ($CD44^+CD25^+$), DN3 ($CD44^-CD25^+$), DN4 ($CD44^-CD25^-$) were identified by staining for CD44 versus CD25. Numbers on the plots denotes the averages ± SD of a minimum of 3 individual mice per group. Numbers in bold blue font represent significant difference calculated in prism with One-Way ANOVA, P<0.001. Data are representative of 4 independent experiments with minimum of 3 mice per group. Three replicate experiments conducted with 7 week old mice, and one with 11 week old mice showed similar results.

Table 4.1 Absolute thymocyte cell numbers in 7 week-old mice (x10^6)

Genotype	Total	DN	DP	CD4 SP	CD8 SP	CD8 SP TCR^+
BALB/c (n=9)	125.2 ± 13.8	7.0 ± 2.7	98.1 ± 8.8	11.5 ± 2.0	4.0 ± 2.3	3.4 ± 1.9
SKG (n=9)	113.3 ± 3.2	4.7 ± 1.5	102.5 ± 3.5	2.7 ± 0.7	0.8 ± 0.3	0.34 ± 0.1
SKG *Ptpn22*$^{-/-}$ (n=12)	112.1 ± 10.4	4.7 ± 3.0	100.8 ± 9.6	3.3 ± 0.5	0.8 ± 0.2	0.45 ± 0.18

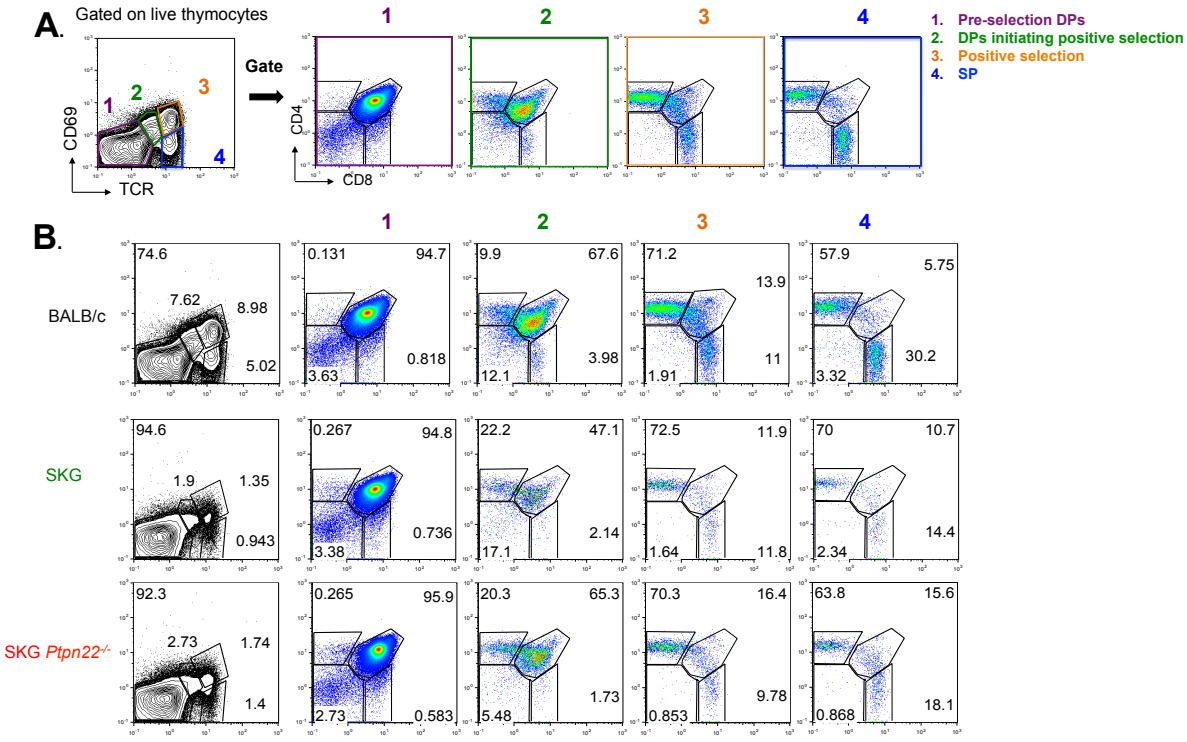

C.

Genotype	Gate 1	Gate 2	Gate 3	Gate 4
BALB/c	73.1 ± 2.4	7.3 ± 0.5	10.4 ± 2.6	5.4 ± 0.8
SKG	93.5 ± 1.7	1.8 ± 0.3	1.9 ± 0.8	1.2 ± 0.3
SKG *Ptpn22*$^{-/-}$	90.8 ± 2.1	**2.8 ± 0.4**	2.6 ± 0.9	1.8 ± 0.3

Figure 4.3 Positive selection is partially restored in SKG *Ptpn22*$^{-/-}$ mice.
(A) CD69 together with TCRβ on total live thymocytes was used to distinguish the stages of positive selection. Gate 1: pre-selection DPs thymocytes denoted by CD69^{-}TCR^{-}; Gate 2: DPs thymocytes initiating positive selection denoted by CD69^{+}TCR^{+}; Gate 3:Thymocytes undergoing positive selection denoted by CD69^{hi}TCR^{hi}; Gate 4: SPs denoted by CD69^{lo}TCR^{hi} **(B)** Representative flow cytometry plots show the CD4 versus CD8 profile for the 4 selecting gates for BALB/c, SKG and SKG *Ptpn22*$^{-/-}$ thymocytes. **(C)** Table shows the proportions of thymocytes within the four stages of positive selection for indicated strains of mice. Data represents the average of 6-9 mice per genotype (±SD) from three independent experiments. Numbers in bold represent significant difference calculated in prism with One-Way ANOVA, **P<0.01**.

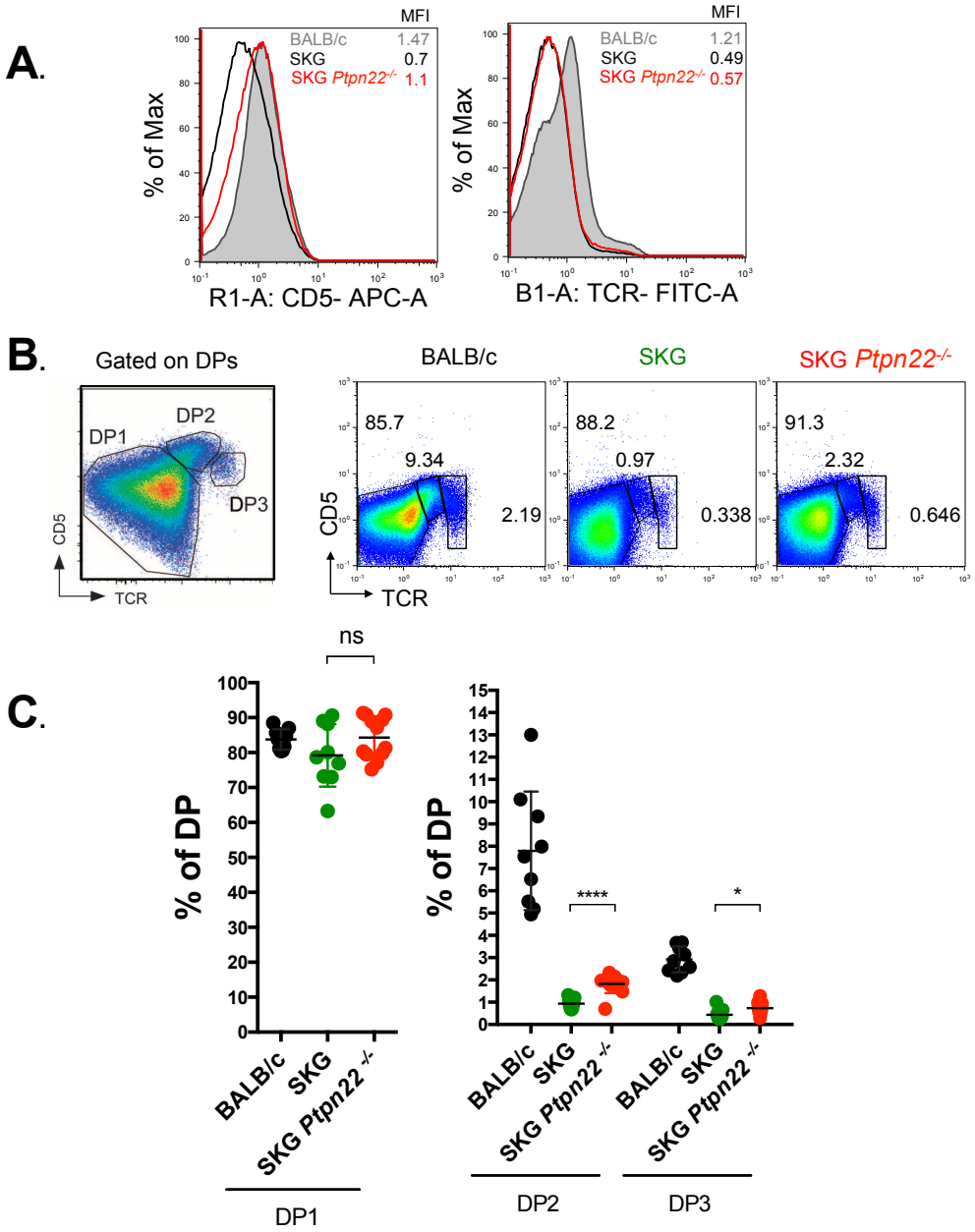

Figure 4.4 SKG *Ptpn22*$^{-/-}$ DP thymocytes show increased expression of CD5 compared to DP thymocytes from SKG mice

(A) FACS histogram plots showing the surface expression of CD5 and TCR gated on CD4^{+}CD8^{+} double positive thymocytes from BALB/c, SKG and SKG *Ptpn22*$^{-/-}$ mice. Gray filled histogram represents BALB/c, SKG is shown by black line overlay while SKG *Ptpn22*$^{-/-}$ is shown by red line. Mean fluorescence of CD5 and TCR is indicated on the FACS plots for the strains. **(B)** Example of dot plots showing the profile of CD5 versus TCRβ gated on DP thymocytes which distinguishes the stages of DP maturation; DP1 (TCR^{lo}CD5^{lo}), DP2 (TCR^{int}CD5^{hi}) and DP3 (TCR^{hi}CD5^{int}) in BALB/c, SKG and SKG *Ptpn22*$^{-/-}$ DP thymocytes. **(C)** Bar chart shows the proportions of thymocytes in in DP1, DP2 and DP3 gate. Data represents the average of 6-9 mice per genotype (±SD) from three independent experiments. Statistical significance calculated with One-Way ANOVA and post-ANOVA Holm-Sidak test for multiple comparison, *P<0.05, **P<0.01, ***P<0.001

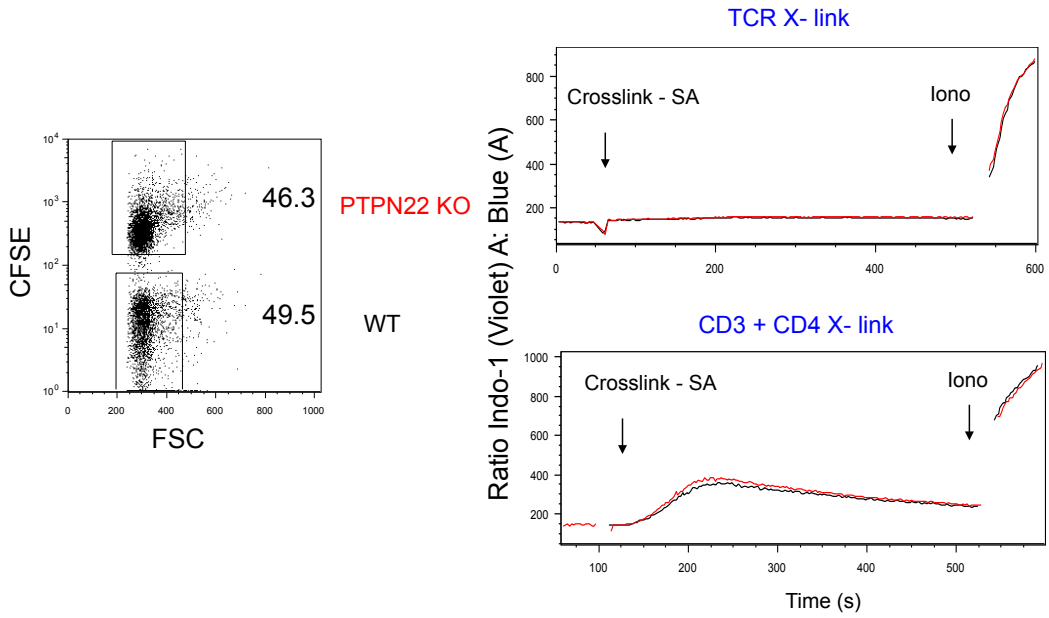

Figure 4.5 No difference in Ca^{2+} Flux in wild-type C57BL/6 and PTPN22 KO $CD4^{+}CD8^{+}$ thymocytes

Single cell suspension of thymocytes from PTPN22KO mice were labelled with 0.012μM CFSE and mixed in 1:1 ratio with unlabelled wild-type C57BL/6 thymocytes (left panel). The cells were then loaded with 2μM indo-1, followed by staining with biotin-conjugated anti-TCRβ and anti CD3 + CD4 (clone RMA 4.4). Basal levels of Ca^{2+} were determined for 45 seconds and induction of Ca^{2+} flux was achieved by crosslinking of anti TCRβ (top right) or anti CD3 + CD4 (bottom right) with streptavidin phycoerythrin conjugates. Arrows on the histogram indicate the time of addition of streptavidin (45 sec) and ionomycin (8min). Wild-type *Ptpn22*$^{+/+}$ is represented in black and *Ptpn22*$^{-/-}$ in red line. Experiment only performed once.

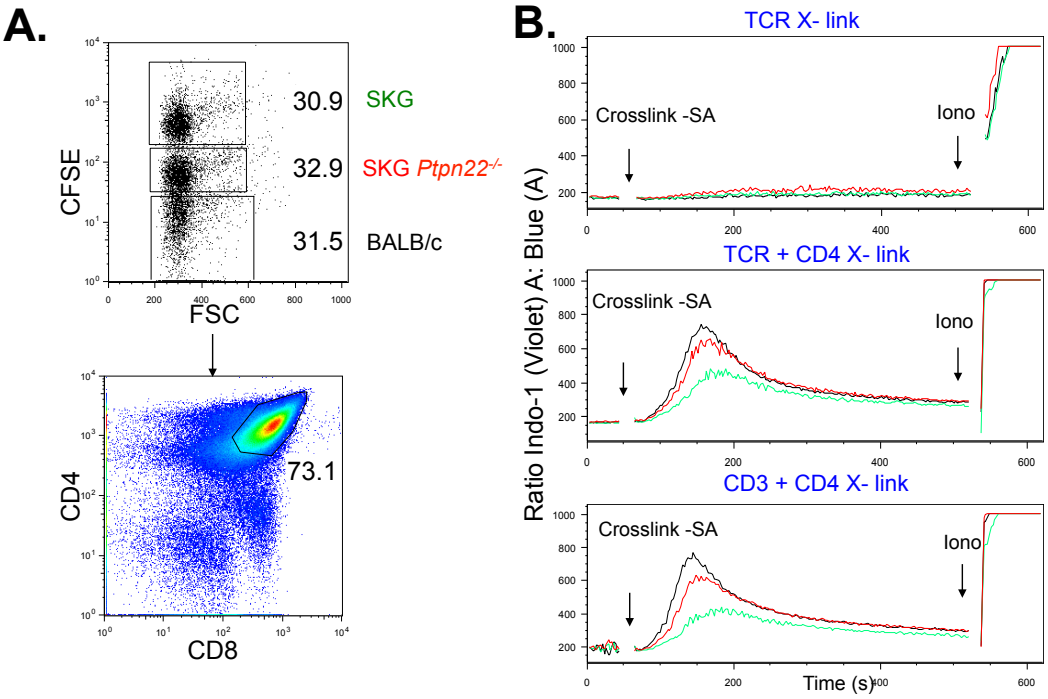

Figure 4.6 Thymocytes from SKG *Ptpn22*$^{-/-}$ show enhanced TCR induced calcium mobilisation compared to SKG mice

Thymocytes from BALB/c, SKG and SKG *Ptpn22*$^{-/-}$ mice were labelled with 2µM indo-1, followed by staining with biotin conjugated antibody anti-TCRβ ± CD4 (clone 145 2C11) and anti CD3 + CD4 (clone RMA 4.4). Additional fluorescently conjugated CD8 and CD4 (clone RMA 4.5 does not compete with clone RMA 4.4 used for crosslinking) Abs were used to identify thymocyte populations and Ca^{+2} flux was analysed by flow cytometry **(A)** Single cell suspension of thymocytes from BALB/c, SKG and SKG *Ptpn22*$^{-/-}$ mice were labelled with different concentration of CFSE: 0µM, 0.012µM, 0.002µM respectively and mixed in 1:1:1 ratio. Ca^{2+} traces were analysed in the DP gate for each genotype as shown on the CD4 versus CD8 dot plot. **(B)** Basal levels were determined for 45 seconds and induction of Ca^{2+} was achieved by addition of crosslinking anti TCRβ ± CD4 and anti CD3 + CD4 with streptavidin phycoerythrin conjugates. Arrows on the histogram indicate the time of addition of streptavidin (45 sec) and ionomycin (8min) BALB/c is represented in black, SKG in green and SKG *Ptpn22*$^{-/-}$ in red line. Data are representative of three independent experiments.

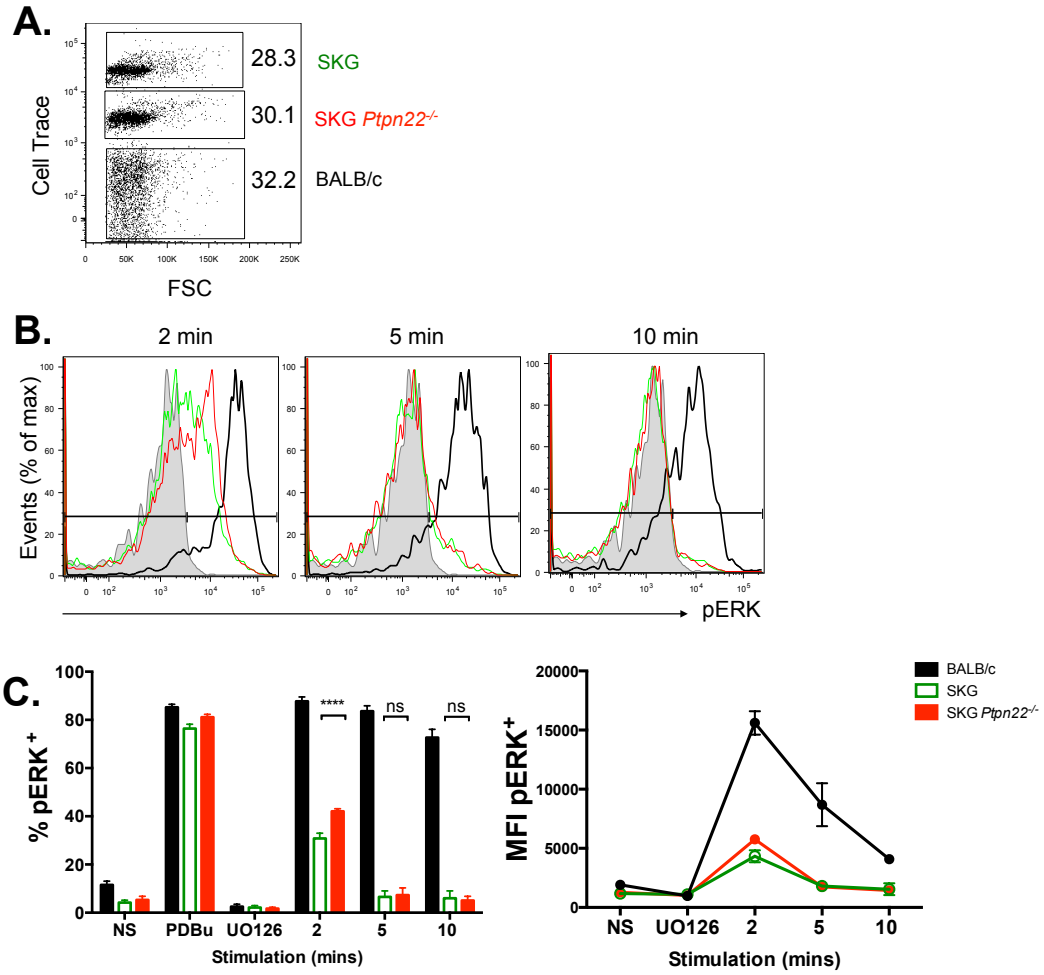

Figure 4.7 *Ptpn22* deficiency results in moderate increase in phosphorylation of ERK on SKG background

(A) Single cell suspension of thymocytes from BALB/c, SKG and SKG *Ptpn22*$^{-/-}$ mice were labelled with different concentration of Cell Trace Violet: 0μM, 0.012 μM, 0.1μM respectively and mixed in 1:1:1 ratio. Cells were stained with biotinylated anti-CD3 and CD4 antibodies and stimulated by crossing linking with streptavidin-allophycocyanin for 0, 2, 5 and 10 minutes. Cells were fixed at end of the time points by addition of 4% PFA, permeabilised with 90% methanol and stained with phospho-ERK specific antibody. **(B)** Representative histograms show overlays of intracellular pERK 2, 5 and 10 min after cross-linking. Filled histogram depicts BALB/c treated with UO126, MEK inhibitor that serves as negative control. pERK levels is shown for BALB/c by black line, SKG in blue overlay line while SKG *Ptpn22*$^{-/-}$ is indicated by red line. Bar graph shows average percentages of pERK^{+} cells ± SD, over the time course. Data are representative of two independent experiments. Statistical significance was calculated in Prism: One way ANOVA, ****P<0.0001.

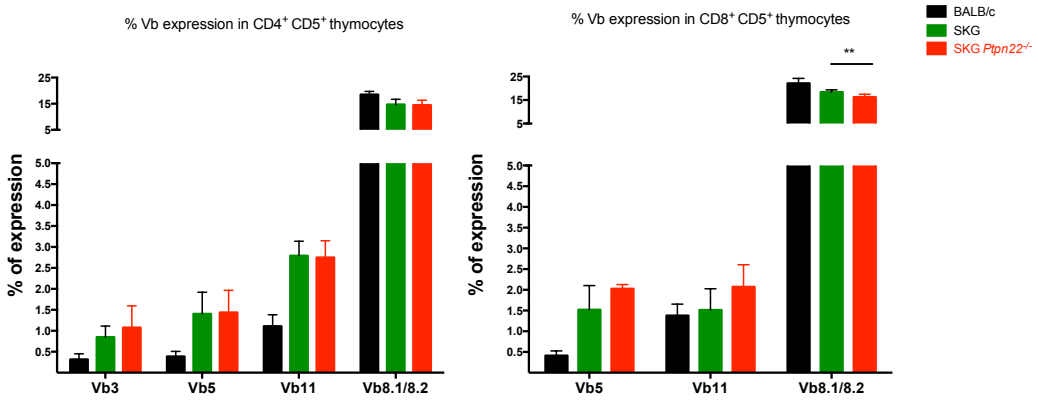

Figure 4.8 *Ptpn22* deficiency does not alter the TCR Vβ repertoire in mature thymocytes compared to SKG mice

The bar charts show the percentage expression of Vβ3, Vβ5, Vβ11 and Vβ8 TCR chains in mature $CD4^+$ $CD5^+$ (left) and in mature $CD8^+$ $CD5^+$ (right) thymocytes for BALB/c (black), SKG (green) and SKG *Ptpn22*$^{-/-}$ (red). The data are representative of three independent experiments and are shown as averages of n=4 for each strain ± SD. Statistical significance was calculated in Prism: One way ANOVA, *P<0.05, **P<0.01, ***P<0.001.

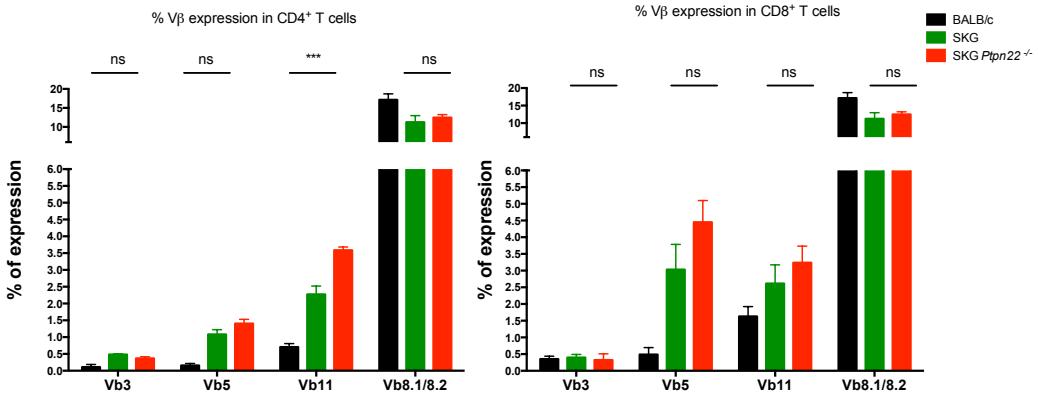

Figure 4.9 Peripheral $CD4^+$ and $CD8^+$ T cells from SKG *Ptpn22*$^{-/-}$ showed no differences in selection of TCR Vβ subfamilies.

The bar charts shows the percentages of expression indicated TCR Vβ chains in $CD4^+$ (left) and $CD8^+$ (right) T lymphocytes for BALB/c (black), SKG (green) and SKG *Ptpn22*$^{-/-}$ (red). The data is from only one experiment and is shown as average of n=4 mice for each strain ± SD. Statistical significance was calculated in Prism: One way ANOVA, ***P<0.001.

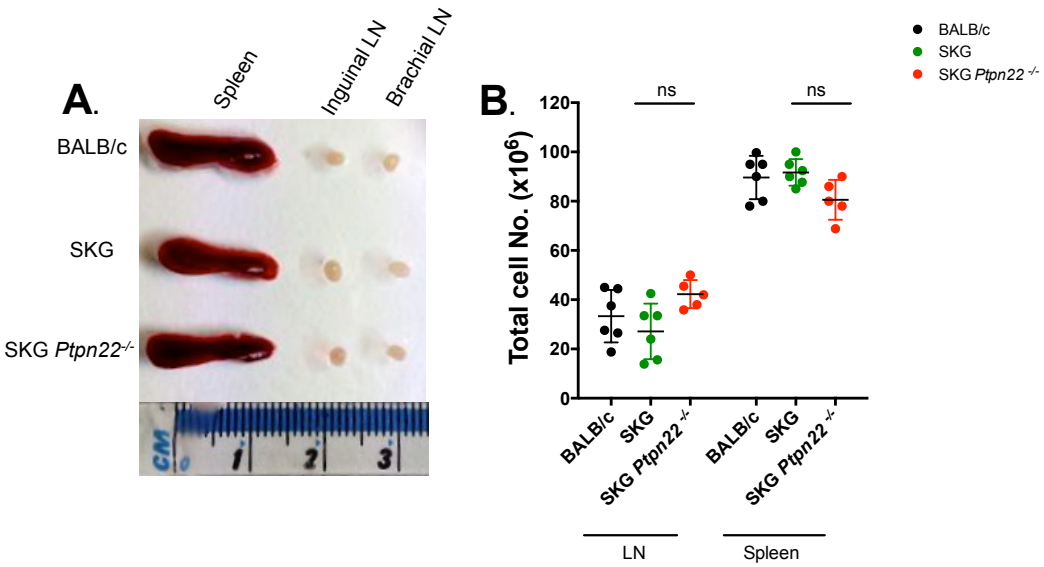

Figure 4.10 Total numbers of LNs and spleen cells were comparable between SKG and SKG *Ptpn22*$^{-/-}$ mice

(A) Representative spleen, inguinal and brachial LNs from 7 week old BALB/c, SKG and SKG *Ptpn22*$^{-/-}$ mice. **(B)** Total cell numbers were counted using CASY counter. Data shown are pooled from 2 independent experiments representing BALB/c (black fill circles), SKG *Ptpn22*$^{+/+}$ (green fill circles) for SKG *Ptpn22*$^{+/-}$ (blue fill circles) and SKG *Ptpn22*$^{-/-}$ (red fill circles). Dot plots shows group means indicated by the horizontal bars ± SD with each point representing individual mice. Statistical significance was calculated in Prism: One way ANOVA, ns - non significant, *P<0.05, **P<0.01, ***P<0.001.

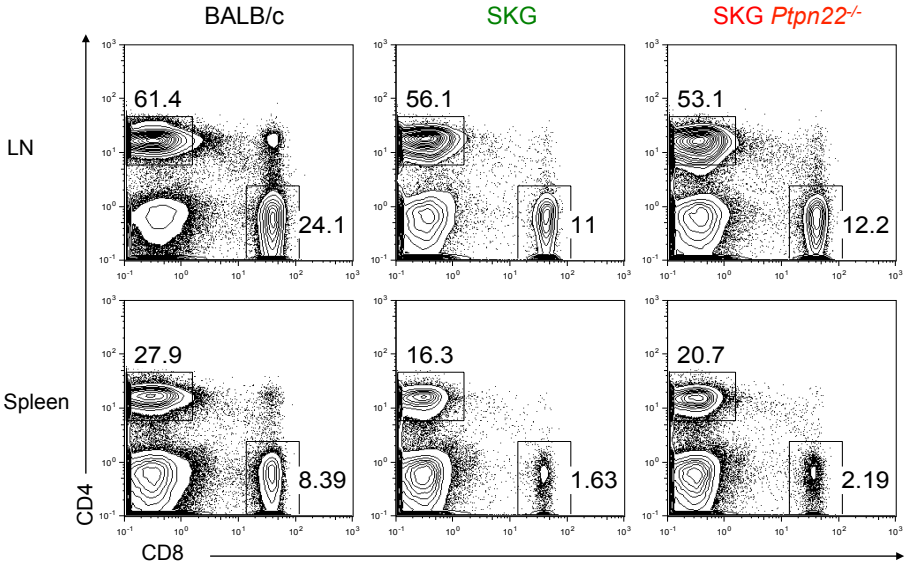

Figure 4.11 The proportions of T cells in LN and spleen on SKG background are not altered by *Ptpn22* deficiency

Representative FACS dot plots showing the CD4 versus CD8 expression in LN (top panel) and spleen (bottom panel) from individual 7-week-old BALB/c, SKG and SKG *Ptpn22*$^{-/-}$ mice.

Table 4.2 Absolute T cell numbers in LN from 7 week old mice (x10^6)

Genotype	Total	CD4	CD8	B220
BALB/c	33.3 ± 10.7	19.7 ± 6.7	7.1 ± 2.6	4.1 ± 1.2
SKG	27.2 ± 11.3	13.3 ± 6.3	3.0 ± 1.2	9.1 ± 4.1
SKG *Ptpn22*$^{-/-}$	42.3 ± 5.7	**19.6 ± 5.9**	4.5 ± 1.0	**13.4 ± 1.9**

Table 4.3 Absolute T cell numbers in Spleen from 7 week old mice (x10^6)

Genotype	Total	CD4	CD8	B220
BALB/c	89.6 ± 8.8	24.1 ± 8.7	7.9 ± 1.8	33.1 ± 2.2
SKG	91.7 ± 5.4	13.4 ± 4.1	1.8 ± 0.3	43.7 ± 11.2
SKG *Ptpn22*$^{-/-}$	80.6 ± 8.1	13.2 ± 4.5	1.5 ± 0.3	39.9 ± 7.5

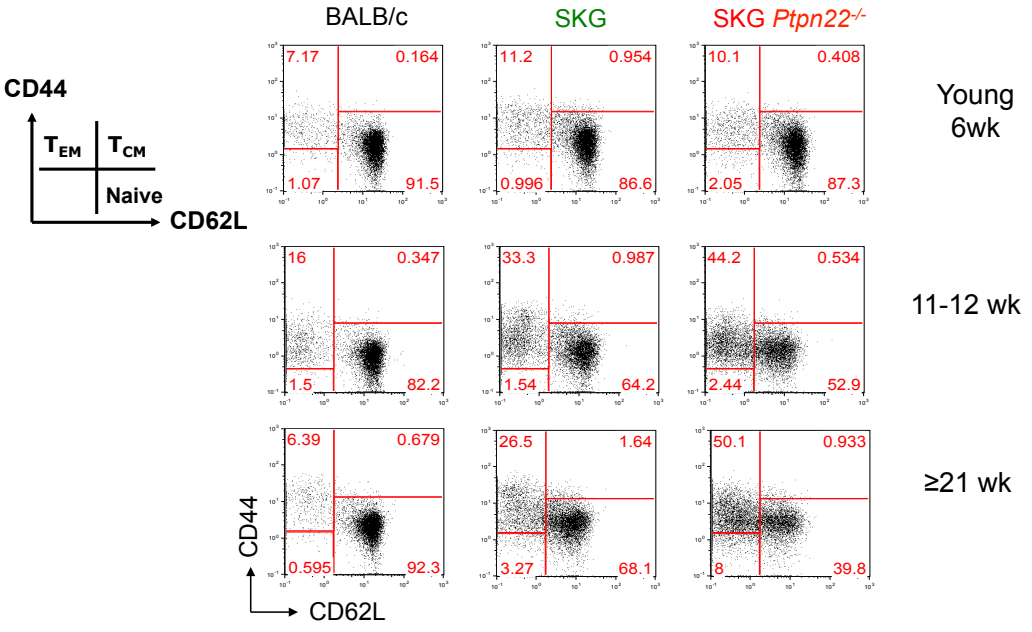

Figure 4.12 SKG *Ptpn22*$^{-/-}$ mice have an expansion of effector/memory T cells than increases with age compared to SKG mice

Single cell suspension from LNs was evaluated for the proportions of naïve (CD44^{lo}CD62L^{hi}) and effector (CD44^{hi}CD62L^{lo}) cells within the CD4$^+$ T cells from young (6 week), 11week and 21 week old BALB/c, SKG and SKG *Ptpn22*$^{-/-}$ mice.

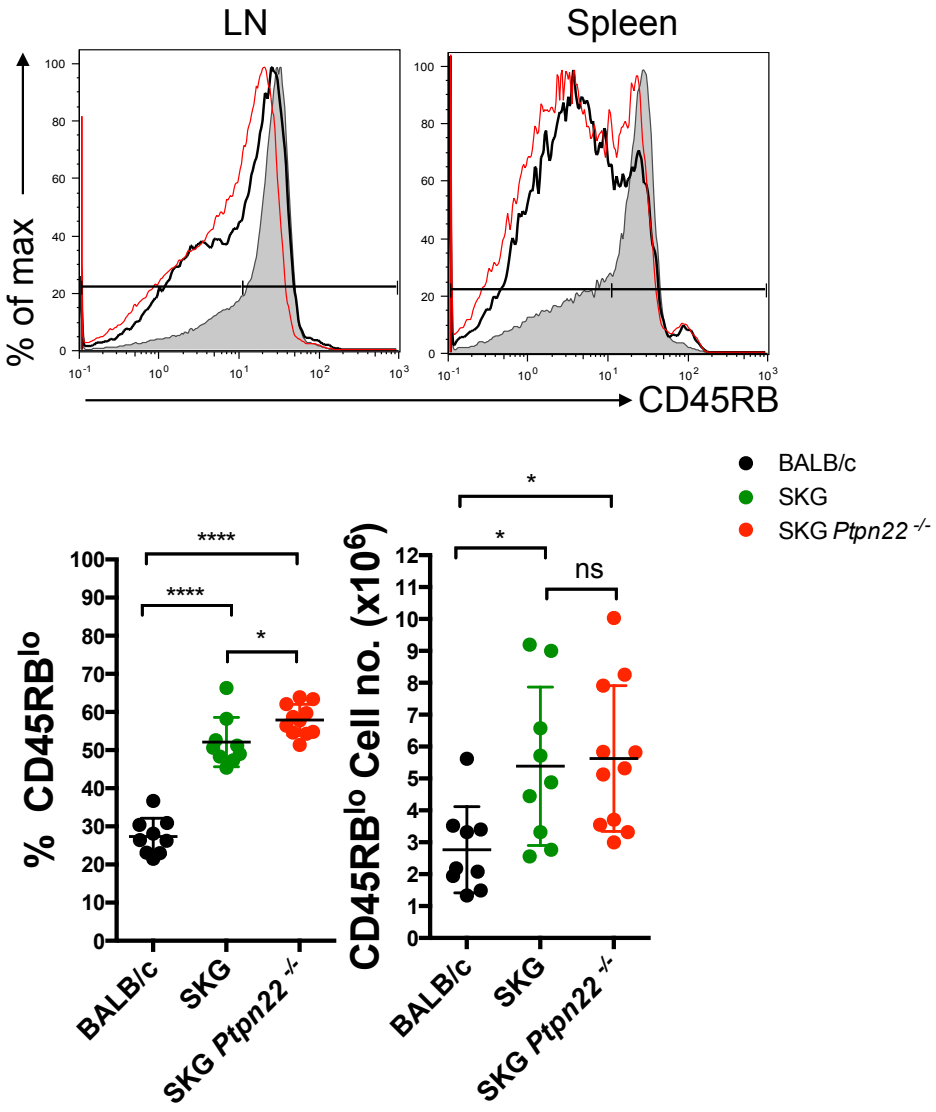

Figure 4.13 Increased proportions of CD4$^+$ CD45RB^{lo}T cells in SKG *Ptpn22*$^{-/-}$ mice compared to SKG mice

Top panel shows representative histograms of CD4$^+$ T cells from 20 week BALB/c (grey shaded), SKG (black overlay line) and SKG *Ptpn22*$^{-/-}$ (red line) for expression of CD45RB. Graph below shows tabulated frequencies and absolute numbers of CD45RB^{lo} population calculated from the FACS plots. Data represents the average of n=6 for BALB/c and SKG mice and n= 12 for SKG *Ptpn22*$^{-/-}$ mice (±SD) from three independent experiments. Statistical significance was calculated in Prism with One-Way ANOVA and Tukey's post-ANOVA multiple comparison test, ns – non significant, *P<0.05, **P<0.01, ***P<0.001.

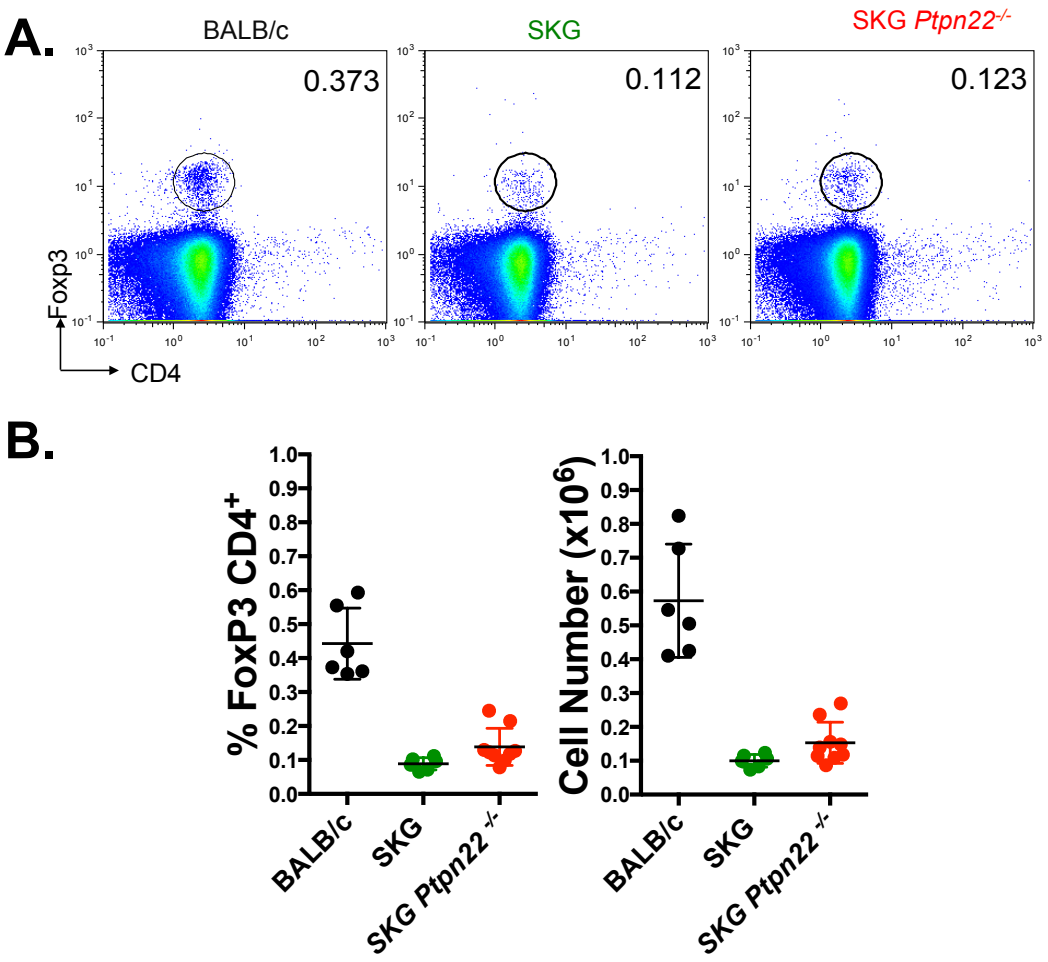

Figure 4.14 Proportion and absolute numbers of thymic Tregs were similar in SKG and SKG *Ptpn22*$^{-/-}$ mice

(A) Representative dot plot showing the thymi from 7 week old BALB/c, SKG and SKG *Ptpn22*$^{-/-}$ mice were examined for the proportions of FoxP3^{+} CD4^{+} Tregs **(B)** Graph showing the percentages and the absolute number of Tregs. Data represent the average of 6-9 mice per genotype (±SD) from three independent experiments.

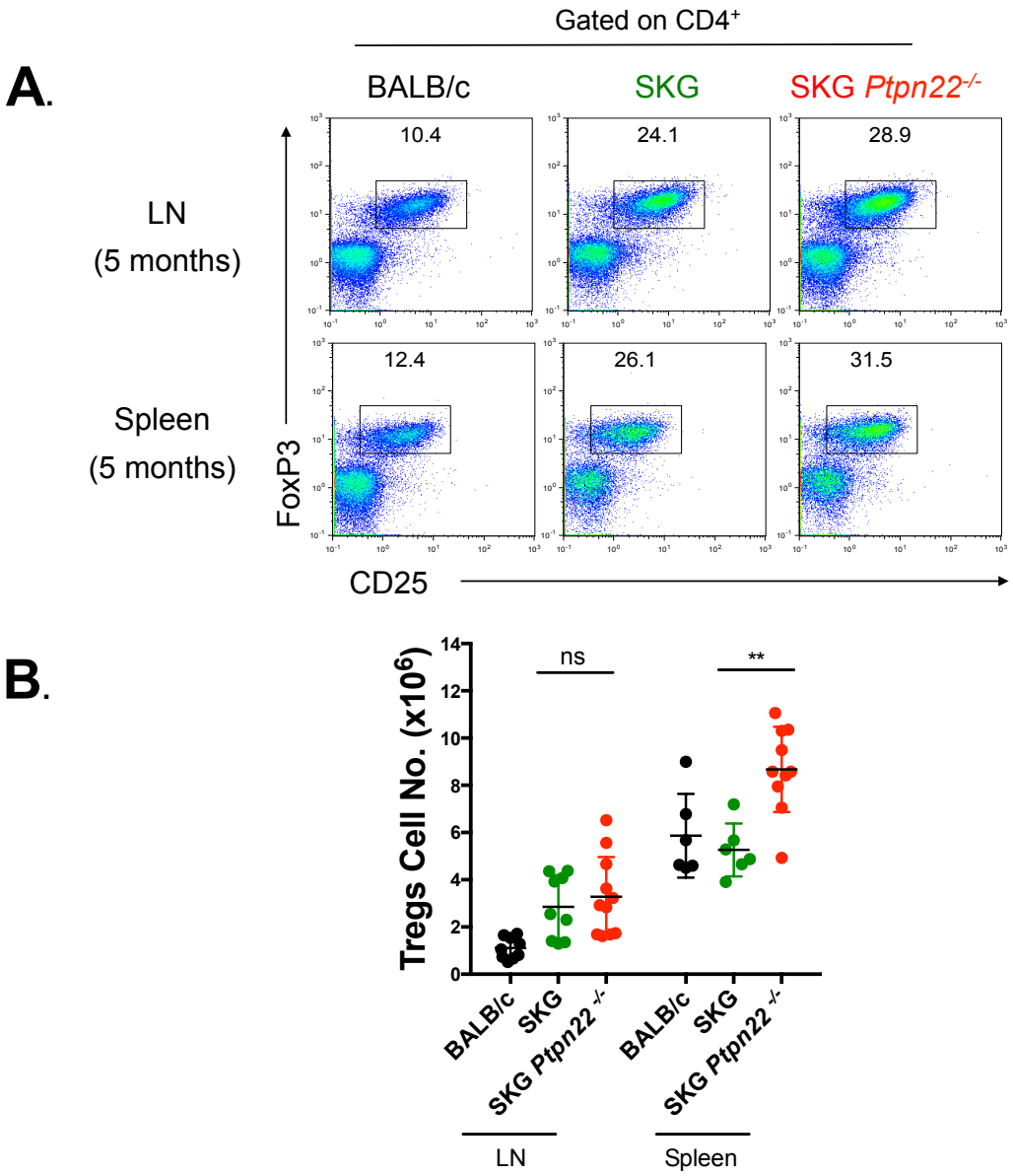

Figure 4.15 SKG *Ptpn22*$^{-/-}$ mice show a subtle increase in proportion and numbers of peripheral Tregs than SKG mice

T cells recovered from LN and spleen from wild-type BALB/c (black), SKG (green) and SKG *Ptpn22*$^{-/-}$ (red) mice were analysed by ex vivo intracellular staining for Tregs (FoxP3^{+}CD25^{+}) within the CD4^{+} T cell population. Example dot plots are shown as well as graphs representing the proportions and absolute cell numbers of CD4^{+} FoxP3^{+}CD25^{+} Tregs. Data represents the average of 6-9 mice per genotype (±SD) from three independent experiments. Statistical significance was calculated in Prism: One-Way ANOVA and Tukey's post-ANOVA multiple comparison test, ns-non significant, *P<0.05, **P<0.01, ***P<0.001.

Chapter 5: Effect of *Ptpn22* deficiency on susceptibility to arthritis in SKG *Ptpn22*$^{-/-}$ mice

5.1 Introduction

Rheumatoid arthritis (RA) is a chronic systemic inflammatory disease, which predominantly affects the synovial membranes of the primary joints. Although autoreactive $CD4^+$ T cells and dysregulated B cell homeostasis are prime mediators of RA, the precise aetiology remains unknown (Burmester et al., 2014). Both genetic and environmental factors contribute to the development of RA. Recent genome wide association analyses identified several HLA and non-HLA disease susceptibility genes among which HLA-DRB1 and PTPN22 are robustly linked to disease predisposition (Choy, 2012).

There are several animal models of RA (Asquith et al., 2009). Here we took advantage of the SKG mouse strain that contains a homozygous W163C mutation in C-terminal SH2 domain of ZAP-70 due to which these mice spontaneously develop $CD4^+$ T-cell-mediated autoimmune arthritis when maintained in conventional environments (Sakaguchi et al., 2003). Arthritis can also be elicited in animals held under SPF conditions either through antigen non-specific activation of innate immunity, e.g. by administration of crude or purified fungal extracts or by provoking homeostatic proliferation of self-reactive T cells upon transfer to the T cell-deficient environment of nude mice (Yoshitomi et al., 2005). Importantly, PTPN22 directly affects ZAP-70 signalling (Wu et al., 2006). Given the association of *PTPN22* polymorphisms with an increased susceptibility of developing RA, it was of interest to assess the impact of the phosphatase in the SKG arthritis model.

Arthritis in SKG mice is characterized by symmetric swelling of small joints that later progress to larger joints accompanied by severe joint destruction (Sakaguchi et al., 2003). Serologically, SKG mice develop high titers of rheumatoid factors (RF), autoantibodies specific for type II collagen, antibodies reactive with heat shock protein of *Mycobacterium tuberculosis* potentially because of cross-reaction with its conserved epitope, severe hypergammaglobulinemia and high concentrations of

circulating immune complexes (Sakaguchi et al., 2003). In addition, cells within the affected joints produce abundant proinflammatory cytokines such as IL-1, IL-6 and TNF and the incidence and severity of arthritis in SKG mice has shown to be significantly reduced by genetic deficiency of these cytokines (Hata et al., 2004).

The underlying mechanism for development of arthritis in SKG mice is decreased signalling downstream of the TCR due to expression of aberrant ZAP-70 which leads to alteration of the thymic selection thresholds resulting in production of autoreactive T cells that would otherwise be deleted due to negative selection (Sakaguchi et al., 2003). As shown in chapter 4, our results illustrate that although both SKG *Ptpn22*$^{-/-}$ and SKG mice exhibit a similar extent of impairment in thymocyte development, SKG *Ptpn22*$^{-/-}$ mice show subtle effects in positive selection and have increased TCR mediated signalling in comparison to SKG mice. These results suggest that both ZAP-70 and PTPN22 act by affecting similar signalling pathways.

In the light of the genetic predisposition to developing autoimmune arthritis in SKG mice, we next set out to investigate whether the increased TCR signalling observed in SKG *Ptpn22*$^{-/-}$ mice influenced their susceptibility in developing autoimmune arthritis. **Figure 5.1** summarises the effect of T cell signalling on the development and immune phenotypes of SKG and PTPN22 KO mouse models. Several possibilities were considered for the impact of *Ptpn22* deletion on the severity of disease in the SKG model of autoimmune arthritis. The increase in the signalling capacity could perhaps balance the "thymic selection shift" and coupled with enhanced peripheral signalling in absence of *Ptpn22* could decrease severity of disease. Alternatively, the increase in signalling capacity might not be sufficient to shift the selection window to avoid release of autoreactive T cells in periphery and with a cumulative lack of negative regulation due to *Ptpn22* deficiency could exacerbate the phenotype resulting in increased severity of disease. In support, of the latter view is the observation that we did not see any differences in the deletion of endogenous provirus-specific TCR Vβ clones in SKG *Ptpn22*$^{-/-}$ mice **(Fig 4.9)** along with increase in ratio of effector/memory T cells **(Fig 4.12)** compared to SKG mice. The *Ptpn22* deficient mouse is a global knock out, therefore there is a third possibility of creating a balanced situation wherein we have augmented thymic

threshold and simultaneously caused a similar increase in the peripheral T cell activation thus having no affect on incidence or severity of arthritis in SKG *Ptpn22*$^{-/-}$ mice and a fourth possibility where the effect of PTPN22-deficiency on non-T cells may influence the T cell responses directly.

5.2 Results

5.2.1 Increased proliferation of naïve SKG *Ptpn22*$^{-/-}$ CD4^{+} T cells in response to TCR stimulation

PTPN22 is an inhibitor of TCR signalling (Bottini and Peterson, 2014). In line with previous studies from *Ptpn22*$^{-/-}$ mice showing TCR signalling is enhanced in the absence of PTPN22 (Brownlie et al., 2012; Hasegawa et al., 2004), we showed in the previous chapter that loss of *Ptpn22* improved TCR signalling defects in SKG *Ptpn22*$^{-/-}$ thymocytes compared to SKG thymocytes **(Fig 4.6 and 4.7)** and SKG *Ptpn22*$^{-/-}$ CD4 T cells presented with increased proportions of effector memory cells (**Fig 4.12)**. Therefore, for analysis of TCR-induced proliferation it was important to sort naïve CD4^{+} T cells, as CD44^{hi} memory-phenotype cells contribute differently than naïve T cells in an immune response (Surh and Sprent, 2002). Naïve CD4^{+} T cells, gated as CD45RB^{hi}CD25^{-} were sorted from LNs of young BALB/c, SKG and SKG *Ptpn22*$^{-/-}$ mice **(Fig. 5.2)**. Subsequently the cells were labelled with Cell Tracer Violet and stimulated *in vitro* by co-culturing with irradiated splenocytes from a BALB/c RAG$^{-/-}$ mouse in the presence of varying doses of anti-CD3 mAb. Proliferation was measured at day 3 by assessing the dilution of Cell Tracer dye by flow cytometry.

As previously reported, there was decreased proliferation of SKG CD4^{+} cells compared with that of wild type BALB/c in response to all doses of anti-CD3 after 72h of stimulation *in vitro* **(Fig 5.3A)** (Sakaguchi et al., 2003). Interestingly, although the proliferation of SKG *Ptpn22*$^{-/-}$ cells was lower compared to BALB/c CD4^{+} T cells **(Fig 5.3A)**, SKG *Ptpn22*$^{-/-}$ cells partially overcame the proliferative defect seen in SKG cells in response to stimulation with anti-CD3, showing that *Ptpn22* deficiency enhanced the proliferative capacity of CD4^{+} SKG *Ptpn22*$^{-/-}$ cells

(Fig 5.3A). The proliferation index is a quantitive analysis calculated by FlowJo software (from the cell violet dilution peaks shown in **Fig 5.3B**) and represents the average number of divisions of the dividing population. Therefore the proliferation index measures only the response of cells that underwent at least one division. **Fig 5.3C** shows that SKG *Ptpn22*$^{-/-}$ CD4^{+} T cells proliferated more than SKG CD4^{+} T cells at all concentrations of anti-CD3 *in vitro*. Additionally, more SKG *Ptpn22*$^{-/-}$ cells went into division which is further quantified in FlowJo by the divison index function, which calculates the average number of cell division that a cell in the original population has undergone and takes into consideration the undivided peak (**Fig 5.3C**, right panel). As shown in **Figure 5.3C**, both SKG and SKG *Ptpn22*$^{-/-}$ cells show very similar proliferation index, however the division index is much lower in SKG cells compared to SKG *Ptpn22*$^{-/-}$ cells suggesting that SKG T cells are less likely to reach the threshold of proliferation than SKG *Ptpn22*$^{-/-}$ T cells, but those SKG cells which do overcome the threshold, undergo similar numbers of cell divisions on an average.

5.2.2 IL-2 production was enhanced in SKG *Ptpn22*$^{-/-}$ T cells

Upon activation, both CD4^{+} and CD8^{+} T cells produce IL-2, the latter to lesser extent (Malek and Castro, 2010). Ca^{2+} signalling has also been shown to be important for IL-2 production (Rao et al., 1997; Smith-Garvin et al., 2009). Our results show that *Ptpn22* deficiency results in increased calcium mobilisation in the thymus (**Fig 4.6)** as well enhanced proliferation in SKG *Ptpn22*$^{-/-}$ T cells **(Fig 5.3)**. IL-2 has an important role in augmenting T cell expansion, differentiation and effector functions (Boyman and Sprent, 2012) therefore we assessed the capacity of CD4^{+} T cells from SKG and SKG *Ptpn22*$^{-/-}$ mice to produce IL-2. To this end naïve sorted CD4^{+} T cells from BALB/c, SKG and SKG *Ptpn22*$^{-/-}$ mice were stimulated with different amounts of anti-CD3ε for 72h and the amount of IL-2 produced was measured by ELISA. BALB/c T cells were used as a positive control. Consistent with increased *in vitro* proliferation **(Fig. 5.3)**, SKG *Ptpn22*$^{-/-}$ CD4^{+} cells produced more IL-2 in a dose dependent manner in response to stimulation with anti-CD3 than SKG CD4^{+} cells **(Fig. 5.4)**. Nonetheless, the levels of IL-2 were greatly reduced in SKG *Ptpn22*$^{-/-}$ CD4^{+} cell cultures as compared to wild type CD4^{+} BALB/c controls. These data need

to be interpreted with caution, as at 72h the data may be biased by differences in the IL-2 consumption and also depend on the number of cells present in the culture.

As seen in Chapter 4 increased signalling strength observed in the thymus correlated with elevated responses in the peripheral pool of T cells with increased *in vitro* proliferation and IL-2 production of $CD4^+$ T lymphocytes from SKG *Ptpn22*$^{-/-}$ relative to SKG, but as noted earlier, in the thymus, the SKG *Ptpn22*$^{-/-}$ cells did not reach the levels of responses seen in BALB/c cells.

5.2.3 *Ptpn22* deficiency results in development of less severe arthritis in SKG *Ptpn22*$^{-/-}$ mice.

Despite production of arthritogenic autoimmune T cells due to imbalances in thymic selection, SKG mice fail to develop arthritis when maintained in a SPF animal facility. However, severe arthritis can be triggered by a single intraperitoneal (i.p.) injection of zymosan, a crude yeast wall extract or purified β glucan, such as laminarin (Yoshitomi et al., 2005). Additionally SKG mice stimulated with mannan, a fungal wall polysacharride, presented a higher arthritis score than mice stimulated with zymosan A (Keller et al., 2013). Therefore, we decided to use mannan to induce arthritis in SKG and SKG *Ptpn22*$^{-/-}$ mice.

The frequency and clinical score of spontaneous arthritis in SKG mice is dependent on the cleanliness of the environment and microbial colonisation. In our animal facilities, SKG mice up to the age of 6 months did not develop any spontaneous arthritis or any systemic inflammation such as interstitial pneumonitis as previously reported (Sakaguchi et al., 2006). Additionally, unlike previously demonstrated, SKG mice, those maintained in our facility failed to develop any signs of arthritis with published doses of mannan (0.2, 2 and 20 mg) (Hashimoto et al., 2010). Furthermore, even a 2mg zymosan boost or doubling the amount of highest dose used in literature either showed no disease or only about 50% disease incidence respectively. Therefore we used a higher dose of 50mg/mouse to provoke arthritis in SKG mice **(Figure 5.5)**.

SKG and SKG *Ptpn22*$^{-/-}$ mice were challenged with mannan and monitored for the development of arthritis. A single i.p. injection of 50 mg mannan triggered joint inflammation in the mice as seen by increased paw swelling compared to untreated control **(Fig 5.6).** Interestingly, *Ptpn22* deficiency delayed the onset and severity of arthritis in SKG mice. In addition, the incidence of disease was decreased in SKG *Ptpn22*$^{-/-}$ mice with one out of the six SKG *Ptpn22*$^{-/-}$ mice failing to develop any clinical signs of arthritis, while there was 100% incidence in the SKG group **(Fig 5.7)**. At the end of the 4-week observation period, arthritic joints from the mannan treated SKG and SKG *Ptpn22*$^{-/-}$ mice (n=3) were collected and were evaluated for histology. The mice were not scored for arthritis by histology and it would be interesting to conduct blinded histological scoring with bigger cohort in future experiments. Consistent with the arthritis scores, SKG *Ptpn22*$^{-/-}$ mice showed less synovial hyperplasia compared to the SKG mice **(Fig 5.8)**. Collectively, these data show that loss of *Ptpn22* reduced the severity of arthritis in SKG *Ptpn22*$^{-/-}$ mice.

5.2.4 Increase in total LN and spleen cell number after mannan treatment

Examination of the SKG and SKG *Ptpn22*$^{-/-}$ mice for other evidence of dysregulation of the T cell compartment following mannan administration revealed that more cells were recovered from LNs of SKG mice relative to SKG *Ptpn22*$^{-/-}$ mice. Overall increased total cell numbers were recovered from LNs and spleen in mannan treated SKG and SKG *Ptpn22*$^{-/-}$ mice compared to untreated SKG control mice **(Fig 5.9 A)**. A decrease in frequency of both $CD4^+$ and $CD8^+$ T cells in LNs was noted in mannan treated SKG and SKG *Ptpn22*$^{-/-}$ mice compared to the untreated BALB/c or SKG controls **(Fig 5.9B)**, possibly due to infiltration of T cells into the sub synovial tissue, a cardinal feature in SKG arthritis (Keller et al., 2013; Kobayashi et al., 2006; Sakaguchi et al., 2003; Sakaguchi et al., 2006). The proportions of $CD4^+$ T cells recovered from the LNs were similar in both mannan treated SKG and SKG *Ptpn22*$^{-/-}$ mice but decreased proportions of $CD8^+$ T were detected in SKG *Ptpn22*$^{-/-}$ compared to SKG mice **(Fig 5.9B left panel)**. Furthermore, no significant difference in the ratio of $CD4^+$ and $CD8^+$ T cells was observed in the spleen between SKG and SKG *Ptpn22*$^{-/-}$ **(Fig 5.9B right panel)** suggesting that the increase noted in the total

cell numbers from LNs and spleen were not primarily because of the expansion of T cell compartment. Furthermore the percentages of activated/memory $CD44^{hi}CD62L^{lo}$ were significantly ($p<0.0001$) increased for both $CD4^+$ and $CD8^+$ T cells in SKG *Ptpn22*$^{-/-}$ compared to SKG mice following mannan challenge **(Fig 5.10)**.

5.2.5 IL17 production is decreased in SKG *Ptpn22*$^{-/-}$ mice

Numerous studies have provided evidence that cytokines are directly involved in the pathogenesis of arthritis (Hata et al., 2004; Hirota et al., 2007a; Kobayashi et al., 2006). Of importance is a recent report showing that the development of arthritis in SKG mice is dependent on IL-17-producing arthritogenic Th17 cells, which are promoted by IL-6, secreted by either activated APCs or T cells (Hirota et al., 2007a). Deficiency of either IL-6 or IL-17 completely inhibited the arthritis, while lack of IFN-γ exacerbated the disease (Hirota et al., 2007a). Collectively, these data suggest that both IL-6 and IL-17 are important in the differentiation of Th17 and IFN-γ plays a critical role in maintenance of immunological self-tolerance, as IFN-γ deficiency can break tolerance facilitating differentiation/expansion of arithogenic Th17 cells (Hirota et al., 2007a).

As SKG *Ptpn22*$^{-/-}$ mice developed less severe arthritis in comparison to SKG mice, we compared *ex vivo* cytokine production in $CD4^+$ T cells from mannan treated SKG and SKG *Ptpn22*$^{-/-}$ mice following stimulation with phorbol ester and ionomycin. As shown in **Fig 5.11A**, a significant fraction of LN $CD4^+$ cells from untreated control SKG mice produced IL-17 compared to BALB/c mice and this proportion was further increased on treatment with mannan in both SKG and SKG *Ptpn22*$^{-/-}$ mice. Importantly, the proportion of $CD4^+$IL-17 producing cells was 2-fold higher in LN cultures from SKG as compared to SKG *Ptpn22*$^{-/-}$ mice **(Fig 5.11B)**. We asked whether there was a direct correlation between the increase in proportions of IL-17 positive cells and severity of arthritis in individual animals in both SKG and SKG *Ptpn22*$^{-/-}$ mice, but no such correlation was observed in two independent arthritis induction experiments **(Fig 5.11C)**. Therefore, these results show that the expansion or differentiation of Th17 cells occurs in both SKG and SKG *Ptpn22*$^{-/-}$ mice, albeit to a much lesser degree in SKG *Ptpn22*$^{-/-}$ mice. Additionally SKG *Ptpn22*$^{-/-}$ $CD4^+$ T cells produced more IFNγ and less TNF relative to SKG $CD4^+$ T cells **(Fig 5.11C)**.

5.2.6 Increased production of IL-10 in SKG *Ptpn22*$^{-/-}$ CD4^{+} T cells

IL-10 is a pleiotropic cytokine made by variety of hematopoietic cells, which modulates both the innate and adaptive immune response. Broadly, in CD4^{+} T cells it exerts its effects by induction of Tregs and by suppressing production of inflammatory Th1 cytokines (Mege et al., 2006). The balance of Th1 and Th17 cytokines play a pivotal role in the pathogenesis of RA (Andreakos et al., 2002). Indeed, the immunosuppressive effects of IL-10 were shown in a study in which IL-10$^{-/-}$ SKG mice had a consistently higher incidence and mean arthritis score than IL-10 sufficient mice (Hata et al., 2004). In line with the reported effect of IL -10 on Th1 cells, we sought to determine, if there was any difference in production of IL-10 from CD4^{+} T cells from SKG and SKG *Ptpn22*$^{-/-}$ mice following stimulation with Phorbol ester and ionomycin. As shown previously, a higher proportion of CD4^{+} T cells from SKG as compared to BALB/c mice produced IL-10, which was further increased upon treatment of mice with mannan (Hata et al., 2004; Hirota et al., 2007a). Interestingly, a higher proportion of CD4^{+} T cells from SKG *Ptpn22*$^{-/-}$ mice produced IL-10 compared to SKG mice **(Fig 5.12)**. Therefore, a generalized increase in the IL-10 production could possibly explain the less arthritis seen in SKG *Ptpn22*$^{-/-}$ mice.

5.2.7 Increased proportion of SKG *Ptpn22*$^{-/-}$ Tregs are more activated

Tregs play a critical role in peripheral tolerance and exert their suppressive effects through various effector mechanisms such as consumption of IL-2, production of IL-10 and increasing the expression of immunosuppressive molecules, CTLA4 (Shevach, 2009). Overall increased proportions of Tregs were recovered from LNs and spleen in mannan treated SKG and SKG *Ptpn22*$^{-/-}$ mice compared to untreated SKG or BALB/c control mice **(Fig 5.13A and B)**. We noted a subtle, albeit not significant increase in the proportions of Tregs in the LN of SKG *Ptpn22*$^{-/-}$ mice **(Fig 5.13B** left panel**)**, however no differences were observed in the proportion of Tregs in the spleen between SKG and SKG *Ptpn22*$^{-/-}$ mice **(Fig 5.13B** right panel**)**.

Furthermore, a significant increase (p=0.02) in the proportions of Tregs in the mesenteric lymph node, a key site of iTreg induction was seen in SKG *Ptpn22*$^{-/-}$ mice suggesting that *Ptpn22* deficiency might enhance the propensity of naïve T cells to differentiate into this lineage **(Fig 5.13B** middle panel**)**. Interestingly, comparison of Tregs/Th17 CD4 cells revealed significantly higher ratios in the SKG *Ptpn22*$^{-/-}$ mice compared to SKG mice following challenge with mannan **(Fig 5.13B** right panel**)**. We found a slight increase in the amounts of surface expression of CTLA4 in SKG *Ptpn22*$^{-/-}$ Tregs recovered from lymph nodes and spleen compared to those of SKG Tregs raising the possibility that SKG *Ptpn22*$^{-/-}$ Tregs might have a greater suppressive capacity **(Fig 5.13C)**. These results provide evidence that Tregs are more proportionally in SKG *Ptpn22*$^{-/-}$ mice consistent with the lower severity of arthritis observed in SKG *Ptpn22*$^{-/-}$ compared to SKG mice. However further studies to determine the suppressive function of SKG *Ptpn22*$^{-/-}$ Tregs and exact mechanism of action need to be undertaken.

5.3 Discussion

The aim of the work presented in this chapter was to determine the effect of *Ptpn22* deficiency on the development of arthritis in the SKG mouse model. Recent evidence from PTPN22^{R619W} knock-in mouse models show a similar phenotype as that of PTPN22-deficient mice suggesting that the disease-associated variant acts as a loss-of function allele, at least in mice (Dai et al., 2013; Zhang et al., 2011). Given the association of the variant allele with increased susceptibility to autoimmunity we sought to use the knockout mouse to gain an understanding of how loss of function alleles might contribute to the development of arthritis. To this end, we compared mannan-induced arthritis in SKG *Ptpn22*$^{-/-}$ and SKG mice to ask whether combined mutations in PTPN22 and ZAP-70 would be synergistic or antagonistic for the development of disease.

Stimulation of naïve CD4^{+} T cells from SKG *Ptpn22*$^{-/-}$ mice with anti-CD3 mAb demonstrated a dose-dependent increase in proliferation relative to CD4^{+} T cells from SKG mice **(Fig. 5.3C)**. Overall both SKG and SKG *Ptpn22*$^{-/-}$ CD4^{+} T cells were capable of proliferation, albeit to a much lesser extent than wild-type BALB/c CD4^{+}

T cells in response to stimulation via the TCR. Of note, the initial population of cells, which overcame the threshold of signalling and underwent division, was enhanced by loss of *Ptpn22*, as noted by the significant differences in division index between SKG and SKG *Ptpn22*$^{-/-}$CD4^{+} T cells suggesting that the loss of *Ptpn22* had a subtle effect in improving the proliferative capacity of CD4^{+} T cells on SKG background, which was more clear at low doses of anti-CD3 stimulation. Furthermore, IL-2 production in response to TCR stimulation was increased in SKG *Ptpn22*$^{-/-}$ T cells relative to SKG cells **(Fig 5.4)**. Taken together these results show that consistent with the increases in TCR signalling capacity observed in thymocytes, *Ptpn22* deficiency also enhanced the responses to stimulation in the periphery and is capable therefore, of reversing the reduction of ZAP-70 activity which results from the SKG mutation.

Of note, both effector and regulatory T cell numbers and function are elevated in *Ptpn22*$^{-/-}$ mice and, on the C57BL/6 background, the mice do not develop spontaneous autoimmunity (Brownlie et al., 2012; Maine et al., 2012). However, *Ptpn22* deficiency cooperates with the mutant CD45 E613R protein, to break tolerance in double mutant mice (Zikherman et al., 2009) suggesting cumulative mutations might underlie the autoimmune phenotypes associated with variant allele. Our initial prediction was that the elevated TCR signalling capacity coupled with an increased propensity of T cells to develop an effector/memory phenotype in the absence of PTPN22 might exacerbate disease in SKG mice upon mannan challenge. Surprisingly, our data show the SKG *Ptpn22*$^{-/-}$ mice developed less severe arthritis when compared to SKG mice; furthermore the onset of arthritis was delayed by almost a week in SKG *Ptpn22*$^{-/-}$ mice **(Fig 5.7)**. CD4^{+} T cells that secrete increased levels of IL-17 mediate arthritis in SKG mice (Hirota et al., 2007a). We examined IL-17 production from CD4^{+} T cells recovered from LNs of the mannan treated SKG and SKG *Ptpn22*$^{-/-}$ mice following stimulation with phorbol ester and ionomycin. The frequency of IL-17 production was significantly two-fold lower in CD4^{+} T cells from SKG *Ptpn22*$^{-/-}$ mice compared to SKG mice **(Fig 5.11B)**. The lack of a direct correlation between the numbers of IL-17 producing T cells and the severity of arthritis **(Fig 5.11C)** could be a result of lack of Th17 cells in peripheral lymphoid organs as the Th17 cells are recruited into the synovial cavity (Hirota et al., 2007b)

or the kinetics of the disease progression dictated the presence of Th17. Therefore, future experiments to assess the IL-17 production from synoviocytes and mice taken at an earlier time point would be more informative and representative of Th17 correlation with disease.

The decrease in proportions of IL-17 producing cells could be explained by either that SKG *Ptpn22*$^{-/-}$ T cells were less able to differentiate into Th17 cells or that the development of Th17 was suppressed. Differentiation of naïve wild type C57BL/6 and *Ptpn22*$^{-/-}$ CD4^{+} T cells was equivalent under optimal Th17 polarising conditions *in vitro* (R. Brownlie, personal communication), therefore it is unlikely that decreases in the ratio of Th17 producing cells observed in SKG *Ptpn22*$^{-/-}$ mice is due to an intrinsic defect in Th17 differentiation. Previously published literature shows that IFN-γ suppresses the differentiation/ expansion of Th17 cells and IFN-γ plays a critical role in the maintenance of immunological self-tolerance as lack of IFN-γ worsened the arthritis by facilitating the differentiation/expansion of arthritogenic T cells which could break tolerance in SKG mice maintained even under SPF conditions (Hirota et al., 2007a). We found an increased tendency of CD4^{+} T cells from SKG *Ptpn22*$^{-/-}$ mice to secrete more IFN-γ compared to SKG mice **(Fig 5.11)**. Further, the proportion of IL-10, producing CD4^{+} T cells was also increased in SKG *Ptpn22*$^{-/-}$ mice **(Fig 5.12)**. Therefore both increased IFN-γ and IL-10 may have contributed to the increased resistance to arthritis induction on the *Ptpn22*-deficient background.

The role of pro- or anti-inflammatory cytokines in facilitating or inhibiting the activation of various types of cells, such as macrophages, neutrophils, T cells which are involved in local inflammation is well documented in arthritis (Arend, 2001; Choy, 2012). It is likely that these cytokines alter the degree of T cell mediated control of autoimmune cells. For instance, among the many pleiotropic effects of IL-10, it plays an important role in augmenting Treg mediated immunoregulation, as seen in studies of autoimmune/inflammatory diseases (Fowler and Powrie, 1999; Goudy et al., 2003).

Phenotypic and functional characterization of Treg cells, which are essential for peripheral self-tolerance, indicated that increased percentages of peripheral Treg were found in SKG *Ptpn22*$^{-/-}$ mice (**Fig 5.13B** left and middle panel**)**. Furthermore, the Treg/Th17 ratio was higher in the SKG *Ptpn22*$^{-/-}$ mice compared with that of SKG mice following mannan treatment **(Fig 5.13B** right panel**)**. Both Th17 and Tregs are mutually antagonistic in their differentiation programs (Bettelli et al., 2006; Zhou et al., 2008), wherein Treg transcription factor, Foxp3 is able to suppress the function of ROR-γt, transcription factor required for Th17 differentiation and this could possibly explain the decreased frequency of IL-17 producing cells noted in SKG *Ptpn22*$^{-/-}$ mice compared to SKG mice. In support, SKG *Ptpn22*$^{-/-}$ T cells produced more IL-2, a major cytokine which is not only important for Treg development and maintenance but has also been reported to inhibit Th17 expansion, as blockage of IL-2 or deletion of STAT5 leads to enhanced production of Th17 cells (Laurence et al., 2007). Therefore, it is possible that enhanced IL-2 production in the absence of PTPN22 may favour the induction of inducible Treg and reduce Th17 polarisation, providing an explanation for the altered frequencies of these populations in SKG *Ptpn22*$^{-/-}$ mice.

A recent report from our group demonstrating that *Ptpn22*$^{-/-}$ Tregs are more effective potent suppressors of *Ptpn22*$^{-/-}$ effector T cells than wild-type Tregs is likely to be pertinent to the current study (Brownlie et al., 2012). SKG *Ptpn22*$^{-/-}$ mice have increases in the absolute numbers of peripheral Tregs that also present with a slightly more activated phenotype than the equivalent populations from SKG mice. Whether SKG *Ptpn22*$^{-/-}$ Tregs are more functional in their suppressive capacity than SKG Tregs remains to be determined. In support of an important role for Tregs in disease, a recent report demonstrated protection from arthritis in SLAP-deficient SKG mice due to an increase in steady-state numbers of Tregs, which further expanded following zymosan challenge without an accompanied increase in expansion of autoreactive Th17 cells leading to an increase in the ratio of Tregs to Th17 cells (Peterson et al., 2011).

SKG mice develop high titers of autoantibodies (Sakaguchi et al., 2003). B cell maturation in germinal centres and autoantibody production are regulated by T cells

(Kobezda et al., 2014) and a recent report shows that *Ptpn22*$^{-/-}$ mice have increased T follicular helper (Tfh) cell activity and formation of germinal centres associated with elevated serum Ig titers (Maine et al., 2014), suggesting importance of PTPN22 in regulating B cells. Therefore it would be interesting to see if *Ptpn22* deficiency affected germinal centres in SKG *Ptpn22*$^{-/-}$ mice. The increase noticed in the total cell numbers could be due to recruitment of neutrophils as the Th17 lineage is also largely responsible for the induction of granulopoiesis, or recruitment of neutrophils (Schwarzenberger et al., 1998). A recent report showed that neutrophils from individuals with the variant *PTPN22* 1858T allele release increased levels of reactive oxygen species when primed with TNF and increased Ca^{2+} after stimulation with a chemotactic bacterial peptide mimic (Bayley et al., 2014). Therefore it would be interesting to examine the neutrophils from SKG *Ptpn22*$^{-/-}$ mice.

Collectively, this chapter highlighted that *Ptpn22* deficiency on SKG background resulted in less severe mannan-induced arthritis in SKG *Ptpn22*$^{-/-}$ mice in comparison to SKG mice. In contrast to SKG mice, SKG *Ptpn22*$^{-/-}$ mice show decreased proportions of Th17 cells and higher numbers of regulatory T cells. Further functional studies to demonstrate that the balance between protection from and induction of autoimmune arthritis depends on the fine Treg/Th17 balance might provide an underlying mechanism of *Ptpn22* action in development of arthritis in SKG mice.

5.4 Figures

ZAP-70	PTPN22	T cell development	Immune cell phenotypes	Disease
WT	WT	Normal	Normal	NO
SKG	WT	Defective	↑ Effectors ↑ Tregs ↓ Tregs Suppression	Arthritis
WT	KO	"Normal"	↑ Effectors ↑ Tregs ↑ Tregs Suppression	Susceptible
SKG	KO	?	?	?

Figure 5.1 Immune phenotypes of SKG and PTPN22 KO mice.
The figure describes the summary of T cell development, immune phenotype of effector and regulatory T cells and the susceptibility to autoimmune disease reported for SKG and PTPN22KO mice.

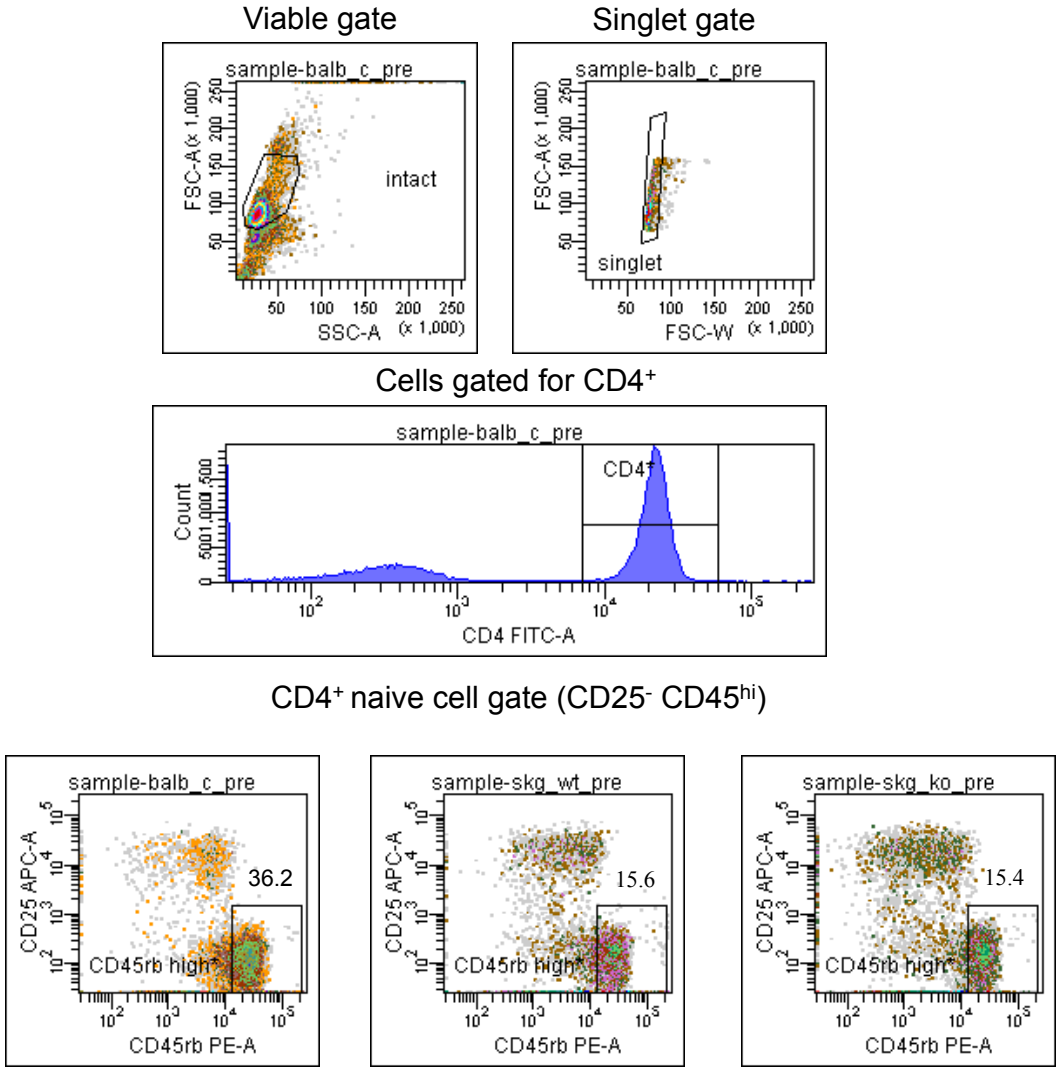

Figure 5.2 Gating strategy for sorting CD4$^+$ naïve T cells from BALB/c, SKG and SKG *Ptpn22*$^{-/-}$ mice

Single cell suspension of lymphocytes from 6 week old BALB/c, SKG and SKG *Ptpn22*$^{-/-}$ mice was first pre-enriched for CD4$^+$ using dynal negative selection, following which the cells were stained with Abs to CD4, CD8, CD25 and CD45RB. Cells were then sorted on the MoFlo on Aria by gating on cells falling within the intact gate as determined by cell size and granularity (FSC versus SSC). Single cells were further gated to on CD4$^+$ population and the naïve cells falling in CD45RB^{hi}CD25$^-$ gate were sorted.

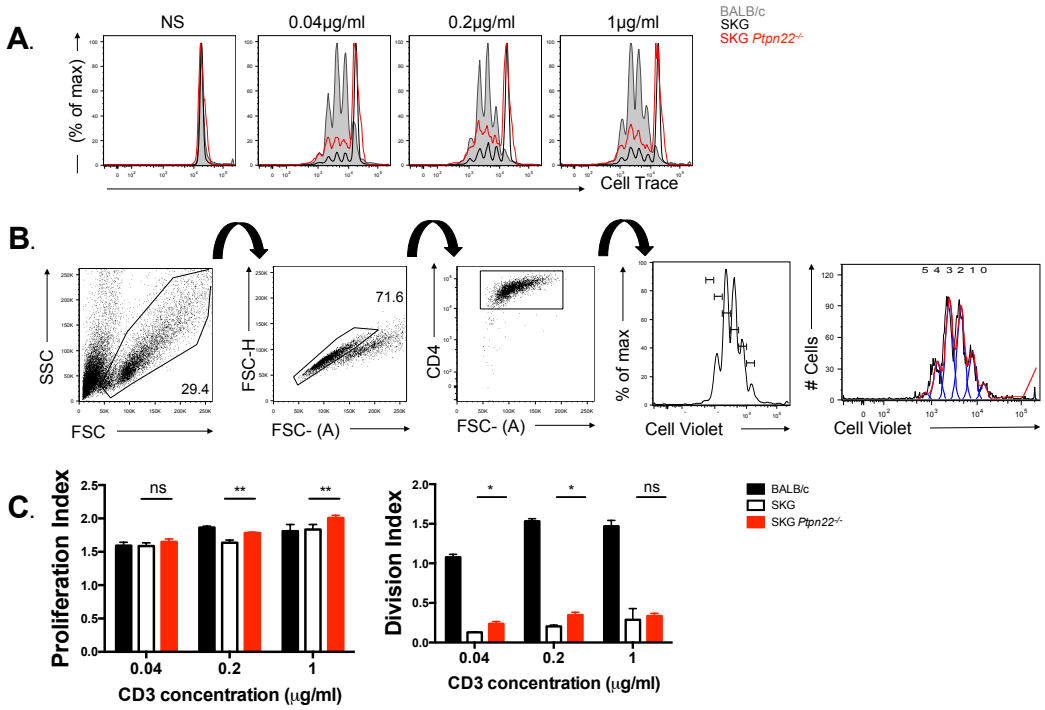

Figure 5.3 Increased proliferation of CD4$^+$ T cells from SKG *Ptpn22*$^{-/-}$ mice compared to SKG mice

Cell Tracer Violet labelled sorted naïve CD4$^+$ T cells (CD45RB^{hi}CD25$^-$) from wild type BALB/c, SKG or SKG *Ptpn22*$^{-/-}$ (10^5cells/well) were stimulated in triplicate wells with irradiated splenocytes ($2x10^5$cells/well) from BALB/c RAG2$^{-/-}$ mice pulsed with mAbs against CD3ε (0.04µg mL^{-1}, 0.2µg mL^{-1} 1µg mL^{-1}). Proliferation of the CD4$^+$ T cells was measured by dilution of Cell Trace on day 3 **(A)** Representative histograms showing the overlay of Cell Tracer dilution in BALB/c (grey shaded), SKG (black overlay line) and SKG *Ptpn22*$^{-/-}$ (red overlay line) in response to stimulation with varying doses of anti-CD3 mAbs on day 3 **(B)** Gating strategy for calculating the proliferation index on FlowJo. First the live cells were gated based on SSC versus FSC followed by gating for FSC-H versus FSC-A (singlet) and finally CD4$^+$ cells were gated for Cell Trace violet expression on histogram gate. **(C)** FlowJo was used to calculate the proliferation index and division index. Bar chart shows the average proliferation and division index at day 3 in BALB/c (black fill bar), SKG (clear bar) and SKG *Ptpn22*$^{-/-}$ (red) at indicated concentration of anti-CD3 stimulation. Data are representative of 4 independent experiments.

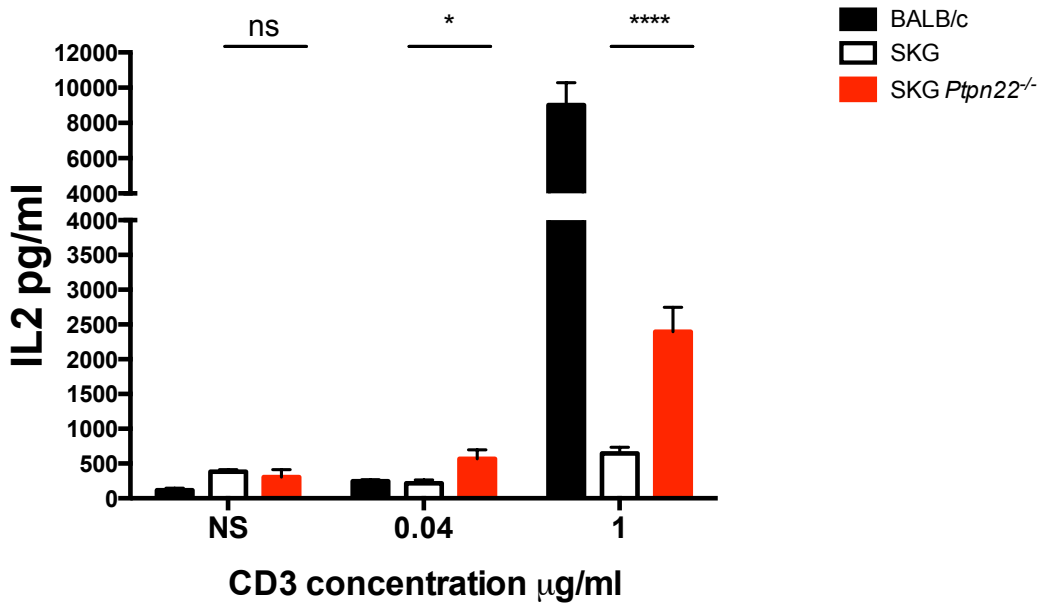

Figure 5.4 CD4$^+$ T cells from SKG *Ptpn22*$^{-/-}$ stimulated with anti-CD3ε mAb produced more IL-2 than SKG CD4$^+$ T cells

Sorted Naïve CD4$^+$ T cells from BALB/c, SKG and SKG *Ptpn22*$^{-/-}$ were stimulated in triplicate wells with irradiated splenocytes (10^5cells/well) were stimulated with irradiated splenocytes ($2x10^5$cells/well) from BALB/c RAG2$^{-/-}$ mice pulsed with mAbs against CD3ε (0.04μg mL^{-1}, 1μg mL^{-1}) for 72h. IL-2 production was assessed from harvested supernatant by ELISA and plotted as average pg mL^{-1}. BALB/c is indicated in black filled bars, SKG in clear bar and SKG *Ptpn22*$^{-/-}$ in red fill bars. Data are representative of 3 independent experiments. Statistical significance was calculated in Prism: multiple t-tests with Holm-Sidak method ns – non significant, *P<0.05, ****P<0.0001.

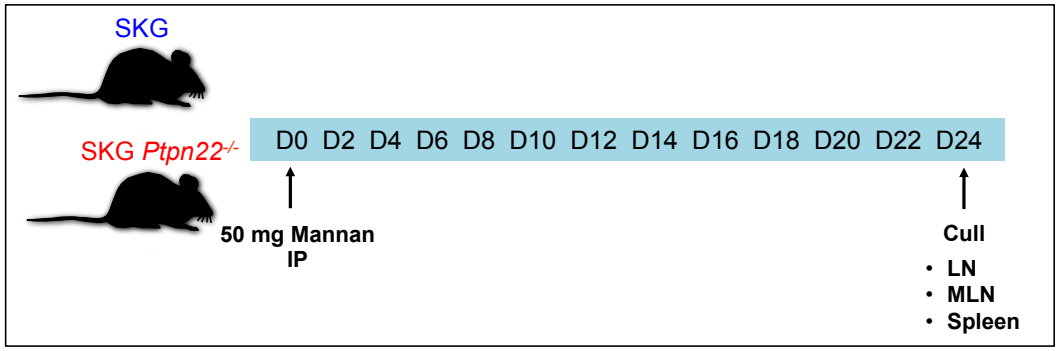

Experiment	Amount of mannan administered per mouse	Incidence of disease
1	2mg	0/7
2	20mg + 2mg Zymosan boost	0/7
3	40 mg	**1/2**
4	50 mg	**6/6**

Figure 5.5 Optimisation of mannan induced arthritis in SKG mice
SKG and SKG *Ptpn22*$^{-/-}$ maintained in SPF facility were given varying dose of mannan via a single intraperitoneal (i.p.) injection to induce arthritis. The animals were sacrificed after 4-6 weeks and the LNs and spleen were analysed.

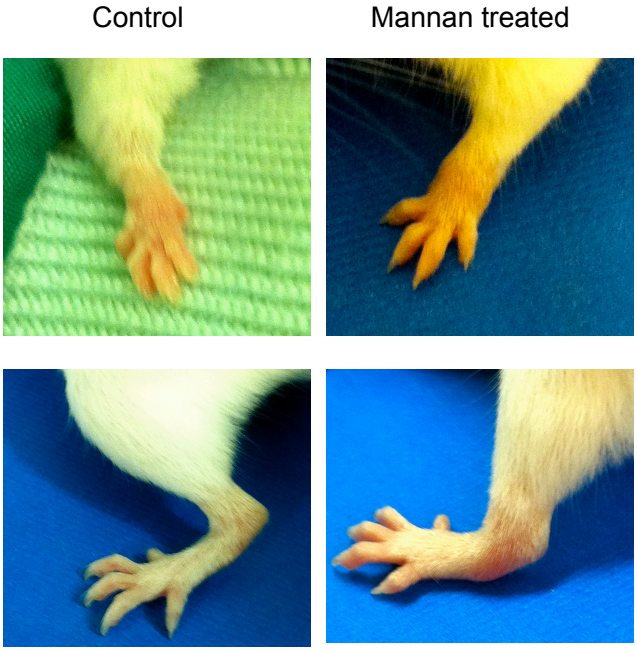

Figure 5.6 Arthritis is induced by 50mg mannan
Representative wrist and ankle joint swelling in SKG mouse, which was administered 50mg of mannan via an i.p. injection compared to an untreated control at 4 weeks, showing an arthritis score of 2

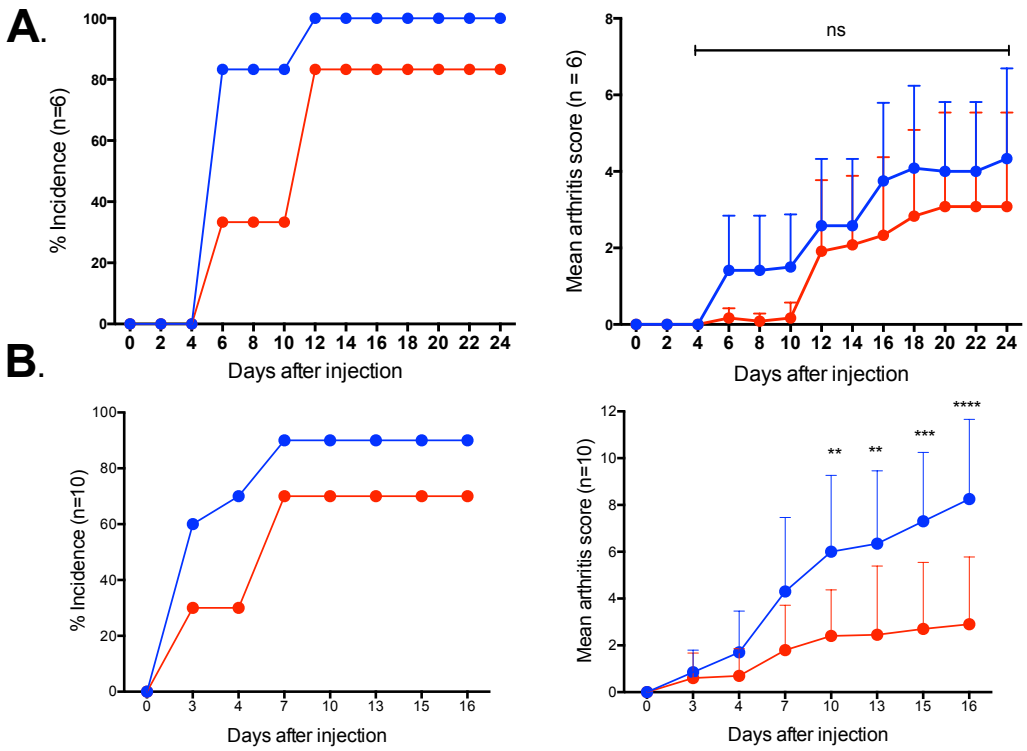

Figure 5.7 SKG *Ptpn22*$^{-/-}$ mice developed less mannan induced arthritis
Incidence of arthritis and joint scores from 11-12 week-old SKG and SKG *Ptpn22*$^{-/-}$ mice that received a single i.p. injection of 50mg mannan over time is shown from two independent experiments **(A)** and **(B)**. Joint swelling was monitored by inspection and scored as follows 0 = no swelling; 1=mild swelling of wrist or ankle; 2=substantial swelling of wrist or ankle; 3=severe swelling of wrist or ankle. Error bars are mean ± SD of the arthritis scores. Statistical significance for the mean arthritis score was calculated in Prism using Two-way Anova, ns = non significant, ** P<0.01, *** P<0.001, ****P<0.0001 and Mantel Cox Test was used to assess the significance of arthritis incidence with P=0.02 for **(A)** and ns for **(B)**

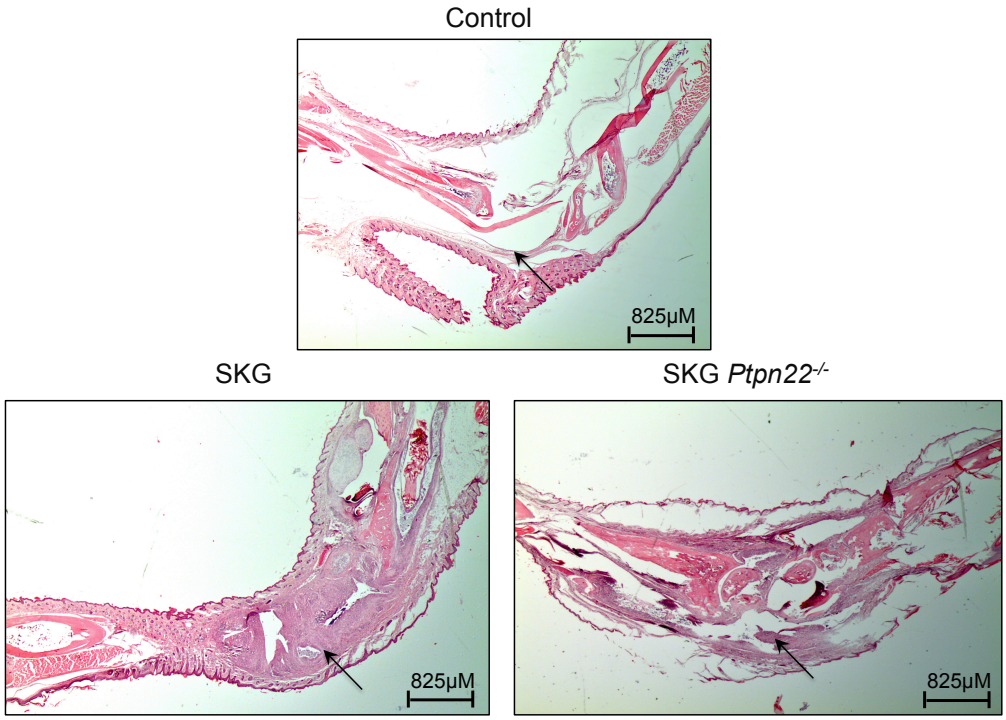

Figure 5.8 Histology of an ankle joint from mannan treated SKG and SKG *Ptpn22*$^{-/-}$ mice
Representative histology of transverse sections of paw and ankle joints from SKG and SKG *Ptpn22*$^{-/-}$ 4 weeks after treatment with 50mg mannan with hematoxylin and eosin staining are shown. H&E staining of ankle joint from untreated SKG mouse serves as control. Arrows highlight the area of infiltration, original magnification 12.5X.

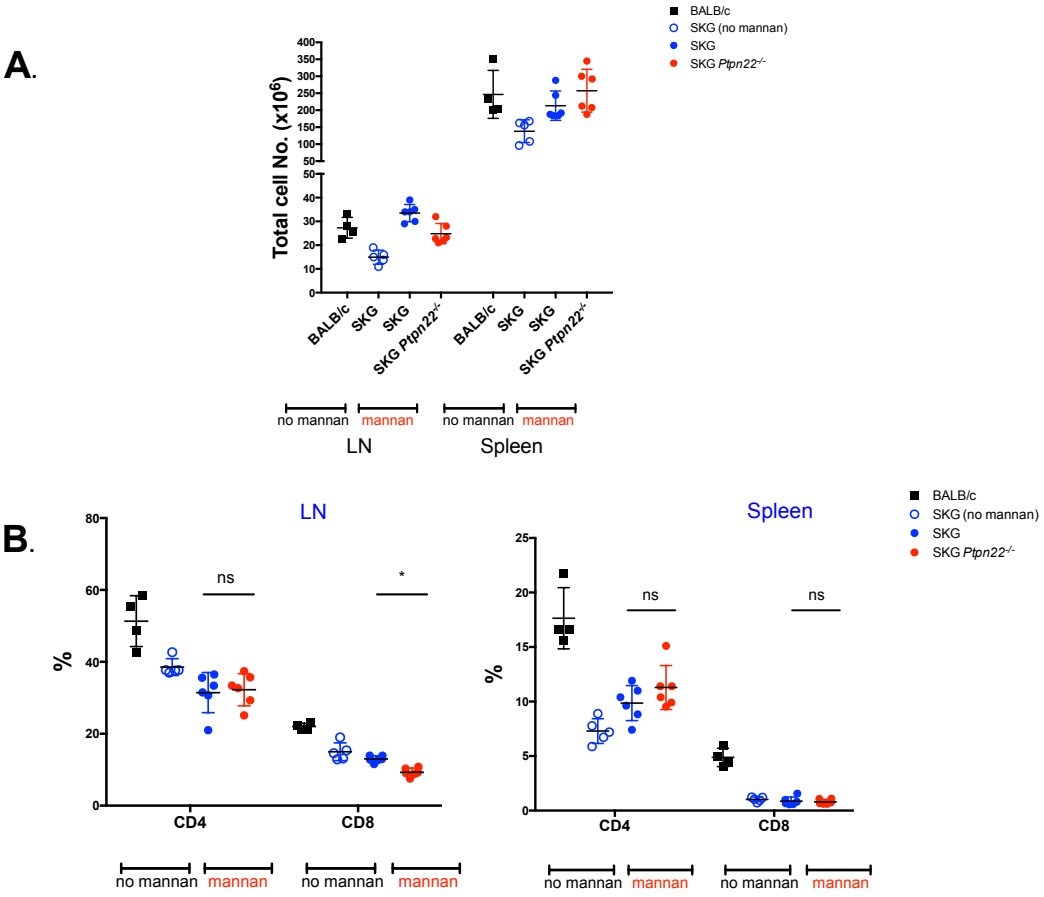

Figure 5.9 Increased numbers of total cells were recovered from SKG and SKG *Ptpn22*$^{-/-}$ mice after mannan treatment.
Axial, Brachial, Inguinal, popliteal LNs and spleen were recovered from the SKG (blue filled circles) and SKG *Ptpn22*$^{-/-}$ mice (red filled circles) 4-week after treatment with mannan. LNs and spleen from untreated BALB/c (black solid squares) and SKG (hollow blue circles) were taken as controls. **(A)** Total cell numbers were counted using CASY counter. **(B)** Single cell suspension of lymphocytes was stained with CD4 and CD8 antibodies and the frequency of CD4 and CD8 in the control and mannan animals treated are shown in LN (left panel) and spleen (right panel). Dot plots shows group means indicated by the horizontal bars ± SD with each point representing individual mice. Statistical significance was calculated in Prism: One-Way ANOVA with post ANOVA Tukey's test for multiple comparisons ns - non significant, *P<0.05.

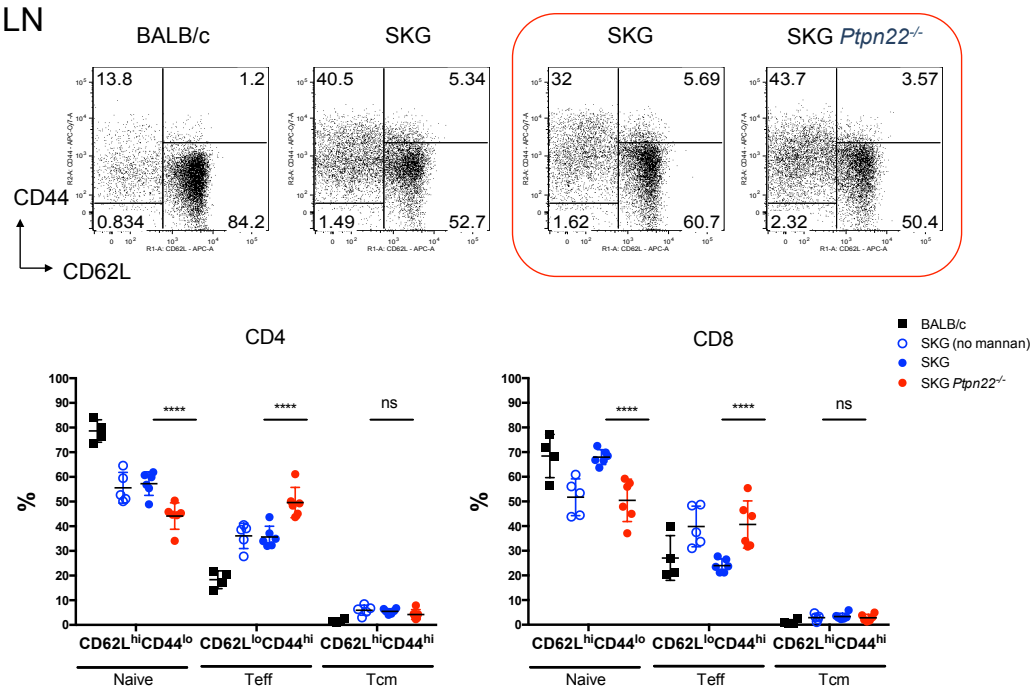

Figure 5.10 Increased proportions of CD4$^+$ effectors in SKG *Ptpn22*$^{-/-}$ mice compared to SKG mice

CD4$^+$ T lymphocytes from LNs were analysed for the frequencies of naïve and effector/memory cells from mannan treated SKG (blue filled circles), SKG *Ptpn22*$^{-/-}$ (red filled circles) control untreated BALB/c (black solid squares) and SKG (hollow blue circles) mice. Example dot plots with frequencies within the CD4 and CD8 gate are shown with mannan treated mice indicated in red square. Statistical significance was calculated in Prism: One-Way ANOVA with post ANOVA Tukey's test for multiple comparisons ns - non significant, ****P<0.0001.

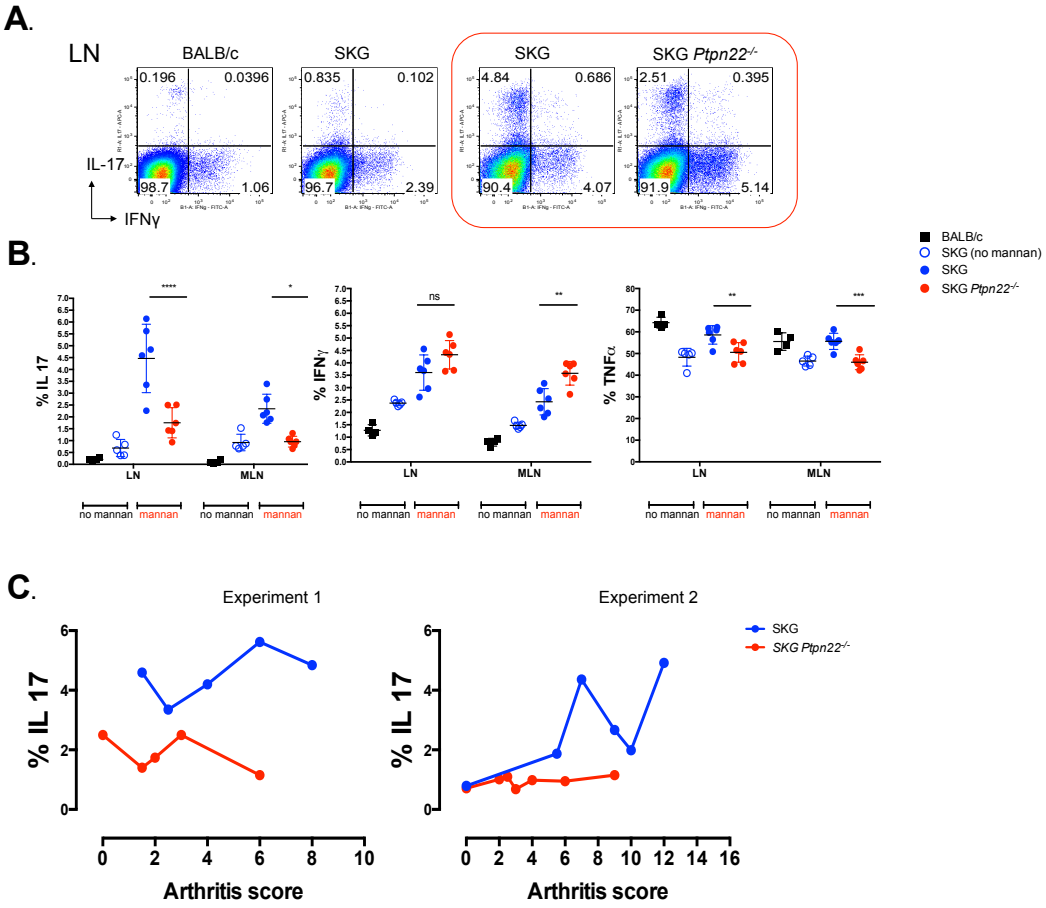

Figure 5.11 *Ptpn22* deficient SKG mice produced less IL-17, TNF and more IFNγ than SKG mice

Ex vivo LNs (axial, brachial, inguinal and popliteal) and mesenteric LNs from mannan treated SKG or SKG *Ptpn22*$^{-/-}$ mice were cultured for 4 h in the presence of PDBu/ ionomycin and BrefeldinA (stimulation). IL-17, IFNγ and TNF production was assessed in CD4^{+} T cells with or without stimulus. **(A)** Representative dot plots of stimulated cells are shown with mannan treated samples shown in red square on the right **(B)** graph representing the frequencies of IL-17, TNF and IFNγ producing CD4^{+} T cells from mannan treated SKG (solid blue circles) or SKG *Ptpn22*$^{-/-}$ mice (red filled circles) compared to untreated BALB/c (black solid squares) and SKG (hollow blue circles) is shown. **(C)** Correlation of IL-17 proportions with severity of arthritis indicated by joint scores for SKG (blue line) and SKG *Ptpn22*$^{-/-}$ (red line) from two independent arthritis experiments is shown. Statistical significance was calculated in Prism: One-Way ANOVA with post ANOVA Tukey's test for multiple comparisons ns – non significant, *P<0.05, **P<0.01, ***P<0.001, ****P<0.0001.

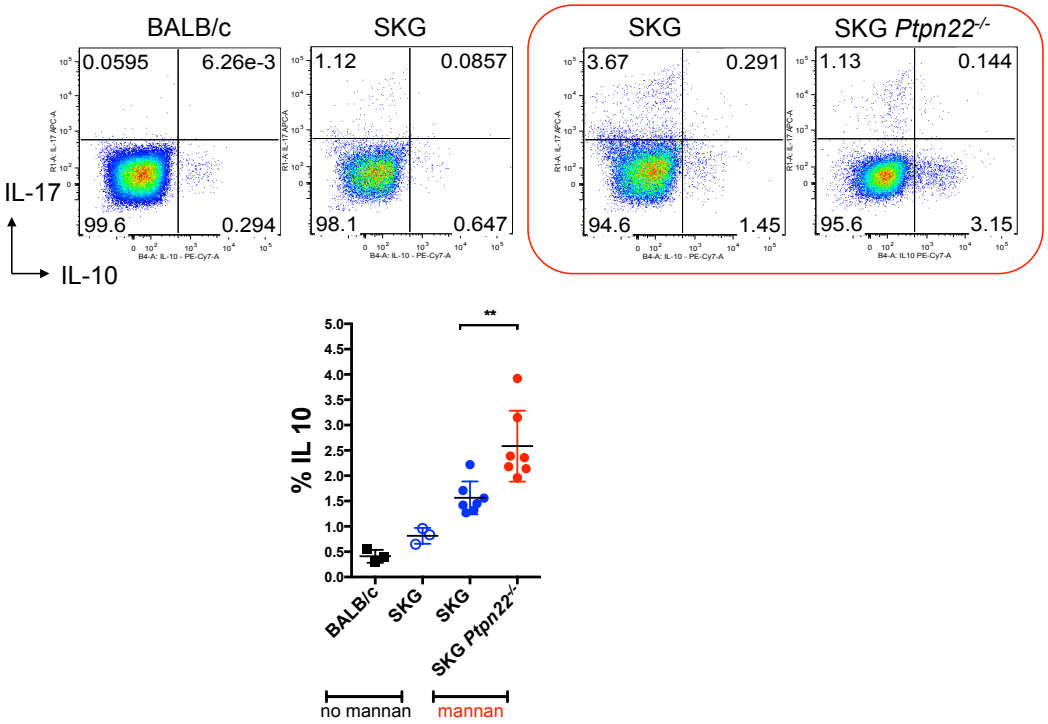

Figure 5.12 *Ptpn22* deficient SKG mice produced more IL-10 than SKG mice
Ex vivo mesenteric LNs from mannan treated SKG or SKG *Ptpn22*$^{-/-}$ mice were cultured for 4 h in the presence of PDBu/ ionomycin and Brefeldin A (stimulation). IL-10 production was assessed in CD4^{+} T cells with or without stimulus. Representative dot plots of stimulated cells are shown from the untreated control BALB/c, SKG and the mannan treated SKG and SKG *Ptpn22*$^{-/-}$ mice (indicated by red square). The graph representing the frequencies of IL-10 producing CD4^{+} T cells from mannan treated SKG (solid blue circles) or SKG *Ptpn22*$^{-/-}$ mice (red filled circles) compared to untreated BALB/c (black solid squares) and SKG (hollow blue circles) is shown. Statistical significance was calculated in Prism: One-Way ANOVA with post ANOVA Tukey's test for multiple comparisons ns-non significant, *P<0.05, **P<0.01, ***P<0.001.

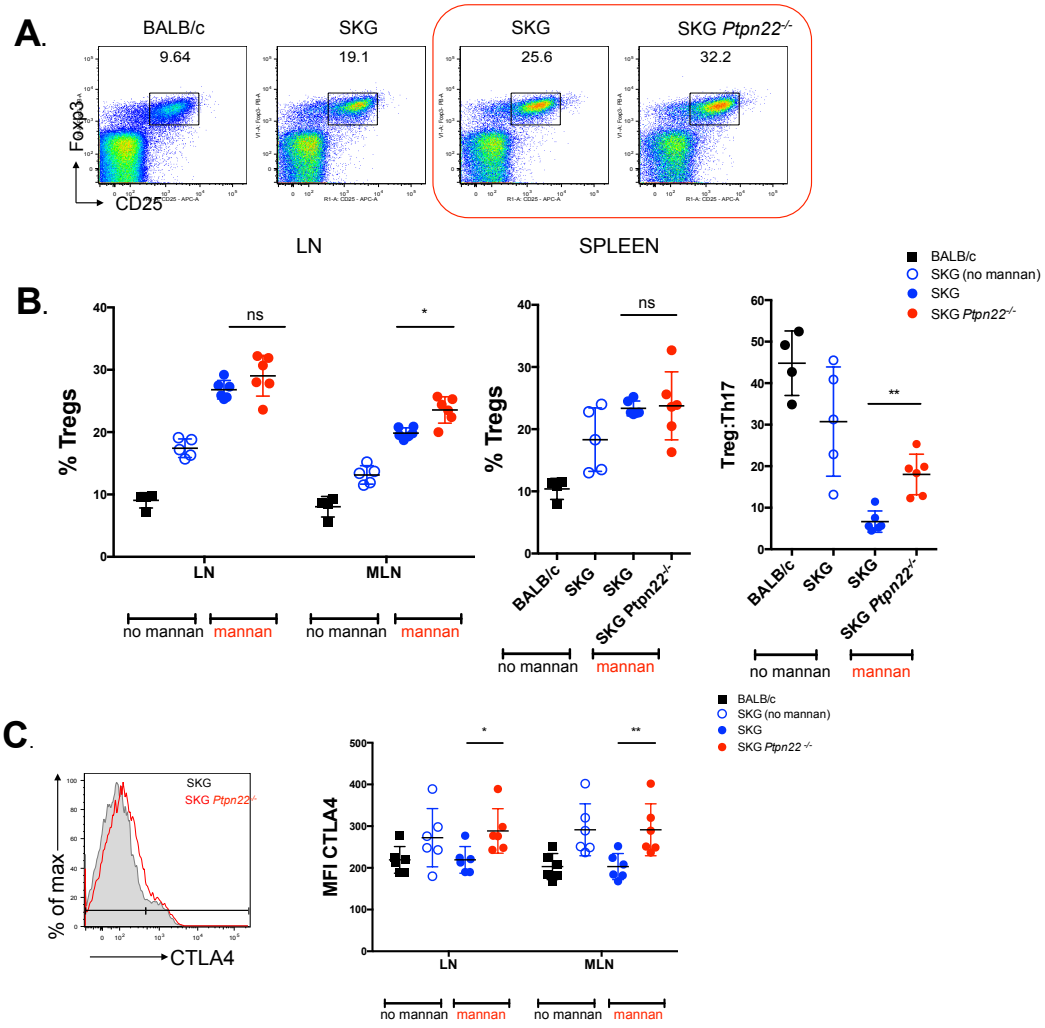

Figure 5.13 *Ptpn22* deficiency results in increased proportions of peripheral Tregs in SKG *Ptpn22*$^{-/-}$ mice after mannan treatment which alter the Treg/Th17 balance
LNs and spleen from SKG and SKG *Ptpn22*$^{-/-}$ mice were analysed for percentages of Tregs (FoxP3^{+}CD25^{+}) within the CD4^{+} T cell population. **(A)** Representative dot plots showing the FoxP3 versus CD25 expression gated on CD4^{+} T cells in control BALB/c, SKG mice or mannan treated SKG and SKG *Ptpn22*$^{-/-}$ mice (indicated in red square) is shown. **(B)** Bar chart shows frequencies of Tregs (CD4^{+} FoxP3^{+}CD25^{+}) in LNs and spleen and the Treg/Th17 CD4 ratio in the LN from control BALB/c, SKG or mannan treated SKG and SKG *Ptpn22*$^{-/-}$ mice. Th17 cells are defined as CD4^{+} IL-17^{+} **(C)** Histogram shows the surface expression of CTLA4 in CD4^{+}FoxP3^{+}CD25^{+} Tregs from LNs of SKG (grey shaded) and SKG *Ptpn22*$^{-/-}$ (red overlay line) mice and the bar chart shows the MFI of CTLA4 expression from the genotypes in LN and MLNs.

Chapter 6: Discussion & Future Directions

Genetic alteration in *PTPN22* gene has been linked to human autoimmunity. The overall objective of this thesis was to understand the functional effect of PTPN22 and its variant in T cell signalling and delineate the molecular mechanism of action in context of an autoimmune disease. Studies from overexpression of PTPN22 in Jurkat T cells or primary human T cells and genetic loss of *Ptpn22* in mice provide strong evidence that PTPN22 negatively regulates TCR signalling (Brownlie et al., 2012; Gjorloff-Wingren et al., 1999; Hasegawa et al., 2004; Vang et al., 2005). A single nucleotide polymorphism of *PTPN22* (*C1858T*) was found to be associated with numerous autoimmune diseases (Bottini and Peterson, 2014), however whether the disease associated variant is a loss-of or gain-of function allele remains controversial.

To clarify the functional effects of $PTPN22^{R619W}$ on T cell signalling, we utilised the lentiviral transduction technology to express $PTPN22^{WT}$ and $PTPN22^{R619W}$ variant in primary T cells from $Ptpn22^{-/-}$ mice. Our data shows that lentiviral induced expression of either $PTPN22^{WT}$ or $PTPN22^{R619W}$ had no effect on cytokine production **(Fig 3.5B)**, suggesting that the lentiviral induced expression might not be sufficient to dampen TCR induced cytokine production. We employed a different approach and used Amaxa nucleofection to express PTPN22 YFP fusion proteins in $Ptpn22^{-/-}$. In this case both $PTPN22^{WT}$ and $PTPN22^{R619W}$ reduced the extent of ERK phosphorylation. Interestingly, at higher levels of $PTPN22^{R619W}$ YFP expression significant reduction in the levels of pERK were noted in comparison to the control $Ptpn22^{-/-}$ T cells **(Fig 3.13)**. However, the results from ectopic expression of PTPN22 needs to be carefully considered, as it is difficult to evaluate if increased levels of expression PTPN22 might alter the stoichiometric balance with Csk and lead to off-target effects. Therefore studying the effect of the R619W variant in physiological setting would be a more relevant approach. Recent studies from two groups, which have independently generated the knock-in mouse model of human ortholog, $PTPN22^{R619W}$ demonstrate that variant phenotypically resembles the $Ptpn22^{-/-}$ mouse, suggesting that at least in mice, R619W variant is a loss-of function allele (Dai et al., 2013; Zhang et al., 2011).

The R620W variation of PTPN22 is a prominent risk factor for RA, T1D and other autoimmune diseases (Bottini and Peterson, 2014). We used the SKG mouse model of arthritis to understand function of PTPN22 in context of an autoimmune disease. Taking advantage of PTPN22-deficient mouse as a model of the loss-of function risk allele, albeit a more extreme allele we generated double mutant SKG *Ptpn22*$^{-/-}$ mice by crossing the *Ptpn22*$^{-/-}$ mice with SKG mice.

Our results show that loss of *Ptpn22* resulted in partial rescue of positive selection in SKG *Ptpn22*$^{-/-}$ mice. Although we did not see significant increases in the CD4^{+} and CD8^{+} SP cells in SKG *Ptpn22*$^{-/-}$ mice, however the expression of CD5 was increased in preselecting DP thymocytes **(Fig 4.4A)**, which correlated with enhanced T cell signalling in response to stimulation in SKG *Ptpn22*$^{-/-}$ thymocytes compared to SKG mice as shown by increase in Ca^{2+} flux **(Fig 4.6)** and moderate increase in pERK **(Fig 4.7)**. In periphery, many T cell associated phenotypes in SKG *Ptpn22*$^{-/-}$ mice recapitulated those observed in *Ptpn22*$^{-/-}$ mice (Brownlie et al., 2012; Hasegawa et al., 2004). Memory/effector CD4^{+} T cells accumulated in aging SKG *Ptpn22*$^{-/-}$ mice **(Fig 4.12)**. CD4^{+} T cells from SKG *Ptpn22*$^{-/-}$ mice proliferated more and produced greater amounts of IL-2 after stimulation in comparison to CD4^{+} T cells from SKG mice **(Fig 5.3 and 5.4)**. Thus these results provided evidence that both PTPN22 and ZAP-70 function by affecting similar signalling pathways *in vivo*. Interestingly despite the tendency to develop effector/memory population, the SKG *Ptpn22*$^{-/-}$ mice developed less severe mannan-induced arthritis in comparison to SKG mice **(Fig 5.7)**.

One of the proposed models as to how the R620W PTPN22 variant allele might promote autoimmunity in humans suggested that the mutation was a gain-of function allele, which suppressed T cell signalling more efficiently resulting in increasing the threshold required for effective TCR signalling in developing thymocytes and allowing the escape of higher number of autoreactive T cells exhibiting a higher functional avidity (Gregersen et al., 2006; Vang et al., 2005). This is exemplified in SKG mouse, where TCR hyporesponsiveness of thymocytes due to aberrant ZAP-70 skews the selection repertoire in a manner that T cells with higher than normal avidity for self escape deletion by negative selection (Sakaguchi et al., 2003). These

negative selection escapees are perpetrators of an autoreactive phenotype in the periphery and cause arthritis in SKG mice **(**see **Fig 6.1)**.

We considered if loss of *Ptpn22* might selectively impact the $CD4^+$ T cell repertoire, however we did not observe any alterations in the selection of TCR Vβ repertoire either in thymus **(Fig 4.8)** or periphery **(Fig 4.9)** of SKG *Ptpn22*$^{-/-}$ mice suggesting that PTPN22 does not have an effect on negative selection in mice, which is in line with a previous published study from *Ptpn22*$^{-/-}$ mice (Hasegawa et al., 2004), Taken together these results suggest that deletion of *Ptpn22* does not majorly impact thymic selection, albeit a subtle effect in augmenting positive selection is noted in SKG *Ptpn22*$^{-/-}$ mice.

The repertoire of both SKG and SKG *Ptpn22*$^{-/-}$ mice contained self-reactive cells but it was perplexing that SKG *Ptpn22*$^{-/-}$ mice still developed less arthritis. Tregs are important in curbing the autoreactive T cells keeping them from causing autoimmunity in the periphery. The alteration of TCR signalling in thymus may alter the amount and repertoire of Treg (Tanaka et al., 2010). Despite the increased signalling observed in SKG *Ptpn22*$^{-/-}$ thymocytes, the numbers of thymic Tregs were not increased in SKG *Ptpn22*$^{-/-}$, which is consistent with C57BL/6 *Ptpn22*$^{-/-}$ mice (Brownlie et al., 2012). However we noticed increased proportions of Tregs in the periphery of SKG *Ptpn22*$^{-/-}$ mice compared to SKG mice, which could provide an explanation for why SKG *Ptpn22*$^{-/-}$ were more resistance to arthritis. A recent study showed that PTPN22 is a direct target of Foxp3, transcription factor important for Treg function (Marson et al., 2007), suggesting that PTPN22 negatively regulates function of Treg cells. In line our previous study showed that Tregs from *Ptpn22*$^{-/-}$ mice are more numerous and suppressive than wild-type Tregs (Brownlie et al., 2012). In support of our proposed mechanism to arthritis resistance in SKG *Ptpn22*$^{-/-}$ mice, *Ptpn22* deficiency has also been shown to be protective in NOD and EAE mice model of disease due to increased Treg numbers (Maine et al., 2012; Zheng and Kissler, 2013).

Tregs are indispensible in immune tolerance and depend on IL-2 for their development, homeostasis and function (Josefowicz and Rudensky, 2009; Malek and

Castro, 2010). The increase in Treg cells might be due to the enhanced responsiveness to IL-2. We found that IL-2 production by $CD4^+$ T cells is increased, which could constitute a source of IL-2 for Treg cells in SKG *Ptpn22*$^{-/-}$ mice. In addition, a recently, published report from our lab showed that *Ptpn22* limits naïve and effector T cell activation in response to very weak self affinity antigens (Salmond et al., 2014). Therefore, it is likely that *Ptpn22* deficiency could enhance homeostatic TCR signalling, which slowly accelerates the turnover of Treg cells and accounts for the increase in Treg proportions seen in the SKG *Ptpn22*$^{-/-}$ mice (Josefowicz and Rudensky, 2009).

SKG mutation impairs the *in vivo* and *in vitro* suppressive function of natural $Foxp3^+$ Tregs as established from cotransfer experiments, wherein transfer of SKG $CD25^-$ $CD4^+$ T cells together with $CD25^+CD4^+$ Treg cells from non-arthritic SKG or BALB/c mice to BALB/c nude mice showed that SKG Treg cells were much less effective in suppressing the development of arthritis (Tanaka et al., 2010). Whether the lack of arthritis in SKG *Ptpn22*$^{-/-}$ mice is exerted through the increased suppressive function of Tregs remains to be determined. It is interesting to note that studies from $PTPN22^{R619W}$ knock-in mice have not reported a diminished Treg function (Dai et al., 2013), thus posing a conflicting argument for our proposed model of protection from arthritis in SKG *Ptpn22*$^{-/-}$ mice.

Another alternative explanation for the role of $PTPN22^{R620W}$ in the pathogenesis of autoimmune disease is that it alters the balance of effector and Treg. This is supported by a study conducted in NOD mouse model wherein, overexpression of T-cell specific transgenic wild-type PTPN22 in NOD mice showed a marked decrease in TCR-mediated effector cell responses such as proliferation and Th1 differentiation but did not affect the differentiation of Tregs or their suppressive activity (Yeh et al., 2013). Importantly the transgenic mice showed lower incidence of spontaneous autoimmune diabetes, which was marked by decreased IFNγ- producing T cells and increased ratios of $CD4^+Foxp3^+$ Tregs to $CD4^+IFN\gamma^+$ or $CD8^+IFN\gamma^+$ effector T cells (Yeh et al., 2013). Our data shows that loss of *Ptpn22* resulted in a significant two-fold decrease in the proportion of $CD4^+$ T cells secreting IL-17 and a concomitant increase in the proportion secreting IFNγ compared to SKG mice **(Fig 5.11)**

suggesting that the balance between autoimmune-promoting effector T cell and autoimmune-protecting Treg cell compartments is finely regulated by PTPN22. In support of this mechanism of PTPN22 action a study showed that Foxp3 induction could restrain differentiation of inflammatory Th17 in response to TGFβ in absence of other inflammatory cytokines by inhibiting RORγT function (Zhou et al., 2008). Further support is provided from a recent study conducted in peripheral blood T cells from healthy PTPN22-C1858T carriers, which revealed that the cytokine production patterns in differentiated effector or memory T cells showed Th1 skewing with increased production of IFNγ, IL-2, TNF but reduced production of Th17 (Vang et al., 2013).

In conclusion, we show that deficiency of *Ptpn22* in SKG mice resulted in accumulation of Treg cells and reduction of autoreactive Th17 cells, which is capable of protecting SKG *Ptpn22*$^{-/-}$ mice from arthritis suggesting that alteration of Treg/Th17 balance could be one of the possible mechanisms of action of PTPN22. It remains to be determined but it is likely that the effects of PTPN22-deficiency on innate cells might have contributed in providing the necessary cytokine milieu for this skewed differentiation **(Fig 6.1)**. Antigen specific Tregs are a potential route for reinstatement of immune tolerance, in light of our results, PTPN22 inhibition (by using a small molecule inhibitor) could be valuable approach to generate either *ex vivo* expanded Tregs or for testing the disease protective effect *in vivo*. Thus our results indicate that PTPN22 could be a valuable target for the treatment of autoimmune diseases.

Future directions

More work is required to understand the function of PTPN22 in immune-cell homeostasis and to clarify the exact molecular mechanism by which the R620W allele of PTPN22 enhances autoimmune disease. Reports have argued a gain-of function, as well as a loss-of function in lymphocytes (Bottini and Peterson, 2014). Recent data provides evidence that *PTPN22* C1858T involves concerted aberration in other cells such as B cells and myeloid cells (Dai et al., 2013; Menard et al., 2011; Wang et al., 2013; Zhang et al., 2011). Selective deficiency of PTPN22 in T

lymphocyte subset and other subsets will help clarify the cellular mechanism of PTPN22 action. Expression of PTPN22^{R619W} variant in autoimmune models will further help to explore immunological function of PTPN22 on disease pathogenesis and will ultimately aid in explaining how it confers risk of disease and reveal any potential as a therapeutic or prognostic target.

Figure 6.1 Model depicting how PTPN22 deficiency might affect development and effector function of T cells in SKG mice.
In SKG mice TCR signal attenuation due to aberrant ZAP-70 leads to a thymic selection shift resulting in positive selection of highly self-reactive T cells and their escape from negative selection, shifting TCR repertoire of conventional T cells to be more self-reactive. In the periphery, these self reactive T cells recognize self pMHC on APCs with greater affinity. This results in the activation and stimulation of APCs to secrete proinflammatory cytokines such as IL-6, IL-1β which together with TGFβ (derived from the tissues) drive the differentiation of self-reactive T cells into Th17 cells. These Th17 cells are then recruited to the inflammation site in the joint by synovial cells where it promotes secretion of inflammatory cytokines by the synovial fibroblasts and activation of other immune cells resulting in bone damage. In thymus, PTPN22 deficiency has minimal effect on selection, albeit shows a very subtle effect on positive selection therefore not majorly altering the thymic selection shift in SKG *Ptpn22*$^{-/-}$ mice. In the periphery, SKG *Ptpn22*$^{-/-}$ mice have a similar pool of autoreactive T cells as that of SKG mice but also have increased number of Tregs. These Tregs might be able to restrain the effector function mediated by Th17 cells by increased immunosuppression or by affecting differentiation of Th17 lineage thereby skewing the Treg:Th17 ratio resulting in the decreased incidence and less severe arthritis observed in these mice.

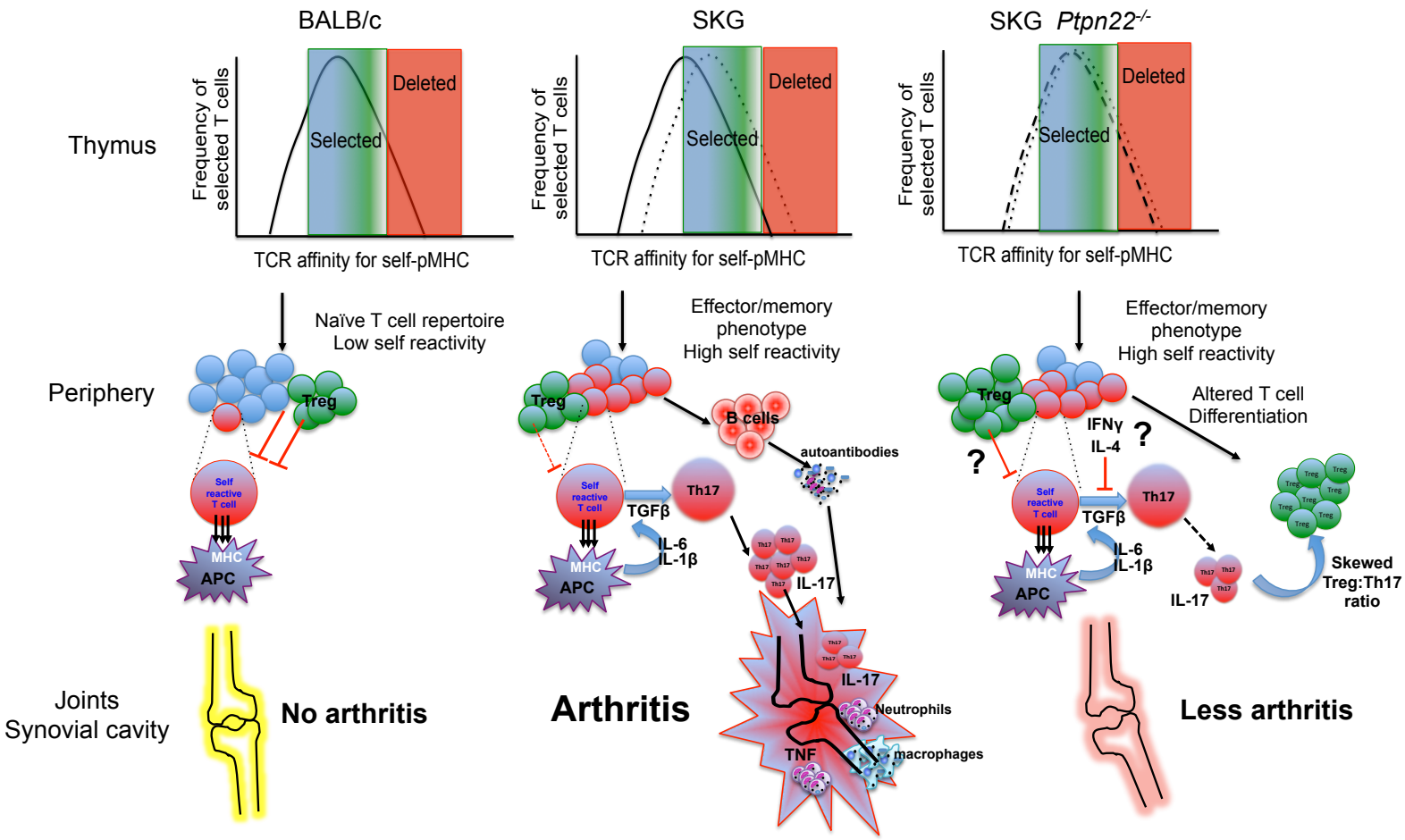

Figure 6.1 Model depicting how PTPN22 deficiency might affect development and effector function of T cells in SKG mice.

Chapter 7: References

Aarnisalo, J., Treszl, A., Svec, P., Marttila, J., Oling, V., Simell, O., Knip, M., Korner, A., Madacsy, L., Vasarhelyi, B.*, et al.* (2008). Reduced CD4+T cell activation in children with type 1 diabetes carrying the PTPN22/Lyp 620Trp variant. J Autoimmun *31*, 13-21.

Acuto, O., Di Bartolo, V., and Michel, F. (2008). Tailoring T-cell receptor signals by proximal negative feedback mechanisms. Nat Rev Immunol *8*, 699-712.

Aggarwal, S., Ghilardi, N., Xie, M.H., de Sauvage, F.J., and Gurney, A.L. (2003). Interleukin-23 promotes a distinct CD4 T cell activation state characterized by the production of interleukin-17. J Biol Chem *278*, 1910-1914.

Alam, S.M., Travers, P.J., Wung, J.L., Nasholds, W., Redpath, S., Jameson, S.C., and Gascoigne, N.R. (1996). T-cell-receptor affinity and thymocyte positive selection. Nature *381*, 616-620.

Alonso, A., Sasin, J., Bottini, N., Friedberg, I., Osterman, A., Godzik, A., Hunter, T., Dixon, J., and Mustelin, T. (2004). Protein tyrosine phosphatases in the human genome. Cell *117*, 699-711.

Andersen, J.N., Jansen, P.G., Echwald, S.M., Mortensen, O.H., Fukada, T., Del Vecchio, R., Tonks, N.K., and Moller, N.P. (2004). A genomic perspective on protein tyrosine phosphatases: gene structure, pseudogenes, and genetic disease linkage. Faseb J *18*, 8-30.

Anderson, G., and Takahama, Y. (2012). Thymic epithelial cells: working class heroes for T cell development and repertoire selection. Trends Immunol *33*, 256-263.

Anderson, M.S., Venanzi, E.S., Klein, L., Chen, Z., Berzins, S.P., Turley, S.J., von Boehmer, H., Bronson, R., Dierich, A., Benoist, C., and Mathis, D. (2002). Projection of an immunological self shadow within the thymus by the aire protein. Science *298*, 1395-1401.

Andreakos, E.T., Foxwell, B.M., Brennan, F.M., Maini, R.N., and Feldmann, M. (2002). Cytokines and anti-cytokine biologicals in autoimmunity: present and future. Cytokine Growth Factor Rev *13*, 299-313.

Apostolou, I., and von Boehmer, H. (2004). In vivo instruction of suppressor commitment in naive T cells. J Exp Med *199*, 1401-1408.

Ardavin, C., Wu, L., Li, C.L., and Shortman, K. (1993). Thymic dendritic cells and T cells develop simultaneously in the thymus from a common precursor population. Nature *362*, 761-763.

Arechiga, A.F., Habib, T., He, Y., Zhang, X., Zhang, Z.Y., Funk, A., and Buckner, J.H. (2009). Cutting edge: the PTPN22 allelic variant associated with autoimmunity impairs B cell signaling. J Immunol *182*, 3343-3347.

Arend, W.P. (2001). Physiology of cytokine pathways in rheumatoid arthritis. Arthritis Rheum *45*, 101-106.

Arimura, Y., Vang, T., Tautz, L., Williams, S., and Mustelin, T. (2008). TCR-induced downregulation of protein tyrosine phosphatase PEST augments secondary T cell responses. Mol Immunol *45*, 3074-3084.

Arimura, Y., and Yagi, J. (2010). Comprehensive expression profiles of genes for protein tyrosine phosphatases in immune cells. Sci Signal *3*, rs1.

Asquith, D.L., Miller, A.M., McInnes, I.B., and Liew, F.Y. (2009). Animal models of rheumatoid arthritis. Eur J Immunol *39*, 2040-2044.

Au-Yeung, B.B., Levin, S.E., Zhang, C., Hsu, L.Y., Cheng, D.A., Killeen, N., Shokat, K.M., and Weiss, A. (2010). A genetically selective inhibitor demonstrates a function for the kinase Zap70 in regulatory T cells independent of its catalytic activity. Nat Immunol *11*, 1085-1092.

Azzam, H.S., DeJarnette, J.B., Huang, K., Emmons, R., Park, C.S., Sommers, C.L., El-Khoury, D., Shores, E.W., and Love, P.E. (2001). Fine tuning of TCR signaling by CD5. J Immunol *166*, 5464-5472.

Azzam, H.S., Grinberg, A., Lui, K., Shen, H., Shores, E.W., and Love, P.E. (1998). CD5 expression is developmentally regulated by T cell receptor (TCR) signals and TCR avidity. J Exp Med *188*, 2301-2311.

Baldwin, T.A., and Hogquist, K.A. (2007). Transcriptional analysis of clonal deletion in vivo. J Immunol *179*, 837-844.

Barcellos, L.F., Caillier, S., Dragone, L., Elder, M., Vittinghoff, E., Bucher, P., Lincoln, R.R., Pericak-Vance, M., Haines, J.L., Weiss, A.*, et al.* (2001). PTPRC (CD45) is not associated with the development of multiple sclerosis in U.S. patients. Nat Genet *29*, 23-24.

Barry, M., and Bleackley, R.C. (2002). Cytotoxic T lymphocytes: all roads lead to death. Nat Rev Immunol *2*, 401-409.

Bayley, R., Kite, K.A., McGettrick, H.M., Smith, J.P., Kitas, G.D., Buckley, C.D., and Young, S.P. (2014). The autoimmune-associated genetic variant PTPN22 R620W enhances neutrophil activation and function in patients with rheumatoid arthritis and healthy individuals. Ann Rheum Dis.

Bedoya, S.K., Lam, B., Lau, K., and Larkin, J., 3rd (2013). Th17 cells in immunity and autoimmunity. Clin Dev Immunol *2013*, 986789.

Begovich, A.B., Caillier, S.J., Alexander, H.C., Penko, J.M., Hauser, S.L., Barcellos, L.F., and Oksenberg, J.R. (2005). The R620W polymorphism of the protein tyrosine phosphatase PTPN22 is not associated with multiple sclerosis. Am J Hum Genet *76*, 184-187.

Begovich, A.B., Carlton, V.E., Honigberg, L.A., Schrodi, S.J., Chokkalingam, A.P., Alexander, H.C., Ardlie, K.G., Huang, Q., Smith, A.M., Spoerke, J.M.*, et al.* (2004). A missense single-nucleotide polymorphism in a gene encoding a protein tyrosine

phosphatase (PTPN22) is associated with rheumatoid arthritis. Am J Hum Genet *75*, 330-337.

Bettelli, E., Carrier, Y., Gao, W., Korn, T., Strom, T.B., Oukka, M., Weiner, H.L., and Kuchroo, V.K. (2006). Reciprocal developmental pathways for the generation of pathogenic effector TH17 and regulatory T cells. Nature *441*, 235-238.

Bottini, N., Musumeci, L., Alonso, A., Rahmouni, S., Nika, K., Rostamkhani, M., MacMurray, J., Meloni, G.F., Lucarelli, P., Pellecchia, M.*, et al.* (2004). A functional variant of lymphoid tyrosine phosphatase is associated with type I diabetes. Nat Genet *36*, 337-338.

Bottini, N., and Peterson, E.J. (2014). Tyrosine phosphatase PTPN22: multifunctional regulator of immune signaling, development, and disease. Annu Rev Immunol *32*, 83-119.

Bottini, N., Vang, T., Cucca, F., and Mustelin, T. (2006). Role of PTPN22 in type 1 diabetes and other autoimmune diseases. Semin Immunol *18*, 207-213.

Bouillet, P., Metcalf, D., Huang, D.C., Tarlinton, D.M., Kay, T.W., Kontgen, F., Adams, J.M., and Strasser, A. (1999). Proapoptotic Bcl-2 relative Bim required for certain apoptotic responses, leukocyte homeostasis, and to preclude autoimmunity. Science *286*, 1735-1738.

Bouillet, P., Purton, J.F., Godfrey, D.I., Zhang, L.C., Coultas, L., Puthalakath, H., Pellegrini, M., Cory, S., Adams, J.M., and Strasser, A. (2002). BH3-only Bcl-2 family member Bim is required for apoptosis of autoreactive thymocytes. Nature *415*, 922-926.

Boyman, O., and Sprent, J. (2012). The role of interleukin-2 during homeostasis and activation of the immune system. Nat Rev Immunol *12*, 180-190.

Brdicka, T., Pavlistova, D., Leo, A., Bruyns, E., Korinek, V., Angelisova, P., Scherer, J., Shevchenko, A., Hilgert, I., Cerny, J.*, et al.* (2000). Phosphoprotein associated with glycosphingolipid-enriched microdomains (PAG), a novel

ubiquitously expressed transmembrane adaptor protein, binds the protein tyrosine kinase csk and is involved in regulation of T cell activation. J Exp Med *191*, 1591-1604.

Brownlie, R.J., Miosge, L.A., Vassilakos, D., Svensson, L.M., Cope, A., and Zamoyska, R. (2012). Lack of the phosphatase PTPN22 increases adhesion of murine regulatory T cells to improve their immunosuppressive function. Sci Signal *5*, ra87.

Broz, P., and Monack, D.M. (2013). Newly described pattern recognition receptors team up against intracellular pathogens. Nat Rev Immunol *13*, 551-565.

Burmester, G.R., Feist, E., and Dorner, T. (2014). Emerging cell and cytokine targets in rheumatoid arthritis. Nat Rev Rheumatol *10*, 77-88.

Burn, G.L., Svensson, L., Sanchez-Blanco, C., Saini, M., and Cope, A.P. (2011). Why is PTPN22 a good candidate susceptibility gene for autoimmune disease? FEBS Lett *585*, 3689-3698.

Burton, P.R. (2007). Genome-wide association study of 14,000 cases of seven common diseases and 3,000 shared controls. Nature *447*, 661-678.

Byth, K.F., Conroy, L.A., Howlett, S., Smith, A.J., May, J., Alexander, D.R., and Holmes, N. (1996). CD45-null transgenic mice reveal a positive regulatory role for CD45 in early thymocyte development, in the selection of CD4+CD8+ thymocytes, and B cell maturation. J Exp Med *183*, 1707-1718.

Cabaniols, J.P., Fazilleau, N., Casrouge, A., Kourilsky, P., and Kanellopoulos, J.M. (2001). Most alpha/beta T cell receptor diversity is due to terminal deoxynucleotidyl transferase. J Exp Med *194*, 1385-1390.

Carlton, V.E., Hu, X., Chokkalingam, A.P., Schrodi, S.J., Brandon, R., Alexander, H.C., Chang, M., Catanese, J.J., Leong, D.U., Ardlie, K.G.*, et al.* (2005). PTPN22 genetic variation: evidence for multiple variants associated with rheumatoid arthritis. Am J Hum Genet *77*, 567-581.

Carpenter, A.C., and Bosselut, R. (2010). Decision checkpoints in the thymus. Nat Immunol *11*, 666-673.

Chan, A.C., Iwashima, M., Turck, C.W., and Weiss, A. (1992). ZAP-70: a 70 kd protein-tyrosine kinase that associates with the TCR zeta chain. Cell *71*, 649-662.

Chan, A.C., Kadlecek, T.A., Elder, M.E., Filipovich, A.H., Kuo, W.L., Iwashima, M., Parslow, T.G., and Weiss, A. (1994). ZAP-70 deficiency in an autosomal recessive form of severe combined immunodeficiency. Science *264*, 1599-1601.

Chang, H.H., Miaw, S.C., Tseng, W., Sun, Y.W., Liu, C.C., Tsao, H.W., and Ho, I.C. (2013). PTPN22 modulates macrophage polarization and susceptibility to dextran sulfate sodium-induced colitis. J Immunol *191*, 2134-2143.

Chien, W., Tidow, N., Williamson, E.A., Shih, L.Y., Krug, U., Kettenbach, A., Fermin, A.C., Roifman, C.M., and Koeffler, H.P. (2003). Characterization of a myeloid tyrosine phosphatase, Lyp, and its role in the Bcr-Abl signal transduction pathway. J Biol Chem *278*, 27413-27420.

Cho, J.H., and Gregersen, P.K. (2011). Genomics and the multifactorial nature of human autoimmune disease. N Engl J Med *365*, 1612-1623.

Choy, E. (2012). Understanding the dynamics: pathways involved in the pathogenesis of rheumatoid arthritis. Rheumatology (Oxford) *51 Suppl 5*, v3-11.

Cloutier, J.F., and Veillette, A. (1996). Association of inhibitory tyrosine protein kinase p50csk with protein tyrosine phosphatase PEP in T cells and other hemopoietic cells. Embo J *15*, 4909-4918.

Cloutier, J.F., and Veillette, A. (1999). Cooperative inhibition of T-cell antigen receptor signaling by a complex between a kinase and a phosphatase. J Exp Med *189*, 111-121.

Cohen, P.L., and Eisenberg, R.A. (1991). Lpr and gld: single gene models of systemic autoimmunity and lymphoproliferative disease. Annu Rev Immunol *9*, 243-269.

Cohen, S., Dadi, H., Shaoul, E., Sharfe, N., and Roifman, C.M. (1999). Cloning and characterization of a lymphoid-specific, inducible human protein tyrosine phosphatase, Lyp. Blood *93*, 2013-2024.

Consortium, T.W.T.C. (2007). Genome-wide association study of 14,000 cases of seven common diseases and 3,000 shared controls. Nature *447*, 661-678.

Cooke, A. (2006). Th17 cells in inflammatory conditions. Rev Diabet Stud *3*, 72-75.

Criswell, L.A., Pfeiffer, K.A., Lum, R.F., Gonzales, B., Novitzke, J., Kern, M., Moser, K.L., Begovich, A.B., Carlton, V.E., Li, W.*, et al.* (2005). Analysis of families in the multiple autoimmune disease genetics consortium (MADGC) collection: the PTPN22 620W allele associates with multiple autoimmune phenotypes. Am J Hum Genet *76*, 561-571.

Crotty, S. (2011). Follicular helper CD4 T cells (TFH). Annu Rev Immunol *29*, 621-663.

Dai, X., James, R.G., Habib, T., Singh, S., Jackson, S., Khim, S., Moon, R.T., Liggitt, D., Wolf-Yadlin, A., Buckner, J.H., and Rawlings, D.J. (2013). A disease-associated PTPN22 variant promotes systemic autoimmunity in murine models. J Clin Invest *123*, 2024-2036.

Daniels, M.A., Teixeiro, E., Gill, J., Hausmann, B., Roubaty, D., Holmberg, K., Werlen, G., Hollander, G.A., Gascoigne, N.R., and Palmer, E. (2006). Thymic selection threshold defined by compartmentalization of Ras/MAPK signalling. Nature *444*, 724-729.

Davidson, D., Cloutier, J.F., Gregorieff, A., and Veillette, A. (1997). Inhibitory tyrosine protein kinase p50csk is associated with protein-tyrosine phosphatase PTP-PEST in hemopoietic and non-hemopoietic cells. J Biol Chem *272*, 23455-23462.

Davidson, D., Schraven, B., and Veillette, A. (2007). PAG-associated FynT regulates calcium signaling and promotes anergy in T lymphocytes. Mol Cell Biol *27*, 1960-1973.

Davidson, D., Shi, X., Zhong, M.C., Rhee, I., and Veillette, A. (2010). The phosphatase PTP-PEST promotes secondary T cell responses by dephosphorylating the protein tyrosine kinase Pyk2. Immunity *33*, 167-180.

Davidson, D., and Veillette, A. (2001). PTP-PEST, a scaffold protein tyrosine phosphatase, negatively regulates lymphocyte activation by targeting a unique set of substrates. Embo J *20*, 3414-3426.

de Souza, A.W., Mesquita Junior, D., Araujo, J.A., Catelan, T.T., Cruvinel Wde, M., Andrade, L.E., and da Silva, N.P. (2010). Immune system: part III. The delicate balance of the immune system between tolerance and autoimmunity. Rev Bras Reumatol *50*, 665-679.

Deindl, S., Kadlecek, T.A., Brdicka, T., Cao, X., Weiss, A., and Kuriyan, J. (2007). Structural basis for the inhibition of tyrosine kinase activity of ZAP-70. Cell *129*, 735-746.

Denzin, L.K., and Cresswell, P. (1995). HLA-DM induces CLIP dissociation from MHC class II alpha beta dimers and facilitates peptide loading. Cell *82*, 155-165.

Di Bartolo, V., Montagne, B., Salek, M., Jungwirth, B., Carrette, F., Fourtane, J., Sol-Foulon, N., Michel, F., Schwartz, O., Lehmann, W.D., and Acuto, O. (2007). A novel pathway down-modulating T cell activation involves HPK-1-dependent recruitment of 14-3-3 proteins on SLP-76. J Exp Med *204*, 681-691.

Diaz-Gallo, L.M., Espino-Paisan, L., Fransen, K., Gomez-Garcia, M., van Sommeren, S., Cardena, C., Rodrigo, L., Mendoza, J.L., Taxonera, C., Nieto, A.*, et al.* (2011). Differential association of two PTPN22 coding variants with Crohn's disease and ulcerative colitis. Inflamm Bowel Dis *17*, 2287-2294.

Dobenecker, M.W., Schmedt, C., Okada, M., and Tarakhovsky, A. (2005). The ubiquitously expressed Csk adaptor protein Cbp is dispensable for embryogenesis and T-cell development and function. Mol Cell Biol *25*, 10533-10542.

Dong, S., Corre, B., Foulon, E., Dufour, E., Veillette, A., Acuto, O., and Michel, F. (2006). T cell receptor for antigen induces linker for activation of T cell-dependent activation of a negative signaling complex involving Dok-2, SHIP-1, and Grb-2. J Exp Med *203*, 2509-2518.

Doody, K.M., Bourdeau, A., and Tremblay, M.L. (2009). T-cell protein tyrosine phosphatase is a key regulator in immune cell signaling: lessons from the knockout mouse model and implications in human disease. Immunol Rev *228*, 325-341.

Duan, B., and Morel, L. (2006). Role of B-1a cells in autoimmunity. Autoimmun Rev *5*, 403-408.

Dupuis, M., De Jesus Ibarra-Sanchez, M., Tremblay, M.L., and Duplay, P. (2003). Gr-1+ myeloid cells lacking T cell protein tyrosine phosphatase inhibit lymphocyte proliferation by an IFN-gamma- and nitric oxide-dependent mechanism. J Immunol *171*, 726-732.

Edmonds, S.D., and Ostergaard, H.L. (2002). Dynamic association of CD45 with detergent-insoluble microdomains in T lymphocytes. J Immunol *169*, 5036-5042.

Elder, M.E., Lin, D., Clever, J., Chan, A.C., Hope, T.J., Weiss, A., and Parslow, T.G. (1994). Human severe combined immunodeficiency due to a defect in ZAP-70, a T cell tyrosine kinase. Science *264*, 1596-1599.

Engel, P., Gomez-Puerta, J.A., Ramos-Casals, M., Lozano, F., and Bosch, X. (2011). Therapeutic targeting of B cells for rheumatic autoimmune diseases. Pharmacol Rev *63*, 127-156.

Fehling, H.J., Krotkova, A., Saint-Ruf, C., and von Boehmer, H. (1995). Crucial role of the pre-T-cell receptor alpha gene in development of alpha beta but not gamma delta T cells. Nature *375*, 795-798.

Filby, A., Seddon, B., Kleczkowska, J., Salmond, R., Tomlinson, P., Smida, M., Lindquist, J.A., Schraven, B., and Zamoyska, R. (2007). Fyn regulates the duration of TCR engagement needed for commitment to effector function. J Immunol *179*, 4635-4644.

Fiorillo, E., Orru, V., Stanford, S.M., Liu, Y., Salek, M., Rapini, N., Schenone, A.D., Saccucci, P., Delogu, L.G., Angelini, F.*, et al.* (2010). Autoimmune-associated PTPN22 R620W variation reduces phosphorylation of lymphoid phosphatase on an inhibitory tyrosine residue. J Biol Chem *285*, 26506-26518.

Flores, E., Roy, G., Patel, D., Shaw, A., and Thomas, M.L. (1994). Nuclear localization of the PEP protein tyrosine phosphatase. Mol Cell Biol *14*, 4938-4946.

Fontenot, J.D., Gavin, M.A., and Rudensky, A.Y. (2003). Foxp3 programs the development and function of CD4+CD25+ regulatory T cells. Nat Immunol *4*, 330-336.

Fontenot, J.D., Rasmussen, J.P., Gavin, M.A., and Rudensky, A.Y. (2005). A function for interleukin 2 in Foxp3-expressing regulatory T cells. Nat Immunol *6*, 1142-1151.

Fowler, S., and Powrie, F. (1999). Control of immune pathology by IL-10-secreting regulatory T cells. Springer Semin Immunopathol *21*, 287-294.

Frecha, C., Levy, C., Cosset, F.L., and Verhoeyen, E. (2010). Advances in the field of lentivector-based transduction of T and B lymphocytes for gene therapy. Mol Ther *18*, 1748-1757.

Freiberg, B.A., Kupfer, H., Maslanik, W., Delli, J., Kappler, J., Zaller, D.M., and Kupfer, A. (2002). Staging and resetting T cell activation in SMACs. Nat Immunol *3*, 911-917.

Fu, G., Vallee, S., Rybakin, V., McGuire, M.V., Ampudia, J., Brockmeyer, C., Salek, M., Fallen, P.R., Hoerter, J.A., Munshi, A.*, et al.* (2009). Themis controls thymocyte

selection through regulation of T cell antigen receptor-mediated signaling. Nat Immunol *10*, 848-856.

Gallegos, A.M., and Bevan, M.J. (2004). Central tolerance to tissue-specific antigens mediated by direct and indirect antigen presentation. J Exp Med *200*, 1039-1049.

Gascoigne, N.R., and Palmer, E. (2011). Signaling in thymic selection. Curr Opin Immunol *23*, 207-212.

Genot, E., and Cantrell, D.A. (2000). Ras regulation and function in lymphocytes. Curr Opin Immunol *12*, 289-294.

Germain, R.N. (2002). T-cell development and the CD4-CD8 lineage decision. Nat Rev Immunol *2*, 309-322.

Ghose, R., Shekhtman, A., Goger, M.J., Ji, H., and Cowburn, D. (2001). A novel, specific interaction involving the Csk SH3 domain and its natural ligand. Nat Struct Biol *8*, 998-1004.

Gilham, D.E., Lie, A.L.M., Taylor, N., and Hawkins, R.E. (2010). Cytokine stimulation and the choice of promoter are critical factors for the efficient transduction of mouse T cells with HIV-1 vectors. J Gene Med *12*, 129-136.

Girardi, M. (2006). Immunosurveillance and immunoregulation by gammadelta T cells. J Invest Dermatol *126*, 25-31.

Gjorloff-Wingren, A., Saxena, M., Han, S., Wang, X., Alonso, A., Renedo, M., Oh, P., Williams, S., Schnitzer, J., and Mustelin, T. (2000). Subcellular localization of intracellular protein tyrosine phosphatases in T cells. Eur J Immunol *30*, 2412-2421.

Gjorloff-Wingren, A., Saxena, M., Williams, S., Hammi, D., and Mustelin, T. (1999). Characterization of TCR-induced receptor-proximal signaling events negatively regulated by the protein tyrosine phosphatase PEP. Eur J Immunol *29*, 3845-3854.

Gol-Ara, M., Jadidi-Niaragh, F., Sadria, R., Azizi, G., and Mirshafiey, A. (2012). The role of different subsets of regulatory T cells in immunopathogenesis of rheumatoid arthritis. Arthritis *2012*, 805875.

Goudy, K.S., Burkhardt, B.R., Wasserfall, C., Song, S., Campbell-Thompson, M.L., Brusko, T., Powers, M.A., Clare-Salzler, M.J., Sobel, E.S., Ellis, T.M.*, et al.* (2003). Systemic overexpression of IL-10 induces CD4+CD25+ cell populations in vivo and ameliorates type 1 diabetes in nonobese diabetic mice in a dose-dependent fashion. J Immunol *171*, 2270-2278.

Gregersen, P.K., Lee, H.S., Batliwalla, F., and Begovich, A.B. (2006). PTPN22: setting thresholds for autoimmunity. Semin Immunol *18*, 214-223.

Gregorieff, A., Cloutier, J.F., and Veillette, A. (1998). Sequence requirements for association of protein-tyrosine phosphatase PEP with the Src homology 3 domain of inhibitory tyrosine protein kinase p50(csk). J Biol Chem *273*, 13217-13222.

Hacker, H., Tseng, P.H., and Karin, M. (2011). Expanding TRAF function: TRAF3 as a tri-faced immune regulator. Nat Rev Immunol *11*, 457-468.

Hardy, R.R. (2006). B-1 B cells: development, selection, natural autoantibody and leukemia. Curr Opin Immunol *18*, 547-555.

Hasegawa, K., Martin, F., Huang, G., Tumas, D., Diehl, L., and Chan, A.C. (2004). PEST domain-enriched tyrosine phosphatase (PEP) regulation of effector/memory T cells. Science *303*, 685-689.

Hasegawa, K., Yajima, H., Katagiri, T., Ogimoto, M., Arimura, Y., Mitomo, K., Mashima, K., Mizuno, K., and Yakura, H. (1999). Requirement of PEST domain tyrosine phosphatase PEP in B cell antigen receptor-induced growth arrest and apoptosis. Eur J Immunol *29*, 887-896.

Hashimoto, M., Hirota, K., Yoshitomi, H., Maeda, S., Teradaira, S., Akizuki, S., Prieto-Martin, P., Nomura, T., Sakaguchi, N., Kohl, J.*, et al.* (2010). Complement

drives Th17 cell differentiation and triggers autoimmune arthritis. J Exp Med *207*, 1135-1143.

Hata, H., Sakaguchi, N., Yoshitomi, H., Iwakura, Y., Sekikawa, K., Azuma, Y., Kanai, C., Moriizumi, E., Nomura, T., Nakamura, T., and Sakaguchi, S. (2004). Distinct contribution of IL-6, TNF-alpha, IL-1, and IL-10 to T cell-mediated spontaneous autoimmune arthritis in mice. J Clin Invest *114*, 582-588.

Hayden, M.S., and Ghosh, S. (2011). NF-kappaB in immunobiology. Cell Res *21*, 223-244.

He, J., Yang, Q., and Chang, L.J. (2005). Dynamic DNA methylation and histone modifications contribute to lentiviral transgene silencing in murine embryonic carcinoma cells. J Virol *79*, 13497-13508.

Heng, T.S., and Painter, M.W. (2008). The Immunological Genome Project: networks of gene expression in immune cells. Nat Immunol *9*, 1091-1094.

Hermiston, M.L., Xu, Z., and Weiss, A. (2003). CD45: a critical regulator of signaling thresholds in immune cells. Annu Rev Immunol *21*, 107-137.

Hermiston, M.L., Zikherman, J., and Zhu, J.W. (2009). CD45, CD148, and Lyp/Pep: critical phosphatases regulating Src family kinase signaling networks in immune cells. Immunol Rev *228*, 288-311.

Hernandez-Hoyos, G., Sohn, S.J., Rothenberg, E.V., and Alberola-Ila, J. (2000). Lck activity controls CD4/CD8 T cell lineage commitment. Immunity *12*, 313-322.

Hill, R.J., Zozulya, S., Lu, Y.L., Ward, K., Gishizky, M., and Jallal, B. (2002). The lymphoid protein tyrosine phosphatase Lyp interacts with the adaptor molecule Grb2 and functions as a negative regulator of T-cell activation. Exp Hematol *30*, 237-244.

Hirota, K., Hashimoto, M., Yoshitomi, H., Tanaka, S., Nomura, T., Yamaguchi, T., Iwakura, Y., Sakaguchi, N., and Sakaguchi, S. (2007a). T cell self-reactivity forms a

cytokine milieu for spontaneous development of IL-17+ Th cells that cause autoimmune arthritis. J Exp Med *204*, 41-47.

Hirota, K., Yoshitomi, H., Hashimoto, M., Maeda, S., Teradaira, S., Sugimoto, N., Yamaguchi, T., Nomura, T., Ito, H., Nakamura, T.*, et al.* (2007b). Preferential recruitment of CCR6-expressing Th17 cells to inflamed joints via CCL20 in rheumatoid arthritis and its animal model. J Exp Med *204*, 2803-2812.

Hogquist, K.A., Baldwin, T.A., and Jameson, S.C. (2005). Central tolerance: learning self-control in the thymus. Nat Rev Immunol *5*, 772-782.

Honda, R., Ohba, Y., Nagata, A., Okayama, H., and Yasuda, H. (1993). Dephosphorylation of human p34cdc2 kinase on both Thr-14 and Tyr-15 by human cdc25B phosphatase. FEBS Lett *318*, 331-334.

Hori, S., Nomura, T., and Sakaguchi, S. (2003). Control of regulatory T cell development by the transcription factor Foxp3. Science *299*, 1057-1061.

Hsieh, C.S., Lee, H.M., and Lio, C.W. (2012). Selection of regulatory T cells in the thymus. Nat Rev Immunol *12*, 157-167.

Hsu, L.Y., Tan, Y.X., Xiao, Z., Malissen, M., and Weiss, A. (2009). A hypomorphic allele of ZAP-70 reveals a distinct thymic threshold for autoimmune disease versus autoimmune reactivity. J Exp Med *206*, 2527-2541.

Huck, S., Le Corre, R., Youinou, P., and Zouali, M. (2001). Expression of B cell receptor-associated signaling molecules in human lupus. Autoimmunity *33*, 213-224.

Huesmann, M., Scott, B., Kisielow, P., and von Boehmer, H. (1991). Kinetics and efficacy of positive selection in the thymus of normal and T cell receptor transgenic mice. Cell *66*, 533-540.

Itoh, M., Takahashi, T., Sakaguchi, N., Kuniyasu, Y., Shimizu, J., Otsuka, F., and Sakaguchi, S. (1999). Thymus and autoimmunity: production of CD25+CD4+

naturally anergic and suppressive T cells as a key function of the thymus in maintaining immunologic self-tolerance. J Immunol *162*, 5317-5326.

Ivanov, II, McKenzie, B.S., Zhou, L., Tadokoro, C.E., Lepelley, A., Lafaille, J.J., Cua, D.J., and Littman, D.R. (2006). The orphan nuclear receptor RORgammat directs the differentiation program of proinflammatory IL-17+ T helper cells. Cell *126*, 1121-1133.

Jacobsen, M., Schweer, D., Ziegler, A., Gaber, R., Schock, S., Schwinzer, R., Wonigeit, K., Lindert, R.B., Kantarci, O., Schaefer-Klein, J*., et al.* (2000). A point mutation in PTPRC is associated with the development of multiple sclerosis. Nat Genet *26*, 495-499.

Janssen, E., and Zhang, W. (2003). Adaptor proteins in lymphocyte activation. Curr Opin Immunol *15*, 269-276.

Javierre, B.M., Hernando, H., and Ballestar, E. (2011). Environmental triggers and epigenetic deregulation in autoimmune disease. Discov Med *12*, 535-545.

Jordan, M.S., Boesteanu, A., Reed, A.J., Petrone, A.L., Holenbeck, A.E., Lerman, M.A., Naji, A., and Caton, A.J. (2001). Thymic selection of CD4+CD25+ regulatory T cells induced by an agonist self-peptide. Nat Immunol *2*, 301-306.

Josefowicz, S.Z., and Rudensky, A. (2009). Control of regulatory T cell lineage commitment and maintenance. Immunity *30*, 616-625.

Kalergis, A.M., Boucheron, N., Doucey, M.A., Palmieri, E., Goyarts, E.C., Vegh, Z., Luescher, I.F., and Nathenson, S.G. (2001). Efficient T cell activation requires an optimal dwell-time of interaction between the TCR and the pMHC complex. Nat Immunol *2*, 229-234.

Kariuki, S.N., Crow, M.K., and Niewold, T.B. (2008). The PTPN22 C1858T polymorphism is associated with skewing of cytokine profiles toward high interferon-alpha activity and low tumor necrosis factor alpha levels in patients with lupus. Arthritis Rheum *58*, 2818-2823.

Kassiotis, G., Zamoyska, R., and Stockinger, B. (2003). Involvement of avidity for major histocompatibility complex in homeostasis of naive and memory T cells. J Exp Med *197*, 1007-1016.

Katagiri, K., Maeda, A., Shimonaka, M., and Kinashi, T. (2003). RAPL, a Rap1-binding molecule that mediates Rap1-induced adhesion through spatial regulation of LFA-1. Nat Immunol *4*, 741-748.

Katagiri, T., Ogimoto, M., Hasegawa, K., Arimura, Y., Mitomo, K., Okada, M., Clark, M.R., Mizuno, K., and Yakura, H. (1999). CD45 negatively regulates lyn activity by dephosphorylating both positive and negative regulatory tyrosine residues in immature B cells. J Immunol *163*, 1321-1326.

Keller, K.K., Lindgaard, L.M., Wogensen, L., Dagnaes-Hansen, F., Thomsen, J.S., Sakaguchi, S., Stengaard-Pedersen, K., and Hauge, E.M. (2013). SKG arthritis as a model for evaluating therapies in rheumatoid arthritis with special focus on bone changes. Rheumatol Int *33*, 1127-1133.

Kersh, G.J., Kersh, E.N., Fremont, D.H., and Allen, P.M. (1998). High- and low-potency ligands with similar affinities for the TCR: the importance of kinetics in TCR signaling. Immunity *9*, 817-826.

Khattri, R., Cox, T., Yasayko, S.A., and Ramsdell, F. (2003). An essential role for Scurfin in CD4+CD25+ T regulatory cells. Nat Immunol *4*, 337-342.

Kieper, W.C., Troy, A., Burghardt, J.T., Ramsey, C., Lee, J.Y., Jiang, H.Q., Dummer, W., Shen, H., Cebra, J.J., and Surh, C.D. (2005). Recent immune status determines the source of antigens that drive homeostatic T cell expansion. J Immunol *174*, 3158-3163.

Kindt, T.J., Goldsby, R.A., Osborne, B.A., and Kuby, J. (2007). Kuby immunology, Sixth edition / edn (New York: W.H. Freeman).

Kishihara, K., Penninger, J., Wallace, V.A., Kundig, T.M., Kawai, K., Wakeham, A., Timms, E., Pfeffer, K., Ohashi, P.S., Thomas, M.L., and et al. (1993). Normal B

lymphocyte development but impaired T cell maturation in CD45-exon6 protein tyrosine phosphatase-deficient mice. Cell *74*, 143-156.

Kobayashi, K., Suda, T., Nan-Ya, K., Sakaguchi, N., Sakaguchi, S., and Miki, I. (2006). Cytokine production profile of splenocytes derived from zymosan A-treated SKG mice developing arthritis. Inflamm Res *55*, 335-341.

Kobezda, T., Ghassemi-Nejad, S., Mikecz, K., Glant, T.T., and Szekanecz, Z. (2014). Of mice and men: how animal models advance our understanding of T-cell function in RA. Nat Rev Rheumatol *10*, 160-170.

Koretzky, G.A., Abtahian, F., and Silverman, M.A. (2006). SLP76 and SLP65: complex regulation of signalling in lymphocytes and beyond. Nat Rev Immunol *6*, 67-78.

Krummel, M.F., and Allison, J.P. (1995). CD28 and CTLA-4 have opposing effects on the response of T cells to stimulation. J Exp Med *182*, 459-465.

Kyogoku, C., Langefeld, C.D., Ortmann, W.A., Lee, A., Selby, S., Carlton, V.E., Chang, M., Ramos, P., Baechler, E.C., Batliwalla, F.M.*, et al.* (2004). Genetic association of the R620W polymorphism of protein tyrosine phosphatase PTPN22 with human SLE. Am J Hum Genet *75*, 504-507.

Laurence, A., Tato, C.M., Davidson, T.S., Kanno, Y., Chen, Z., Yao, Z., Blank, R.B., Meylan, F., Siegel, R., Hennighausen, L.*, et al.* (2007). Interleukin-2 signaling via STAT5 constrains T helper 17 cell generation. Immunity *26*, 371-381.

Leavy, O. (2008). Apoptosis: BIM and FAS: the ultimate death squad. Nat Rev Immunol *8*, 245-245.

Lefvert, A.K., Zhao, Y., Ramanujam, R., Yu, S., Pirskanen, R., and Hammarstrom, L. (2008). PTPN22 R620W promotes production of anti-AChR autoantibodies and IL-2 in myasthenia gravis. J Neuroimmunol *197*, 110-113.

Legname, G., Seddon, B., Lovatt, M., Tomlinson, P., Sarner, N., Tolaini, M., Williams, K., Norton, T., Kioussis, D., and Zamoyska, R. (2000). Inducible expression of a p56Lck transgene reveals a central role for Lck in the differentiation of CD4 SP thymocytes. Immunity *12*, 537-546.

Lehuen, A., Diana, J., Zaccone, P., and Cooke, A. (2010). Immune cell crosstalk in type 1 diabetes. Nat Rev Immunol *10*, 501-513.

Liston, A., and Gray, D.H. (2014). Homeostatic control of regulatory T cell diversity. Nat Rev Immunol *14*, 154-165.

Liu, C., Saito, F., Liu, Z., Lei, Y., Uehara, S., Love, P., Lipp, M., Kondo, S., Manley, N., and Takahama, Y. (2006). Coordination between CCR7- and CCR9-mediated chemokine signals in prevascular fetal thymus colonization. Blood *108*, 2531-2539.

Liu, G.Y., Fairchild, P.J., Smith, R.M., Prowle, J.R., Kioussis, D., and Wraith, D.C. (1995). Low avidity recognition of self-antigen by T cells permits escape from central tolerance. Immunity *3*, 407-415.

Liu, Y., Stanford, S.M., Jog, S.P., Fiorillo, E., Orru, V., Comai, L., and Bottini, N. (2009). Regulation of lymphoid tyrosine phosphatase activity: inhibition of the catalytic domain by the proximal interdomain. Biochemistry *48*, 7525-7532.

Loeser, S., and Penninger, J.M. (2007). Regulation of peripheral T cell tolerance by the E3 ubiquitin ligase Cbl-b. Semin Immunol *19*, 206-214.

Long, S.A., Cerosaletti, K., Wan, J.Y., Ho, J.C., Tatum, M., Wei, S., Shilling, H.G., and Buckner, J.H. (2011). An autoimmune-associated variant in PTPN2 reveals an impairment of IL-2R signaling in CD4(+) T cells. Genes Immun *12*, 116-125.

Lorenz, U. (2009). SHP-1 and SHP-2 in T cells: two phosphatases functioning at many levels. Immunol Rev *228*, 342-359.

Ma, Y., Ramezani, A., Lewis, R., Hawley, R.G., and Thomson, J.A. (2003). High-level sustained transgene expression in human embryonic stem cells using lentiviral vectors. Stem Cells *21*, 111-117.

Maine, C.J., Hamilton-Williams, E.E., Cheung, J., Stanford, S.M., Bottini, N., Wicker, L.S., and Sherman, L.A. (2012). PTPN22 alters the development of regulatory T cells in the thymus. J Immunol *188*, 5267-5275.

Maine, C.J., Marquardt, K., Cheung, J., and Sherman, L.A. (2014). PTPN22 controls the germinal center by influencing the numbers and activity of T follicular helper cells. J Immunol *192*, 1415-1424.

Majeti, R., Xu, Z., Parslow, T.G., Olson, J.L., Daikh, D.I., Killeen, N., and Weiss, A. (2000). An inactivating point mutation in the inhibitory wedge of CD45 causes lymphoproliferation and autoimmunity. Cell *103*, 1059-1070.

Malek, T.R., and Castro, I. (2010). Interleukin-2 receptor signaling: at the interface between tolerance and immunity. Immunity *33*, 153-165.

Malissen, B., Aguado, E., and Malissen, M. (2005). Role of the LAT adaptor in T-cell development and Th2 differentiation. Adv Immunol *87*, 1-25.

Malissen, B., and Malissen, M. (1996). Functions of TCR and pre-TCR subunits: lessons from gene ablation. Curr Opin Immunol *8*, 383-393.

Malissen, M., Gillet, A., Ardouin, L., Bouvier, G., Trucy, J., Ferrier, P., Vivier, E., and Malissen, B. (1995). Altered T cell development in mice with a targeted mutation of the CD3-epsilon gene. Embo J *14*, 4641-4653.

Manley, N.R., and Blackburn, C.C. (2003). A developmental look at thymus organogenesis: where do the non-hematopoietic cells in the thymus come from? Curr Opin Immunol *15*, 225-232.

Mariathasan, S., Zakarian, A., Bouchard, D., Michie, A.M., Zuniga-Pflucker, J.C., and Ohashi, P.S. (2001). Duration and strength of extracellular signal-regulated

kinase signals are altered during positive versus negative thymocyte selection. J Immunol *167*, 4966-4973.

Marie, J.C., Letterio, J.J., Gavin, M., and Rudensky, A.Y. (2005). TGF-beta1 maintains suppressor function and Foxp3 expression in CD4+CD25+ regulatory T cells. J Exp Med *201*, 1061-1067.

Marrack, P., and Kappler, J. (2004). Control of T cell viability. Annu Rev Immunol *22*, 765-787.

Marson, A., Kretschmer, K., Frampton, G.M., Jacobsen, E.S., Polansky, J.K., MacIsaac, K.D., Levine, S.S., Fraenkel, E., von Boehmer, H., and Young, R.A. (2007). Foxp3 occupancy and regulation of key target genes during T-cell stimulation. Nature *445*, 931-935.

Masuda, E.S., Imamura, R., Amasaki, Y., Arai, K., and Arai, N. (1998). Signalling into the T-cell nucleus: NFAT regulation. Cell Signal *10*, 599-611.

Matsutani, T., Ohmori, T., Ogata, M., Soga, H., Yoshioka, T., Suzuki, R., and Itoh, T. (2006). Alteration of T-cell receptor repertoires during thymic T-cell development. Scand J Immunol *64*, 53-60.

Matthews, R.J., Bowne, D.B., Flores, E., and Thomas, M.L. (1992). Characterization of hematopoietic intracellular protein tyrosine phosphatases: description of a phosphatase containing an SH2 domain and another enriched in proline-, glutamic acid-, serine-, and threonine-rich sequences. Mol Cell Biol *12*, 2396-2405.

McGargill, M.A., Derbinski, J.M., and Hogquist, K.A. (2000). Receptor editing in developing T cells. Nat Immunol *1*, 336-341.

McKeithan, T.W. (1995). Kinetic proofreading in T-cell receptor signal transduction. Proc Natl Acad Sci U S A *92*, 5042-5046.

McNeil, L.K., Starr, T.K., and Hogquist, K.A. (2005). A requirement for sustained ERK signaling during thymocyte positive selection in vivo. Proc Natl Acad Sci U S A *102*, 13574-13579.

Mege, J.L., Meghari, S., Honstettre, A., Capo, C., and Raoult, D. (2006). The two faces of interleukin 10 in human infectious diseases. Lancet Infect Dis *6*, 557-569.

Menard, L., Saadoun, D., Isnardi, I., Ng, Y.S., Meyers, G., Massad, C., Price, C., Abraham, C., Motaghedi, R., Buckner, J.H.*, et al.* (2011). The PTPN22 allele encoding an R620W variant interferes with the removal of developing autoreactive B cells in humans. J Clin Invest *121*, 3635-3644.

Menasche, G., Kliche, S., Bezman, N., and Schraven, B. (2007). Regulation of T-cell antigen receptor-mediated inside-out signaling by cytosolic adapter proteins and Rap1 effector molecules. Immunol Rev *218*, 82-91.

Mombaerts, P., Iacomini, J., Johnson, R.S., Herrup, K., Tonegawa, S., and Papaioannou, V.E. (1992). RAG-1-deficient mice have no mature B and T lymphocytes. Cell *68*, 869-877.

Mosmann, T.R., Cherwinski, H., Bond, M.W., Giedlin, M.A., and Coffman, R.L. (1986). Two types of murine helper T cell clone. I. Definition according to profiles of lymphokine activities and secreted proteins. J Immunol *136*, 2348-2357.

Murali-Krishna, K., Altman, J.D., Suresh, M., Sourdive, D.J., Zajac, A.J., Miller, J.D., Slansky, J., and Ahmed, R. (1998). Counting antigen-specific CD8 T cells: a reevaluation of bystander activation during viral infection. Immunity *8*, 177-187.

Murphy, K., Travers, P., Walport, M., and Janeway, C. (2012). Janeway's immunobiology, Eighth edition. edn (New York: Garland Science).

Murphy, K.M., and Reiner, S.L. (2002). The lineage decisions of helper T cells. Nat Rev Immunol *2*, 933-944.

Murphy, M.A., Schnall, R.G., Venter, D.J., Barnett, L., Bertoncello, I., Thien, C.B., Langdon, W.Y., and Bowtell, D.D. (1998). Tissue hyperplasia and enhanced T-cell signalling via ZAP-70 in c-Cbl-deficient mice. Mol Cell Biol *18*, 4872-4882.

Mustelin, T., Alonso, A., Bottini, N., Huynh, H., Rahmouni, S., Nika, K., Louis-dit-Sully, C., Tautz, L., Togo, S.H., Bruckner, S.*, et al.* (2004). Protein tyrosine phosphatases in T cell physiology. Mol Immunol *41*, 687-700.

Mustelin, T., Coggeshall, K.M., and Altman, A. (1989). Rapid activation of the T-cell tyrosine protein kinase pp56lck by the CD45 phosphotyrosine phosphatase. Proc Natl Acad Sci U S A *86*, 6302-6306.

Mustelin, T., and Tasken, K. (2003). Positive and negative regulation of T-cell activation through kinases and phosphatases. Biochem J *371*, 15-27.

Naramura, M., Jang, I.K., Kole, H., Huang, F., Haines, D., and Gu, H. (2002). c-Cbl and Cbl-b regulate T cell responsiveness by promoting ligand-induced TCR down-modulation. Nat Immunol *3*, 1192-1199.

Neel, B.G., Gu, H., and Pao, L. (2003). The 'Shp'ing news: SH2 domain-containing tyrosine phosphatases in cell signaling. Trends Biochem Sci *28*, 284-293.

Negishi, I., Motoyama, N., Nakayama, K., Senju, S., Hatakeyama, S., Zhang, Q., Chan, A.C., and Loh, D.Y. (1995). Essential role for ZAP-70 in both positive and negative selection of thymocytes. Nature *376*, 435-438.

Negro, R., Gobessi, S., Longo, P.G., He, Y., Zhang, Z.-Y., Laurenti, L., and Efremov, D.G. (2012). Overexpression of the autoimmunity-associated phosphatase PTPN22 promotes survival of antigen-stimulated CLL cells by selectively activating AKT, Vol 119.

Nika, K., Soldani, C., Salek, M., Paster, W., Gray, A., Etzensperger, R., Fugger, L., Polzella, P., Cerundolo, V., Dushek, O.*, et al.* (2010). Constitutively active Lck kinase in T cells drives antigen receptor signal transduction. Immunity *32*, 766-777.

Nishimura, H., Nose, M., Hiai, H., Minato, N., and Honjo, T. (1999). Development of lupus-like autoimmune diseases by disruption of the PD-1 gene encoding an ITIM motif-carrying immunoreceptor. Immunity *11*, 141-151.

Oh-hora, M., and Rao, A. (2008). Calcium signaling in lymphocytes. Curr Opin Immunol *20*, 250-258.

Orru, V., Tsai, S.J., Rueda, B., Fiorillo, E., Stanford, S.M., Dasgupta, J., Hartiala, J., Zhao, L., Ortego-Centeno, N., D'Alfonso, S.*, et al.* (2009). A loss-of-function variant of PTPN22 is associated with reduced risk of systemic lupus erythematosus. Hum Mol Genet *18*, 569-579.

Ostergaard, H.L., Shackelford, D.A., Hurley, T.R., Johnson, P., Hyman, R., Sefton, B.M., and Trowbridge, I.S. (1989). Expression of CD45 alters phosphorylation of the lck-encoded tyrosine protein kinase in murine lymphoma T-cell lines. Proc Natl Acad Sci U S A *86*, 8959-8963.

Otsu, M., Steinberg, M., Ferrand, C., Merida, P., Rebouissou, C., Tiberghien, P., Taylor, N., Candotti, F., and Noraz, N. (2002). Reconstitution of lymphoid development and function in ZAP-70-deficient mice following gene transfer into bone marrow cells. Blood *100*, 1248-1256.

Palacios, E.H., and Weiss, A. (2004). Function of the Src-family kinases, Lck and Fyn, in T-cell development and activation. Oncogene *23*, 7990-8000.

Palmer, E. (2003). Negative selection--clearing out the bad apples from the T-cell repertoire. Nat Rev Immunol *3*, 383-391.

Palmer, E., and Naeher, D. (2009). Affinity threshold for thymic selection through a T-cell receptor-co-receptor zipper. Nat Rev Immunol *9*, 207-213.

Pani, G., Fischer, K.D., Mlinaric-Rascan, I., and Siminovitch, K.A. (1996). Signaling capacity of the T cell antigen receptor is negatively regulated by the PTP1C tyrosine phosphatase. J Exp Med *184*, 839-852.

Parkin, J., and Cohen, B. (2001). An overview of the immune system. Lancet *357*, 1777-1789.

Penninger, J.M., Irie-Sasaki, J., Sasaki, T., and Oliveira-dos-Santos, A.J. (2001). CD45: new jobs for an old acquaintance. Nat Immunol *2*, 389-396.

Perez, V.L., Van Parijs, L., Biuckians, A., Zheng, X.X., Strom, T.B., and Abbas, A.K. (1997). Induction of peripheral T cell tolerance in vivo requires CTLA-4 engagement. Immunity *6*, 411-417.

Peterson, L.K., Shaw, L.A., Joetham, A., Sakaguchi, S., Gelfand, E.W., and Dragone, L.L. (2011). SLAP deficiency enhances number and function of regulatory T cells preventing chronic autoimmune arthritis in SKG mice. J Immunol *186*, 2273-2281.

Peterson, P., Nagamine, K., Scott, H., Heino, M., Kudoh, J., Shimizu, N., Antonarakis, S.E., and Krohn, K.J. (1998). APECED: a monogenic autoimmune disease providing new clues to self-tolerance. Immunol Today *19*, 384-386.

Petrie, H.T., and Zuniga-Pflucker, J.C. (2007). Zoned out: functional mapping of stromal signaling microenvironments in the thymus. Annu Rev Immunol *25*, 649-679.

Pfeifer, A., Ikawa, M., Dayn, Y., and Verma, I.M. (2002). Transgenesis by lentiviral vectors: lack of gene silencing in mammalian embryonic stem cells and preimplantation embryos. Proc Natl Acad Sci U S A *99*, 2140-2145.

Pieper, K., Grimbacher, B., and Eibel, H. (2013). B-cell biology and development. J Allergy Clin Immunol *131*, 959-971.

Pui, J.C., Allman, D., Xu, L., DeRocco, S., Karnell, F.G., Bakkour, S., Lee, J.Y., Kadesch, T., Hardy, R.R., Aster, J.C., and Pear, W.S. (1999). Notch1 expression in early lymphopoiesis influences B versus T lineage determination. Immunity *11*, 299-308.

Rachmilewitz, J., and Lanzavecchia, A. (2002). A temporal and spatial summation model for T-cell activation: signal integration and antigen decoding. Trends Immunol *23*, 592-595.

Radtke, F., Wilson, A., Stark, G., Bauer, M., van Meerwijk, J., MacDonald, H.R., and Aguet, M. (1999). Deficient T cell fate specification in mice with an induced inactivation of Notch1. Immunity *10*, 547-558.

Rao, A., Luo, C., and Hogan, P.G. (1997). Transcription factors of the NFAT family: regulation and function. Annu Rev Immunol *15*, 707-747.

Rellahan, B.L., Graham, L.J., Tysgankov, A.Y., DeBell, K.E., Veri, M.-C., Noviello, C., and Bonvini, E. (2003). A dynamic constitutive and inducible binding of c-Cbl by PLCŒ≥1 SH3 and SH2 domains (negatively) regulates antigen receptor-induced PLCŒ≥1 activation in lymphocytes. Exp Cell Res *289*, 184-194.

Rhee, I., and Veillette, A. (2012). Protein tyrosine phosphatases in lymphocyte activation and autoimmunity. Nat Immunol *13*, 439-447.

Rieck, M., Arechiga, A., Onengut-Gumuscu, S., Greenbaum, C., Concannon, P., and Buckner, J.H. (2007). Genetic variation in PTPN22 corresponds to altered function of T and B lymphocytes. J Immunol *179*, 4704-4710.

Rioux, J.D., and Abbas, A.K. (2005). Paths to understanding the genetic basis of autoimmune disease. Nature *435*, 584-589.

Rodriguez-Rodriguez, L., Taib, W.R., Topless, R., Steer, S., Gonzalez-Escribano, M.F., Balsa, A., Pascual-Salcedo, D., Gonzalez-Gay, M.A., Raya, E., Fernandez-Gutierrez, B.*, et al.* (2011). The PTPN22 R263Q polymorphism is a risk factor for rheumatoid arthritis in Caucasian case-control samples. Arthritis Rheum *63*, 365-372.

Rogers, S., Wells, R., and Rechsteiner, M. (1986). Amino acid sequences common to rapidly degraded proteins: the PEST hypothesis. Science *234*, 364-368.

Rossi, F.M., Corbel, S.Y., Merzaban, J.S., Carlow, D.A., Gossens, K., Duenas, J., So, L., Yi, L., and Ziltener, H.J. (2005). Recruitment of adult thymic progenitors is regulated by P-selectin and its ligand PSGL-1. Nat Immunol *6*, 626-634.

Rothenberg, E.V., Moore, J.E., and Yui, M.A. (2008). Launching the T-cell-lineage developmental programme. Nat Rev Immunol *8*, 9-21.

Rudensky, A.Y. (2011). Regulatory T cells and Foxp3. Immunol Rev *241*, 260-268.

Rudolph, M.G., Stanfield, R.L., and Wilson, I.A. (2006). How TCRs bind MHCs, peptides, and coreceptors. Annu Rev Immunol *24*, 419-466.

Sadasivan, B., Lehner, P.J., Ortmann, B., Spies, T., and Cresswell, P. (1996). Roles for calreticulin and a novel glycoprotein, tapasin, in the interaction of MHC class I molecules with TAP. Immunity *5*, 103-114.

Saini, M., Sinclair, C., Marshall, D., Tolaini, M., Sakaguchi, S., and Seddon, B. (2010). Regulation of Zap70 expression during thymocyte development enables temporal separation of CD4 and CD8 repertoire selection at different signaling thresholds. Sci Signal *3*, ra23.

Sakaguchi, N., Takahashi, T., Hata, H., Nomura, T., Tagami, T., Yamazaki, S., Sakihama, T., Matsutani, T., Negishi, I., Nakatsuru, S., and Sakaguchi, S. (2003). Altered thymic T-cell selection due to a mutation of the ZAP-70 gene causes autoimmune arthritis in mice. Nature *426*, 454-460.

Sakaguchi, S., Sakaguchi, N., Asano, M., Itoh, M., and Toda, M. (1995). Immunologic self-tolerance maintained by activated T cells expressing IL-2 receptor alpha-chains (CD25). Breakdown of a single mechanism of self-tolerance causes various autoimmune diseases. J Immunol *155*, 1151-1164.

Sakaguchi, S., Sakaguchi, N., Yoshitomi, H., Hata, H., Takahashi, T., and Nomura, T. (2006). Spontaneous development of autoimmune arthritis due to genetic anomaly of T cell signal transduction: Part 1. Semin Immunol *18*, 199-206.

Sakaguchi, S., Yamaguchi, T., Nomura, T., and Ono, M. (2008). Regulatory T cells and immune tolerance. Cell *133*, 775-787.

Sallusto, F., and Lanzavecchia, A. (2009). Heterogeneity of CD4+ memory T cells: functional modules for tailored immunity. Eur J Immunol *39*, 2076-2082.

Sallusto, F., Lenig, D., Forster, R., Lipp, M., and Lanzavecchia, A. (2014). Pillars article: two subsets of memory T lymphocytes with distinct homing potentials and effector functions. Nature. 1999. 401: 708-712. J Immunol *192*, 840-844.

Salmond, R.J., Brownlie, R.J., Morrison, V.L., and Zamoyska, R. (2014). The tyrosine phosphatase PTPN22 discriminates weak self peptides from strong agonist TCR signals. Nat Immunol.

Salmond, R.J., Filby, A., Qureshi, I., Caserta, S., and Zamoyska, R. (2009). T-cell receptor proximal signaling via the Src-family kinases, Lck and Fyn, influences T-cell activation, differentiation, and tolerance. Immunol Rev *228*, 9-22.

Savage, P.A., and Davis, M.M. (2001). A kinetic window constricts the T cell receptor repertoire in the thymus. Immunity *14*, 243-252.

Saxton, T.M., Henkemeyer, M., Gasca, S., Shen, R., Rossi, D.J., Shalaby, F., Feng, G.S., and Pawson, T. (1997). Abnormal mesoderm patterning in mouse embryos mutant for the SH2 tyrosine phosphatase Shp-2. Embo J *16*, 2352-2364.

Schluns, K.S., and Lefrancois, L. (2003). Cytokine control of memory T-cell development and survival. Nat Rev Immunol *3*, 269-279.

Schmitt, T.M., and Zuniga-Pflucker, J.C. (2002). Induction of T cell development from hematopoietic progenitor cells by delta-like-1 in vitro. Immunity *17*, 749-756.

Schoenborn, J.R., Tan, Y.X., Zhang, C., Shokat, K.M., and Weiss, A. (2011). Feedback circuits monitor and adjust basal Lck-dependent events in T cell receptor signaling. Sci Signal *4*, ra59.

Schwartz, R.H. (2003). T cell anergy. Annu Rev Immunol *21*, 305-334.

Schwarzenberger, P., La Russa, V., Miller, A., Ye, P., Huang, W., Zieske, A., Nelson, S., Bagby, G.J., Stoltz, D., Mynatt, R.L.*, et al.* (1998). IL-17 stimulates granulopoiesis in mice: use of an alternate, novel gene therapy-derived method for in vivo evaluation of cytokines. J Immunol *161*, 6383-6389.

Sebzda, E., Bracke, M., Tugal, T., Hogg, N., and Cantrell, D.A. (2002). Rap1A positively regulates T cells via integrin activation rather than inhibiting lymphocyte signaling. Nat Immunol *3*, 251-258.

Seddon, B., and Zamoyska, R. (2002). TCR signals mediated by Src family kinases are essential for the survival of naive T cells. J Immunol *169*, 2997-3005.

Shevach, E.M. (2009). Mechanisms of foxp3+ T regulatory cell-mediated suppression. Immunity *30*, 636-645.

Shinkai, Y., Rathbun, G., Lam, K.P., Oltz, E.M., Stewart, V., Mendelsohn, M., Charron, J., Datta, M., Young, F., Stall, A.M., and et al. (1992). RAG-2-deficient mice lack mature lymphocytes owing to inability to initiate V(D)J rearrangement. Cell *68*, 855-867.

Shui, J.W., Boomer, J.S., Han, J., Xu, J., Dement, G.A., Zhou, G., and Tan, T.H. (2007). Hematopoietic progenitor kinase 1 negatively regulates T cell receptor signaling and T cell-mediated immune responses. Nat Immunol *8*, 84-91.

Shultz, L.D., Rajan, T.V., and Greiner, D.L. (1997). Severe defects in immunity and hematopoiesis caused by SHP-1 protein-tyrosine-phosphatase deficiency. Trends Biotechnol *15*, 302-307.

Shultz, L.D., Schweitzer, P.A., Rajan, T.V., Yi, T., Ihle, J.N., Matthews, R.J., Thomas, M.L., and Beier, D.R. (1993). Mutations at the murine motheaten locus are within the hematopoietic cell protein-tyrosine phosphatase (Hcph) gene. Cell *73*, 1445-1454.

Siggs, O.M., Miosge, L.A., Yates, A.L., Kucharska, E.M., Sheahan, D., Brdicka, T., Weiss, A., Liston, A., and Goodnow, C.C. (2007). Opposing functions of the T cell

receptor kinase ZAP-70 in immunity and tolerance differentially titrate in response to nucleotide substitutions. Immunity *27*, 912-926.

Sirois, J., Cote, J.F., Charest, A., Uetani, N., Bourdeau, A., Duncan, S.A., Daniels, E., and Tremblay, M.L. (2006). Essential function of PTP-PEST during mouse embryonic vascularization, mesenchyme formation, neurogenesis and early liver development. Mech Dev *123*, 869-880.

Smith-Garvin, J.E., Koretzky, G.A., and Jordan, M.S. (2009). T cell activation. Annu Rev Immunol *27*, 591-619.

Smyth, D.J., Plagnol, V., Walker, N.M., Cooper, J.D., Downes, K., Yang, J.H., Howson, J.M., Stevens, H., McManus, R., Wijmenga, C*., et al.* (2008). Shared and distinct genetic variants in type 1 diabetes and celiac disease. N Engl J Med *359*, 2767-2777.

Sommers, C.L., Samelson, L.E., and Love, P.E. (2004). LAT: a T lymphocyte adapter protein that couples the antigen receptor to downstream signaling pathways. Bioessays *26*, 61-67.

Sprent, J., and Surh, C.D. (2011). Normal T cell homeostasis: the conversion of naive cells into memory-phenotype cells. Nat Immunol *12*, 478-484.

Starr, T.K., Jameson, S.C., and Hogquist, K.A. (2003). Positive and negative selection of T cells. Annu Rev Immunol *21*, 139-176.

Stefanova, I., Dorfman, J.R., and Germain, R.N. (2002). Self-recognition promotes the foreign antigen sensitivity of naive T lymphocytes. Nature *420*, 429-434.

Stefanova, I., Hemmer, B., Vergelli, M., Martin, R., Biddison, W.E., and Germain, R.N. (2003). TCR ligand discrimination is enforced by competing ERK positive and SHP-1 negative feedback pathways. Nat Immunol *4*, 248-254.

Surh, C.D., and Sprent, J. (2000). Homeostatic T cell proliferation: how far can T cells be activated to self-ligands? J Exp Med *192*, F9-F14.

Surh, C.D., and Sprent, J. (2002). Regulation of naive and memory T-cell homeostasis. Microbes Infect *4*, 51-56.

Tanaka, S., Maeda, S., Hashimoto, M., Fujimori, C., Ito, Y., Teradaira, S., Hirota, K., Yoshitomi, H., Katakai, T., Shimizu, A.*, et al.* (2010). Graded attenuation of TCR signaling elicits distinct autoimmune diseases by altering thymic T cell selection and regulatory T cell function. J Immunol *185*, 2295-2305.

Tarakhovsky, A., Kanner, S.B., Hombach, J., Ledbetter, J.A., Muller, W., Killeen, N., and Rajewsky, K. (1995). A role for CD5 in TCR-mediated signal transduction and thymocyte selection. Science *269*, 535-537.

Tartaglia, M., Mehler, E.L., Goldberg, R., Zampino, G., Brunner, H.G., Kremer, H., van der Burgt, I., Crosby, A.H., Ion, A., Jeffery, S.*, et al.* (2001). Mutations in PTPN11, encoding the protein tyrosine phosphatase SHP-2, cause Noonan syndrome. Nat Genet *29*, 465-468.

Thien, C.B., and Langdon, W.Y. (2001). Cbl: many adaptations to regulate protein tyrosine kinases. Nat Rev Mol Cell Biol *2*, 294-307.

Tivol, E.A., Borriello, F., Schweitzer, A.N., Lynch, W.P., Bluestone, J.A., and Sharpe, A.H. (1995). Loss of CTLA-4 leads to massive lymphoproliferation and fatal multiorgan tissue destruction, revealing a critical negative regulatory role of CTLA-4. Immunity *3*, 541-547.

Todd, J.A., Walker, N.M., Cooper, J.D., Smyth, D.J., Downes, K., Plagnol, V., Bailey, R., Nejentsev, S., Field, S.F., Payne, F.*, et al.* (2007). Robust associations of four new chromosome regions from genome-wide analyses of type 1 diabetes. Nat Genet *39*, 857-864.

Tonks, N.K. (2006). Protein tyrosine phosphatases: from genes, to function, to disease. Nat Rev Mol Cell Biol *7*, 833-846.

Tootle, T.L., Silver, S.J., Davies, E.L., Newman, V., Latek, R.R., Mills, I.A., Selengut, J.D., Parlikar, B.E., and Rebay, I. (2003). The transcription factor Eyes absent is a protein tyrosine phosphatase. Nature *426*, 299-302.

Tsai, S.J., Sen, U., Zhao, L., Greenleaf, W.B., Dasgupta, J., Fiorillo, E., Orru, V., Bottini, N., and Chen, X.S. (2009). Crystal structure of the human lymphoid tyrosine phosphatase catalytic domain: insights into redox regulation. Biochemistry *48*, 4838-4845.

Tsui, H.W., Siminovitch, K.A., de Souza, L., and Tsui, F.W. (1993). Motheaten and viable motheaten mice have mutations in the haematopoietic cell phosphatase gene. Nat Genet *4*, 124-129.

Valitutti, S., Muller, S., Cella, M., Padovan, E., and Lanzavecchia, A. (1995). Serial triggering of many T-cell receptors by a few peptide-MHC complexes. Nature *375*, 148-151.

van Oene, M., Wintle, R.F., Liu, X., Yazdanpanah, M., Gu, X., Newman, B., Kwan, A., Johnson, B., Owen, J., Greer, W.*, et al.* (2005). Association of the lymphoid tyrosine phosphatase R620W variant with rheumatoid arthritis, but not Crohn's disease, in Canadian populations. Arthritis Rheum *52*, 1993-1998.

Vang, T., Congia, M., Macis, M.D., Musumeci, L., Orru, V., Zavattari, P., Nika, K., Tautz, L., Tasken, K., Cucca, F.*, et al.* (2005). Autoimmune-associated lymphoid tyrosine phosphatase is a gain-of-function variant. Nat Genet *37*, 1317-1319.

Vang, T., Landskron, J., Viken, M.K., Oberprieler, N., Torgersen, K.M., Mustelin, T., Tasken, K., Tautz, L., Rickert, R.C., and Lie, B.A. (2013). The autoimmune-predisposing variant of lymphoid tyrosine phosphatase favors T helper 1 responses. Hum Immunol *74*, 574-585.

Vang, T., Liu, W.H., Delacroix, L., Wu, S., Vasile, S., Dahl, R., Yang, L., Musumeci, L., Francis, D., Landskron, J.*, et al.* (2012). LYP inhibits T-cell activation when dissociated from CSK. Nat Chem Biol *8*, 437-446.

Vang, T., Miletic, A.V., Arimura, Y., Tautz, L., Rickert, R.C., and Mustelin, T. (2008). Protein tyrosine phosphatases in autoimmunity. Annu Rev Immunol *26*, 29-55.

Veillette, A., Bookman, M.A., Horak, E.M., and Bolen, J.B. (1988). The CD4 and CD8 T cell surface antigens are associated with the internal membrane tyrosine-protein kinase p56lck. Cell *55*, 301-308.

Veillette, A., Latour, S., and Davidson, D. (2002). Negative regulation of immunoreceptor signaling. Annu Rev Immunol *20*, 669-707.

Veillette, A., Rhee, I., Souza, C.M., and Davidson, D. (2009). PEST family phosphatases in immunity, autoimmunity, and autoinflammatory disorders. Immunol Rev *228*, 312-324.

Veldhoen, M., Hocking, R.J., Atkins, C.J., Locksley, R.M., and Stockinger, B. (2006). TGFbeta in the context of an inflammatory cytokine milieu supports de novo differentiation of IL-17-producing T cells. Immunity *24*, 179-189.

Vignali, D.A.A., Collison, L.W., and Workman, C.J. (2008). How regulatory T cells work. Nat Rev Immunol *8*, 523-532.

von Boehmer, H., and Melchers, F. (2010). Checkpoints in lymphocyte development and autoimmune disease. Nat Immunol *11*, 14-20.

Walunas, T.L., Bakker, C.Y., and Bluestone, J.A. (1996). CTLA-4 ligation blocks CD28-dependent T cell activation. J Exp Med *183*, 2541-2550.

Wang, S., Dong, H., Han, J., Ho, W.T., Fu, X., and Zhao, Z.J. (2010). Identification of a variant form of tyrosine phosphatase LYP. BMC Mol Biol *11*, 78.

Wang, Y., Shaked, I., Stanford, S.M., Zhou, W., Curtsinger, J.M., Mikulski, Z., Shaheen, Z.R., Cheng, G., Sawatzke, K., Campbell, A.M*., et al.* (2013). The autoimmunity-associated gene PTPN22 potentiates toll-like receptor-driven, type 1 interferon-dependent immunity. Immunity *39*, 111-122.

Wiede, F., Shields, B.J., Chew, S.H., Kyparissoudis, K., van Vliet, C., Galic, S., Tremblay, M.L., Russell, S.M., Godfrey, D.I., and Tiganis, T. (2011). T cell protein tyrosine phosphatase attenuates T cell signaling to maintain tolerance in mice. J Clin Invest *121*, 4758-4774.

Williams, M.A., and Bevan, M.J. (2007). Effector and memory CTL differentiation. Annu Rev Immunol *25*, 171-192.

Wu, J., Katrekar, A., Honigberg, L.A., Smith, A.M., Conn, M.T., Tang, J., Jeffery, D., Mortara, K., Sampang, J., Williams, S.R.*, et al.* (2006). Identification of substrates of human protein-tyrosine phosphatase PTPN22. J Biol Chem *281*, 11002-11010.

Wucherpfennig, K.W., Gagnon, E., Call, M.J., Huseby, E.S., and Call, M.E. (2010). Structural biology of the T-cell receptor: insights into receptor assembly, ligand recognition, and initiation of signaling. Cold Spring Harb Perspect Biol *2*, a005140.

Xu, S., Huo, J., Tan, J.E., and Lam, K.P. (2005). Cbp deficiency alters Csk localization in lipid rafts but does not affect T-cell development. Mol Cell Biol *25*, 8486-8495.

Xu, Z., and Weiss, A. (2002). Negative regulation of CD45 by differential homodimerization of the alternatively spliced isoforms. Nat Immunol *3*, 764-771.

Yamashita, I., Nagata, T., Tada, T., and Nakayama, T. (1993). CD69 cell surface expression identifies developing thymocytes which audition for T cell antigen receptor-mediated positive selection. Int Immunol *5*, 1139-1150.

Yasuda, K., Nagafuku, M., Shima, T., Okada, M., Yagi, T., Yamada, T., Minaki, Y., Kato, A., Tani-Ichi, S., Hamaoka, T., and Kosugi, A. (2002). Cutting edge: Fyn is essential for tyrosine phosphorylation of Csk-binding protein/phosphoprotein associated with glycolipid-enriched microdomains in lipid rafts in resting T cells. J Immunol *169*, 2813-2817.

Yasuda, T., Bundo, K., Hino, A., Honda, K., Inoue, A., Shirakata, M., Osawa, M., Tamura, T., Nariuchi, H., Oda, H.*, et al.* (2007). Dok-1 and Dok-2 are negative regulators of T cell receptor signaling. Int Immunol *19*, 487-495.

Yeh, L.T., Miaw, S.C., Lin, M.H., Chou, F.C., Shieh, S.J., Chuang, Y.P., Lin, S.H., Chang, D.M., and Sytwu, H.K. (2013). Different modulation of Ptpn22 in effector and regulatory T cells leads to attenuation of autoimmune diabetes in transgenic nonobese diabetic mice. J Immunol *191*, 594-607.

Yoshitomi, H., Sakaguchi, N., Kobayashi, K., Brown, G.D., Tagami, T., Sakihama, T., Hirota, K., Tanaka, S., Nomura, T., Miki, I.*, et al.* (2005). A role for fungal {beta}-glucans and their receptor Dectin-1 in the induction of autoimmune arthritis in genetically susceptible mice. J Exp Med *201*, 949-960.

Yu, X., Chen, M., Zhang, S., Yu, Z.H., Sun, J.P., Wang, L., Liu, S., Imasaki, T., Takagi, Y., and Zhang, Z.Y. (2011). Substrate specificity of lymphoid-specific tyrosine phosphatase (Lyp) and identification of Src kinase-associated protein of 55 kDa homolog (SKAP-HOM) as a Lyp substrate. J Biol Chem *286*, 30526-30534.

Yu, X., Sun, J.P., He, Y., Guo, X., Liu, S., Zhou, B., Hudmon, A., and Zhang, Z.Y. (2007). Structure, inhibitor, and regulatory mechanism of Lyp, a lymphoid-specific tyrosine phosphatase implicated in autoimmune diseases. Proc Natl Acad Sci U S A *104*, 19767-19772.

Zehn, D., and Bevan, M.J. (2006). T cells with low avidity for a tissue-restricted antigen routinely evade central and peripheral tolerance and cause autoimmunity. Immunity *25*, 261-270.

Zhang, J., Zahir, N., Jiang, Q., Miliotis, H., Heyraud, S., Meng, X., Dong, B., Xie, G., Qiu, F., Hao, Z.*, et al.* (2011). The autoimmune disease-associated PTPN22 variant promotes calpain-mediated Lyp/Pep degradation associated with lymphocyte and dendritic cell hyperresponsiveness. Nat Genet *43*, 902-907.

Zhang, S.Q., Yang, W., Kontaridis, M.I., Bivona, T.G., Wen, G., Araki, T., Luo, J., Thompson, J.A., Schraven, B.L., Philips, M.R., and Neel, B.G. (2004). Shp2

regulates SRC family kinase activity and Ras/Erk activation by controlling Csk recruitment. Mol Cell *13*, 341-355.

Zhang, T., Tsang, T.C., and Harris, D.T. (2003). Efficient transduction of murine primary T cells requires a combination of high viral titer, preferred tropism, and proper timing of transduction. J Hematother Stem Cell Res *12*, 123-130.

Zheng, P., and Kissler, S. (2013). PTPN22 silencing in the NOD model indicates the type 1 diabetes-associated allele is not a loss-of-function variant. Diabetes *62*, 896-904.

Zhou, L., Lopes, J.E., Chong, M.M., Ivanov, II, Min, R., Victora, G.D., Shen, Y., Du, J., Rubtsov, Y.P., Rudensky, A.Y.*, et al.* (2008). TGF-beta-induced Foxp3 inhibits T(H)17 cell differentiation by antagonizing RORgammat function. Nature *453*, 236-240.

Zhu, J., Yamane, H., and Paul, W.E. (2010). Differentiation of effector CD4 T cell populations (*). Annu Rev Immunol *28*, 445-489.

Zhu, J.W., Brdicka, T., Katsumoto, T.R., Lin, J., and Weiss, A. (2008). Structurally distinct phosphatases CD45 and CD148 both regulate B cell and macrophage immunoreceptor signaling. Immunity *28*, 183-196.

Zikherman, J., Hermiston, M., Steiner, D., Hasegawa, K., Chan, A., and Weiss, A. (2009). PTPN22 deficiency cooperates with the CD45 E613R allele to break tolerance on a non-autoimmune background. J Immunol *182*, 4093-4106.